

CERN-PH-EP-2011-069  
10 May 2011

## Cross-sections of large-angle hadron production in proton– and pion–nucleus interactions VII: tin nuclei and beam momenta from $\pm 3 \text{ GeV}/c$ to $\pm 15 \text{ GeV}/c$

### Abstract

We report on double-differential inclusive cross-sections of the production of secondary protons, charged pions, and deuterons, in the interactions with a 5%  $\lambda_{\text{int}}$  thick stationary tin target, of proton and pion beams with momentum from  $\pm 3 \text{ GeV}/c$  to  $\pm 15 \text{ GeV}/c$ . Results are given for secondary particles with production angles  $20^\circ < \theta < 125^\circ$ . Cross-sections on tin nuclei are compared with cross-sections on beryllium, carbon, copper, tantalum and lead nuclei.

### The HARP–CDP group

A. Bolshakova<sup>1</sup>, I. Boyko<sup>1</sup>, G. Chelkov<sup>1a</sup>, D. Dedovitch<sup>1</sup>, A. Elagin<sup>1b</sup>, D. Emelyanov<sup>1</sup>, M. Gostkin<sup>1</sup>, A. Guskov<sup>1</sup>, Z. Kroumchtein<sup>1</sup>, Yu. Nefedov<sup>1</sup>, K. Nikolaev<sup>1</sup>, A. Zhemchugov<sup>1</sup>, F. Dydak<sup>2</sup>, J. Wotschack<sup>2\*</sup>, A. De Min<sup>3c</sup>, V. Ammosov<sup>4†</sup>, V. Gapienko<sup>4</sup>, V. Koreshev<sup>4</sup>, A. Semak<sup>4</sup>, Yu. Sviridov<sup>4</sup>, E. Usenko<sup>4d</sup>, V. Zaets<sup>4</sup>

<sup>1</sup> Joint Institute for Nuclear Research, Dubna, Russia

<sup>2</sup> CERN, Geneva, Switzerland

<sup>3</sup> Politecnico di Milano and INFN, Sezione di Milano-Bicocca, Milan, Italy

<sup>4</sup> Institute of High Energy Physics, Protvino, Russia

*(To be submitted to Eur. Phys. J. C)*

<sup>a</sup> Also at the Moscow Institute of Physics and Technology, Moscow, Russia

<sup>b</sup> Now at Texas A&M University, College Station, USA

<sup>c</sup> On leave of absence

<sup>d</sup> Now at Institute for Nuclear Research RAS, Moscow, Russia

<sup>†</sup> Deceased

\* Corresponding author; e-mail: joerg.wotschack@cern.ch

## 1 INTRODUCTION

The HARP experiment arose from the realization that the inclusive differential cross-sections of hadron production in the interactions of few  $\text{GeV}/c$  protons with nuclei were known only within a factor of two to three, while more precise cross-sections are in demand for several reasons.

These are the optimization of the design parameters of the proton driver of a neutrino factory (see Ref. [1] and further references cited therein), but also the understanding of the underlying physics and the modelling of Monte Carlo generators of hadron–nucleus collisions, flux predictions for conventional neutrino beams, and more precise calculations of the atmospheric neutrino flux.

The HARP experiment was designed to carry out a programme of systematic and precise (i.e., at the few per cent level) measurements of hadron production by protons and pions with momenta from 1.5 to 15  $\text{GeV}/c$ , on a variety of target nuclei. It took data at the CERN Proton Synchrotron in 2001 and 2002.

The HARP detector combined a forward spectrometer with a large-angle spectrometer. The latter comprised a cylindrical Time Projection Chamber (TPC) around the target and an array of Resistive Plate Chambers (RPCs) that surrounded the TPC. The purpose of the TPC was track reconstruction and particle identification by  $dE/dx$ . The purpose of the RPCs was to complement the particle identification by time of flight.

This is the seventh of a series of cross-section papers with results from the HARP experiment. In the first paper [2] we described the detector characteristics and our analysis algorithms, on the example of  $+8.9 \text{ GeV}/c$  and  $-8.0 \text{ GeV}/c$  beams impinging on a 5%  $\lambda_{\text{int}}$  Be target. The second paper [3] presented results for all beam momenta from this Be target. The third [4], fourth [5], fifth [6], and sixth [7] papers presented results from the interactions with 5%  $\lambda_{\text{int}}$  tantalum, copper, lead, and carbon targets. In this paper, we report on the large-angle production (polar angle  $\theta$  in the range  $20^\circ < \theta < 125^\circ$ ) of secondary protons and charged pions, and of deuterons, in the interactions with a 5%  $\lambda_{\text{int}}$  tin target of protons and pions with beam momenta of  $\pm 3.0, \pm 5.0, \pm 8.0, \pm 12.0$ , and  $\pm 15.0 \text{ GeV}/c$ .

Our work involves only the HARP large-angle spectrometer.

## 2 THE BEAMS AND THE HARP SPECTROMETER

The protons and pions were delivered by the T9 beam line in the East Hall of CERN’s Proton Synchrotron. This beam line supports beam momenta between 1.5 and 15  $\text{GeV}/c$ , with a momentum bite  $\Delta p/p \sim 1\%$ .

The beam instrumentation, the definition of the beam particle trajectory, the cuts to select ‘good’ beam particles, and the muon and electron contaminations of the particle beams, are the same as described, e.g., in Ref. [2].

The target was a disc made of high-purity (99.99%) tin, with a radius of 15.1 mm, a thickness of 11.1 mm (5%  $\lambda_{\text{int}}$ ), and a measured density of  $7.24 \text{ g/cm}^3$ .

The finite thickness of the target leads to a small attenuation of the number of incident beam particles. The attenuation factor is  $f_{\text{att}} = 0.975$ .

Our calibration work on the HARP TPC and RPCs is described in detail in Refs. [8] and [9], and in references cited therein.

The momentum resolution  $\sigma(1/p_T)$  of the TPC is typically  $0.2 (\text{GeV}/c)^{-1}$  and worsens towards small relative particle velocity  $\beta$  and small polar angle  $\theta$ . The absolute momentum scale is determined to be correct to better than 2%, both for positively and negatively charged particles.

The polar angle  $\theta$  is measured in the TPC with a resolution of  $\sim 9$  mrad, for a representative angle of  $\theta = 60^\circ$ . In addition, a multiple scattering error must be considered that is for a proton with  $p_T = 500$  MeV/c in the TPC gas  $\sim 6$  mrad at  $\theta = 20^\circ$ , and  $\sim 18$  mrad at  $\theta = 90^\circ$ . For a pion with the same characteristics, the multiple scattering errors are  $\sim 3$  mrad and  $\sim 10$  mrad, respectively. The polar-angle scale is correct to better than 2 mrad.

The TPC measures  $dE/dx$  with a resolution of 16% for a track length of 300 mm.

The intrinsic efficiency of the RPCs that surround the TPC is better than 98%.

The intrinsic time resolution of the RPCs is 127 ps and the system time-of-flight resolution (that includes the jitter of the arrival time of the beam particle at the target) is 175 ps.

To separate measured particles into species, we assign on the basis of  $dE/dx$  and  $\beta$  to each particle a probability of being a proton, a pion (muon), or an electron, respectively. The probabilities add up to unity, so that the number of particles is conserved. These probabilities are used for weighting when entering tracks into plots or tables.

A general discussion of the systematic errors can be found, e.g., in Ref. [2]. All systematic errors are propagated into the momentum spectra of secondaries and then added in quadrature. They add up to a systematic uncertainty of our inclusive cross-sections at the few-per-cent level, mainly from errors in the normalization, in the momentum measurement, in particle identification, and in the corrections applied to the data.

### 3 MONTE CARLO SIMULATION

We used the Geant4 tool kit [10] for the simulation of the HARP large-angle spectrometer.

Geant4's QGSP\_BIC physics list provided us with reasonably realistic spectra of secondaries from incoming beam protons with momentum below 12 GeV/c. For the secondaries from beam protons at 12 and 15 GeV/c momentum, and from beam pions at all momenta, we found the standard physics lists of Geant4 unsuitable [11].

To overcome this problem, we built our own HARP\_CDP physics list. It starts from Geant4's standard QBBC physics list, but the Quark–Gluon String Model is replaced by the FRITIOF string fragmentation model for kinetic energy  $E > 6$  GeV; for  $E < 6$  GeV, the Bertini Cascade is used for pions, and the Binary Cascade for protons; elastic and quasi-elastic scattering is disabled. Examples of the good performance of the HARP\_CDP physics list are given in Ref. [11].

### 4 CROSS-SECTION RESULTS

In Tables A.1–A.45, collated in the Appendix of this paper, we give the double-differential inclusive cross-sections  $d^2\sigma/dpd\Omega$  for various combinations of incoming beam particle and secondary particle, including statistical and systematic errors. In each bin, the average momentum at the vertex and the average polar angle are also given.

The data of Tables A.1–A.45 are available in ASCII format in Ref. [12].

Some bins in the tables are empty. Cross-sections are only given if the total error is not larger than the cross-section itself. Since our track reconstruction algorithm is optimized for tracks with  $p_T$  above  $\sim 70$  MeV/c in the TPC volume, we do not give cross-sections from tracks with  $p_T$  below this value. Because of the absorption of slow protons in the material between the vertex and the TPC gas, and with a view to keeping the correction for absorption losses below 30%, cross-sections from protons are limited to  $p > 450$  MeV/c at the interaction vertex. Proton cross-sections are also not given if a 10% error on the proton energy loss in materials between the interaction vertex and the TPC volume leads to a momentum change larger than

2%. Pion cross-sections are not given if pions are separated from protons by less than twice the time-of-flight resolution.

The large errors and/or absence of results from the  $+15 \text{ GeV}/c$  pion beam are caused by scarce statistics because the beam composition was dominated by protons.

We present in Figs. 1 to 7 what we consider salient features of our cross-sections.

Figure 1 shows the inclusive cross-sections of the production of protons,  $\pi^+$ 's, and  $\pi^-$ 's, by incoming protons between  $3 \text{ GeV}/c$  and  $15 \text{ GeV}/c$  momentum, as a function of their charge-signed  $p_T$ . The data refer to the polar-angle range  $20^\circ < \theta < 30^\circ$ . Figures 2 and 3 show the same for incoming  $\pi^+$ 's and  $\pi^-$ 's.

Figure 4 shows inclusive Lorentz-invariant cross-sections of the production of protons,  $\pi^+$ 's and  $\pi^-$ 's, by incoming protons between  $3 \text{ GeV}/c$  and  $15 \text{ GeV}/c$  momentum, in the rapidity range  $0.6 < y < 0.8$ , as a function of the charge-signed reduced transverse particle mass,  $m_T - m_0$ , where  $m_0$  is the rest mass of the respective particle. Figures 5 and 6 show the same for incoming  $\pi^+$ 's and  $\pi^-$ 's. We note the good representation of particle production by an exponential falloff with increasing reduced transverse mass.

In Fig. 7, we present the inclusive cross-sections of the production of secondary  $\pi^+$ 's and  $\pi^-$ 's, integrated over the momentum range  $0.2 < p < 1.0 \text{ GeV}/c$  and the polar-angle range  $30^\circ < \theta < 90^\circ$  in the forward hemisphere, as a function of the beam momentum.

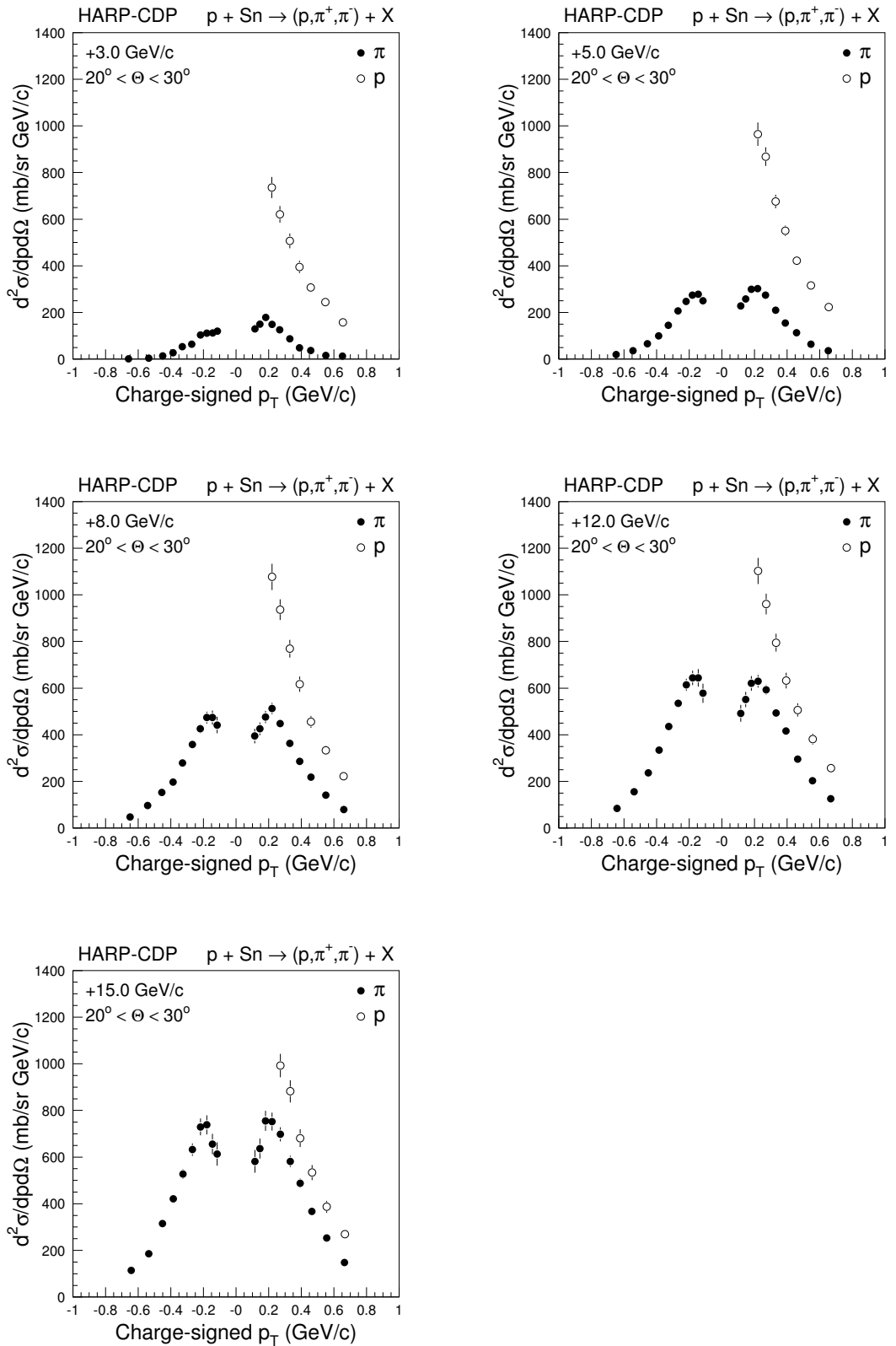


Fig. 1: Inclusive cross-sections of the production of secondary protons,  $\pi^+$ 's, and  $\pi^-$ 's, by protons on tin nuclei, in the polar-angle range  $20^\circ < \theta < 30^\circ$ , for different proton beam momenta, as a function of the charge-signed  $p_T$  of the secondaries; the shown errors are total errors.

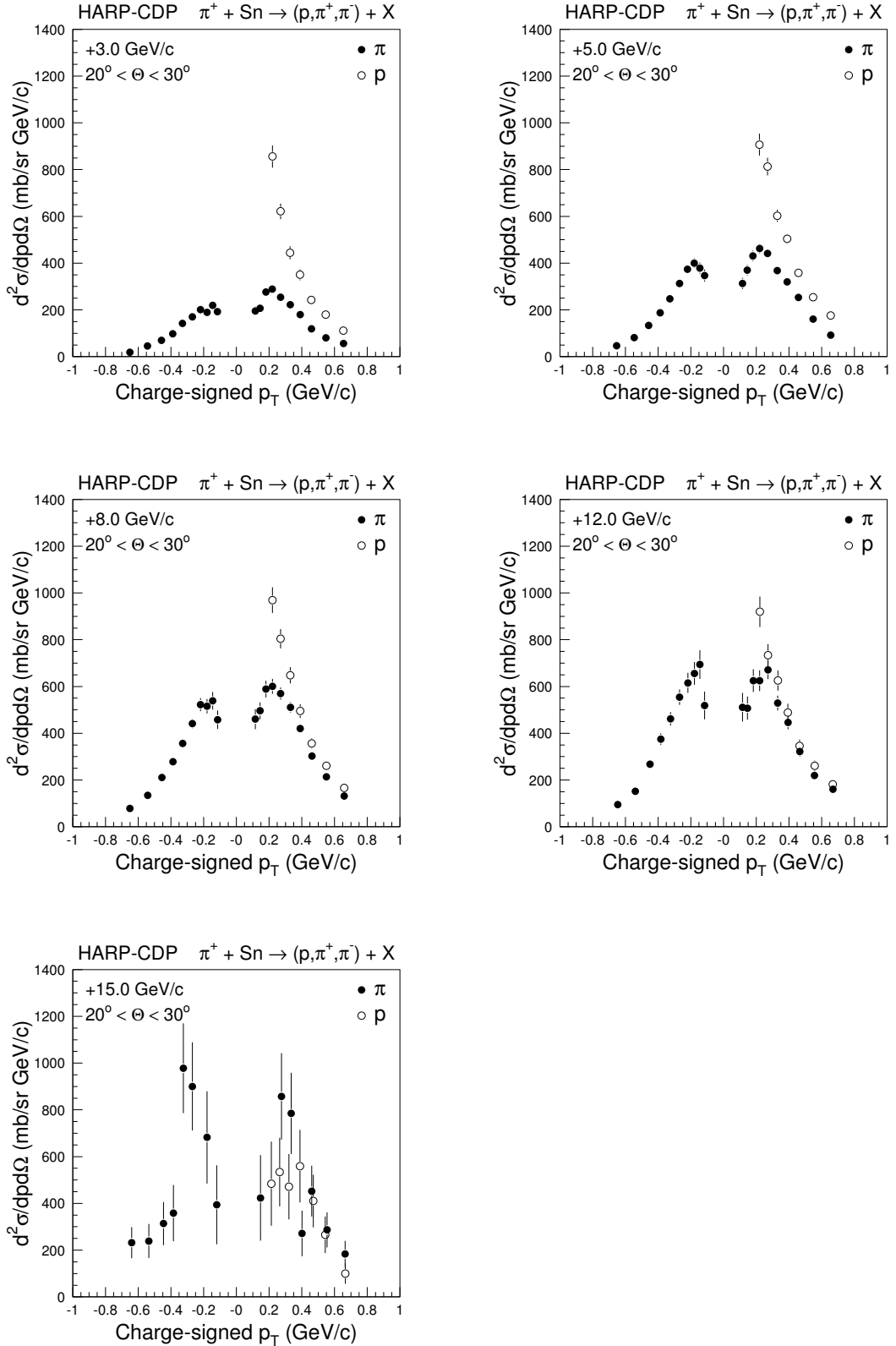


Fig. 2: Inclusive cross-sections of the production of secondary protons,  $\pi^+$ 's, and  $\pi^-$ 's, by  $\pi^+$ 's on tin nuclei, in the polar-angle range  $20^\circ < \theta < 30^\circ$ , for different  $\pi^+$  beam momenta, as a function of the charge-signed  $p_T$  of the secondaries; the shown errors are total errors.

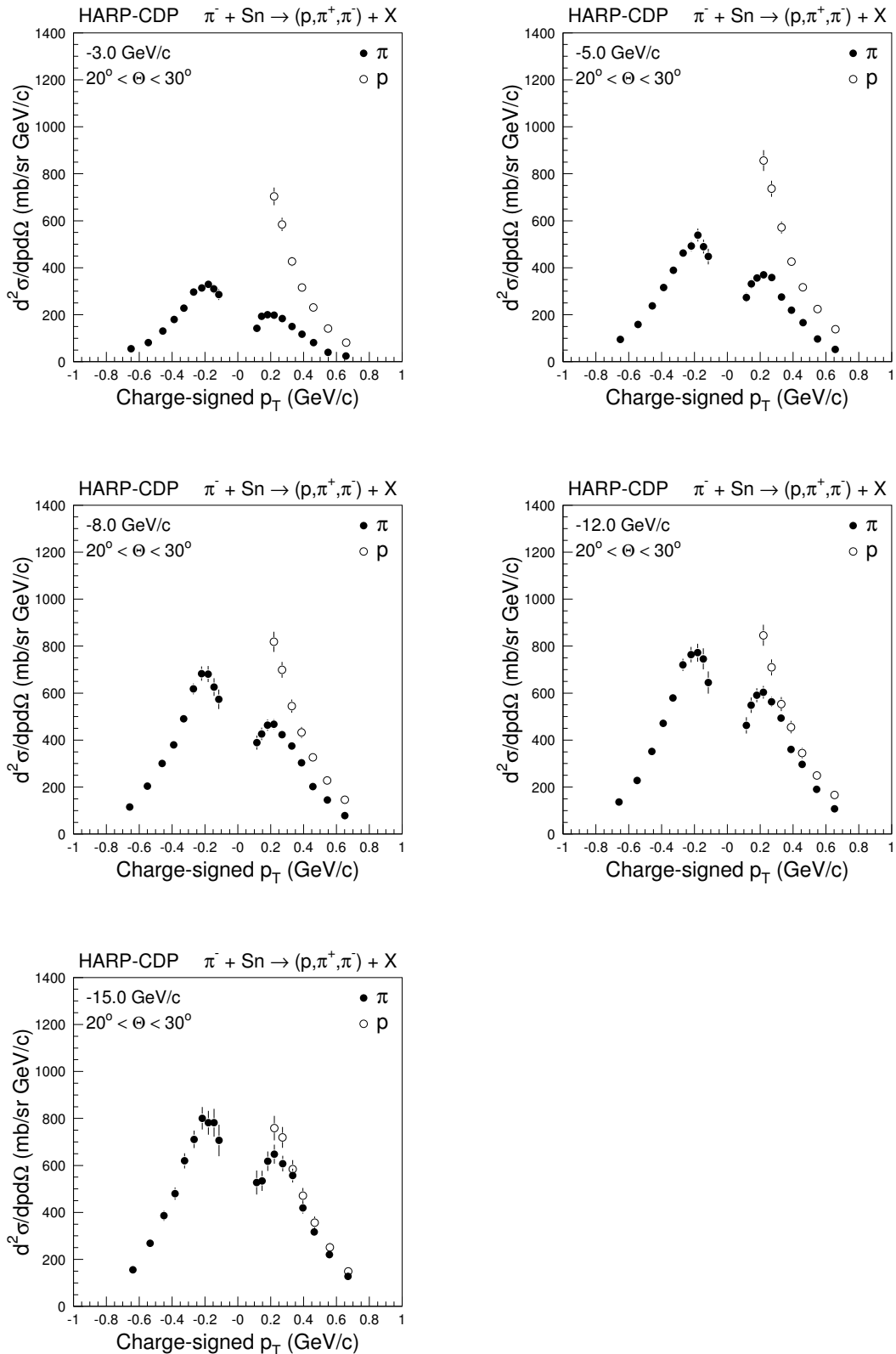


Fig. 3: Inclusive cross-sections of the production of secondary protons,  $\pi^+$ 's, and  $\pi^-$ 's, by  $\pi^-$ 's on tin nuclei, in the polar-angle range  $20^\circ < \theta < 30^\circ$ , for different  $\pi^-$  beam momenta, as a function of the charge-signed  $p_T$  of the secondaries; the shown errors are total errors.

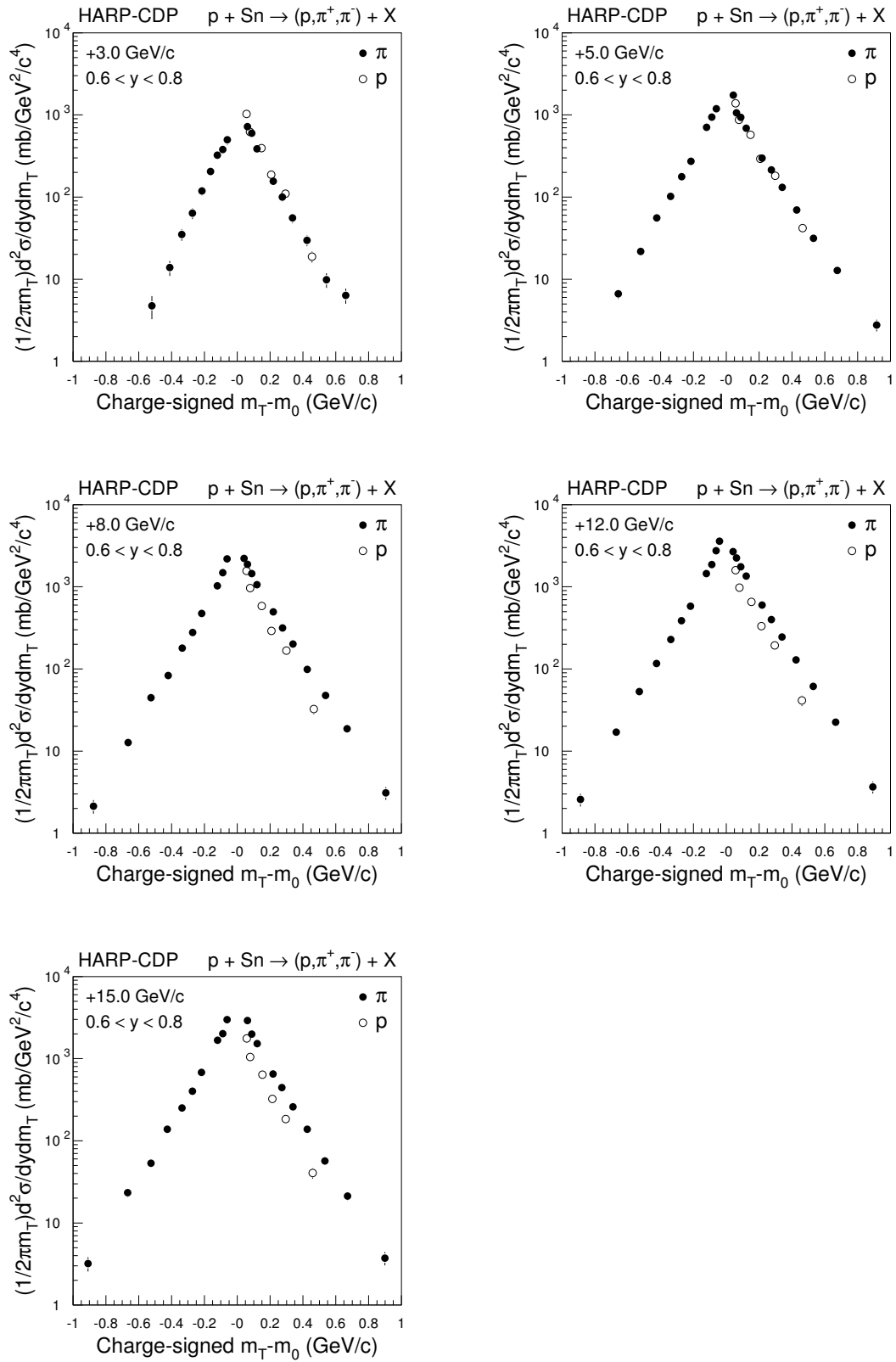


Fig. 4: Inclusive Lorentz-invariant cross-sections of the production of protons,  $\pi^+$ 's and  $\pi^-$ 's, by incoming protons between  $3 \text{ GeV}/c$  and  $15 \text{ GeV}/c$  momentum, in the rapidity range  $0.6 < y < 0.8$ , as a function of the charge-signed reduced transverse particle mass,  $m_T - m_0$ , where  $m_0$  is the rest mass of the respective particle; the shown errors are total errors.

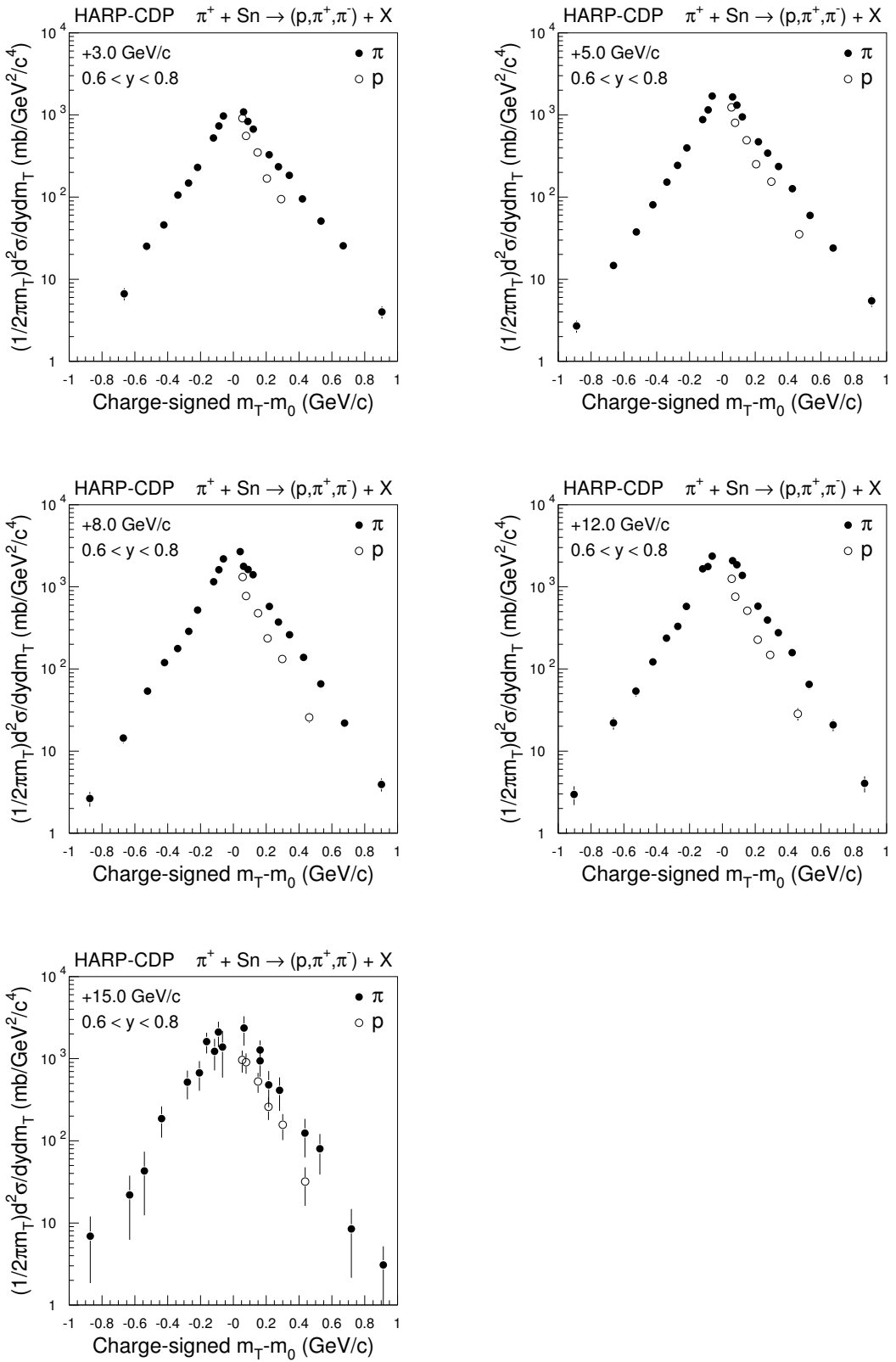


Fig. 5: Inclusive Lorentz-invariant cross-sections of the production of protons,  $\pi^+$ 's and  $\pi^-$ 's, by incoming  $\pi^+$ 's between 3 GeV/c and 15 GeV/c momentum, in the rapidity range  $0.6 < y < 0.8$ , as a function of the charge-signed reduced transverse pion mass,  $m_T - m_0$ , where  $m_0$  is the rest mass of the respective particle; the shown errors are total errors.

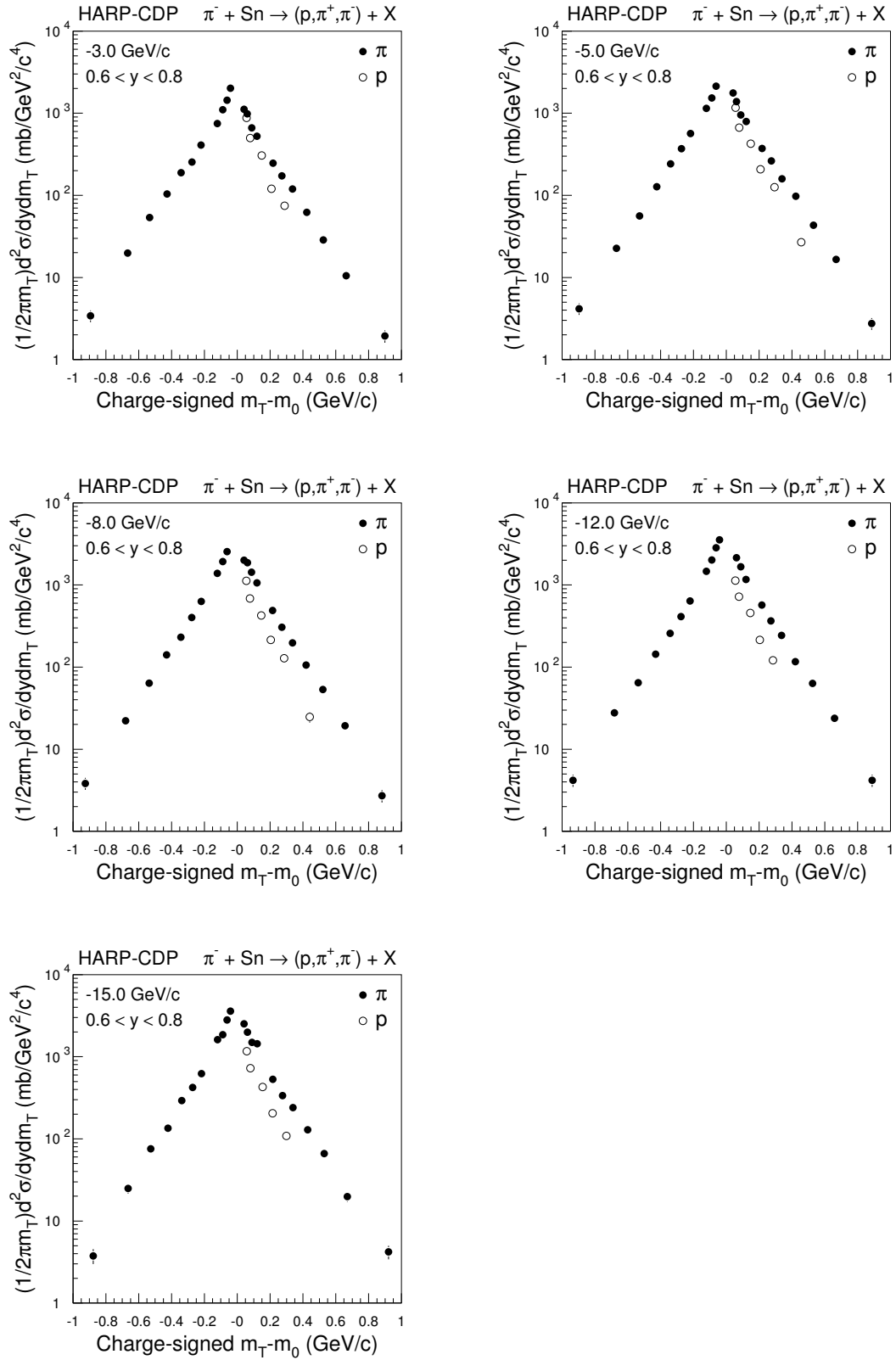


Fig. 6: Inclusive Lorentz-invariant cross-sections of the production of protons,  $\pi^+$ 's and  $\pi^-$ 's, by incoming  $\pi^-$ 's between  $3 \text{ GeV}/c$  and  $15 \text{ GeV}/c$  momentum, in the rapidity range  $0.6 < y < 0.8$ , as a function of the charge-signed reduced transverse pion mass,  $m_T - m_0$ , where  $m_0$  is the rest mass of the respective particle; the shown errors are total errors.

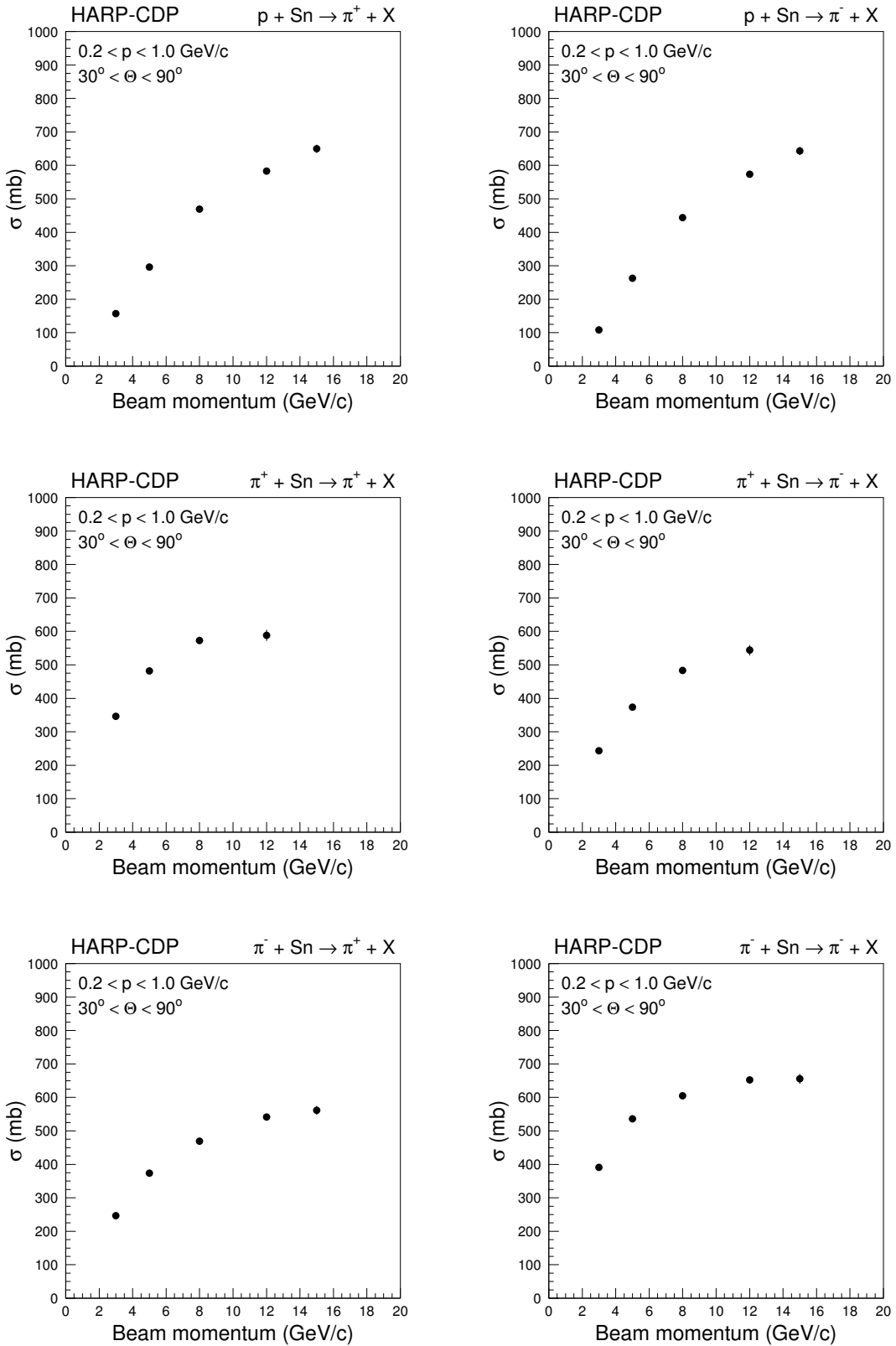


Fig. 7: Inclusive cross-sections of the production of secondary  $\pi^+$ 's and  $\pi^-$ 's, integrated over the momentum range  $0.2 < p < 1.0 \text{ GeV}/c$  and the polar-angle range  $30^\circ < \theta < 90^\circ$ , from the interactions on tin nuclei of protons (top row),  $\pi^+$ 's (middle row), and  $\pi^-$ 's (bottom row), as a function of the beam momentum; the shown errors are total errors and mostly smaller than the symbol size.

## 5 COMPARISON OF OUR RESULTS WITH RESULTS FROM THE HARP COLLABORATION

Figure 8 shows the comparison of our cross-sections of  $\pi^\pm$  production by protons,  $\pi^+$ 's and  $\pi^-$ 's of  $3.0 \text{ GeV}/c$  and  $8.0 \text{ GeV}/c$  momentum, off tin nuclei, with the ones published by the HARP Collaboration [14, 15], in the polar-angle range  $20^\circ < \theta < 30^\circ$ . The latter cross-sections are plotted as published, while we expressed our cross-sections in the unit used by the HARP Collaboration. The errors shown are the published total errors.

The discrepancy between our results and those published by the HARP Collaboration is evident. It shows the same pattern as observed in inclusive cross-sections off other targets that we analyzed and compared. We hold that the discrepancy is caused by problems in the HARP Collaboration's data analysis, discussed in detail in Refs [16–20], and summarized in the Appendix of Ref. [2].

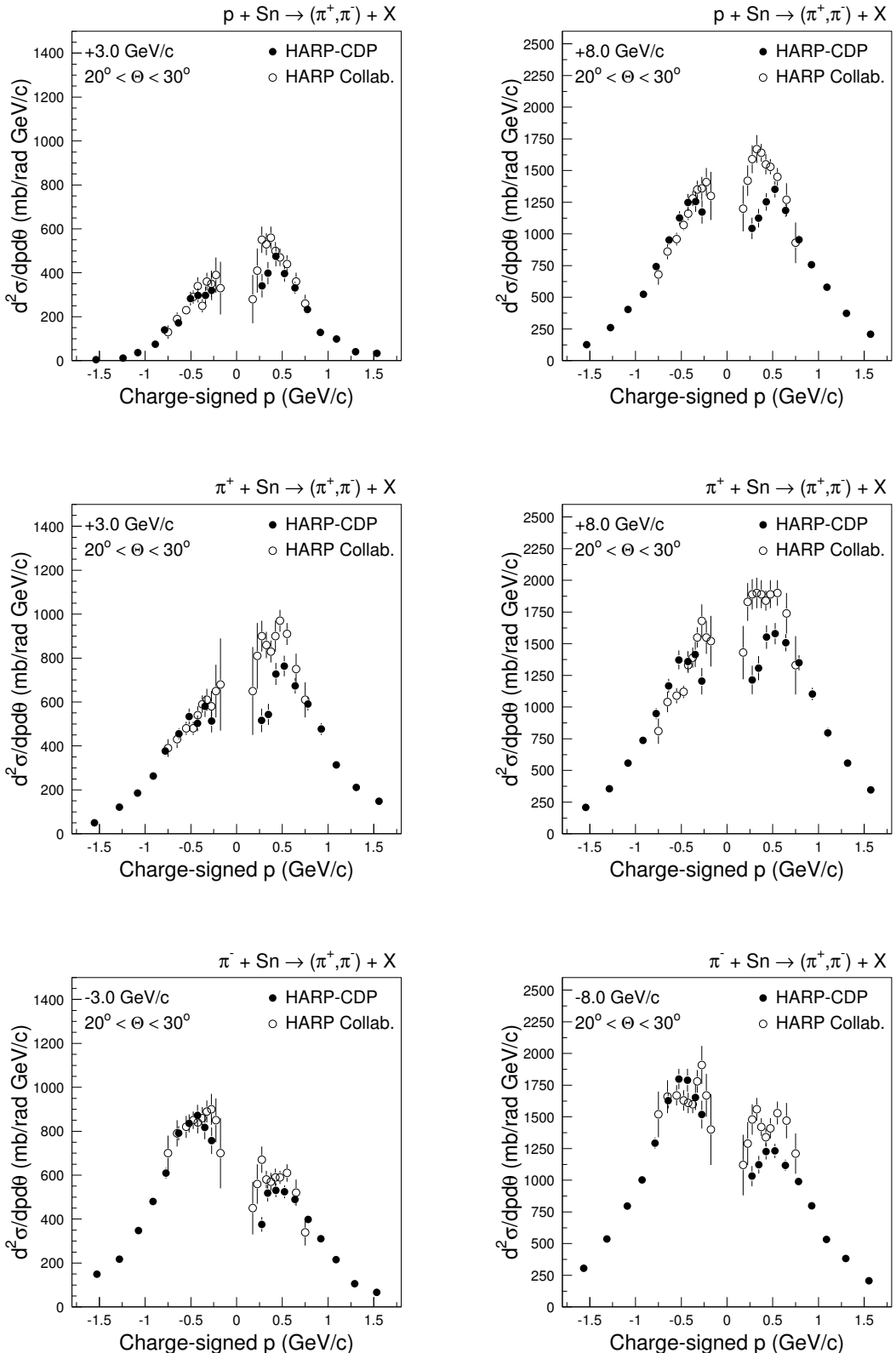


Fig. 8: Comparison of HARP-CDP cross-sections (full circles) of  $\pi^\pm$  production by protons,  $\pi^+$ 's and  $\pi^-$ 's of  $3.0 \text{ GeV}/c$  (left panels) and  $8.0 \text{ GeV}/c$  momentum (right panels), off tin nuclei, with the cross-sections published by the HARP Collaboration (open circles).

## 6 COMPARISON OF CHARGED-PION PRODUCTION ON BERYLLIUM, CARBON, COPPER, TIN, TANTALUM AND LEAD

Figure 9 presents a comparison between the inclusive cross-sections of  $\pi^+$  and  $\pi^-$  production, integrated over the secondaries' momentum range  $0.2 < p < 1.0 \text{ GeV}/c$  and polar-angle range  $30^\circ < \theta < 90^\circ$ , in the interactions of protons,  $\pi^+$  and  $\pi^-$ , with beryllium ( $A = 9.01$ ), carbon ( $A = 12.01$ ), copper ( $A = 63.55$ ), tin ( $A = 118.7$ ), tantalum ( $A = 181.0$ ), and lead ( $A = 207.2$ ) nuclei<sup>1)</sup>. The comparison employs the scaling variable  $A^{2/3}$  where  $A$  is the atomic number of the respective nucleus. We note the approximately linear dependence on this scaling variable. At low beam momentum, the slope exhibits a strong dependence on beam particle type, which tends to disappear with higher beam momentum.

Linearity with  $A^{2/3}$  means that inclusive pion production scales with the geometrical cross-section of the nucleus. We note that at the lowest beam momenta the inclusive pion cross-section tends to fall below a linear dependence on  $A^{2/3}$ , while at the highest beam momenta the cross-sections tend to lie above a linear dependence. We conjecture that this behaviour arises from the production of tertiary pions from the interactions of secondaries in nuclear matter. At high beam momenta, the acceptance cut of  $p > 0.2 \text{ GeV}/c$  has a minor effect on the tertiary pions. The transition of the inclusive pion cross-section from an approximate  $A^{2/3}$  dependence for light nuclei toward an approximate  $A$  dependence for heavy nuclei (owing to the increasing contribution of pions from the reinteractions in nuclear matter) becomes apparent. At low beam momenta, the acceptance cut of  $p > 0.2 \text{ GeV}/c$  suppresses a large fraction of the primarily low-momentum tertiaries, thus hiding this transition.

Figure 10 compares the ‘forward multiplicity’ of secondary  $\pi^+$ ’s and  $\pi^-$ ’s in the interaction of protons and pions with beryllium, carbon, copper, tin, tantalum, and lead target nuclei. The forward multiplicities are averaged over the momentum range  $0.2 < p < 1.0 \text{ GeV}/c$  and the polar-angle range  $30^\circ < \theta < 90^\circ$ . They have been obtained by dividing the measured inclusive cross-section by the total cross-section inferred from the nuclear interaction lengths and pion interaction lengths, respectively, as published by the Particle Data Group [13] and reproduced in Table 1. The errors of the forward multiplicities are dominated by a 3% systematic uncertainty.

Table 1: Nuclear and pion interaction lengths used for the calculation of pion forward multiplicities.

Nucleus	$\lambda_{\text{int}}^{\text{nucl}} [\text{g cm}^{-2}]$	$\lambda_{\text{int}}^{\text{pion}} [\text{g cm}^{-2}]$
Beryllium	77.8	109.9
Carbon	85.8	117.8
Copper	137.3	165.9
Tin	166.7	194.3
Tantalum	191.0	217.7
Lead	199.6	226.2

The forward multiplicities display a ‘leading particle effect’ that mirrors the incoming beam particle. It is also interesting that the forward multiplicity decreases with the nuclear mass at low beam momentum but increases at high beam momentum. Again, we interpret this as the

---

<sup>1)</sup>The beryllium data with  $+8.9 \text{ GeV}/c$  beam momentum [2, 3] have been scaled, by interpolation, to a beam momentum of  $+8.0 \text{ GeV}/c$ .

effect of pion reinteractions in the nuclear matter in conjunction with the acceptance cut of  $p > 0.2 \text{ GeV}/c$ .

Figure 11 shows the increase of the inclusive cross-sections of  $\pi^+$ 's and  $\pi^-$ 's production by incoming protons of  $8.0 \text{ GeV}/c$  (in the case of beryllium target nuclei:  $+8.9 \text{ GeV}/c$ ) from the light beryllium nucleus to the heavy lead nucleus, for pions in the polar angle range  $20^\circ < \theta < 30^\circ$ . It is interesting to note that  $\pi^-$  production is slightly favoured on heavy nuclei, while  $\pi^+$  production is slightly favoured on light nuclei.

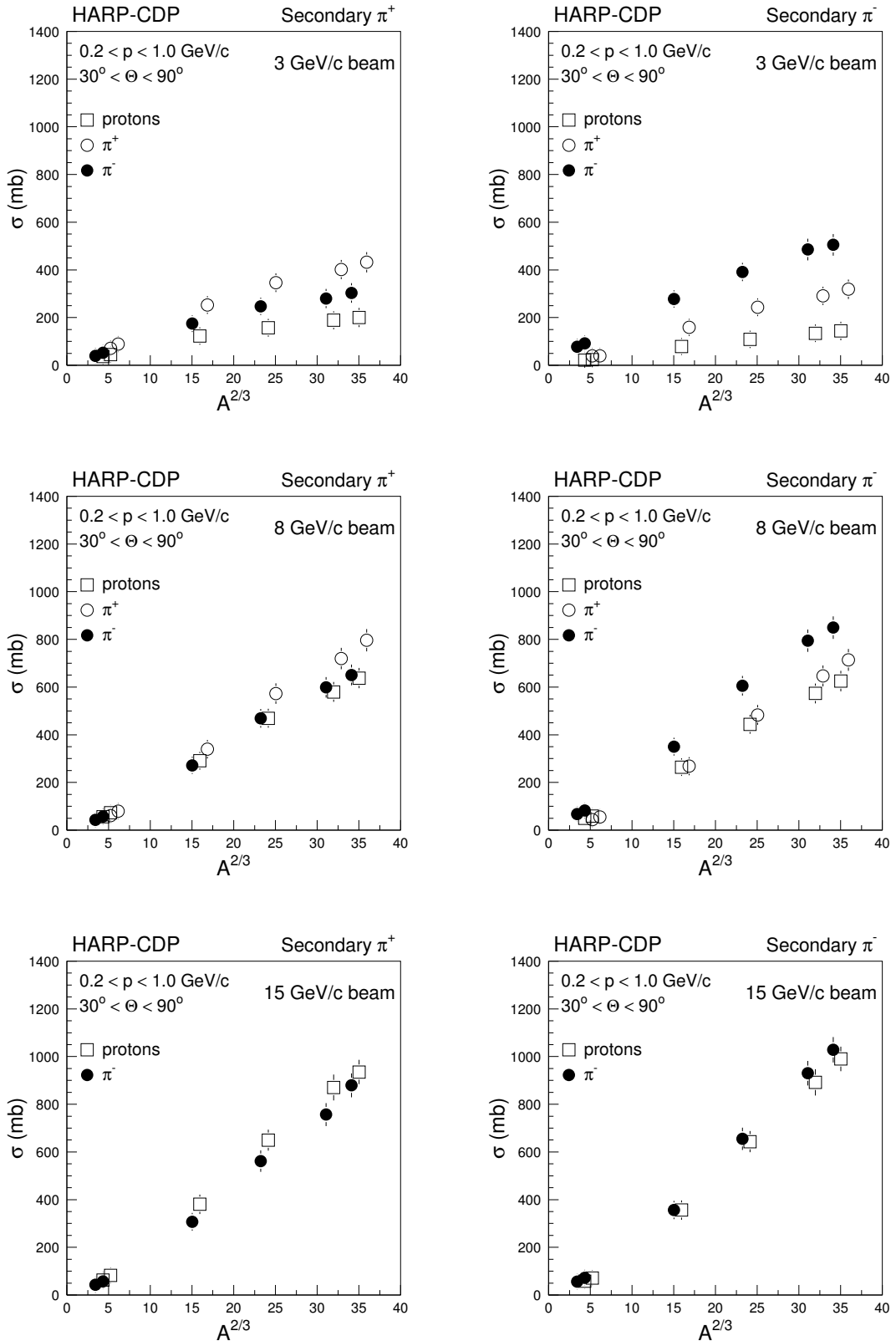


Fig. 9: Inclusive cross-sections of  $\pi^+$  and  $\pi^-$  production by protons (open squares),  $\pi^+$ 's (open circles), and  $\pi^-$ 's (black circles), as a function of  $A^{2/3}$  for, from left to right, beryllium, carbon, copper, tin, tantalum, and lead nuclei; the cross-sections are integrated over the momentum range  $0.2 < p < 1.0 \text{ GeV}/c$  and the polar-angle range  $30^\circ < \theta < 90^\circ$ ; the shown errors are total errors and often smaller than the symbol size.

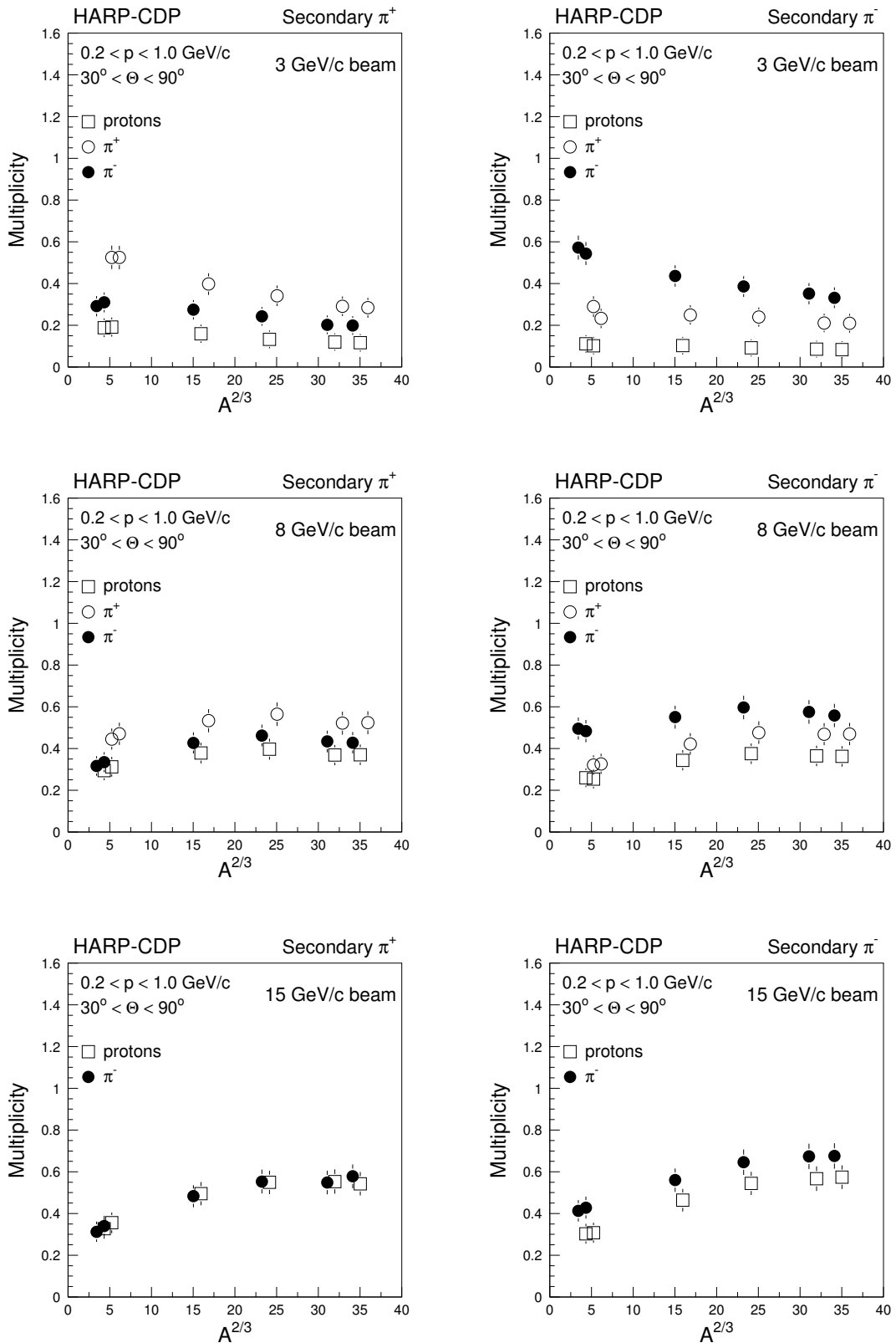


Fig. 10: Forward multiplicity of  $\pi^+$ 's and  $\pi^-$ 's produced by protons (open squares),  $\pi^+$ 's (open circles), and  $\pi^-$ 's (black circles), as a function of  $A^{2/3}$  for, from left to right, beryllium, carbon, copper, tin, tantalum, and lead nuclei; the forward multiplicity refers to the momentum range  $0.2 < p < 1.0 \text{ GeV}/c$  and the polar-angle range  $30^\circ < \theta < 90^\circ$  of secondary pions.

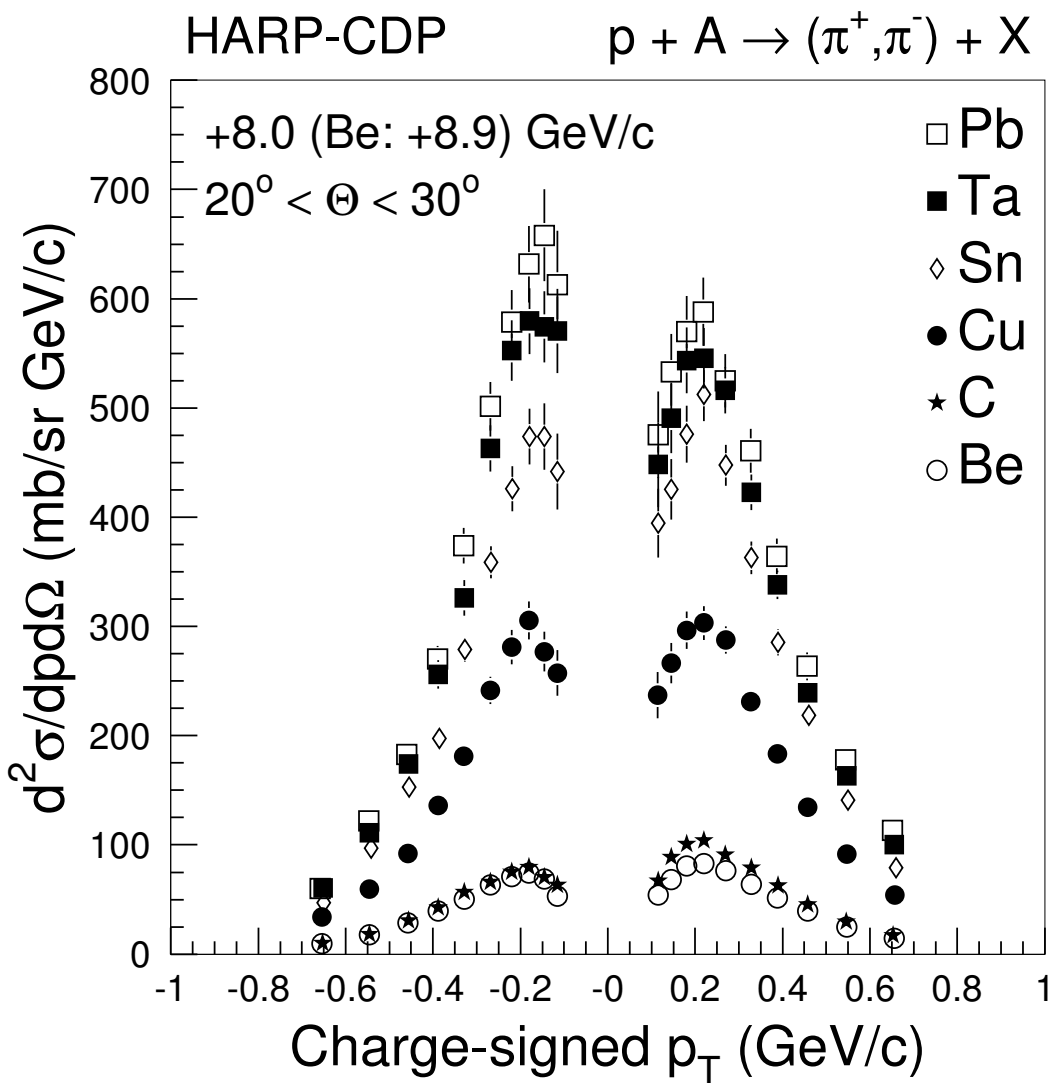


Fig. 11: Comparison of inclusive pion production cross-sections in the forward region between beryllium, carbon, copper, tin, tantalum, and lead target nuclei, as a function of the pion momentum.

## 7 DEUTERON PRODUCTION

Besides pions and protons, also deuterons are produced in sizeable quantities on tin nuclei. Up to momenta of about  $1 \text{ GeV}/c$ , deuterons are easily separated from protons by  $dE/dx$ .

Table 2 gives the deuteron-to-proton production ratio as a function of the momentum at the vertex, for  $8 \text{ GeV}/c$  beam protons,  $\pi^+$ 's, and  $\pi^-$ 's<sup>2)</sup>. Cross-section ratios are not given if the data are scarce and the statistical error becomes comparable with the ratio itself—which is the case for deuterons at the high-momentum end of the spectrum.

The measured deuteron-to-proton production ratios are illustrated in Fig. 12, and compared with the predictions of Geant4's FRITIOF model. FRITIOF's predictions are shown for  $\pi^+$  beam particles<sup>3)</sup>. FRITIOF's estimate of deuteron production falls short of the data.

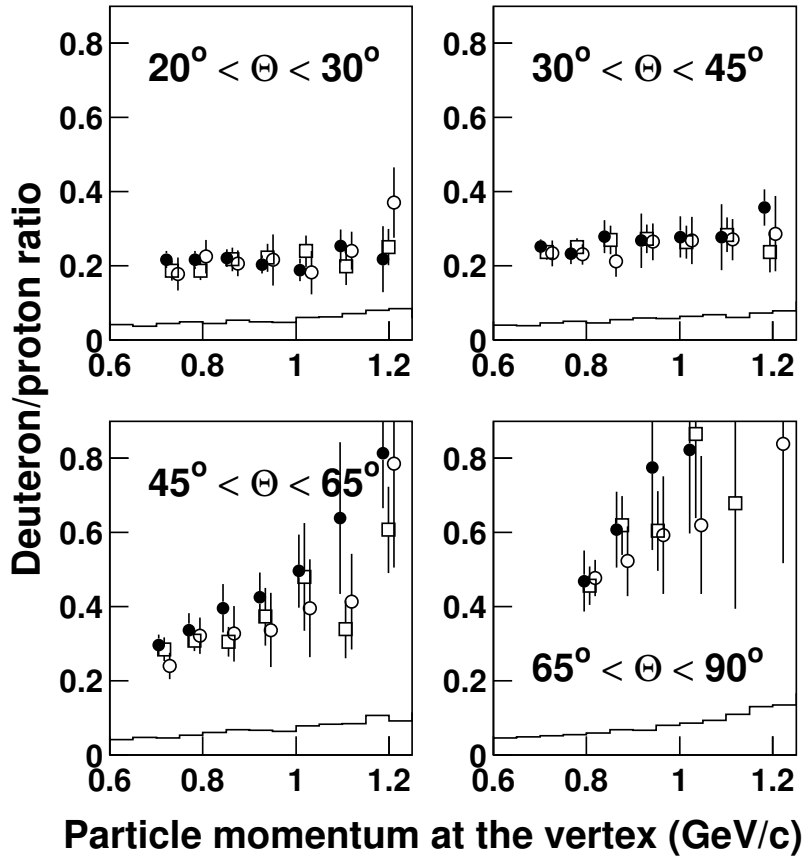


Fig. 12: Deuteron-to-proton production ratios for  $8 \text{ GeV}/c$  beam particles on tin nuclei, as a function of the momentum at the vertex, for four polar-angle regions; open squares denote beam protons, open circles beam  $\pi^+$ 's, and full circles beam  $\pi^-$ 's; the full lines denotes predictions of Geant4's FRITIOF model for  $\pi^+$  beam particles.

In Fig. 13 we show, for the polar-angle region  $30^\circ < \theta < 45^\circ$ , how the deuteron-to-proton

---

<sup>2)</sup>We observe no appreciable dependence of the deuteron-to-proton production ratio on beam momentum.

<sup>3)</sup>There is virtually no difference between its predictions for incoming protons,  $\pi^+$ 's and  $\pi^-$ 's.

ratio varies with the mass of the target nucleus. The ratios are for 8  $\text{GeV}/c$  beam protons on beryllium, carbon, copper, tin, tantalum and lead nuclei.

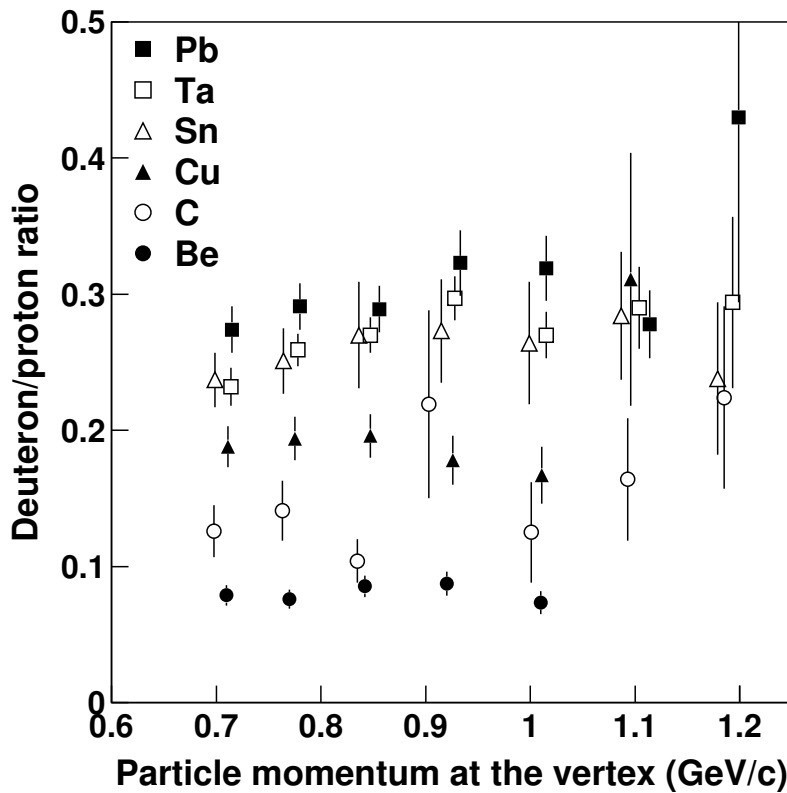


Fig. 13: Deuteron-to-proton production ratios for 8  $\text{GeV}/c$  beam protons on beryllium, carbon, copper, tin, tantalum and lead nuclei, as a function of the momentum at the vertex, for the polar-angle region  $30^\circ < \theta < 45^\circ$ .

Table 2: Ratio  $d/p$  of deuterons to protons produced by beam protons,  $\pi^+$ 's and  $\pi^-$ 's of 8 GeV/c momentum, as a function of the particle momentum  $p$  [GeV/c] at the vertex, for different bins of polar angle  $\theta$ .

$p$	Beam p d/p	Beam $\pi^+$ d/p	Beam $\pi^-$ d/p
$\theta = 20^\circ - 30^\circ$			
0.734	$0.187 \pm 0.027$	$0.178 \pm 0.044$	$0.217 \pm 0.023$
0.795	$0.187 \pm 0.025$	$0.225 \pm 0.045$	$0.216 \pm 0.024$
0.863	$0.218 \pm 0.032$	$0.207 \pm 0.035$	$0.221 \pm 0.024$
0.939	$0.222 \pm 0.038$	$0.216 \pm 0.069$	$0.204 \pm 0.024$
1.021	$0.240 \pm 0.042$	$0.182 \pm 0.058$	$0.189 \pm 0.030$
1.108	$0.199 \pm 0.051$	$0.241 \pm 0.051$	$0.254 \pm 0.044$
1.199	$0.251 \pm 0.049$	$0.371 \pm 0.095$	$0.218 \pm 0.089$
$\theta = 30^\circ - 45^\circ$			
0.714	$0.237 \pm 0.020$	$0.234 \pm 0.035$	$0.252 \pm 0.020$
0.779	$0.251 \pm 0.024$	$0.231 \pm 0.027$	$0.233 \pm 0.028$
0.851	$0.270 \pm 0.039$	$0.212 \pm 0.041$	$0.279 \pm 0.045$
0.930	$0.273 \pm 0.038$	$0.265 \pm 0.050$	$0.268 \pm 0.073$
1.014	$0.264 \pm 0.045$	$0.269 \pm 0.064$	$0.278 \pm 0.056$
1.102	$0.284 \pm 0.047$	$0.271 \pm 0.056$	$0.278 \pm 0.089$
1.194	$0.238 \pm 0.056$	$0.287 \pm 0.102$	$0.358 \pm 0.049$
$\theta = 45^\circ - 65^\circ$			
0.717	$0.285 \pm 0.032$	$0.240 \pm 0.035$	$0.297 \pm 0.027$
0.782	$0.308 \pm 0.028$	$0.321 \pm 0.049$	$0.337 \pm 0.045$
0.855	$0.306 \pm 0.040$	$0.327 \pm 0.075$	$0.396 \pm 0.065$
0.934	$0.373 \pm 0.078$	$0.337 \pm 0.100$	$0.425 \pm 0.067$
1.018	$0.480 \pm 0.145$	$0.396 \pm 0.132$	$0.496 \pm 0.099$
1.107	$0.339 \pm 0.078$	$0.414 \pm 0.129$	$0.639 \pm 0.204$
1.199	$0.607 \pm 0.117$	$0.786 \pm 0.281$	$0.813 \pm 0.148$
$\theta = 65^\circ - 90^\circ$			
0.807	$0.456 \pm 0.052$	$0.477 \pm 0.049$	$0.469 \pm 0.082$
0.876	$0.619 \pm 0.079$	$0.523 \pm 0.094$	$0.608 \pm 0.102$
0.953	$0.604 \pm 0.107$	$0.593 \pm 0.158$	$0.775 \pm 0.222$
1.034	$0.866 \pm 0.227$	$0.620 \pm 0.186$	$0.823 \pm 0.225$
1.120	$0.679 \pm 0.285$	$1.019 \pm 0.340$	$1.152 \pm 0.436$
1.210	$1.006 \pm 0.354$	$0.839 \pm 0.321$	
$\theta = 90^\circ - 125^\circ$			
0.874	$0.749 \pm 0.113$	$0.749 \pm 0.152$	
0.950	$0.931 \pm 0.147$	$0.790 \pm 0.188$	$1.016 \pm 0.176$
1.032	$0.941 \pm 0.261$	$1.514 \pm 0.634$	$1.038 \pm 0.252$

## 8 SUMMARY

From the analysis of data from the HARP large-angle spectrometer (polar angle  $\theta$  in the range  $20^\circ < \theta < 125^\circ$ ), double-differential cross-sections  $d^2\sigma/dpd\Omega$  of the production of secondary protons,  $\pi^+$ 's, and  $\pi^-$ 's, and of deuterons, have been obtained. The incoming beam particles were protons and pions with momenta from  $\pm 3$  to  $\pm 15$  GeV/c, impinging on a 5%  $\lambda_{\text{int}}$  thick stationary tin target.

In the same way as for the other target nuclei which we have analyzed, our cross-sections for  $\pi^+$  and  $\pi^-$  production disagree with results of the HARP Collaboration that were obtained from the same raw data.

We have compared the inclusive tin  $\pi^+$  and  $\pi^-$  production cross-sections with those on beryllium, carbon, copper, tantalum, and lead and find an approximately linear dependence on the scaling variable  $A^{2/3}$ .

We also observe a sizeable production of deuterons off tin nuclei that we compared to the deuteron production on beryllium, carbon, copper, tantalum, and lead.

## ACKNOWLEDGEMENTS

We are greatly indebted to many technical collaborators whose diligent and hard work made the HARP detector a well-functioning instrument. We thank all HARP colleagues who devoted time and effort to the design and construction of the detector, to data taking, and to setting up the computing and software infrastructure. We express our sincere gratitude to HARP's funding agencies for their support.

## REFERENCES

- [1] M. Apollonio *et al.*, J. Instrum. **4** (2009) P07001
- [2] A. Bolshakova *et al.*, Eur. Phys. J. **C62** (2009) 293 (CERN-PH-EP-2008-022, arXiv:0901.3648)
- [3] A. Bolshakova *et al.*, Eur. Phys. J. **C62** (2009) 697 (CERN-PH-EP-2008-025, arXiv:0903.2145)
- [4] A. Bolshakova *et al.*, Eur. Phys. J. **C63** (2009) 549 (CERN-PH-EP-2009-009, arXiv:0906.0471)
- [5] A. Bolshakova *et al.*, Eur. Phys. J. **C64** (2009) 181 (CERN-PH-EP-2009-012, arXiv:0906.3653)
- [6] A. Bolshakova *et al.*, Eur. Phys. J. **C66** (2010) 57 (CERN-PH-EP-2009-025, arXiv:0912.0378v1)
- [7] A. Bolshakova *et al.*, Eur. Phys. J. **C70** (2010) 573 (CERN-PH-EP-2010-026, arXiv:1007.5482)
- [8] V. Ammosov *et al.*, Nucl. Instrum. Methods Phys. Res. **A588** (2008) 294
- [9] V. Ammosov *et al.*, Nucl. Instrum. Methods Phys. Res. **A578** (2007) 119
- [10] S. Agostinelli *et al.*, Nucl. Instrum. Methods Phys. Res. **A506** (2003) 250; J. Allison *et al.*, IEEE Trans. Nucl. Sci. **53** (2006) 270
- [11] A. Bolshakova *et al.*, Eur. Phys. J. **C56** (2008) 323
- [12] A. Bolshakova *et al.*, Tables of cross-sections of large-angle hadron production in proton– and pion–nucleus interactions VII: tin nuclei and beam momenta from  $\pm 3$  GeV/c to  $\pm 15$  GeV/c, CERN–HARP–CDP–2011–001
- [13] <http://pdg.lbl.gov/2010/AtomicNuclearProperties>

- [14] M.G. Catanesi *et al.*, Phys. Rev. **C77** (2008) 055207 (arXiv:0805.2871)
- [15] M. Apollonio *et al.*, Phys. Rev. **C80** (2009) 065207 (arXiv:0907.1428)
- [16] V. Ammosov *et al.*, J. Instrum. **3** (2008) P01002
- [17] V. Ammosov *et al.*, Eur. Phys. J. **C54** (2008) 169
- [18] V. Ammosov *et al.*, CERN–HARP–CDP–2006–003
- [19] V. Ammosov *et al.*, CERN–HARP–CDP–2006–007
- [20] V. Ammosov *et al.*, CERN–HARP–CDP–2007–001

## APPENDIX A: CROSS-SECTION TABLES

Table A.1: Double-differential inclusive cross-section  $d^2\sigma/dpd\Omega$  [mb/(GeV/c sr)] of the production of protons in  $p + \text{Sn} \rightarrow p + X$  interactions with  $+3.0 \text{ GeV}/c$  beam momentum; the first error is statistical, the second systematic;  $p_T$  in  $\text{GeV}/c$ , polar angle  $\theta$  in degrees.

$p_T$	20 < $\theta$ < 30						30 < $\theta$ < 40					
	$\langle p_T \rangle$	$\langle \theta \rangle$	$d^2\sigma/dpd\Omega$				$\langle p_T \rangle$	$\langle \theta \rangle$	$d^2\sigma/dpd\Omega$			
			735.68	$\pm$	26.83	$\pm$	36.52	749.00	$\pm$	21.47	$\pm$	30.62
0.20–0.24	0.220	25.0	735.68	$\pm$	26.83	$\pm$	36.52	0.271	34.8	749.00	$\pm$	21.47
0.24–0.30	0.269	25.3	620.77	$\pm$	19.94	$\pm$	29.43	0.328	35.0	604.52	$\pm$	19.31
0.30–0.36	0.329	25.2	507.15	$\pm$	18.79	$\pm$	25.98	0.389	35.2	472.57	$\pm$	17.83
0.36–0.42	0.389	25.3	395.30	$\pm$	16.73	$\pm$	20.32	0.457	35.2	365.53	$\pm$	14.03
0.42–0.50	0.458	25.2	306.88	$\pm$	12.32	$\pm$	14.44	0.546	35.1	265.93	$\pm$	10.69
0.50–0.60	0.547	25.2	244.05	$\pm$	10.02	$\pm$	11.15	0.655	35.3	163.99	$\pm$	7.76
0.60–0.72	0.654	25.1	157.24	$\pm$	7.20	$\pm$	7.43	0.802	35.0	94.16	$\pm$	4.93
0.72–0.90												
	40 < $\theta$ < 50						50 < $\theta$ < 60					
$p_T$	$\langle p_T \rangle$	$\langle \theta \rangle$	$d^2\sigma/dpd\Omega$				$\langle p_T \rangle$	$\langle \theta \rangle$	$d^2\sigma/dpd\Omega$			
0.30–0.36	0.329	45.1	746.01	$\pm$	23.21	$\pm$	22.98	0.389	55.1	604.12	$\pm$	18.50
0.36–0.42	0.389	45.1	578.63	$\pm$	18.56	$\pm$	17.43	0.458	55.0	474.09	$\pm$	14.68
0.42–0.50	0.459	45.0	431.66	$\pm$	14.58	$\pm$	17.05	0.546	55.1	323.00	$\pm$	11.48
0.50–0.60	0.546	45.0	289.30	$\pm$	11.23	$\pm$	17.90	0.653	55.1	197.42	$\pm$	8.89
0.60–0.72	0.656	45.0	185.32	$\pm$	8.44	$\pm$	13.52	0.797	54.8	88.39	$\pm$	5.04
0.72–0.90	0.798	45.1	95.36	$\pm$	5.08	$\pm$	9.06					
0.90–1.25	1.029	45.2	23.01	$\pm$	1.71	$\pm$	3.16					
	60 < $\theta$ < 75						75 < $\theta$ < 90					
$p_T$	$\langle p_T \rangle$	$\langle \theta \rangle$	$d^2\sigma/dpd\Omega$				$\langle p_T \rangle$	$\langle \theta \rangle$	$d^2\sigma/dpd\Omega$			
0.50–0.60	0.552	67.4	318.74	$\pm$	8.63	$\pm$	12.06	0.552	81.7	243.26	$\pm$	7.30
0.60–0.72	0.663	66.9	163.22	$\pm$	6.25	$\pm$	11.93	0.660	81.8	126.18	$\pm$	5.21
	90 < $\theta$ < 105						105 < $\theta$ < 125					
$p_T$	$\langle p_T \rangle$	$\langle \theta \rangle$	$d^2\sigma/dpd\Omega$				$\langle p_T \rangle$	$\langle \theta \rangle$	$d^2\sigma/dpd\Omega$			
0.42–0.50							0.461	113.1	129.94	$\pm$	4.98	$\pm$
0.50–0.60	0.548	96.9	139.52	$\pm$	5.56	$\pm$	8.82	0.548	113.0	54.39	$\pm$	3.23
0.60–0.72	0.660	96.6	61.72	$\pm$	3.79	$\pm$	5.82					

Table A.2: Double-differential inclusive cross-section  $d^2\sigma/dpd\Omega$  [mb/(GeV/c sr)] of the production of  $\pi^+$ 's in  $p + \text{Sn} \rightarrow \pi^+ + X$  interactions with  $+3.0$  GeV/c beam momentum; the first error is statistical, the second systematic;  $p_T$  in GeV/c, polar angle  $\theta$  in degrees.

$p_T$	20 < $\theta$ < 30						30 < $\theta$ < 40					
	$\langle p_T \rangle$	$\langle \theta \rangle$	$d^2\sigma/dpd\Omega$				$\langle p_T \rangle$	$\langle \theta \rangle$	$d^2\sigma/dpd\Omega$			
			129.48	$\pm$ 15.14	$\pm$ 13.38	118.33	$\pm$ 13.81	$\pm$ 9.51	118.33	$\pm$ 13.81	$\pm$ 9.51	
0.10–0.13	0.116	24.8	129.48	$\pm$ 15.14	$\pm$ 13.38	0.115	34.9	118.33	$\pm$ 13.81	$\pm$ 9.51		
0.13–0.16	0.146	25.1	149.54	$\pm$ 14.53	$\pm$ 12.17	0.147	34.9	143.19	$\pm$ 14.10	$\pm$ 10.19		
0.16–0.20	0.181	25.1	178.53	$\pm$ 13.43	$\pm$ 10.67	0.181	34.7	146.00	$\pm$ 11.78	$\pm$ 9.10		
0.20–0.24	0.221	25.0	149.32	$\pm$ 11.94	$\pm$ 7.28	0.219	35.2	121.28	$\pm$ 10.45	$\pm$ 6.37		
0.24–0.30	0.268	24.8	125.69	$\pm$ 8.91	$\pm$ 5.44	0.269	34.6	109.28	$\pm$ 8.18	$\pm$ 4.81		
0.30–0.36	0.329	25.2	87.08	$\pm$ 7.33	$\pm$ 3.78	0.329	34.9	85.64	$\pm$ 7.28	$\pm$ 3.57		
0.36–0.42	0.388	25.1	48.25	$\pm$ 5.29	$\pm$ 2.48	0.387	35.1	66.97	$\pm$ 6.36	$\pm$ 3.03		
0.42–0.50	0.458	24.8	37.42	$\pm$ 3.87	$\pm$ 2.33	0.457	34.6	37.19	$\pm$ 3.94	$\pm$ 1.87		
0.50–0.60	0.551	25.1	15.43	$\pm$ 2.03	$\pm$ 1.34	0.543	35.8	23.50	$\pm$ 2.76	$\pm$ 1.48		
0.60–0.72	0.652	25.2	12.42	$\pm$ 1.56	$\pm$ 1.39	0.649	35.0	13.64	$\pm$ 1.79	$\pm$ 1.12		
0.72–0.90						0.807	34.0	7.53	$\pm$ 0.97	$\pm$ 0.96		
$p_T$	40 < $\theta$ < 50						50 < $\theta$ < 60					
	$\langle p_T \rangle$	$\langle \theta \rangle$	$d^2\sigma/dpd\Omega$				$\langle p_T \rangle$	$\langle \theta \rangle$	$d^2\sigma/dpd\Omega$			
			112.49	$\pm$ 13.27	$\pm$ 8.86	0.146	54.9	124.78	$\pm$ 13.32	$\pm$ 8.15		
0.10–0.13	0.116	45.3	123.68	$\pm$ 12.67	$\pm$ 7.71	0.179	54.8	127.61	$\pm$ 10.67	$\pm$ 6.66		
0.13–0.16	0.146	44.8	134.68	$\pm$ 11.40	$\pm$ 7.50	0.216	54.9	88.90	$\pm$ 9.06	$\pm$ 4.33		
0.16–0.20	0.181	44.9	109.58	$\pm$ 10.03	$\pm$ 5.84	0.268	54.6	76.63	$\pm$ 6.77	$\pm$ 3.44		
0.20–0.24	0.220	44.8	107.18	$\pm$ 8.15	$\pm$ 4.79	0.331	54.9	59.55	$\pm$ 5.92	$\pm$ 2.61		
0.24–0.30	0.269	44.9	67.06	$\pm$ 6.35	$\pm$ 2.93	0.390	54.5	45.96	$\pm$ 5.39	$\pm$ 2.20		
0.30–0.36	0.327	45.1	54.01	$\pm$ 5.70	$\pm$ 2.36	0.455	55.2	29.92	$\pm$ 3.84	$\pm$ 1.64		
0.36–0.42	0.388	44.5	44.92	$\pm$ 4.56	$\pm$ 2.26	0.547	54.9	19.43	$\pm$ 2.67	$\pm$ 1.28		
0.42–0.50	0.456	44.7	27.23	$\pm$ 3.06	$\pm$ 1.61	0.668	55.2	7.89	$\pm$ 1.44	$\pm$ 0.67		
0.50–0.60	0.543	45.0	11.72	$\pm$ 1.77	$\pm$ 0.96	0.788	54.6	6.08	$\pm$ 1.07	$\pm$ 0.69		
0.60–0.72	0.663	45.2	7.22	$\pm$ 1.07	$\pm$ 0.81	1.051	54.5	1.41	$\pm$ 0.25	$\pm$ 0.23		
0.72–0.90	0.798	45.0										
0.90–1.25												
$p_T$	60 < $\theta$ < 75						75 < $\theta$ < 90					
	$\langle p_T \rangle$	$\langle \theta \rangle$	$d^2\sigma/dpd\Omega$				$\langle p_T \rangle$	$\langle \theta \rangle$	$d^2\sigma/dpd\Omega$			
			118.21	$\pm$ 11.26	$\pm$ 7.97	0.146	82.2	91.54	$\pm$ 10.61	$\pm$ 6.55		
0.13–0.16	0.145	67.3	102.42	$\pm$ 7.89	$\pm$ 5.06	0.181	82.3	97.17	$\pm$ 8.07	$\pm$ 5.03		
0.16–0.20	0.181	67.6	84.75	$\pm$ 7.14	$\pm$ 3.75	0.221	82.9	68.37	$\pm$ 6.57	$\pm$ 3.05		
0.20–0.24	0.221	67.0	63.90	$\pm$ 5.15	$\pm$ 2.74	0.268	82.3	51.63	$\pm$ 4.75	$\pm$ 2.28		
0.24–0.30	0.268	67.6	47.69	$\pm$ 4.43	$\pm$ 2.11	0.327	81.1	36.50	$\pm$ 4.01	$\pm$ 2.01		
0.30–0.36	0.330	66.6	32.68	$\pm$ 3.78	$\pm$ 1.63	0.390	81.3	17.80	$\pm$ 2.74	$\pm$ 1.19		
0.36–0.42	0.391	67.0	27.22	$\pm$ 2.95	$\pm$ 1.55	0.458	81.8	10.88	$\pm$ 1.91	$\pm$ 0.84		
0.42–0.50	0.459	66.9	12.46	$\pm$ 1.77	$\pm$ 0.91	0.554	81.1	7.83	$\pm$ 1.37	$\pm$ 0.73		
0.50–0.60	0.554	66.6	6.87	$\pm$ 1.16	$\pm$ 0.65	0.659	81.6	5.14	$\pm$ 1.07	$\pm$ 0.62		
0.60–0.72	0.662	66.5	3.52	$\pm$ 0.64	$\pm$ 0.43	0.817	81.7	1.13	$\pm$ 0.35	$\pm$ 0.17		
0.72–0.90	0.792	66.9	0.61	$\pm$ 0.15	$\pm$ 0.12	1.087	80.6	0.13	$\pm$ 0.04	$\pm$ 0.03		
0.90–1.25	1.073	65.6										
$p_T$	90 < $\theta$ < 105						105 < $\theta$ < 125					
	$\langle p_T \rangle$	$\langle \theta \rangle$	$d^2\sigma/dpd\Omega$				$\langle p_T \rangle$	$\langle \theta \rangle$	$d^2\sigma/dpd\Omega$			
			99.68	$\pm$ 11.06	$\pm$ 7.55	0.146	114.6	108.04	$\pm$ 9.42	$\pm$ 6.65		
0.13–0.16	0.145	98.2	81.24	$\pm$ 7.64	$\pm$ 4.36	0.180	113.8	65.54	$\pm$ 5.74	$\pm$ 2.71		
0.16–0.20	0.178	96.9	74.76	$\pm$ 6.91	$\pm$ 3.38	0.218	113.9	45.54	$\pm$ 4.60	$\pm$ 1.99		
0.20–0.24	0.219	97.2	33.19	$\pm$ 3.81	$\pm$ 1.54	0.269	113.0	20.57	$\pm$ 2.54	$\pm$ 1.20		
0.24–0.30	0.266	97.4	17.89	$\pm$ 2.69	$\pm$ 1.18	0.326	113.7	11.60	$\pm$ 1.92	$\pm$ 1.02		
0.30–0.36	0.329	97.2	12.98	$\pm$ 2.35	$\pm$ 1.17	0.383	112.8	4.55	$\pm$ 1.30	$\pm$ 0.60		
0.36–0.42	0.387	96.1	7.60	$\pm$ 1.58	$\pm$ 0.83	0.471	113.0	2.15	$\pm$ 0.71	$\pm$ 0.38		
0.42–0.50	0.461	96.3	3.97	$\pm$ 1.02	$\pm$ 0.53	0.562	108.4	1.39	$\pm$ 0.52	$\pm$ 0.32		
0.50–0.60	0.551	97.1	1.32	$\pm$ 0.50	$\pm$ 0.22	0.664	119.6	0.22	$\pm$ 0.17	$\pm$ 0.08		
0.60–0.72	0.671	94.8	0.43	$\pm$ 0.20	$\pm$ 0.10							
0.72–0.90	0.843	94.1										

Table A.3: Double-differential inclusive cross-section  $d^2\sigma/dpd\Omega$  [mb/(GeV/c sr)] of the production of  $\pi^-$ 's in  $p + \text{Sn} \rightarrow \pi^- + \text{X}$  interactions with  $+3.0 \text{ GeV}/c$  beam momentum; the first error is statistical, the second systematic;  $p_T$  in  $\text{GeV}/c$ , polar angle  $\theta$  in degrees.

$p_T$	20 < $\theta$ < 30				30 < $\theta$ < 40					
	$\langle p_T \rangle$	$\langle \theta \rangle$	$d^2\sigma/dpd\Omega$		$\langle p_T \rangle$	$\langle \theta \rangle$	$d^2\sigma/dpd\Omega$			
0.10–0.13	0.115	25.0	120.38	$\pm$ 13.59	9.41	0.115	35.1	107.57	$\pm$ 12.88	8.45
0.13–0.16	0.143	24.9	112.38	$\pm$ 12.76	8.03	0.144	35.7	101.89	$\pm$ 11.34	7.08
0.16–0.20	0.179	25.1	111.42	$\pm$ 10.38	6.34	0.181	34.7	102.00	$\pm$ 9.52	5.91
0.20–0.24	0.218	25.7	103.89	$\pm$ 10.00	5.45	0.218	34.8	91.80	$\pm$ 9.18	4.77
0.24–0.30	0.271	25.3	64.11	$\pm$ 6.18	2.75	0.268	35.0	79.61	$\pm$ 6.92	3.38
0.30–0.36	0.329	24.7	53.06	$\pm$ 5.59	2.40	0.326	35.4	52.63	$\pm$ 5.61	2.19
0.36–0.42	0.386	25.8	27.35	$\pm$ 4.07	1.44	0.389	34.6	44.90	$\pm$ 5.19	2.19
0.42–0.50	0.449	24.6	14.00	$\pm$ 2.48	0.88	0.450	35.3	18.38	$\pm$ 2.81	1.01
0.50–0.60	0.535	25.5	4.35	$\pm$ 1.26	0.38	0.533	34.1	8.03	$\pm$ 1.64	0.59
0.60–0.72	0.659	25.4	1.67	$\pm$ 0.69	0.23	0.638	34.8	3.52	$\pm$ 1.02	0.38
0.72–0.90						0.771	35.3	1.76	$\pm$ 0.66	0.32
$p_T$	40 < $\theta$ < 50				50 < $\theta$ < 60					
	$\langle p_T \rangle$	$\langle \theta \rangle$	$d^2\sigma/dpd\Omega$		$\langle p_T \rangle$	$\langle \theta \rangle$	$d^2\sigma/dpd\Omega$			
0.10–0.13	0.115	45.0	114.52	$\pm$ 13.34	9.01	0.145	55.3	121.76	$\pm$ 12.96	8.06
0.13–0.16	0.144	45.7	82.35	$\pm$ 9.93	5.55	0.179	54.8	103.03	$\pm$ 9.65	5.79
0.16–0.20	0.179	44.5	85.30	$\pm$ 8.46	5.01	0.221	55.1	77.80	$\pm$ 8.46	4.47
0.20–0.24	0.221	44.7	92.37	$\pm$ 8.82	4.93	0.269	54.4	71.46	$\pm$ 6.53	3.34
0.24–0.30	0.269	45.0	73.20	$\pm$ 6.42	3.10	0.325	55.1	44.37	$\pm$ 5.04	1.94
0.30–0.36	0.327	45.2	59.85	$\pm$ 6.00	2.66	0.389	55.2	28.95	$\pm$ 4.19	1.46
0.36–0.42	0.393	45.1	29.94	$\pm$ 4.14	1.39	0.456	55.1	18.92	$\pm$ 2.92	1.07
0.42–0.50	0.455	44.3	20.37	$\pm$ 2.98	1.10	0.533	54.0	8.92	$\pm$ 1.72	0.67
0.50–0.60	0.551	45.3	11.88	$\pm$ 2.04	0.85	0.644	53.7	3.74	$\pm$ 1.08	0.44
0.60–0.72	0.641	45.2	2.20	$\pm$ 0.78	0.24	0.801	54.8	1.17	$\pm$ 0.52	0.24
$p_T$	60 < $\theta$ < 75				75 < $\theta$ < 90					
	$\langle p_T \rangle$	$\langle \theta \rangle$	$d^2\sigma/dpd\Omega$		$\langle p_T \rangle$	$\langle \theta \rangle$	$d^2\sigma/dpd\Omega$			
0.13–0.16	0.143	67.5	123.14	$\pm$ 11.17	7.47	0.145	82.5	121.80	$\pm$ 12.17	7.92
0.16–0.20	0.179	67.6	87.38	$\pm$ 7.23	4.30	0.178	82.2	101.65	$\pm$ 8.23	4.93
0.20–0.24	0.218	67.2	68.22	$\pm$ 6.20	3.18	0.218	82.4	61.02	$\pm$ 6.23	3.04
0.24–0.30	0.267	67.0	53.55	$\pm$ 4.56	2.28	0.265	81.9	36.36	$\pm$ 3.79	1.63
0.30–0.36	0.324	67.1	34.67	$\pm$ 3.74	1.51	0.326	81.3	24.43	$\pm$ 3.13	1.24
0.36–0.42	0.380	66.6	21.37	$\pm$ 2.91	1.04	0.386	80.9	15.31	$\pm$ 2.53	0.97
0.42–0.50	0.452	65.9	14.38	$\pm$ 2.06	0.83	0.460	81.5	9.33	$\pm$ 1.65	0.69
0.50–0.60	0.536	66.2	5.47	$\pm$ 1.16	0.44	0.541	84.6	2.33	$\pm$ 0.74	0.24
0.60–0.72	0.627	66.2	1.47	$\pm$ 0.56	0.18	0.621	80.0	1.60	$\pm$ 0.57	0.29
0.72–0.90	0.823	66.6	0.69	$\pm$ 0.35	0.19	0.741	85.0	0.90	$\pm$ 0.48	0.44
$p_T$	90 < $\theta$ < 105				105 < $\theta$ < 125					
	$\langle p_T \rangle$	$\langle \theta \rangle$	$d^2\sigma/dpd\Omega$		$\langle p_T \rangle$	$\langle \theta \rangle$	$d^2\sigma/dpd\Omega$			
0.13–0.16	0.145	97.3	89.43	$\pm$ 10.15	5.86	0.145	113.9	99.93	$\pm$ 9.10	6.09
0.16–0.20	0.178	97.3	86.11	$\pm$ 7.75	4.51	0.177	114.2	60.54	$\pm$ 5.43	2.67
0.20–0.24	0.220	97.1	52.89	$\pm$ 5.76	2.60	0.217	113.5	28.17	$\pm$ 3.53	1.44
0.24–0.30	0.267	97.0	23.20	$\pm$ 3.05	1.15	0.269	113.5	14.25	$\pm$ 2.06	0.87
0.30–0.36	0.320	96.9	15.73	$\pm$ 2.63	1.07	0.330	114.8	6.55	$\pm$ 1.43	0.54
0.36–0.42	0.386	98.5	10.36	$\pm$ 2.07	0.86	0.382	111.4	3.25	$\pm$ 0.98	0.36
0.42–0.50	0.447	99.1	4.92	$\pm$ 1.23	0.51	0.464	113.7	2.14	$\pm$ 0.68	0.32
0.50–0.60	0.540	93.8	2.64	$\pm$ 0.80	0.40	0.555	114.5	0.64	$\pm$ 0.32	0.15
0.60–0.72	0.649	98.4	0.32	$\pm$ 0.22	0.09					

Table A.4: Double-differential inclusive cross-section  $d^2\sigma/dpd\Omega$  [mb/(GeV/c sr)] of the production of protons in  $\pi^+ + \text{Sn} \rightarrow p + X$  interactions with  $+3.0 \text{ GeV}/c$  beam momentum; the first error is statistical, the second systematic;  $p_T$  in  $\text{GeV}/c$ , polar angle  $\theta$  in degrees.

$p_T$	20 < $\theta$ < 30			30 < $\theta$ < 40		
	$\langle p_T \rangle$	$\langle \theta \rangle$	$d^2\sigma/dpd\Omega$	$\langle p_T \rangle$	$\langle \theta \rangle$	$d^2\sigma/dpd\Omega$
0.20–0.24	0.221	25.1	855.97 $\pm$ 21.71 $\pm$ 42.97	0.271	34.9	805.09 $\pm$ 16.50 $\pm$ 33.16
0.24–0.30	0.270	25.3	621.57 $\pm$ 14.74 $\pm$ 30.06	0.329	35.3	644.43 $\pm$ 14.81 $\pm$ 24.85
0.30–0.36	0.328	25.3	444.31 $\pm$ 13.10 $\pm$ 24.39	0.389	35.1	494.75 $\pm$ 13.53 $\pm$ 24.03
0.36–0.42	0.389	25.3	350.22 $\pm$ 11.73 $\pm$ 20.28	0.458	35.2	348.50 $\pm$ 10.18 $\pm$ 20.48
0.42–0.50	0.457	25.3	243.03 $\pm$ 8.19 $\pm$ 13.78	0.546	35.1	235.50 $\pm$ 7.48 $\pm$ 14.92
0.50–0.60	0.547	25.3	179.90 $\pm$ 6.39 $\pm$ 10.14	0.653	35.3	145.67 $\pm$ 5.43 $\pm$ 11.14
0.60–0.72	0.654	25.5	111.46 $\pm$ 4.43 $\pm$ 6.00	0.796	35.2	72.12 $\pm$ 3.18 $\pm$ 6.38
0.72–0.90						
40 < $\theta$ < 50						
$p_T$	$\langle p_T \rangle$	$\langle \theta \rangle$	$d^2\sigma/dpd\Omega$	$\langle p_T \rangle$	$\langle \theta \rangle$	$d^2\sigma/dpd\Omega$
0.30–0.36	0.329	45.0	740.78 $\pm$ 15.26 $\pm$ 23.13	0.390	55.2	695.77 $\pm$ 14.75 $\pm$ 18.99
0.36–0.42	0.389	44.9	617.78 $\pm$ 14.18 $\pm$ 18.96	0.457	55.0	526.99 $\pm$ 11.46 $\pm$ 15.93
0.42–0.50	0.458	45.2	453.19 $\pm$ 11.09 $\pm$ 18.58	0.547	55.0	335.39 $\pm$ 8.67 $\pm$ 16.45
0.50–0.60	0.548	45.2	268.52 $\pm$ 8.06 $\pm$ 17.80	0.654	55.0	184.10 $\pm$ 6.41 $\pm$ 15.75
0.60–0.72	0.655	45.0	172.82 $\pm$ 6.08 $\pm$ 13.78	0.796	55.1	81.58 $\pm$ 3.65 $\pm$ 9.89
0.72–0.90	0.794	45.3	80.98 $\pm$ 3.50 $\pm$ 8.60			
60 < $\theta$ < 75						
$p_T$	$\langle p_T \rangle$	$\langle \theta \rangle$	$d^2\sigma/dpd\Omega$	$\langle p_T \rangle$	$\langle \theta \rangle$	$d^2\sigma/dpd\Omega$
0.50–0.60	0.551	67.2	344.19 $\pm$ 6.63 $\pm$ 13.14	0.551	82.1	297.74 $\pm$ 5.99 $\pm$ 13.93
0.60–0.72	0.663	67.2	166.16 $\pm$ 4.68 $\pm$ 12.44	0.660	81.8	154.55 $\pm$ 4.26 $\pm$ 10.59
90 < $\theta$ < 105						
$p_T$	$\langle p_T \rangle$	$\langle \theta \rangle$	$d^2\sigma/dpd\Omega$	$\langle p_T \rangle$	$\langle \theta \rangle$	$d^2\sigma/dpd\Omega$
0.42–0.50	0.551	97.3	206.92 $\pm$ 5.02 $\pm$ 13.04	0.461	113.8	196.05 $\pm$ 4.52 $\pm$ 10.95
0.50–0.60	0.551	97.3	93.08 $\pm$ 3.35 $\pm$ 8.13	0.549	113.2	92.21 $\pm$ 3.02 $\pm$ 8.18
0.60–0.72	0.664	97.1				
75 < $\theta$ < 90						
105 < $\theta$ < 125						
$p_T$	$\langle p_T \rangle$	$\langle \theta \rangle$	$d^2\sigma/dpd\Omega$	$\langle p_T \rangle$	$\langle \theta \rangle$	$d^2\sigma/dpd\Omega$

Table A.5: Double-differential inclusive cross-section  $d^2\sigma/dpd\Omega$  [mb/(GeV/c sr)] of the production of  $\pi^+$ 's in  $\pi^+ + \text{Sn} \rightarrow \pi^+ + \text{X}$  interactions with +3.0 GeV/c beam momentum; the first error is statistical, the second systematic;  $p_T$  in GeV/c, polar angle  $\theta$  in degrees.

$p_T$	20 < $\theta$ < 30						30 < $\theta$ < 40					
	$\langle p_T \rangle$	$\langle \theta \rangle$	$d^2\sigma/dpd\Omega$				$\langle p_T \rangle$	$\langle \theta \rangle$	$d^2\sigma/dpd\Omega$			
			$\langle p_T \rangle$	$\langle \theta \rangle$	$d^2\sigma/dpd\Omega$	$d^2\sigma/dpd\Omega$			$\langle p_T \rangle$	$\langle \theta \rangle$	$d^2\sigma/dpd\Omega$	$d^2\sigma/dpd\Omega$
0.10–0.13	0.115	24.9	194.99	$\pm$ 12.89	$\pm$ 15.71	0.115	35.1	185.30	$\pm$ 12.06	$\pm$ 13.71		
0.13–0.16	0.145	24.7	207.23	$\pm$ 12.35	$\pm$ 13.41	0.145	35.0	194.08	$\pm$ 11.83	$\pm$ 12.21		
0.16–0.20	0.180	24.8	276.44	$\pm$ 12.26	$\pm$ 14.71	0.180	34.8	195.26	$\pm$ 9.94	$\pm$ 10.49		
0.20–0.24	0.220	24.9	288.70	$\pm$ 12.31	$\pm$ 12.79	0.220	34.8	232.27	$\pm$ 10.61	$\pm$ 10.58		
0.24–0.30	0.270	25.0	253.95	$\pm$ 9.36	$\pm$ 9.56	0.269	34.9	216.72	$\pm$ 8.55	$\pm$ 8.13		
0.30–0.36	0.330	25.0	222.13	$\pm$ 8.62	$\pm$ 7.59	0.328	35.0	195.85	$\pm$ 8.11	$\pm$ 6.59		
0.36–0.42	0.390	24.9	179.97	$\pm$ 7.75	$\pm$ 6.74	0.390	35.0	169.11	$\pm$ 7.47	$\pm$ 5.69		
0.42–0.50	0.459	24.9	118.61	$\pm$ 5.28	$\pm$ 4.81	0.458	34.9	132.93	$\pm$ 5.64	$\pm$ 4.87		
0.50–0.60	0.547	24.7	80.38	$\pm$ 3.67	$\pm$ 4.35	0.547	34.9	85.48	$\pm$ 3.93	$\pm$ 4.13		
0.60–0.72	0.655	24.9	56.05	$\pm$ 2.80	$\pm$ 4.45	0.653	34.9	54.22	$\pm$ 2.72	$\pm$ 3.70		
0.72–0.90						0.794	34.9	30.10	$\pm$ 1.66	$\pm$ 3.44		
$p_T$	40 < $\theta$ < 50						50 < $\theta$ < 60					
	$\langle p_T \rangle$	$\langle \theta \rangle$	$d^2\sigma/dpd\Omega$				$\langle p_T \rangle$	$\langle \theta \rangle$	$d^2\sigma/dpd\Omega$			
			$\langle p_T \rangle$	$\langle \theta \rangle$	$d^2\sigma/dpd\Omega$	$d^2\sigma/dpd\Omega$			$\langle p_T \rangle$	$\langle \theta \rangle$	$d^2\sigma/dpd\Omega$	$d^2\sigma/dpd\Omega$
0.10–0.13	0.116	45.6	160.38	$\pm$ 11.47	$\pm$ 12.16	0.146	54.8	203.49	$\pm$ 12.25	$\pm$ 12.48		
0.13–0.16	0.145	45.1	184.34	$\pm$ 11.18	$\pm$ 10.85	0.179	55.0	158.33	$\pm$ 8.61	$\pm$ 7.85		
0.16–0.20	0.180	44.8	187.62	$\pm$ 9.84	$\pm$ 9.80	0.220	55.1	165.12	$\pm$ 9.00	$\pm$ 7.40		
0.20–0.24	0.220	44.8	191.87	$\pm$ 9.80	$\pm$ 9.00	0.269	55.0	133.08	$\pm$ 6.60	$\pm$ 5.15		
0.24–0.30	0.270	44.8	186.34	$\pm$ 7.89	$\pm$ 7.22	0.329	54.9	124.23	$\pm$ 6.31	$\pm$ 4.38		
0.30–0.36	0.331	44.7	155.56	$\pm$ 7.13	$\pm$ 5.42	0.390	54.9	106.94	$\pm$ 6.00	$\pm$ 3.87		
0.36–0.42	0.389	44.6	136.48	$\pm$ 6.65	$\pm$ 4.63	0.459	54.7	100.60	$\pm$ 5.11	$\pm$ 4.32		
0.42–0.50	0.458	44.7	113.99	$\pm$ 5.37	$\pm$ 4.39	0.543	54.6	61.83	$\pm$ 3.50	$\pm$ 3.04		
0.50–0.60	0.547	44.5	77.02	$\pm$ 3.78	$\pm$ 3.54	0.658	54.6	40.51	$\pm$ 2.57	$\pm$ 2.74		
0.60–0.72	0.656	44.6	51.79	$\pm$ 2.87	$\pm$ 3.44	0.795	54.7	24.68	$\pm$ 1.65	$\pm$ 2.44		
0.72–0.90	0.796	44.5	27.21	$\pm$ 1.64	$\pm$ 2.71	1.035	54.6	5.05	$\pm$ 0.42	$\pm$ 0.77		
$p_T$	60 < $\theta$ < 75						75 < $\theta$ < 90					
	$\langle p_T \rangle$	$\langle \theta \rangle$	$d^2\sigma/dpd\Omega$				$\langle p_T \rangle$	$\langle \theta \rangle$	$d^2\sigma/dpd\Omega$			
			$\langle p_T \rangle$	$\langle \theta \rangle$	$d^2\sigma/dpd\Omega$	$d^2\sigma/dpd\Omega$			$\langle p_T \rangle$	$\langle \theta \rangle$	$d^2\sigma/dpd\Omega$	$d^2\sigma/dpd\Omega$
0.13–0.16	0.146	67.0	195.61	$\pm$ 10.68	$\pm$ 13.53	0.146	81.9	179.69	$\pm$ 11.59	$\pm$ 15.13		
0.16–0.20	0.180	67.3	164.25	$\pm$ 7.26	$\pm$ 7.83	0.181	82.5	160.50	$\pm$ 7.55	$\pm$ 7.64		
0.20–0.24	0.220	67.3	157.75	$\pm$ 7.10	$\pm$ 6.59	0.221	82.1	145.94	$\pm$ 6.98	$\pm$ 6.11		
0.24–0.30	0.271	67.2	123.23	$\pm$ 5.30	$\pm$ 4.82	0.271	82.2	96.23	$\pm$ 4.77	$\pm$ 4.08		
0.30–0.36	0.332	67.1	94.40	$\pm$ 4.63	$\pm$ 3.45	0.331	81.8	72.05	$\pm$ 4.20	$\pm$ 3.42		
0.36–0.42	0.392	67.2	79.50	$\pm$ 4.31	$\pm$ 3.24	0.392	81.7	51.56	$\pm$ 3.48	$\pm$ 2.50		
0.42–0.50	0.461	66.6	73.31	$\pm$ 3.55	$\pm$ 3.27	0.462	82.0	46.84	$\pm$ 2.89	$\pm$ 2.67		
0.50–0.60	0.554	66.9	47.28	$\pm$ 2.53	$\pm$ 2.74	0.551	82.0	30.66	$\pm$ 2.05	$\pm$ 2.15		
0.60–0.72	0.663	67.0	29.08	$\pm$ 1.77	$\pm$ 2.23	0.660	81.6	19.08	$\pm$ 1.54	$\pm$ 1.92		
0.72–0.90	0.805	67.3	12.21	$\pm$ 0.90	$\pm$ 1.31	0.808	81.3	7.62	$\pm$ 0.71	$\pm$ 0.99		
0.90–1.25	1.028	66.8	2.69	$\pm$ 0.25	$\pm$ 0.47	1.043	81.8	0.88	$\pm$ 0.13	$\pm$ 0.20		
$p_T$	90 < $\theta$ < 105						105 < $\theta$ < 125					
	$\langle p_T \rangle$	$\langle \theta \rangle$	$d^2\sigma/dpd\Omega$				$\langle p_T \rangle$	$\langle \theta \rangle$	$d^2\sigma/dpd\Omega$			
			$\langle p_T \rangle$	$\langle \theta \rangle$	$d^2\sigma/dpd\Omega$	$d^2\sigma/dpd\Omega$			$\langle p_T \rangle$	$\langle \theta \rangle$	$d^2\sigma/dpd\Omega$	$d^2\sigma/dpd\Omega$
0.13–0.16	0.146	97.5	174.68	$\pm$ 11.93	$\pm$ 12.27	0.145	115.0	161.00	$\pm$ 8.71	$\pm$ 10.03		
0.16–0.20	0.180	97.6	163.49	$\pm$ 7.72	$\pm$ 7.31	0.179	114.6	132.89	$\pm$ 5.97	$\pm$ 5.09		
0.20–0.24	0.220	97.0	120.42	$\pm$ 6.49	$\pm$ 5.02	0.219	114.2	87.46	$\pm$ 4.69	$\pm$ 3.34		
0.24–0.30	0.268	97.7	77.40	$\pm$ 4.29	$\pm$ 3.34	0.269	113.5	48.12	$\pm$ 2.86	$\pm$ 2.17		
0.30–0.36	0.331	96.7	45.41	$\pm$ 3.18	$\pm$ 2.21	0.330	113.7	28.98	$\pm$ 2.24	$\pm$ 1.72		
0.36–0.42	0.390	97.3	38.35	$\pm$ 3.01	$\pm$ 2.39	0.391	114.0	24.34	$\pm$ 2.17	$\pm$ 2.04		
0.42–0.50	0.461	97.2	24.99	$\pm$ 2.09	$\pm$ 1.87	0.461	113.8	11.73	$\pm$ 1.20	$\pm$ 1.17		
0.50–0.60	0.550	96.6	16.96	$\pm$ 1.53	$\pm$ 1.66	0.542	112.3	4.64	$\pm$ 0.65	$\pm$ 0.62		
0.60–0.72	0.658	96.7	6.31	$\pm$ 0.80	$\pm$ 0.83	0.650	111.0	1.50	$\pm$ 0.31	$\pm$ 0.30		
0.72–0.90	0.797	96.0	1.76	$\pm$ 0.32	$\pm$ 0.32	0.813	114.4	0.11	$\pm$ 0.05	$\pm$ 0.04		
0.90–1.25	0.998	95.6	0.17	$\pm$ 0.04	$\pm$ 0.07							

Table A.6: Double-differential inclusive cross-section  $d^2\sigma/dpd\Omega$  [mb/(GeV/c sr)] of the production of  $\pi^-$ 's in  $\pi^+ + \text{Sn} \rightarrow \pi^- + \text{X}$  interactions with +3.0 GeV/c beam momentum; the first error is statistical, the second systematic;  $p_T$  in GeV/c, polar angle  $\theta$  in degrees.

$p_T$	20 < $\theta$ < 30						30 < $\theta$ < 40						
	$\langle p_T \rangle$	$\langle \theta \rangle$	$d^2\sigma/dpd\Omega$				$\langle p_T \rangle$	$\langle \theta \rangle$	$d^2\sigma/dpd\Omega$				
			192.85	$\pm$ 12.59	$\pm$ 14.74	194.29	$\pm$ 12.29	$\pm$ 14.67	189.23	$\pm$ 11.00	$\pm$ 11.83		
0.10–0.13	0.116	25.0	192.85	$\pm$ 12.59	$\pm$ 14.74	0.114	35.1	194.29	$\pm$ 12.29	$\pm$ 14.67	189.23	$\pm$ 11.00	$\pm$ 11.83
0.13–0.16	0.145	24.9	219.31	$\pm$ 12.42	$\pm$ 13.48	0.145	35.1	189.23	$\pm$ 11.00	$\pm$ 11.83	185.51	$\pm$ 9.30	$\pm$ 9.57
0.16–0.20	0.180	24.9	189.78	$\pm$ 9.76	$\pm$ 9.55	0.179	34.8	185.51	$\pm$ 9.30	$\pm$ 9.57	182.81	$\pm$ 9.48	$\pm$ 8.43
0.20–0.24	0.219	25.0	200.85	$\pm$ 10.13	$\pm$ 9.16	0.219	34.8	182.81	$\pm$ 9.48	$\pm$ 8.43	172.37	$\pm$ 7.51	$\pm$ 6.45
0.24–0.30	0.269	25.3	169.78	$\pm$ 7.43	$\pm$ 6.12	0.268	34.9	172.37	$\pm$ 7.51	$\pm$ 6.45	130.46	$\pm$ 6.44	$\pm$ 4.40
0.30–0.36	0.329	25.0	141.74	$\pm$ 6.84	$\pm$ 4.96	0.329	34.8	96.47	$\pm$ 5.64	$\pm$ 3.65	72.03	$\pm$ 4.10	$\pm$ 2.96
0.36–0.42	0.389	25.3	97.79	$\pm$ 5.68	$\pm$ 3.62	0.390	34.9	45.48	$\pm$ 2.94	$\pm$ 2.43	34.9	$\pm$ 2.94	$\pm$ 2.43
0.42–0.50	0.457	25.0	69.70	$\pm$ 4.17	$\pm$ 3.03	0.457	34.9	18.62	$\pm$ 1.75	$\pm$ 1.35	10.54	$\pm$ 1.14	$\pm$ 1.08
0.50–0.60	0.543	25.0	45.45	$\pm$ 3.01	$\pm$ 2.55	0.545	34.9	10.54	$\pm$ 1.14	$\pm$ 1.08	7.95	$\pm$ 1.14	$\pm$ 1.08
0.60–0.72	0.651	24.8	19.07	$\pm$ 1.76	$\pm$ 1.41	0.655	35.0	35.4	$\pm$ 1.14	$\pm$ 1.08	35.4	$\pm$ 1.14	$\pm$ 1.08
0.72–0.90													
$p_T$	40 < $\theta$ < 50						50 < $\theta$ < 60						
	$\langle p_T \rangle$	$\langle \theta \rangle$	$d^2\sigma/dpd\Omega$				$\langle p_T \rangle$	$\langle \theta \rangle$	$d^2\sigma/dpd\Omega$				
			204.04	$\pm$ 12.85	$\pm$ 15.62	0.144	54.8	194.04	$\pm$ 11.82	$\pm$ 12.06	171.52	$\pm$ 9.13	$\pm$ 8.86
0.10–0.13	0.115	45.0	162.50	$\pm$ 9.95	$\pm$ 10.07	0.180	54.9	140.56	$\pm$ 8.29	$\pm$ 7.31	115.70	$\pm$ 6.15	$\pm$ 4.79
0.13–0.16	0.144	45.3	163.81	$\pm$ 8.64	$\pm$ 8.63	0.219	54.8	115.70	$\pm$ 6.15	$\pm$ 4.79	87.17	$\pm$ 5.22	$\pm$ 3.11
0.16–0.20	0.180	45.0	148.98	$\pm$ 8.28	$\pm$ 6.91	0.269	54.9	67.60	$\pm$ 4.73	$\pm$ 2.79	57.65	$\pm$ 3.77	$\pm$ 2.60
0.20–0.24	0.220	44.8	137.06	$\pm$ 6.48	$\pm$ 5.07	0.329	55.0	29.97	$\pm$ 2.36	$\pm$ 1.70	54.6	$\pm$ 2.36	$\pm$ 1.70
0.24–0.30	0.267	44.6	118.40	$\pm$ 6.30	$\pm$ 4.53	0.388	54.7	19.95	$\pm$ 1.85	$\pm$ 1.60	19.95	$\pm$ 1.85	$\pm$ 1.60
0.30–0.36	0.330	45.0	89.49	$\pm$ 5.35	$\pm$ 3.26	0.456	54.7	0.786	$\pm$ 0.91	$\pm$ 0.82	0.994	$\pm$ 0.23	$\pm$ 0.23
0.36–0.42	0.389	45.3	42.78	$\pm$ 2.71	$\pm$ 2.06	0.545	54.6	1.27	$\pm$ 0.23	$\pm$ 0.23	54.6	$\pm$ 0.23	$\pm$ 0.23
0.42–0.50	0.456	44.8	37.28	$\pm$ 2.71	$\pm$ 2.06	0.654	54.4	0.791	$\pm$ 0.82	$\pm$ 0.82	0.994	$\pm$ 0.23	$\pm$ 0.23
0.50–0.60	0.544	45.1	18.39	$\pm$ 1.67	$\pm$ 1.38	0.786	67.7	6.33	$\pm$ 0.82	$\pm$ 0.69	6.33	$\pm$ 0.82	$\pm$ 0.69
0.60–0.72	0.655	45.0	7.91	$\pm$ 0.91	$\pm$ 0.82	0.983	67.7	0.791	$\pm$ 0.82	$\pm$ 0.69	0.994	$\pm$ 0.23	$\pm$ 0.23
0.72–0.90													
$p_T$	60 < $\theta$ < 75						75 < $\theta$ < 90						
	$\langle p_T \rangle$	$\langle \theta \rangle$	$d^2\sigma/dpd\Omega$				$\langle p_T \rangle$	$\langle \theta \rangle$	$d^2\sigma/dpd\Omega$				
			171.70	$\pm$ 9.37	$\pm$ 10.13	0.145	82.7	170.85	$\pm$ 10.39	$\pm$ 11.27	111.40	$\pm$ 6.15	$\pm$ 5.18
0.13–0.16	0.144	67.2	143.99	$\pm$ 6.79	$\pm$ 6.74	0.178	81.9	146.09	$\pm$ 7.21	$\pm$ 6.91	78.12	$\pm$ 4.11	$\pm$ 3.05
0.16–0.20	0.179	67.3	117.59	$\pm$ 5.99	$\pm$ 4.93	0.219	82.0	59.46	$\pm$ 3.64	$\pm$ 2.53	52.00	$\pm$ 3.15	$\pm$ 2.27
0.20–0.24	0.219	67.2	106.09	$\pm$ 4.77	$\pm$ 4.05	0.268	82.1	28.60	$\pm$ 2.16	$\pm$ 1.70	22.62	$\pm$ 1.97	$\pm$ 1.55
0.24–0.30	0.268	67.3	54.21	$\pm$ 3.45	$\pm$ 2.21	0.386	81.5	11.90	$\pm$ 0.90	$\pm$ 0.78	10.79	$\pm$ 1.31	$\pm$ 0.97
0.30–0.36	0.326	66.9	42.71	$\pm$ 2.64	$\pm$ 2.01	0.450	82.3	6.69	$\pm$ 0.50	$\pm$ 0.44	6.69	$\pm$ 0.50	$\pm$ 0.44
0.36–0.42	0.387	66.8	27.80	$\pm$ 1.94	$\pm$ 1.77	0.535	82.8	2.77	$\pm$ 0.50	$\pm$ 0.44	2.77	$\pm$ 0.50	$\pm$ 0.44
0.42–0.50	0.453	66.5	14.92	$\pm$ 1.60	$\pm$ 1.26	0.642	81.0	0.791	$\pm$ 0.82	$\pm$ 0.69	0.791	$\pm$ 0.82	$\pm$ 0.69
0.50–0.60	0.538	67.1	10.10	$\pm$ 1.16	$\pm$ 1.14	0.786	99.0	0.786	$\pm$ 0.82	$\pm$ 0.69	0.786	$\pm$ 0.82	$\pm$ 0.69
0.60–0.72	0.638	99.0	3.77	$\pm$ 0.57	$\pm$ 0.62	0.983	67.7	0.983	$\pm$ 0.82	$\pm$ 0.69	0.983	$\pm$ 0.82	$\pm$ 0.69
0.72–0.90													
$p_T$	90 < $\theta$ < 105						105 < $\theta$ < 125						
	$\langle p_T \rangle$	$\langle \theta \rangle$	$d^2\sigma/dpd\Omega$				$\langle p_T \rangle$	$\langle \theta \rangle$	$d^2\sigma/dpd\Omega$				
			143.73	$\pm$ 9.75	$\pm$ 9.22	0.144	114.4	151.31	$\pm$ 8.01	$\pm$ 7.88	114.0	$\pm$ 5.00	$\pm$ 3.79
0.13–0.16	0.145	97.0	128.15	$\pm$ 6.97	$\pm$ 6.57	0.217	113.9	48.97	$\pm$ 3.45	$\pm$ 2.11	36.01	$\pm$ 2.46	$\pm$ 1.85
0.16–0.20	0.179	97.5	97.12	$\pm$ 5.80	$\pm$ 4.30	0.327	113.5	22.62	$\pm$ 1.97	$\pm$ 1.55	111.9	$\pm$ 0.90	$\pm$ 0.78
0.20–0.24	0.218	97.4	52.45	$\pm$ 3.37	$\pm$ 2.17	0.449	114.9	10.79	$\pm$ 1.31	$\pm$ 0.97	113.0	$\pm$ 0.90	$\pm$ 0.78
0.24–0.30	0.263	97.3	38.79	$\pm$ 3.04	$\pm$ 2.23	0.523	111.9	2.77	$\pm$ 0.50	$\pm$ 0.44	114.4	$\pm$ 0.50	$\pm$ 0.44
0.30–0.36	0.326	97.5	28.13	$\pm$ 2.56	$\pm$ 1.89	0.642	114.4	1.07	$\pm$ 0.26	$\pm$ 0.26	111.1	$\pm$ 0.06	$\pm$ 0.11
0.36–0.42	0.383	97.2	10.10	$\pm$ 1.16	$\pm$ 1.14	0.769	111.1	0.18	$\pm$ 0.06	$\pm$ 0.11	0.769	$\pm$ 0.06	$\pm$ 0.11
0.42–0.50	0.449	96.9	3.77	$\pm$ 0.57	$\pm$ 0.62	0.983	67.7	0.983	$\pm$ 0.82	$\pm$ 0.69	0.983	$\pm$ 0.82	$\pm$ 0.69
0.50–0.60	0.538	96.3	0.90	$\pm$ 0.23	$\pm$ 0.21	0.786	99.0	0.786	$\pm$ 0.82	$\pm$ 0.69	0.786	$\pm$ 0.82	$\pm$ 0.69
0.60–0.72	0.638	99.0	0.90	$\pm$ 0.23	$\pm$ 0.21	0.983	67.7	0.983	$\pm$ 0.82	$\pm$ 0.69	0.983	$\pm$ 0.82	$\pm$ 0.69
0.72–0.90													

Table A.7: Double-differential inclusive cross-section  $d^2\sigma/dpd\Omega$  [mb/(GeV/c sr)] of the production of protons in  $\pi^- + \text{Sn} \rightarrow p + X$  interactions with  $-3.0$  GeV/c beam momentum; the first error is statistical, the second systematic;  $p_T$  in GeV/c, polar angle  $\theta$  in degrees.

$p_T$	20 < $\theta$ < 30						30 < $\theta$ < 40							
	$\langle p_T \rangle$	$\langle \theta \rangle$	$d^2\sigma/dpd\Omega$				$\langle p_T \rangle$	$\langle \theta \rangle$	$d^2\sigma/dpd\Omega$					
			704.17	$\pm$	14.37	$\pm$	34.77	771.73	$\pm$	11.84	$\pm$	31.48		
0.20–0.24	0.220	25.2	584.42	$\pm$	10.39	$\pm$	26.41	0.271	34.9	589.94	$\pm$	10.08	$\pm$	21.22
0.24–0.30	0.269	25.4	426.42	$\pm$	9.01	$\pm$	18.89	0.330	35.2	438.91	$\pm$	9.00	$\pm$	15.99
0.30–0.36	0.330	25.4	315.68	$\pm$	7.75	$\pm$	13.57	0.390	35.2	324.46	$\pm$	6.88	$\pm$	13.77
0.36–0.42	0.390	25.4	231.41	$\pm$	5.79	$\pm$	10.19	0.459	35.2	207.27	$\pm$	4.96	$\pm$	9.98
0.42–0.50	0.459	25.5	141.45	$\pm$	4.04	$\pm$	6.49	0.549	35.1	106.04	$\pm$	3.27	$\pm$	6.56
0.50–0.60	0.549	25.4	81.71	$\pm$	2.76	$\pm$	4.19	0.658	35.1	45.32	$\pm$	1.75	$\pm$	3.59
0.60–0.72	0.658	25.4						0.800	35.2					
0.72–0.90														
$p_T$	40 < $\theta$ < 50						50 < $\theta$ < 60							
	$\langle p_T \rangle$	$\langle \theta \rangle$	$d^2\sigma/dpd\Omega$				$\langle p_T \rangle$	$\langle \theta \rangle$	$d^2\sigma/dpd\Omega$					
			720.30	$\pm$	11.31	$\pm$	22.06		608.72	$\pm$	9.89	$\pm$	16.12	
0.30–0.36	0.328	45.0	561.10	$\pm$	9.77	$\pm$	16.03	0.387	55.1	462.96	$\pm$	7.70	$\pm$	13.03
0.36–0.42	0.387	45.2	394.32	$\pm$	7.30	$\pm$	12.94	0.456	55.0	296.78	$\pm$	5.72	$\pm$	11.70
0.42–0.50	0.456	45.0	265.26	$\pm$	5.64	$\pm$	12.65	0.544	55.1	163.01	$\pm$	4.16	$\pm$	10.68
0.50–0.60	0.543	45.2	148.07	$\pm$	3.96	$\pm$	9.25	0.649	55.0	71.60	$\pm$	2.34	$\pm$	6.70
0.60–0.72	0.650	45.1	63.56	$\pm$	2.17	$\pm$	5.72	0.790	55.0					
0.72–0.90	0.789	45.2												
$p_T$	60 < $\theta$ < 75						75 < $\theta$ < 90							
	$\langle p_T \rangle$	$\langle \theta \rangle$	$d^2\sigma/dpd\Omega$				$\langle p_T \rangle$	$\langle \theta \rangle$	$d^2\sigma/dpd\Omega$					
			297.49	$\pm$	4.40	$\pm$	10.66	0.547	82.0	256.75	$\pm$	4.03	$\pm$	11.87
0.50–0.60	0.549	67.5	152.13	$\pm$	3.14	$\pm$	9.68	0.657	81.9	124.38	$\pm$	2.68	$\pm$	8.04
0.60–0.72	0.657	67.2	54.88	$\pm$	1.70	$\pm$	6.52							
0.72–0.90	0.801	67.1												
$p_T$	90 < $\theta$ < 105						105 < $\theta$ < 125							
	$\langle p_T \rangle$	$\langle \theta \rangle$	$d^2\sigma/dpd\Omega$				$\langle p_T \rangle$	$\langle \theta \rangle$	$d^2\sigma/dpd\Omega$					
			173.11	$\pm$	3.31	$\pm$	10.86	0.458	113.3	168.70	$\pm$	3.05	$\pm$	9.19
0.42–0.50	0.547	96.9	73.20	$\pm$	2.09	$\pm$	6.00	0.547	113.0	76.52	$\pm$	1.97	$\pm$	6.61
0.50–0.60	0.656	97.0						0.653	112.6	22.59	$\pm$	1.15	$\pm$	3.75
0.60–0.72														

Table A.8: Double-differential inclusive cross-section  $d^2\sigma/dpd\Omega$  [mb/(GeV/c sr)] of the production of  $\pi^+$ 's in  $\pi^- + \text{Sn} \rightarrow \pi^+ + \text{X}$  interactions with  $-3.0$  GeV/c beam momentum; the first error is statistical, the second systematic;  $p_T$  in GeV/c, polar angle  $\theta$  in degrees.

$p_T$	20 < $\theta$ < 30			30 < $\theta$ < 40		
	$\langle p_T \rangle$	$\langle \theta \rangle$	$d^2\sigma/dpd\Omega$	$\langle p_T \rangle$	$\langle \theta \rangle$	$d^2\sigma/dpd\Omega$
0.10–0.13	0.116	24.9	142.19 $\pm$ 7.78 $\pm$ 10.21	0.116	35.2	158.26 $\pm$ 7.89 $\pm$ 11.36
0.13–0.16	0.145	25.2	193.27 $\pm$ 8.58 $\pm$ 11.15	0.145	34.8	158.31 $\pm$ 7.08 $\pm$ 8.98
0.16–0.20	0.181	25.0	200.04 $\pm$ 7.23 $\pm$ 9.43	0.181	34.9	175.27 $\pm$ 6.51 $\pm$ 8.30
0.20–0.24	0.221	24.9	197.95 $\pm$ 7.17 $\pm$ 8.52	0.221	34.7	167.20 $\pm$ 6.36 $\pm$ 6.82
0.24–0.30	0.270	25.1	183.77 $\pm$ 5.61 $\pm$ 6.53	0.270	34.8	168.64 $\pm$ 5.28 $\pm$ 5.83
0.30–0.36	0.330	24.9	150.36 $\pm$ 4.97 $\pm$ 4.74	0.329	34.7	138.98 $\pm$ 4.73 $\pm$ 4.30
0.36–0.42	0.390	25.1	116.78 $\pm$ 4.37 $\pm$ 3.76	0.390	35.0	122.19 $\pm$ 4.56 $\pm$ 4.09
0.42–0.50	0.460	25.0	81.02 $\pm$ 3.12 $\pm$ 3.22	0.459	34.9	84.59 $\pm$ 3.25 $\pm$ 3.09
0.50–0.60	0.549	25.2	39.62 $\pm$ 1.79 $\pm$ 2.08	0.549	34.8	47.76 $\pm$ 2.06 $\pm$ 2.23
0.60–0.72	0.657	25.4	24.68 $\pm$ 1.27 $\pm$ 1.90	0.657	34.9	24.82 $\pm$ 1.28 $\pm$ 1.70
0.72–0.90				0.795	35.2	11.87 $\pm$ 0.68 $\pm$ 1.29
$p_T$	40 < $\theta$ < 50			50 < $\theta$ < 60		
	$\langle p_T \rangle$	$\langle \theta \rangle$	$d^2\sigma/dpd\Omega$	$\langle p_T \rangle$	$\langle \theta \rangle$	$d^2\sigma/dpd\Omega$
0.10–0.13	0.115	44.7	139.57 $\pm$ 7.71 $\pm$ 10.22	0.145	54.9	149.93 $\pm$ 7.68 $\pm$ 9.00
0.13–0.16	0.145	45.0	166.15 $\pm$ 7.67 $\pm$ 9.40	0.180	55.0	140.98 $\pm$ 5.86 $\pm$ 6.66
0.16–0.20	0.179	45.0	147.03 $\pm$ 5.96 $\pm$ 7.04	0.219	54.6	117.32 $\pm$ 5.35 $\pm$ 4.89
0.20–0.24	0.219	44.9	148.64 $\pm$ 6.08 $\pm$ 6.37	0.268	54.8	113.05 $\pm$ 4.32 $\pm$ 4.03
0.24–0.30	0.269	44.6	134.29 $\pm$ 4.67 $\pm$ 4.65	0.329	54.7	93.77 $\pm$ 3.96 $\pm$ 3.19
0.30–0.36	0.328	44.9	124.02 $\pm$ 4.50 $\pm$ 3.86	0.387	54.9	78.38 $\pm$ 3.66 $\pm$ 2.74
0.36–0.42	0.387	44.9	98.25 $\pm$ 4.07 $\pm$ 3.31	0.456	54.7	64.52 $\pm$ 2.95 $\pm$ 2.92
0.42–0.50	0.457	44.5	77.45 $\pm$ 3.13 $\pm$ 2.87	0.545	54.6	40.58 $\pm$ 2.04 $\pm$ 2.05
0.50–0.60	0.544	44.7	47.16 $\pm$ 2.12 $\pm$ 2.10	0.649	54.5	22.54 $\pm$ 1.34 $\pm$ 1.49
0.60–0.72	0.649	44.5	26.11 $\pm$ 1.40 $\pm$ 1.69	0.790	54.8	10.04 $\pm$ 0.69 $\pm$ 0.94
0.72–0.90	0.791	44.6	12.17 $\pm$ 0.72 $\pm$ 1.15	1.029	54.5	2.44 $\pm$ 0.20 $\pm$ 0.37
0.90–1.25						
$p_T$	60 < $\theta$ < 75			75 < $\theta$ < 90		
	$\langle p_T \rangle$	$\langle \theta \rangle$	$d^2\sigma/dpd\Omega$	$\langle p_T \rangle$	$\langle \theta \rangle$	$d^2\sigma/dpd\Omega$
0.13–0.16	0.145	67.8	136.70 $\pm$ 6.26 $\pm$ 8.20	0.146	82.1	122.08 $\pm$ 6.45 $\pm$ 8.57
0.16–0.20	0.180	67.5	133.12 $\pm$ 4.76 $\pm$ 6.19	0.180	82.2	130.43 $\pm$ 4.96 $\pm$ 6.35
0.20–0.24	0.220	67.1	116.30 $\pm$ 4.33 $\pm$ 4.58	0.219	82.1	99.07 $\pm$ 4.13 $\pm$ 3.96
0.24–0.30	0.269	67.3	85.71 $\pm$ 3.01 $\pm$ 2.84	0.269	82.0	76.21 $\pm$ 2.96 $\pm$ 2.78
0.30–0.36	0.330	66.9	71.62 $\pm$ 2.83 $\pm$ 2.40	0.329	82.0	52.99 $\pm$ 2.52 $\pm$ 2.24
0.36–0.42	0.391	67.1	57.94 $\pm$ 2.59 $\pm$ 2.25	0.388	82.0	42.82 $\pm$ 2.26 $\pm$ 2.01
0.42–0.50	0.459	66.9	45.49 $\pm$ 1.99 $\pm$ 2.10	0.461	81.9	29.78 $\pm$ 1.60 $\pm$ 1.59
0.50–0.60	0.549	67.0	31.27 $\pm$ 1.46 $\pm$ 1.82	0.549	81.7	17.01 $\pm$ 1.07 $\pm$ 1.17
0.60–0.72	0.658	67.2	18.03 $\pm$ 1.00 $\pm$ 1.41	0.664	81.8	10.61 $\pm$ 0.79 $\pm$ 1.02
0.72–0.90	0.803	66.7	6.08 $\pm$ 0.42 $\pm$ 0.65	0.798	81.4	2.60 $\pm$ 0.26 $\pm$ 0.34
0.90–1.25	1.035	66.6	1.14 $\pm$ 0.10 $\pm$ 0.21	1.020	81.9	0.51 $\pm$ 0.06 $\pm$ 0.11
$p_T$	90 < $\theta$ < 105			105 < $\theta$ < 125		
	$\langle p_T \rangle$	$\langle \theta \rangle$	$d^2\sigma/dpd\Omega$	$\langle p_T \rangle$	$\langle \theta \rangle$	$d^2\sigma/dpd\Omega$
0.13–0.16	0.146	97.4	121.76 $\pm$ 6.69 $\pm$ 8.70	0.145	114.5	109.62 $\pm$ 4.87 $\pm$ 5.48
0.16–0.20	0.180	97.3	121.82 $\pm$ 4.82 $\pm$ 5.42	0.180	113.9	84.53 $\pm$ 3.44 $\pm$ 3.13
0.20–0.24	0.220	97.0	82.25 $\pm$ 3.86 $\pm$ 3.15	0.218	114.2	60.25 $\pm$ 2.80 $\pm$ 2.16
0.24–0.30	0.267	96.8	60.04 $\pm$ 2.70 $\pm$ 2.46	0.268	113.8	36.33 $\pm$ 1.77 $\pm$ 1.49
0.30–0.36	0.329	97.5	38.91 $\pm$ 2.09 $\pm$ 1.66	0.328	114.1	20.80 $\pm$ 1.36 $\pm$ 1.18
0.36–0.42	0.391	97.3	30.31 $\pm$ 1.84 $\pm$ 1.66	0.390	112.9	15.69 $\pm$ 1.19 $\pm$ 1.17
0.42–0.50	0.460	96.7	19.17 $\pm$ 1.30 $\pm$ 1.40	0.457	112.7	9.15 $\pm$ 0.74 $\pm$ 0.87
0.50–0.60	0.552	96.4	10.94 $\pm$ 0.89 $\pm$ 1.08	0.552	112.5	3.84 $\pm$ 0.41 $\pm$ 0.50
0.60–0.72	0.657	96.1	4.71 $\pm$ 0.48 $\pm$ 0.61	0.650	112.3	1.19 $\pm$ 0.20 $\pm$ 0.21
0.72–0.90	0.798	95.7	0.80 $\pm$ 0.13 $\pm$ 0.15	0.799	112.1	0.11 $\pm$ 0.03 $\pm$ 0.04
0.90–1.25	1.020	94.8	0.08 $\pm$ 0.02 $\pm$ 0.03	1.102	111.0	0.05 $\pm$ 0.02 $\pm$ 0.02

Table A.9: Double-differential inclusive cross-section  $d^2\sigma/dpd\Omega$  [mb/(GeV/c sr)] of the production of  $\pi^-$ 's in  $\pi^- + \text{Sn} \rightarrow \pi^- + \text{X}$  interactions with  $-3.0$  GeV/c beam momentum; the first error is statistical, the second systematic;  $p_T$  in GeV/c, polar angle  $\theta$  in degrees.

$p_T$	20 < $\theta$ < 30						30 < $\theta$ < 40						
	$\langle p_T \rangle$	$\langle \theta \rangle$	$d^2\sigma/dpd\Omega$				$\langle p_T \rangle$	$\langle \theta \rangle$	$d^2\sigma/dpd\Omega$				
			$\langle p_T \rangle$	$\langle \theta \rangle$	$d^2\sigma/dpd\Omega$	$d^2\sigma/dpd\Omega$			$\langle p_T \rangle$	$\langle \theta \rangle$	$d^2\sigma/dpd\Omega$	$d^2\sigma/dpd\Omega$	
0.10–0.13	0.115	24.9	285.97	$\pm$ 11.43	$\pm$ 19.87	0.115	35.3	247.88	$\pm$ 10.19	$\pm$ 17.81			
0.13–0.16	0.146	24.8	309.71	$\pm$ 11.03	$\pm$ 17.52	0.145	35.1	272.69	$\pm$ 10.09	$\pm$ 15.39			
0.16–0.20	0.179	24.9	329.29	$\pm$ 9.65	$\pm$ 15.75	0.180	35.0	255.26	$\pm$ 8.14	$\pm$ 11.99			
0.20–0.24	0.219	25.0	314.29	$\pm$ 9.23	$\pm$ 12.50	0.219	34.8	268.90	$\pm$ 8.42	$\pm$ 10.82			
0.24–0.30	0.268	25.1	296.67	$\pm$ 7.30	$\pm$ 9.93	0.269	34.8	250.49	$\pm$ 6.56	$\pm$ 8.21			
0.30–0.36	0.328	25.1	228.50	$\pm$ 6.34	$\pm$ 6.64	0.328	34.9	216.39	$\pm$ 6.11	$\pm$ 6.28			
0.36–0.42	0.388	25.2	179.79	$\pm$ 5.65	$\pm$ 5.51	0.388	34.9	173.84	$\pm$ 5.50	$\pm$ 5.21			
0.42–0.50	0.456	25.1	130.29	$\pm$ 4.16	$\pm$ 4.67	0.454	34.9	135.21	$\pm$ 4.23	$\pm$ 4.79			
0.50–0.60	0.544	25.1	81.37	$\pm$ 2.93	$\pm$ 3.85	0.544	35.0	95.33	$\pm$ 3.16	$\pm$ 4.37			
0.60–0.72	0.649	25.2	55.74	$\pm$ 2.28	$\pm$ 3.77	0.650	34.9	60.28	$\pm$ 2.31	$\pm$ 3.81			
0.72–0.90						0.791	35.1	34.68	$\pm$ 1.53	$\pm$ 3.33			
$p_T$	40 < $\theta$ < 50						50 < $\theta$ < 60						
	$\langle p_T \rangle$	$\langle \theta \rangle$	$d^2\sigma/dpd\Omega$				$\langle p_T \rangle$	$\langle \theta \rangle$	$d^2\sigma/dpd\Omega$				
			$\langle p_T \rangle$	$\langle \theta \rangle$	$d^2\sigma/dpd\Omega$	$d^2\sigma/dpd\Omega$			$\langle p_T \rangle$	$\langle \theta \rangle$	$d^2\sigma/dpd\Omega$	$d^2\sigma/dpd\Omega$	
0.10–0.13	0.115	44.9	249.61	$\pm$ 10.75	$\pm$ 18.32		0.145	55.1	235.76	$\pm$ 9.56	$\pm$ 13.79		
0.13–0.16	0.145	44.9	243.91	$\pm$ 9.45	$\pm$ 13.82		0.180	54.8	238.52	$\pm$ 7.88	$\pm$ 11.20		
0.16–0.20	0.180	45.1	245.04	$\pm$ 7.91	$\pm$ 11.63		0.220	54.8	189.03	$\pm$ 6.94	$\pm$ 7.69		
0.20–0.24	0.220	44.8	213.81	$\pm$ 7.21	$\pm$ 8.69		0.270	54.9	166.03	$\pm$ 5.30	$\pm$ 5.46		
0.24–0.30	0.271	44.8	213.75	$\pm$ 6.09	$\pm$ 7.28		0.332	54.9	157.00	$\pm$ 5.26	$\pm$ 4.99		
0.30–0.36	0.331	44.7	173.55	$\pm$ 5.41	$\pm$ 5.08		0.391	54.5	117.49	$\pm$ 4.49	$\pm$ 3.73		
0.36–0.42	0.390	45.1	149.97	$\pm$ 5.12	$\pm$ 4.66		0.461	54.7	103.21	$\pm$ 3.70	$\pm$ 3.98		
0.42–0.50	0.459	45.0	122.06	$\pm$ 4.01	$\pm$ 4.54		0.549	54.9	68.27	$\pm$ 2.68	$\pm$ 3.44		
0.50–0.60	0.550	44.9	84.21	$\pm$ 2.94	$\pm$ 4.06		0.658	54.6	42.72	$\pm$ 1.99	$\pm$ 3.06		
0.60–0.72	0.659	45.1	55.54	$\pm$ 2.25	$\pm$ 3.79		0.795	54.8	19.04	$\pm$ 1.10	$\pm$ 1.88		
0.72–0.90	0.801	44.9	25.57	$\pm$ 1.27	$\pm$ 2.45		1.023	54.7	4.26	$\pm$ 0.32	$\pm$ 0.63		
$p_T$	60 < $\theta$ < 75						75 < $\theta$ < 90						
	$\langle p_T \rangle$	$\langle \theta \rangle$	$d^2\sigma/dpd\Omega$				$\langle p_T \rangle$	$\langle \theta \rangle$	$d^2\sigma/dpd\Omega$				
			$\langle p_T \rangle$	$\langle \theta \rangle$	$d^2\sigma/dpd\Omega$	$d^2\sigma/dpd\Omega$			$\langle p_T \rangle$	$\langle \theta \rangle$	$d^2\sigma/dpd\Omega$	$d^2\sigma/dpd\Omega$	
0.13–0.16	0.145	67.2	261.92	$\pm$ 8.99	$\pm$ 15.40		0.145	82.2	244.92	$\pm$ 10.76	$\pm$ 20.15		
0.16–0.20	0.178	67.6	217.01	$\pm$ 6.29	$\pm$ 9.51		0.179	82.6	209.84	$\pm$ 6.53	$\pm$ 10.04		
0.20–0.24	0.219	67.4	183.86	$\pm$ 5.62	$\pm$ 6.87		0.218	82.1	160.37	$\pm$ 5.42	$\pm$ 6.21		
0.24–0.30	0.268	67.2	139.90	$\pm$ 3.98	$\pm$ 4.41		0.267	82.0	111.94	$\pm$ 3.65	$\pm$ 3.99		
0.30–0.36	0.329	67.0	107.14	$\pm$ 3.53	$\pm$ 3.36		0.328	81.9	81.13	$\pm$ 3.19	$\pm$ 3.43		
0.36–0.42	0.388	67.3	94.08	$\pm$ 3.34	$\pm$ 3.38		0.387	81.9	61.32	$\pm$ 2.71	$\pm$ 2.68		
0.42–0.50	0.457	66.7	67.78	$\pm$ 2.46	$\pm$ 2.99		0.455	82.2	45.99	$\pm$ 2.06	$\pm$ 2.61		
0.50–0.60	0.544	66.8	50.49	$\pm$ 1.90	$\pm$ 2.92		0.544	81.6	32.14	$\pm$ 1.54	$\pm$ 2.40		
0.60–0.72	0.647	66.6	29.85	$\pm$ 1.35	$\pm$ 2.37		0.645	81.4	15.12	$\pm$ 0.94	$\pm$ 1.46		
0.72–0.90	0.785	66.6	13.06	$\pm$ 0.72	$\pm$ 1.39		0.785	81.8	5.35	$\pm$ 0.43	$\pm$ 0.71		
0.90–1.25	1.007	67.1	2.29	$\pm$ 0.18	$\pm$ 0.39		1.005	80.4	0.74	$\pm$ 0.09	$\pm$ 0.16		
$p_T$	90 < $\theta$ < 105						105 < $\theta$ < 125						
	$\langle p_T \rangle$	$\langle \theta \rangle$	$d^2\sigma/dpd\Omega$				$\langle p_T \rangle$	$\langle \theta \rangle$	$d^2\sigma/dpd\Omega$				
			$\langle p_T \rangle$	$\langle \theta \rangle$	$d^2\sigma/dpd\Omega$	$d^2\sigma/dpd\Omega$			$\langle p_T \rangle$	$\langle \theta \rangle$	$d^2\sigma/dpd\Omega$	$d^2\sigma/dpd\Omega$	
0.13–0.16	0.145	97.5	230.67	$\pm$ 9.23	$\pm$ 15.25		0.144	114.8	190.55	$\pm$ 6.60	$\pm$ 9.07		
0.16–0.20	0.178	97.3	188.65	$\pm$ 6.22	$\pm$ 8.61		0.178	114.0	143.33	$\pm$ 4.57	$\pm$ 5.09		
0.20–0.24	0.218	97.3	127.58	$\pm$ 4.87	$\pm$ 4.75		0.218	114.2	82.26	$\pm$ 3.39	$\pm$ 3.02		
0.24–0.30	0.266	97.0	85.84	$\pm$ 3.25	$\pm$ 3.32		0.267	114.4	54.95	$\pm$ 2.22	$\pm$ 2.41		
0.30–0.36	0.326	97.2	59.19	$\pm$ 2.66	$\pm$ 2.61		0.327	113.9	34.91	$\pm$ 1.78	$\pm$ 2.16		
0.36–0.42	0.387	96.7	43.43	$\pm$ 2.31	$\pm$ 2.59		0.388	113.4	25.12	$\pm$ 1.52	$\pm$ 2.06		
0.42–0.50	0.454	97.4	29.20	$\pm$ 1.64	$\pm$ 2.26		0.454	113.7	14.22	$\pm$ 0.96	$\pm$ 1.50		
0.50–0.60	0.541	96.2	17.12	$\pm$ 1.12	$\pm$ 1.77		0.540	111.9	5.38	$\pm$ 0.51	$\pm$ 0.76		
0.60–0.72	0.646	96.4	7.22	$\pm$ 0.63	$\pm$ 0.99		0.637	111.8	1.44	$\pm$ 0.21	$\pm$ 0.28		
0.72–0.90	0.779	96.0	1.72	$\pm$ 0.22	$\pm$ 0.34		0.783	111.6	0.25	$\pm$ 0.06	$\pm$ 0.08		
0.90–1.25	1.012	95.1	0.15	$\pm$ 0.03	$\pm$ 0.05								

Table A.10: Double-differential inclusive cross-section  $d^2\sigma/dpd\Omega$  [mb/(GeV/c sr)] of the production of protons in  $p + \text{Sn} \rightarrow p + X$  interactions with  $+5.0$  GeV/c beam momentum; the first error is statistical, the second systematic;  $p_T$  in GeV/c, polar angle  $\theta$  in degrees.

$p_T$	20 < $\theta$ < 30				30 < $\theta$ < 40					
	$\langle p_T \rangle$	$\langle \theta \rangle$	$d^2\sigma/dpd\Omega$		$\langle p_T \rangle$	$\langle \theta \rangle$	$d^2\sigma/dpd\Omega$			
0.20–0.24	0.220	25.0	964.27	$\pm$ 17.29	$\pm$ 47.09	0.270	34.9	926.20	$\pm$ 13.44	$\pm$ 37.35
0.24–0.30	0.269	25.3	868.27	$\pm$ 12.75	$\pm$ 37.98	0.329	35.1	829.98	$\pm$ 12.19	$\pm$ 29.11
0.30–0.36	0.329	25.3	676.06	$\pm$ 11.26	$\pm$ 26.96	0.389	35.1	658.81	$\pm$ 11.04	$\pm$ 21.95
0.36–0.42	0.389	25.3	550.12	$\pm$ 10.23	$\pm$ 20.15	0.458	35.2	517.25	$\pm$ 8.53	$\pm$ 17.32
0.42–0.50	0.459	25.3	422.31	$\pm$ 7.59	$\pm$ 14.09	0.546	35.3	384.60	$\pm$ 6.62	$\pm$ 13.17
0.50–0.60	0.547	25.2	315.70	$\pm$ 5.81	$\pm$ 10.66	0.655	35.2	257.02	$\pm$ 4.94	$\pm$ 10.78
0.60–0.72	0.655	25.2	223.40	$\pm$ 4.42	$\pm$ 8.67	0.801	35.1	147.24	$\pm$ 3.03	$\pm$ 8.08
0.72–0.90										
$p_T$	40 < $\theta$ < 50				50 < $\theta$ < 60					
	$\langle p_T \rangle$	$\langle \theta \rangle$	$d^2\sigma/dpd\Omega$		$\langle p_T \rangle$	$\langle \theta \rangle$	$d^2\sigma/dpd\Omega$			
0.30–0.36	0.331	45.0	920.36	$\pm$ 12.77	$\pm$ 27.61	0.390	55.0	796.45	$\pm$ 11.53	$\pm$ 20.49
0.36–0.42	0.390	45.1	763.93	$\pm$ 11.53	$\pm$ 20.93	0.460	55.1	659.58	$\pm$ 9.30	$\pm$ 17.68
0.42–0.50	0.460	45.1	583.50	$\pm$ 8.91	$\pm$ 16.61	0.550	55.0	449.36	$\pm$ 7.04	$\pm$ 15.40
0.50–0.60	0.550	45.1	423.80	$\pm$ 7.05	$\pm$ 15.47	0.660	54.9	283.33	$\pm$ 5.37	$\pm$ 14.24
0.60–0.72	0.660	45.0	275.42	$\pm$ 5.21	$\pm$ 12.44	0.804	54.9	142.93	$\pm$ 3.14	$\pm$ 9.69
0.72–0.90	0.805	45.0	159.23	$\pm$ 3.27	$\pm$ 9.57	1.048	55.0	37.57	$\pm$ 1.13	$\pm$ 3.80
0.90–1.25	1.043	45.0	52.27	$\pm$ 1.31	$\pm$ 4.47					
$p_T$	60 < $\theta$ < 75				75 < $\theta$ < 90					
	$\langle p_T \rangle$	$\langle \theta \rangle$	$d^2\sigma/dpd\Omega$		$\langle p_T \rangle$	$\langle \theta \rangle$	$d^2\sigma/dpd\Omega$			
0.50–0.60	0.553	67.4	422.96	$\pm$ 5.33	$\pm$ 14.47	0.551	81.9	335.04	$\pm$ 4.68	$\pm$ 15.34
0.60–0.72	0.662	67.2	248.97	$\pm$ 3.95	$\pm$ 13.28	0.662	81.8	171.98	$\pm$ 3.18	$\pm$ 10.98
0.72–0.90	0.810	66.8	100.74	$\pm$ 2.18	$\pm$ 9.16	0.808	81.8	58.54	$\pm$ 1.74	$\pm$ 6.82
0.90–1.25	1.044	66.7	24.31	$\pm$ 0.77	$\pm$ 3.52					
$p_T$	90 < $\theta$ < 105				105 < $\theta$ < 125					
	$\langle p_T \rangle$	$\langle \theta \rangle$	$d^2\sigma/dpd\Omega$		$\langle p_T \rangle$	$\langle \theta \rangle$	$d^2\sigma/dpd\Omega$			
0.42–0.50					0.460	113.1	195.11	$\pm$ 3.32	$\pm$ 10.97	
0.50–0.60	0.549	96.9	209.82	$\pm$ 3.70	$\pm$ 13.08	0.548	112.6	85.23	$\pm$ 2.08	$\pm$ 7.13
0.60–0.72	0.660	96.4	98.88	$\pm$ 2.47	$\pm$ 7.97	0.659	112.3	22.59	$\pm$ 1.18	$\pm$ 3.80

Table A.11: Double-differential inclusive cross-section  $d^2\sigma/dpd\Omega$  [mb/(GeV/c sr)] of the production of  $\pi^+$ 's in  $p + \text{Sn} \rightarrow \pi^+ + X$  interactions with +5.0 GeV/c beam momentum; the first error is statistical, the second systematic;  $p_T$  in GeV/c, polar angle  $\theta$  in degrees.

$p_T$	20 < $\theta$ < 30						30 < $\theta$ < 40							
	$\langle p_T \rangle$	$\langle \theta \rangle$	$d^2\sigma/dpd\Omega$				$\langle p_T \rangle$	$\langle \theta \rangle$	$d^2\sigma/dpd\Omega$					
			227.92	$\pm$	10.46	$\pm$	15.49	201.22	$\pm$	9.16	$\pm$	14.07		
0.10–0.13	0.115	25.0	227.92	$\pm$	10.46	$\pm$	15.49	0.115	35.0	201.22	$\pm$	9.16	$\pm$	14.07
0.13–0.16	0.146	24.7	258.24	$\pm$	10.20	$\pm$	14.21	0.145	34.9	226.99	$\pm$	9.26	$\pm$	12.54
0.16–0.20	0.180	24.6	299.20	$\pm$	9.34	$\pm$	14.13	0.180	34.8	228.97	$\pm$	8.12	$\pm$	10.92
0.20–0.24	0.219	24.7	302.17	$\pm$	9.18	$\pm$	12.21	0.220	34.9	221.38	$\pm$	7.73	$\pm$	8.91
0.24–0.30	0.268	24.7	274.09	$\pm$	7.06	$\pm$	9.54	0.269	34.8	217.34	$\pm$	6.23	$\pm$	7.35
0.30–0.36	0.329	24.9	210.22	$\pm$	6.07	$\pm$	6.44	0.329	34.8	182.84	$\pm$	5.78	$\pm$	5.64
0.36–0.42	0.389	24.9	154.37	$\pm$	5.14	$\pm$	4.75	0.389	34.9	127.71	$\pm$	4.71	$\pm$	3.80
0.42–0.50	0.458	25.1	112.80	$\pm$	3.76	$\pm$	4.20	0.458	34.8	103.59	$\pm$	3.69	$\pm$	3.63
0.50–0.60	0.546	25.0	64.10	$\pm$	2.37	$\pm$	3.29	0.545	34.9	63.88	$\pm$	2.48	$\pm$	2.93
0.60–0.72	0.653	24.9	36.32	$\pm$	1.47	$\pm$	2.80	0.656	34.9	34.47	$\pm$	1.53	$\pm$	2.33
0.72–0.90							0.795	35.0	13.36	$\pm$	0.66	$\pm$	1.42	
$p_T$	40 < $\theta$ < 50						50 < $\theta$ < 60							
	$\langle p_T \rangle$	$\langle \theta \rangle$	$d^2\sigma/dpd\Omega$				$\langle p_T \rangle$	$\langle \theta \rangle$	$d^2\sigma/dpd\Omega$					
			219.18	$\pm$	10.21	$\pm$	15.82	0.145	54.8	209.95	$\pm$	9.18	$\pm$	12.15
0.10–0.13	0.117	45.0	219.18	$\pm$	10.21	$\pm$	15.82	0.145	54.8	209.95	$\pm$	9.18	$\pm$	12.15
0.13–0.16	0.146	45.2	179.54	$\pm$	8.07	$\pm$	9.94	0.180	54.8	186.64	$\pm$	7.05	$\pm$	8.64
0.16–0.20	0.180	44.8	209.37	$\pm$	7.55	$\pm$	9.88	0.220	54.9	158.06	$\pm$	6.43	$\pm$	6.39
0.20–0.24	0.220	44.8	196.41	$\pm$	7.32	$\pm$	8.09	0.271	54.8	142.15	$\pm$	5.11	$\pm$	4.94
0.24–0.30	0.271	44.9	164.27	$\pm$	5.43	$\pm$	5.65	0.329	54.7	113.18	$\pm$	4.55	$\pm$	3.52
0.30–0.36	0.329	44.9	139.22	$\pm$	4.98	$\pm$	4.26	0.389	54.8	97.74	$\pm$	4.28	$\pm$	3.40
0.36–0.42	0.390	44.8	114.95	$\pm$	4.64	$\pm$	3.96	0.459	54.6	71.81	$\pm$	3.13	$\pm$	2.68
0.42–0.50	0.459	44.6	87.03	$\pm$	3.46	$\pm$	3.15	0.552	54.7	46.19	$\pm$	2.25	$\pm$	2.31
0.50–0.60	0.552	44.7	53.06	$\pm$	2.32	$\pm$	2.35	0.659	54.7	24.97	$\pm$	1.47	$\pm$	1.68
0.60–0.72	0.659	44.4	28.09	$\pm$	1.47	$\pm$	1.75	0.800	54.6	12.45	$\pm$	0.76	$\pm$	1.15
0.72–0.90							1.046	54.2	3.55	$\pm$	0.25	$\pm$	0.52	
$p_T$	60 < $\theta$ < 75						75 < $\theta$ < 90							
	$\langle p_T \rangle$	$\langle \theta \rangle$	$d^2\sigma/dpd\Omega$				$\langle p_T \rangle$	$\langle \theta \rangle$	$d^2\sigma/dpd\Omega$					
			170.83	$\pm$	7.06	$\pm$	9.96	0.147	82.1	136.47	$\pm$	6.52	$\pm$	8.12
0.13–0.16	0.145	67.4	170.83	$\pm$	7.06	$\pm$	9.96	0.180	82.0	152.49	$\pm$	5.43	$\pm$	6.89
0.16–0.20	0.180	67.2	169.32	$\pm$	5.50	$\pm$	7.73	0.221	81.9	135.84	$\pm$	5.08	$\pm$	5.69
0.20–0.24	0.220	67.1	147.36	$\pm$	5.09	$\pm$	5.66	0.271	82.1	91.99	$\pm$	3.36	$\pm$	3.09
0.24–0.30	0.271	67.2	107.12	$\pm$	3.61	$\pm$	3.57	0.330	82.2	52.09	$\pm$	2.54	$\pm$	1.83
0.30–0.36	0.330	66.9	89.94	$\pm$	3.36	$\pm$	3.07	0.390	82.0	40.54	$\pm$	2.26	$\pm$	1.74
0.36–0.42	0.392	66.9	71.63	$\pm$	2.97	$\pm$	2.51	0.461	82.1	27.48	$\pm$	1.61	$\pm$	1.45
0.42–0.50	0.463	66.7	46.46	$\pm$	2.06	$\pm$	1.95	0.551	81.8	16.39	$\pm$	1.11	$\pm$	1.16
0.50–0.60	0.551	67.0	30.64	$\pm$	1.50	$\pm$	1.74	0.664	81.8	9.07	$\pm$	0.73	$\pm$	0.84
0.60–0.72	0.664	66.6	15.55	$\pm$	0.94	$\pm$	1.18	0.805	81.6	3.22	$\pm$	0.33	$\pm$	0.41
0.72–0.90							1.041	80.6	0.46	$\pm$	0.07	$\pm$	0.10	
$p_T$	90 < $\theta$ < 105						105 < $\theta$ < 125							
	$\langle p_T \rangle$	$\langle \theta \rangle$	$d^2\sigma/dpd\Omega$				$\langle p_T \rangle$	$\langle \theta \rangle$	$d^2\sigma/dpd\Omega$					
			188.17	$\pm$	8.82	$\pm$	17.14	0.145	114.4	143.89	$\pm$	5.64	$\pm$	7.02
0.13–0.16	0.146	97.6	147.23	$\pm$	5.65	$\pm$	7.68	0.179	114.2	103.65	$\pm$	3.89	$\pm$	3.74
0.16–0.20	0.180	97.7	101.55	$\pm$	4.42	$\pm$	3.79	0.219	113.5	67.06	$\pm$	3.11	$\pm$	2.34
0.20–0.24	0.219	97.3	68.94	$\pm$	2.98	$\pm$	2.64	0.331	113.1	34.04	$\pm$	1.77	$\pm$	1.41
0.24–0.30	0.268	97.1	36.05	$\pm$	2.15	$\pm$	1.62	0.390	113.3	18.58	$\pm$	1.35	$\pm$	1.06
0.30–0.36	0.330	96.8	23.01	$\pm$	1.72	$\pm$	1.35	0.460	113.9	11.72	$\pm$	1.07	$\pm$	0.89
0.36–0.42	0.393	96.3	14.96	$\pm$	1.22	$\pm$	1.13	0.545	112.8	6.88	$\pm$	0.71	$\pm$	0.68
0.42–0.50	0.460	95.9	8.90	$\pm$	0.82	$\pm$	0.88	0.665	112.2	1.97	$\pm$	0.33	$\pm$	0.26
0.50–0.60	0.656	96.5	3.98	$\pm$	0.48	$\pm$	0.52	0.791	114.5	0.71	$\pm$	0.15	$\pm$	0.15
0.60–0.72							1.029	114.5	0.09	$\pm$	0.03	$\pm$	0.03	

Table A.12: Double-differential inclusive cross-section  $d^2\sigma/dpd\Omega$  [mb/(GeV/c sr)] of the production of  $\pi^-$ 's in  $p + \text{Sn} \rightarrow \pi^- + X$  interactions with  $+5.0$  GeV/c beam momentum; the first error is statistical, the second systematic;  $p_T$  in GeV/c, polar angle  $\theta$  in degrees.

$p_T$	20 < $\theta$ < 30			30 < $\theta$ < 40		
	$\langle p_T \rangle$	$\langle \theta \rangle$	$d^2\sigma/dpd\Omega$	$\langle p_T \rangle$	$\langle \theta \rangle$	$d^2\sigma/dpd\Omega$
0.10–0.13	0.116	25.1	250.59 ± 10.74 ± 17.56	0.115	35.2	222.19 ± 9.69 ± 15.99
0.13–0.16	0.145	24.8	278.35 ± 10.67 ± 16.08	0.145	34.9	247.11 ± 9.79 ± 14.40
0.16–0.20	0.180	24.9	274.12 ± 8.85 ± 13.11	0.179	34.8	221.26 ± 7.69 ± 10.43
0.20–0.24	0.219	25.1	247.54 ± 8.30 ± 10.04	0.219	35.0	224.47 ± 7.82 ± 9.04
0.24–0.30	0.268	25.0	206.55 ± 6.09 ± 6.81	0.269	34.9	181.84 ± 5.71 ± 6.00
0.30–0.36	0.327	25.2	144.75 ± 5.16 ± 4.53	0.328	34.8	143.73 ± 5.03 ± 4.24
0.36–0.42	0.388	25.2	99.66 ± 4.22 ± 3.14	0.389	34.9	111.79 ± 4.52 ± 3.64
0.42–0.50	0.456	25.2	65.79 ± 3.01 ± 2.52	0.457	35.1	74.43 ± 3.16 ± 2.69
0.50–0.60	0.545	25.1	35.77 ± 1.94 ± 1.79	0.543	34.7	39.95 ± 2.05 ± 1.93
0.60–0.72	0.647	24.9	19.35 ± 1.33 ± 1.37	0.651	35.1	20.80 ± 1.37 ± 1.38
0.72–0.90				0.799	35.0	8.25 ± 0.71 ± 0.77
$p_T$	40 < $\theta$ < 50			50 < $\theta$ < 60		
	$\langle p_T \rangle$	$\langle \theta \rangle$	$d^2\sigma/dpd\Omega$	$\langle p_T \rangle$	$\langle \theta \rangle$	$d^2\sigma/dpd\Omega$
0.10–0.13	0.115	45.1	238.53 ± 10.48 ± 17.57	0.144	54.8	233.86 ± 9.60 ± 13.69
0.13–0.16	0.144	44.8	201.71 ± 8.60 ± 11.48	0.179	54.9	183.44 ± 7.01 ± 8.66
0.16–0.20	0.179	45.1	208.17 ± 7.39 ± 9.91	0.219	54.7	159.26 ± 6.37 ± 6.47
0.20–0.24	0.219	44.9	199.91 ± 7.26 ± 8.17	0.268	54.8	130.25 ± 4.80 ± 4.37
0.24–0.30	0.268	44.8	153.85 ± 5.26 ± 5.23	0.326	54.9	102.34 ± 4.31 ± 3.26
0.30–0.36	0.329	44.7	124.62 ± 4.69 ± 3.70	0.386	54.7	80.36 ± 3.86 ± 2.87
0.36–0.42	0.387	44.8	89.34 ± 4.05 ± 2.97	0.458	54.8	55.36 ± 2.74 ± 2.21
0.42–0.50	0.457	45.1	74.16 ± 3.20 ± 2.85	0.546	54.9	36.50 ± 2.00 ± 1.97
0.50–0.60	0.542	44.9	36.80 ± 1.99 ± 1.86	0.646	54.9	16.90 ± 1.24 ± 1.23
0.60–0.72	0.647	45.0	16.80 ± 1.22 ± 1.18	0.785	54.5	6.36 ± 0.62 ± 0.64
0.72–0.90	0.786	45.0	8.97 ± 0.75 ± 0.89	1.004	55.0	1.61 ± 0.22 ± 0.24
$p_T$	60 < $\theta$ < 75			75 < $\theta$ < 90		
	$\langle p_T \rangle$	$\langle \theta \rangle$	$d^2\sigma/dpd\Omega$	$\langle p_T \rangle$	$\langle \theta \rangle$	$d^2\sigma/dpd\Omega$
0.13–0.16	0.145	67.3	209.19 ± 7.92 ± 11.84	0.145	82.2	201.19 ± 8.76 ± 14.61
0.16–0.20	0.179	67.4	179.47 ± 5.68 ± 7.86	0.178	82.2	162.16 ± 5.73 ± 7.31
0.20–0.24	0.218	67.5	143.52 ± 4.97 ± 5.35	0.218	82.2	128.06 ± 4.89 ± 5.01
0.24–0.30	0.266	66.9	107.40 ± 3.52 ± 3.38	0.266	82.2	79.23 ± 3.10 ± 2.66
0.30–0.36	0.326	66.9	74.96 ± 3.01 ± 2.41	0.327	82.2	50.93 ± 2.47 ± 1.82
0.36–0.42	0.385	67.2	56.06 ± 2.63 ± 2.09	0.387	82.2	34.43 ± 2.07 ± 1.58
0.42–0.50	0.452	67.0	37.88 ± 1.86 ± 1.71	0.452	81.4	23.81 ± 1.51 ± 1.40
0.50–0.60	0.540	67.1	24.00 ± 1.33 ± 1.43	0.536	82.3	14.98 ± 1.07 ± 1.16
0.60–0.72	0.641	67.1	11.89 ± 0.86 ± 0.96	0.646	81.6	7.02 ± 0.66 ± 0.71
0.72–0.90	0.783	66.1	4.30 ± 0.42 ± 0.48	0.783	81.1	2.09 ± 0.27 ± 0.29
0.90–1.25	1.025	66.3	0.78 ± 0.11 ± 0.13	0.992	81.2	0.26 ± 0.06 ± 0.06
$p_T$	90 < $\theta$ < 105			105 < $\theta$ < 125		
	$\langle p_T \rangle$	$\langle \theta \rangle$	$d^2\sigma/dpd\Omega$	$\langle p_T \rangle$	$\langle \theta \rangle$	$d^2\sigma/dpd\Omega$
0.13–0.16	0.145	97.8	194.34 ± 10.38 ± 13.98	0.143	114.1	160.68 ± 8.64 ± 7.71
0.16–0.20	0.178	97.3	154.72 ± 5.73 ± 7.18	0.177	113.7	103.54 ± 3.91 ± 3.74
0.20–0.24	0.218	97.4	95.94 ± 4.24 ± 3.45	0.217	113.3	57.42 ± 2.80 ± 2.17
0.24–0.30	0.267	97.2	64.64 ± 2.83 ± 2.36	0.263	113.4	32.54 ± 1.74 ± 1.51
0.30–0.36	0.326	97.0	36.58 ± 2.18 ± 1.85	0.325	114.0	15.68 ± 1.20 ± 1.01
0.36–0.42	0.385	96.7	21.02 ± 1.62 ± 1.28	0.383	112.9	12.92 ± 1.10 ± 1.11
0.42–0.50	0.448	96.2	15.38 ± 1.19 ± 1.21	0.446	112.9	6.33 ± 0.67 ± 0.70
0.50–0.60	0.538	96.9	6.69 ± 0.71 ± 0.71	0.531	112.8	2.55 ± 0.36 ± 0.39
0.60–0.72	0.646	96.9	2.90 ± 0.41 ± 0.42	0.636	110.3	0.55 ± 0.12 ± 0.14
0.72–0.90	0.766	95.7	0.45 ± 0.12 ± 0.10	0.767	109.4	0.10 ± 0.04 ± 0.04
0.90–1.25	1.008	95.2	0.08 ± 0.03 ± 0.03			

Table A.13: Double-differential inclusive cross-section  $d^2\sigma/dpd\Omega$  [mb/(GeV/c sr)] of the production of protons in  $\pi^+ + \text{Sn} \rightarrow p + X$  interactions with +5.0 GeV/c beam momentum; the first error is statistical, the second systematic;  $p_T$  in GeV/c, polar angle  $\theta$  in degrees.

$p_T$	20 < $\theta$ < 30						30 < $\theta$ < 40					
	$\langle p_T \rangle$	$\langle \theta \rangle$	$d^2\sigma/dpd\Omega$				$\langle p_T \rangle$	$\langle \theta \rangle$	$d^2\sigma/dpd\Omega$			
			906.81	$\pm$	14.99	$\pm$	44.53	913.95	$\pm$	13.91	$\pm$	37.15
0.20–0.24	0.220	25.1	906.81	$\pm$	14.99	$\pm$	44.53	913.95	$\pm$	13.91	$\pm$	37.15
0.24–0.30	0.269	25.2	813.11	$\pm$	11.06	$\pm$	35.87	913.95	$\pm$	13.91	$\pm$	37.15
0.30–0.36	0.328	25.2	602.40	$\pm$	9.51	$\pm$	24.49	763.01	$\pm$	10.47	$\pm$	27.06
0.36–0.42	0.389	25.4	503.61	$\pm$	8.75	$\pm$	19.04	613.85	$\pm$	9.54	$\pm$	20.86
0.42–0.50	0.458	25.3	358.72	$\pm$	6.20	$\pm$	12.48	470.86	$\pm$	7.28	$\pm$	16.30
0.50–0.60	0.547	25.4	253.74	$\pm$	4.59	$\pm$	9.02	333.92	$\pm$	5.49	$\pm$	11.93
0.60–0.72	0.654	25.3	175.56	$\pm$	3.40	$\pm$	7.04	220.34	$\pm$	4.05	$\pm$	9.67
0.72–0.90								126.82	$\pm$	2.46	$\pm$	7.16
			0.798		35.1							
$p_T$	40 < $\theta$ < 50						50 < $\theta$ < 60					
	$\langle p_T \rangle$	$\langle \theta \rangle$	$d^2\sigma/dpd\Omega$				$\langle p_T \rangle$	$\langle \theta \rangle$	$d^2\sigma/dpd\Omega$			
			893.05	$\pm$	11.19	$\pm$	27.17	771.46	$\pm$	10.16	$\pm$	20.22
0.30–0.36	0.330	45.1	731.12	$\pm$	10.10	$\pm$	20.39	638.25	$\pm$	8.20	$\pm$	17.43
0.36–0.42	0.391	45.1	556.40	$\pm$	7.78	$\pm$	16.23	422.53	$\pm$	6.13	$\pm$	14.81
0.42–0.50	0.460	45.1	391.31	$\pm$	6.08	$\pm$	14.84	250.68	$\pm$	4.54	$\pm$	13.02
0.50–0.60	0.550	45.1	247.36	$\pm$	4.42	$\pm$	11.63	122.70	$\pm$	2.62	$\pm$	8.61
0.60–0.72	0.659	45.1	134.95	$\pm$	2.69	$\pm$	8.39	31.60	$\pm$	0.93	$\pm$	3.31
0.72–0.90	0.805	45.0	44.20	$\pm$	1.06	$\pm$	3.85	1.043				
0.90–1.25	1.047	45.0										
$p_T$	60 < $\theta$ < 75						75 < $\theta$ < 90					
	$\langle p_T \rangle$	$\langle \theta \rangle$	$d^2\sigma/dpd\Omega$				$\langle p_T \rangle$	$\langle \theta \rangle$	$d^2\sigma/dpd\Omega$			
			409.29	$\pm$	4.70	$\pm$	14.17	345.51	$\pm$	4.26	$\pm$	15.90
0.50–0.60	0.552	67.5	239.96	$\pm$	3.48	$\pm$	12.93	180.82	$\pm$	2.92	$\pm$	11.55
0.60–0.72	0.662	67.4	97.74	$\pm$	1.93	$\pm$	9.04	63.12	$\pm$	1.61	$\pm$	7.15
0.72–0.90	0.809	67.0	22.60	$\pm$	0.67	$\pm$	3.33					
0.90–1.25	1.049	66.8										
$p_T$	90 < $\theta$ < 105						105 < $\theta$ < 125					
	$\langle p_T \rangle$	$\langle \theta \rangle$	$d^2\sigma/dpd\Omega$				$\langle p_T \rangle$	$\langle \theta \rangle$	$d^2\sigma/dpd\Omega$			
			241.98	$\pm$	3.56	$\pm$	15.11	234.08	$\pm$	3.26	$\pm$	12.81
0.42–0.50	0.550	97.1	112.25	$\pm$	2.34	$\pm$	8.98	113.1	$\pm$	2.13	$\pm$	9.40
0.50–0.60	0.660	96.9						34.87	$\pm$	1.25	$\pm$	5.22
0.60–0.72												

Table A.14: Double-differential inclusive cross-section  $d^2\sigma/dpd\Omega$  [mb/(GeV/c sr)] of the production of  $\pi^+$ 's in  $\pi^+ + \text{Sn} \rightarrow \pi^+ + \text{X}$  interactions with +5.0 GeV/c beam momentum; the first error is statistical, the second systematic;  $p_T$  in GeV/c, polar angle  $\theta$  in degrees.

			20 < $\theta$ < 30					30 < $\theta$ < 40						
$p_T$	$\langle p_T \rangle$	$\langle \theta \rangle$	$d^2\sigma/dpd\Omega$					$\langle p_T \rangle$	$\langle \theta \rangle$	$d^2\sigma/dpd\Omega$				
0.10–0.13	0.115	24.8	313.16	±	10.96	±	21.50	0.115	35.0	295.47	±	10.16	±	20.54
0.13–0.16	0.145	24.8	369.66	±	10.84	±	19.84	0.145	34.8	296.42	±	9.34	±	16.10
0.16–0.20	0.180	24.8	431.13	±	9.94	±	20.15	0.181	34.8	342.93	±	8.82	±	15.98
0.20–0.24	0.220	24.8	462.94	±	10.13	±	18.54	0.220	34.8	349.50	±	8.67	±	13.74
0.24–0.30	0.269	24.9	441.08	±	8.06	±	15.28	0.270	34.7	336.90	±	6.95	±	11.15
0.30–0.36	0.329	25.0	368.43	±	7.23	±	10.96	0.330	34.8	296.36	±	6.57	±	8.94
0.36–0.42	0.389	24.8	319.99	±	6.68	±	9.60	0.389	34.8	243.55	±	5.83	±	6.89
0.42–0.50	0.458	25.0	253.54	±	5.11	±	9.24	0.457	34.8	201.16	±	4.63	±	6.82
0.50–0.60	0.547	25.0	160.67	±	3.49	±	7.94	0.546	34.8	133.03	±	3.25	±	5.89
0.60–0.72	0.655	25.0	92.13	±	2.24	±	6.81	0.655	34.7	79.21	±	2.13	±	5.19
0.72–0.90								0.798	34.7	38.80	±	1.12	±	4.05
			40 < $\theta$ < 50					50 < $\theta$ < 60						
$p_T$	$\langle p_T \rangle$	$\langle \theta \rangle$	$d^2\sigma/dpd\Omega$					$\langle p_T \rangle$	$\langle \theta \rangle$	$d^2\sigma/dpd\Omega$				
0.10–0.13	0.115	45.1	267.08	±	10.40	±	19.56	0.145	55.0	249.74	±	9.02	±	14.34
0.13–0.16	0.145	44.9	281.86	±	9.01	±	15.43	0.180	54.8	275.06	±	7.71	±	12.59
0.16–0.20	0.180	44.9	294.16	±	8.01	±	13.64	0.220	55.0	229.93	±	6.96	±	9.06
0.20–0.24	0.220	44.9	269.39	±	7.63	±	10.76	0.269	54.7	213.41	±	5.58	±	7.23
0.24–0.30	0.270	44.8	271.53	±	6.21	±	9.06	0.331	54.7	181.15	±	5.14	±	5.44
0.30–0.36	0.330	44.8	225.18	±	5.65	±	6.61	0.391	54.7	157.41	±	4.84	±	5.26
0.36–0.42	0.390	44.8	201.33	±	5.49	±	6.75	0.460	54.7	129.11	±	3.74	±	4.60
0.42–0.50	0.460	44.7	163.66	±	4.24	±	5.70	0.548	54.7	83.04	±	2.71	±	3.97
0.50–0.60	0.550	44.6	108.69	±	2.99	±	4.60	0.659	54.7	47.54	±	1.82	±	3.10
0.60–0.72	0.658	44.6	67.89	±	2.10	±	4.07	0.802	54.7	23.40	±	0.97	±	2.12
0.72–0.90	0.800	44.6	30.59	±	1.06	±	2.81	1.039	54.5	6.92	±	0.35	±	1.01
			60 < $\theta$ < 75					75 < $\theta$ < 90						
$p_T$	$\langle p_T \rangle$	$\langle \theta \rangle$	$d^2\sigma/dpd\Omega$					$\langle p_T \rangle$	$\langle \theta \rangle$	$d^2\sigma/dpd\Omega$				
0.13–0.16	0.146	67.5	227.11	±	7.33	±	13.40	0.147	82.1	184.19	±	9.00	±	11.21
0.16–0.20	0.181	67.2	228.08	±	5.74	±	10.38	0.181	82.2	205.60	±	5.68	±	9.35
0.20–0.24	0.221	67.3	202.41	±	5.36	±	7.69	0.220	82.0	176.24	±	5.19	±	7.47
0.24–0.30	0.271	67.1	166.77	±	4.04	±	5.52	0.270	82.1	124.70	±	3.51	±	4.17
0.30–0.36	0.331	67.0	135.89	±	3.70	±	4.56	0.330	81.9	92.89	±	3.03	±	3.13
0.36–0.42	0.392	66.7	104.01	±	3.19	±	3.53	0.393	82.2	65.39	±	2.55	±	2.64
0.42–0.50	0.462	66.8	83.38	±	2.46	±	3.37	0.463	81.9	51.26	±	1.95	±	2.58
0.50–0.60	0.552	66.9	57.36	±	1.84	±	3.18	0.553	81.7	35.19	±	1.46	±	2.41
0.60–0.72	0.662	66.6	28.71	±	1.15	±	2.14	0.662	81.8	18.84	±	0.95	±	1.70
0.72–0.90	0.809	66.4	14.78	±	0.65	±	1.56	0.804	81.8	5.60	±	0.39	±	0.70
0.90–1.25	1.039	66.8	2.79	±	0.16	±	0.47	1.036	82.0	1.08	±	0.10	±	0.22
			90 < $\theta$ < 105					105 < $\theta$ < 125						
$p_T$	$\langle p_T \rangle$	$\langle \theta \rangle$	$d^2\sigma/dpd\Omega$					$\langle p_T \rangle$	$\langle \theta \rangle$	$d^2\sigma/dpd\Omega$				
0.13–0.16	0.146	97.7	239.53	±	9.17	±	24.98	0.146	114.9	177.21	±	5.61	±	8.61
0.16–0.20	0.180	97.4	203.48	±	5.90	±	9.91	0.179	114.3	145.23	±	4.12	±	5.17
0.20–0.24	0.220	97.3	154.71	±	4.88	±	5.60	0.221	113.8	97.06	±	3.34	±	3.24
0.24–0.30	0.269	97.1	99.01	±	3.20	±	3.71	0.269	113.7	56.27	±	2.02	±	2.21
0.30–0.36	0.330	96.9	56.69	±	2.40	±	2.41	0.330	113.6	35.50	±	1.66	±	1.95
0.36–0.42	0.393	96.7	45.98	±	2.17	±	2.52	0.391	113.6	25.17	±	1.39	±	1.82
0.42–0.50	0.461	96.7	29.88	±	1.52	±	2.13	0.461	113.4	12.77	±	0.86	±	1.19
0.50–0.60	0.550	96.5	18.75	±	1.06	±	1.76	0.548	112.3	6.08	±	0.51	±	0.76
0.60–0.72	0.655	96.4	8.12	±	0.61	±	1.01	0.659	112.6	1.51	±	0.20	±	0.27
0.72–0.90	0.811	94.7	2.14	±	0.23	±	0.37	0.804	112.4	0.29	±	0.05	±	0.08
0.90–1.25	1.035	95.6	0.22	±	0.04	±	0.07							

Table A.15: Double-differential inclusive cross-section  $d^2\sigma/dpd\Omega$  [mb/(GeV/c sr)] of the production of  $\pi^-$ 's in  $\pi^+ + \text{Sn} \rightarrow \pi^- + \text{X}$  interactions with +5.0 GeV/c beam momentum; the first error is statistical, the second systematic;  $p_T$  in GeV/c, polar angle  $\theta$  in degrees.

$p_T$	20 < $\theta$ < 30						30 < $\theta$ < 40						
	$\langle p_T \rangle$	$\langle \theta \rangle$	$d^2\sigma/dpd\Omega$				$\langle p_T \rangle$	$\langle \theta \rangle$	$d^2\sigma/dpd\Omega$				
			$\langle p_T \rangle$	$\langle \theta \rangle$	$d^2\sigma/dpd\Omega$	$d^2\sigma/dpd\Omega$			$\langle p_T \rangle$	$\langle \theta \rangle$	$d^2\sigma/dpd\Omega$	$d^2\sigma/dpd\Omega$	
0.10–0.13	0.115	24.9	346.43	$\pm$ 11.01	$\pm$ 23.48	0.115	35.0	283.37	$\pm$ 9.56	$\pm$ 20.26			
0.13–0.16	0.145	24.8	378.45	$\pm$ 10.97	$\pm$ 21.51	0.145	34.9	338.27	$\pm$ 10.17	$\pm$ 19.41			
0.16–0.20	0.180	24.9	399.88	$\pm$ 9.54	$\pm$ 18.92	0.180	35.0	308.56	$\pm$ 8.11	$\pm$ 14.40			
0.20–0.24	0.220	24.9	373.77	$\pm$ 9.08	$\pm$ 15.02	0.220	34.9	294.47	$\pm$ 7.99	$\pm$ 11.78			
0.24–0.30	0.269	25.0	313.21	$\pm$ 6.69	$\pm$ 10.18	0.269	34.7	275.99	$\pm$ 6.26	$\pm$ 9.04			
0.30–0.36	0.329	24.9	247.09	$\pm$ 5.99	$\pm$ 7.58	0.329	34.7	209.73	$\pm$ 5.44	$\pm$ 6.06			
0.36–0.42	0.388	25.0	187.11	$\pm$ 5.17	$\pm$ 5.58	0.389	34.9	180.55	$\pm$ 5.15	$\pm$ 5.76			
0.42–0.50	0.458	24.9	133.87	$\pm$ 3.83	$\pm$ 4.96	0.456	34.8	117.86	$\pm$ 3.55	$\pm$ 4.13			
0.50–0.60	0.546	24.9	81.15	$\pm$ 2.61	$\pm$ 3.87	0.546	35.0	77.30	$\pm$ 2.57	$\pm$ 3.59			
0.60–0.72	0.654	25.0	46.73	$\pm$ 1.87	$\pm$ 3.17	0.656	35.1	41.60	$\pm$ 1.73	$\pm$ 2.65			
0.72–0.90						0.794	35.1	16.91	$\pm$ 0.91	$\pm$ 1.51			
$p_T$	40 < $\theta$ < 50						50 < $\theta$ < 60						
	$\langle p_T \rangle$	$\langle \theta \rangle$	$d^2\sigma/dpd\Omega$				$\langle p_T \rangle$	$\langle \theta \rangle$	$d^2\sigma/dpd\Omega$				
			$\langle p_T \rangle$	$\langle \theta \rangle$	$d^2\sigma/dpd\Omega$	$d^2\sigma/dpd\Omega$			$\langle p_T \rangle$	$\langle \theta \rangle$	$d^2\sigma/dpd\Omega$	$d^2\sigma/dpd\Omega$	
0.10–0.13	0.115	45.1	283.79	$\pm$ 10.23	$\pm$ 20.82		0.145	55.0	252.07	$\pm$ 8.87	$\pm$ 14.72		
0.13–0.16	0.145	44.8	287.98	$\pm$ 9.15	$\pm$ 16.29		0.179	54.9	226.50	$\pm$ 6.88	$\pm$ 10.64		
0.16–0.20	0.179	44.9	255.82	$\pm$ 7.28	$\pm$ 12.08		0.219	54.7	190.90	$\pm$ 6.23	$\pm$ 7.66		
0.20–0.24	0.219	44.9	248.29	$\pm$ 7.22	$\pm$ 10.03		0.269	54.9	173.56	$\pm$ 4.97	$\pm$ 5.79		
0.24–0.30	0.269	44.8	219.43	$\pm$ 5.60	$\pm$ 7.46		0.328	54.8	150.71	$\pm$ 4.68	$\pm$ 4.72		
0.30–0.36	0.328	44.9	172.18	$\pm$ 4.95	$\pm$ 5.02		0.388	54.7	110.78	$\pm$ 4.03	$\pm$ 3.83		
0.36–0.42	0.388	44.9	141.06	$\pm$ 4.54	$\pm$ 4.62		0.456	54.8	82.32	$\pm$ 2.99	$\pm$ 3.16		
0.42–0.50	0.455	44.9	105.87	$\pm$ 3.41	$\pm$ 3.98		0.542	54.8	52.56	$\pm$ 2.14	$\pm$ 2.72		
0.50–0.60	0.542	44.6	67.94	$\pm$ 2.41	$\pm$ 3.33		0.647	54.6	29.51	$\pm$ 1.46	$\pm$ 2.06		
0.60–0.72	0.647	44.7	37.64	$\pm$ 1.63	$\pm$ 2.54		0.72–0.90	54.9	14.09	$\pm$ 0.82	$\pm$ 1.36		
0.72–0.90	0.785	45.0	15.00	$\pm$ 0.88	$\pm$ 1.44		0.90–1.25	54.7	3.34	$\pm$ 0.29	$\pm$ 0.49		
$p_T$	60 < $\theta$ < 75						75 < $\theta$ < 90						
	$\langle p_T \rangle$	$\langle \theta \rangle$	$d^2\sigma/dpd\Omega$				$\langle p_T \rangle$	$\langle \theta \rangle$	$d^2\sigma/dpd\Omega$				
			$\langle p_T \rangle$	$\langle \theta \rangle$	$d^2\sigma/dpd\Omega$	$d^2\sigma/dpd\Omega$			$\langle p_T \rangle$	$\langle \theta \rangle$	$d^2\sigma/dpd\Omega$	$d^2\sigma/dpd\Omega$	
0.13–0.16	0.145	67.3	247.24	$\pm$ 7.75	$\pm$ 14.04		0.145	82.0	225.05	$\pm$ 9.24	$\pm$ 15.13		
0.16–0.20	0.179	67.4	214.30	$\pm$ 5.56	$\pm$ 9.40		0.179	82.4	189.27	$\pm$ 5.49	$\pm$ 8.63		
0.20–0.24	0.218	67.0	162.52	$\pm$ 4.69	$\pm$ 6.03		0.218	82.3	150.20	$\pm$ 4.75	$\pm$ 5.97		
0.24–0.30	0.267	67.2	132.92	$\pm$ 3.51	$\pm$ 4.15		0.266	82.2	108.26	$\pm$ 3.24	$\pm$ 3.63		
0.30–0.36	0.327	67.0	110.89	$\pm$ 3.27	$\pm$ 3.51		0.326	82.1	74.82	$\pm$ 2.69	$\pm$ 2.61		
0.36–0.42	0.385	67.0	85.88	$\pm$ 2.90	$\pm$ 3.10		0.386	81.9	55.29	$\pm$ 2.34	$\pm$ 2.44		
0.42–0.50	0.454	67.1	61.31	$\pm$ 2.12	$\pm$ 2.68		0.452	81.6	38.73	$\pm$ 1.71	$\pm$ 2.20		
0.50–0.60	0.540	67.1	38.38	$\pm$ 1.50	$\pm$ 2.22		0.539	81.6	25.46	$\pm$ 1.25	$\pm$ 1.91		
0.60–0.72	0.643	66.6	22.09	$\pm$ 1.05	$\pm$ 1.74		0.638	81.7	11.56	$\pm$ 0.76	$\pm$ 1.13		
0.72–0.90	0.777	67.1	8.27	$\pm$ 0.52	$\pm$ 0.89		0.776	80.9	4.33	$\pm$ 0.35	$\pm$ 0.58		
0.90–1.25	0.994	66.8	1.79	$\pm$ 0.15	$\pm$ 0.29		1.005	81.3	0.74	$\pm$ 0.09	$\pm$ 0.16		
$p_T$	90 < $\theta$ < 105						105 < $\theta$ < 125						
	$\langle p_T \rangle$	$\langle \theta \rangle$	$d^2\sigma/dpd\Omega$				$\langle p_T \rangle$	$\langle \theta \rangle$	$d^2\sigma/dpd\Omega$				
			$\langle p_T \rangle$	$\langle \theta \rangle$	$d^2\sigma/dpd\Omega$	$d^2\sigma/dpd\Omega$			$\langle p_T \rangle$	$\langle \theta \rangle$	$d^2\sigma/dpd\Omega$	$d^2\sigma/dpd\Omega$	
0.13–0.16	0.145	97.4	247.56	$\pm$ 8.77	$\pm$ 16.18		0.144	114.9	178.50	$\pm$ 5.71	$\pm$ 8.57		
0.16–0.20	0.178	97.4	181.85	$\pm$ 5.52	$\pm$ 8.31		0.177	114.1	126.07	$\pm$ 3.86	$\pm$ 4.54		
0.20–0.24	0.217	97.3	123.68	$\pm$ 4.30	$\pm$ 4.40		0.218	114.0	68.64	$\pm$ 2.74	$\pm$ 2.51		
0.24–0.30	0.266	97.0	76.30	$\pm$ 2.74	$\pm$ 2.73		0.267	113.9	46.13	$\pm$ 1.84	$\pm$ 2.06		
0.30–0.36	0.325	97.1	52.90	$\pm$ 2.36	$\pm$ 2.63		0.326	113.6	28.62	$\pm$ 1.45	$\pm$ 1.77		
0.36–0.42	0.386	97.1	37.42	$\pm$ 1.94	$\pm$ 2.19		0.386	113.2	17.58	$\pm$ 1.15	$\pm$ 1.44		
0.42–0.50	0.454	97.1	23.83	$\pm$ 1.33	$\pm$ 1.82		0.451	113.5	11.80	$\pm$ 0.81	$\pm$ 1.26		
0.50–0.60	0.540	96.9	14.05	$\pm$ 0.91	$\pm$ 1.44		0.535	112.8	3.79	$\pm$ 0.40	$\pm$ 0.54		
0.60–0.72	0.639	96.4	5.40	$\pm$ 0.51	$\pm$ 0.75		0.634	112.1	1.13	$\pm$ 0.16	$\pm$ 0.25		
0.72–0.90	0.772	96.5	1.49	$\pm$ 0.19	$\pm$ 0.30		0.767	114.0	0.32	$\pm$ 0.07	$\pm$ 0.10		
0.90–1.25	0.987	95.7	0.19	$\pm$ 0.04	$\pm$ 0.06								

Table A.16: Double-differential inclusive cross-section  $d^2\sigma/dpd\Omega$  [mb/(GeV/c sr)] of the production of protons in  $\pi^- + \text{Sn} \rightarrow p + X$  interactions with  $-5.0 \text{ GeV}/c$  beam momentum; the first error is statistical, the second systematic;  $p_T$  in  $\text{GeV}/c$ , polar angle  $\theta$  in degrees.

$p_T$	20 < $\theta$ < 30				30 < $\theta$ < 40			
	$\langle p_T \rangle$	$\langle \theta \rangle$	$d^2\sigma/dpd\Omega$		$\langle p_T \rangle$	$\langle \theta \rangle$	$d^2\sigma/dpd\Omega$	
0.20–0.24	0.220	25.2	856.58	$\pm$	13.52	$\pm$	42.10	
0.24–0.30	0.269	25.3	736.45	$\pm$	10.07	$\pm$	32.66	0.271
0.30–0.36	0.330	25.3	571.22	$\pm$	8.88	$\pm$	23.62	0.330
0.36–0.42	0.390	25.3	425.50	$\pm$	7.64	$\pm$	16.19	0.390
0.42–0.50	0.459	25.3	316.82	$\pm$	5.64	$\pm$	11.65	0.460
0.50–0.60	0.549	25.4	224.24	$\pm$	4.24	$\pm$	8.38	0.550
0.60–0.72	0.657	25.4	138.00	$\pm$	3.00	$\pm$	5.95	0.659
0.72–0.90								0.805
								35.2
								92.70
								$\pm$
								2.08
								$\pm$
								5.55
$40 < \theta < 50$								
$p_T$	$\langle p_T \rangle$	$\langle \theta \rangle$	$d^2\sigma/dpd\Omega$		$\langle p_T \rangle$	$\langle \theta \rangle$	$d^2\sigma/dpd\Omega$	
0.30–0.36	0.329	45.0	804.65	$\pm$	10.15	$\pm$	24.53	
0.36–0.42	0.389	45.1	647.56	$\pm$	9.06	$\pm$	18.21	0.389
0.42–0.50	0.458	45.1	513.84	$\pm$	7.21	$\pm$	15.64	0.458
0.50–0.60	0.547	45.2	340.54	$\pm$	5.47	$\pm$	13.92	0.547
0.60–0.72	0.655	45.1	215.94	$\pm$	4.00	$\pm$	11.01	0.655
0.72–0.90	0.799	45.2	108.90	$\pm$	2.35	$\pm$	7.27	0.800
0.90–1.25	1.032	45.1	33.02	$\pm$	0.90	$\pm$	3.16	1.032
								55.1
								30.56
								$\pm$
								0.91
								$\pm$
								3.46
$60 < \theta < 75$								
$p_T$	$\langle p_T \rangle$	$\langle \theta \rangle$	$d^2\sigma/dpd\Omega$		$\langle p_T \rangle$	$\langle \theta \rangle$	$d^2\sigma/dpd\Omega$	
0.50–0.60	0.546	67.5	354.43	$\pm$	4.19	$\pm$	12.49	0.544
0.60–0.72	0.654	67.2	199.42	$\pm$	3.09	$\pm$	11.69	0.653
0.72–0.90	0.798	66.9	85.39	$\pm$	1.76	$\pm$	8.34	0.793
								81.8
								45.17
								$\pm$
								1.35
								$\pm$
								5.92
$90 < \theta < 105$								
$p_T$	$\langle p_T \rangle$	$\langle \theta \rangle$	$d^2\sigma/dpd\Omega$		$\langle p_T \rangle$	$\langle \theta \rangle$	$d^2\sigma/dpd\Omega$	
0.42–0.50								
0.50–0.60	0.544	97.1	210.20	$\pm$	3.15	$\pm$	13.29	0.544
0.60–0.72	0.652	97.0	92.43	$\pm$	2.02	$\pm$	7.49	0.649
								113.0
								113.1
								89.97
								$\pm$
								1.84
								$\pm$
								7.64
								1.02
								$\pm$
								4.00

Table A.17: Double-differential inclusive cross-section  $d^2\sigma/dpd\Omega$  [mb/(GeV/c sr)] of the production of  $\pi^+$ 's in  $\pi^- + \text{Sn} \rightarrow \pi^+ + \text{X}$  interactions with  $-5.0$  GeV/c beam momentum; the first error is statistical, the second systematic;  $p_T$  in GeV/c, polar angle  $\theta$  in degrees.

		20 < $\theta$ < 30				30 < $\theta$ < 40								
$p_T$	$\langle p_T \rangle$	$\langle \theta \rangle$	$d^2\sigma/dpd\Omega$			$\langle p_T \rangle$	$\langle \theta \rangle$	$d^2\sigma/dpd\Omega$						
0.10–0.13	0.116	25.0	273.83	$\pm$	9.27	$\pm$	18.20	0.116	35.0	228.48	$\pm$	8.27	$\pm$	16.00
0.13–0.16	0.146	24.7	331.82	$\pm$	9.68	$\pm$	18.31	0.145	34.9	255.38	$\pm$	8.07	$\pm$	14.02
0.16–0.20	0.181	24.8	356.87	$\pm$	8.46	$\pm$	16.81	0.180	34.8	280.93	$\pm$	7.37	$\pm$	12.98
0.20–0.24	0.220	24.8	369.98	$\pm$	8.40	$\pm$	14.71	0.220	34.8	297.91	$\pm$	7.55	$\pm$	11.84
0.24–0.30	0.271	24.9	358.42	$\pm$	6.85	$\pm$	12.77	0.270	34.6	274.84	$\pm$	5.84	$\pm$	9.13
0.30–0.36	0.329	24.8	275.64	$\pm$	5.84	$\pm$	8.29	0.331	34.8	227.52	$\pm$	5.36	$\pm$	6.70
0.36–0.42	0.391	24.9	219.23	$\pm$	5.26	$\pm$	6.95	0.390	34.9	192.13	$\pm$	4.95	$\pm$	5.67
0.42–0.50	0.460	25.0	166.30	$\pm$	3.91	$\pm$	6.40	0.460	34.7	139.37	$\pm$	3.60	$\pm$	4.70
0.50–0.60	0.549	25.0	96.95	$\pm$	2.51	$\pm$	4.84	0.550	34.9	98.24	$\pm$	2.66	$\pm$	4.53
0.60–0.72	0.656	25.0	52.18	$\pm$	1.57	$\pm$	3.89	0.657	34.7	51.56	$\pm$	1.65	$\pm$	3.41
0.72–0.90	0.801	34.9	20.20	$\pm$	0.74	$\pm$	2.12	0.801	34.9	20.20	$\pm$	0.74	$\pm$	2.12
		40 < $\theta$ < 50				50 < $\theta$ < 60								
$p_T$	$\langle p_T \rangle$	$\langle \theta \rangle$	$d^2\sigma/dpd\Omega$			$\langle p_T \rangle$	$\langle \theta \rangle$	$d^2\sigma/dpd\Omega$						
0.10–0.13	0.115	44.8	220.24	$\pm$	8.87	$\pm$	16.30	0.145	54.8	202.06	$\pm$	7.40	$\pm$	11.70
0.13–0.16	0.146	45.1	235.30	$\pm$	7.92	$\pm$	13.01	0.180	55.0	210.93	$\pm$	6.38	$\pm$	9.74
0.16–0.20	0.180	44.9	213.45	$\pm$	6.22	$\pm$	9.92	0.219	54.8	188.86	$\pm$	5.85	$\pm$	7.54
0.20–0.24	0.220	44.9	224.92	$\pm$	6.42	$\pm$	8.98	0.269	54.8	156.93	$\pm$	4.43	$\pm$	5.21
0.24–0.30	0.270	44.7	208.32	$\pm$	5.13	$\pm$	7.01	0.329	54.8	141.78	$\pm$	4.25	$\pm$	4.36
0.30–0.36	0.329	44.7	171.45	$\pm$	4.64	$\pm$	5.10	0.389	54.9	120.05	$\pm$	4.03	$\pm$	4.52
0.36–0.42	0.390	44.8	149.24	$\pm$	4.42	$\pm$	4.75	0.458	54.7	86.68	$\pm$	2.90	$\pm$	3.16
0.42–0.50	0.458	44.7	121.22	$\pm$	3.50	$\pm$	4.76	0.546	54.6	63.76	$\pm$	2.24	$\pm$	3.17
0.50–0.60	0.545	44.7	71.17	$\pm$	2.26	$\pm$	3.05	0.656	54.8	34.22	$\pm$	1.47	$\pm$	2.25
0.60–0.72	0.656	44.8	46.72	$\pm$	1.67	$\pm$	2.92	0.796	54.6	16.00	$\pm$	0.76	$\pm$	1.46
0.72–0.90	0.796	44.5	19.90	$\pm$	0.81	$\pm$	1.84	1.015	54.7	3.40	$\pm$	0.20	$\pm$	0.51
		60 < $\theta$ < 75				75 < $\theta$ < 90								
$p_T$	$\langle p_T \rangle$	$\langle \theta \rangle$	$d^2\sigma/dpd\Omega$			$\langle p_T \rangle$	$\langle \theta \rangle$	$d^2\sigma/dpd\Omega$						
0.13–0.16	0.145	67.4	184.37	$\pm$	6.30	$\pm$	10.91	0.146	82.5	154.07	$\pm$	6.14	$\pm$	9.65
0.16–0.20	0.180	67.6	182.86	$\pm$	4.75	$\pm$	8.37	0.179	82.3	173.12	$\pm$	4.97	$\pm$	8.05
0.20–0.24	0.219	67.4	165.38	$\pm$	4.55	$\pm$	6.34	0.219	82.1	141.31	$\pm$	4.30	$\pm$	5.39
0.24–0.30	0.269	67.1	130.49	$\pm$	3.29	$\pm$	4.16	0.268	82.2	103.23	$\pm$	2.98	$\pm$	3.35
0.30–0.36	0.328	67.0	106.90	$\pm$	3.05	$\pm$	3.47	0.328	82.0	75.09	$\pm$	2.55	$\pm$	2.60
0.36–0.42	0.389	67.0	86.06	$\pm$	2.73	$\pm$	2.98	0.388	81.9	57.85	$\pm$	2.28	$\pm$	2.57
0.42–0.50	0.459	67.0	64.49	$\pm$	2.04	$\pm$	2.66	0.459	81.8	39.67	$\pm$	1.61	$\pm$	2.00
0.50–0.60	0.546	66.9	43.87	$\pm$	1.50	$\pm$	2.41	0.546	81.7	26.09	$\pm$	1.18	$\pm$	1.83
0.60–0.72	0.654	67.0	24.56	$\pm$	1.02	$\pm$	1.88	0.655	81.3	13.53	$\pm$	0.75	$\pm$	1.24
0.72–0.90	0.795	66.4	10.31	$\pm$	0.50	$\pm$	1.09	0.792	81.4	4.65	$\pm$	0.32	$\pm$	0.59
0.90–1.25	1.020	65.6	1.89	$\pm$	0.12	$\pm$	0.33	1.035	81.5	0.63	$\pm$	0.06	$\pm$	0.13
		90 < $\theta$ < 105				105 < $\theta$ < 125								
$p_T$	$\langle p_T \rangle$	$\langle \theta \rangle$	$d^2\sigma/dpd\Omega$			$\langle p_T \rangle$	$\langle \theta \rangle$	$d^2\sigma/dpd\Omega$						
0.13–0.16	0.146	97.6	164.20	$\pm$	6.37	$\pm$	10.03	0.145	114.6	146.98	$\pm$	5.08	$\pm$	7.67
0.16–0.20	0.179	97.3	152.13	$\pm$	4.72	$\pm$	6.58	0.179	113.8	111.85	$\pm$	3.45	$\pm$	4.07
0.20–0.24	0.219	97.3	119.13	$\pm$	4.05	$\pm$	4.40	0.219	113.7	76.28	$\pm$	2.73	$\pm$	2.65
0.24–0.30	0.268	97.2	75.03	$\pm$	2.58	$\pm$	2.58	0.266	113.7	41.68	$\pm$	1.65	$\pm$	1.67
0.30–0.36	0.329	97.0	48.13	$\pm$	2.09	$\pm$	2.16	0.327	114.0	28.79	$\pm$	1.40	$\pm$	1.61
0.36–0.42	0.387	97.1	32.90	$\pm$	1.70	$\pm$	1.79	0.389	113.7	17.43	$\pm$	1.07	$\pm$	1.26
0.42–0.50	0.456	96.5	25.07	$\pm$	1.31	$\pm$	1.82	0.457	113.1	11.95	$\pm$	0.79	$\pm$	1.14
0.50–0.60	0.547	96.8	12.85	$\pm$	0.81	$\pm$	1.21	0.542	112.6	4.77	$\pm$	0.40	$\pm$	0.60
0.60–0.72	0.646	96.2	6.42	$\pm$	0.51	$\pm$	0.82	0.647	111.1	1.07	$\pm$	0.16	$\pm$	0.19
0.72–0.90	0.788	96.6	1.61	$\pm$	0.17	$\pm$	0.29	0.780	111.8	0.20	$\pm$	0.04	$\pm$	0.06
0.90–1.25	1.025	95.3	0.15	$\pm$	0.02	$\pm$	0.05							

Table A.18: Double-differential inclusive cross-section  $d^2\sigma/dpd\Omega$  [mb/(GeV/c sr)] of the production of  $\pi^-$ 's in  $\pi^- + \text{Sn} \rightarrow \pi^- + \text{X}$  interactions with  $-5.0$  GeV/c beam momentum; the first error is statistical, the second systematic;  $p_T$  in GeV/c, polar angle  $\theta$  in degrees.

$p_T$	20 < $\theta$ < 30						30 < $\theta$ < 40					
	$\langle p_T \rangle$	$\langle \theta \rangle$	$d^2\sigma/dpd\Omega$				$\langle p_T \rangle$	$\langle \theta \rangle$	$d^2\sigma/dpd\Omega$			
			447.70	$\pm$ 12.44	$\pm$ 30.88	394.69	$\pm$ 11.57	$\pm$ 28.01	386.19	$\pm$ 10.36	$\pm$ 21.33	
0.10–0.13	0.115	24.9	447.70	$\pm$ 12.44	$\pm$ 30.88	0.115	35.0	394.69	$\pm$ 11.57	$\pm$ 28.01		
0.13–0.16	0.145	24.8	490.00	$\pm$ 11.99	$\pm$ 26.81	0.145	34.8	386.19	$\pm$ 10.36	$\pm$ 21.33		
0.16–0.20	0.179	25.0	538.99	$\pm$ 10.68	$\pm$ 25.30	0.179	34.8	416.58	$\pm$ 9.14	$\pm$ 19.19		
0.20–0.24	0.219	24.9	492.36	$\pm$ 9.99	$\pm$ 19.37	0.220	34.8	401.97	$\pm$ 8.87	$\pm$ 15.64		
0.24–0.30	0.268	24.9	462.15	$\pm$ 7.85	$\pm$ 14.98	0.268	34.7	387.18	$\pm$ 7.14	$\pm$ 12.54		
0.30–0.36	0.328	24.9	389.24	$\pm$ 7.23	$\pm$ 11.56	0.329	34.9	319.33	$\pm$ 6.52	$\pm$ 9.30		
0.36–0.42	0.387	25.0	315.59	$\pm$ 6.45	$\pm$ 9.06	0.387	34.9	256.09	$\pm$ 5.76	$\pm$ 7.30		
0.42–0.50	0.456	24.9	237.40	$\pm$ 4.93	$\pm$ 8.80	0.456	34.8	204.80	$\pm$ 4.52	$\pm$ 7.05		
0.50–0.60	0.543	25.0	158.66	$\pm$ 3.50	$\pm$ 7.38	0.544	34.9	130.51	$\pm$ 3.15	$\pm$ 5.87		
0.60–0.72	0.650	24.9	95.31	$\pm$ 2.48	$\pm$ 6.13	0.650	34.9	81.23	$\pm$ 2.29	$\pm$ 5.05		
0.72–0.90						0.792	34.7	38.91	$\pm$ 1.30	$\pm$ 3.39		
$p_T$	40 < $\theta$ < 50						50 < $\theta$ < 60					
	$\langle p_T \rangle$	$\langle \theta \rangle$	$d^2\sigma/dpd\Omega$				$\langle p_T \rangle$	$\langle \theta \rangle$	$d^2\sigma/dpd\Omega$			
			375.59	$\pm$ 11.94	$\pm$ 27.96	0.145	54.9	338.95	$\pm$ 10.02	$\pm$ 19.66		
0.10–0.13	0.116	45.1	359.28	$\pm$ 9.99	$\pm$ 20.11	0.180	55.0	311.48	$\pm$ 7.99	$\pm$ 14.49		
0.13–0.16	0.145	45.1	342.36	$\pm$ 8.26	$\pm$ 15.91	0.220	54.8	282.54	$\pm$ 7.38	$\pm$ 11.03		
0.16–0.20	0.180	44.9	324.90	$\pm$ 7.85	$\pm$ 12.90	0.269	54.8	243.71	$\pm$ 5.68	$\pm$ 8.13		
0.20–0.24	0.220	44.9	300.92	$\pm$ 6.30	$\pm$ 10.02	0.329	54.8	215.88	$\pm$ 5.38	$\pm$ 6.61		
0.24–0.30	0.269	44.8	251.76	$\pm$ 5.73	$\pm$ 7.14	0.389	54.8	168.77	$\pm$ 4.81	$\pm$ 5.83		
0.30–0.36	0.329	44.8	215.07	$\pm$ 5.37	$\pm$ 6.64	0.459	54.9	131.50	$\pm$ 3.63	$\pm$ 4.99		
0.36–0.42	0.389	44.8	175.44	$\pm$ 4.29	$\pm$ 7.06	0.545	54.8	83.12	$\pm$ 2.57	$\pm$ 4.15		
0.42–0.50	0.459	44.9	104.59	$\pm$ 2.84	$\pm$ 4.99	0.652	54.9	44.07	$\pm$ 1.69	$\pm$ 3.01		
0.50–0.60	0.545	44.8	59.85	$\pm$ 1.94	$\pm$ 3.95	0.796	54.7	21.79	$\pm$ 1.00	$\pm$ 2.10		
0.60–0.72	0.656	44.8	29.03	$\pm$ 1.14	$\pm$ 2.70	1.026	54.3	5.23	$\pm$ 0.35	$\pm$ 0.75		
$p_T$	60 < $\theta$ < 75						75 < $\theta$ < 90					
	$\langle p_T \rangle$	$\langle \theta \rangle$	$d^2\sigma/dpd\Omega$				$\langle p_T \rangle$	$\langle \theta \rangle$	$d^2\sigma/dpd\Omega$			
			297.62	$\pm$ 8.05	$\pm$ 16.59	0.146	82.5	289.41	$\pm$ 9.91	$\pm$ 19.51		
0.13–0.16	0.145	67.4	289.60	$\pm$ 6.28	$\pm$ 12.59	0.179	82.4	255.76	$\pm$ 6.16	$\pm$ 11.22		
0.16–0.20	0.180	67.2	235.28	$\pm$ 5.50	$\pm$ 8.54	0.220	82.2	202.96	$\pm$ 5.37	$\pm$ 8.32		
0.20–0.24	0.219	67.1	186.30	$\pm$ 4.05	$\pm$ 5.91	0.268	82.3	139.87	$\pm$ 3.57	$\pm$ 4.70		
0.24–0.30	0.269	67.0	154.39	$\pm$ 3.76	$\pm$ 5.25	0.328	82.0	97.35	$\pm$ 2.96	$\pm$ 3.36		
0.30–0.36	0.329	66.9	114.74	$\pm$ 3.20	$\pm$ 3.90	0.389	82.1	76.10	$\pm$ 2.62	$\pm$ 3.24		
0.36–0.42	0.388	66.9	89.85	$\pm$ 2.44	$\pm$ 3.77	0.456	81.8	57.84	$\pm$ 1.99	$\pm$ 3.18		
0.42–0.50	0.458	66.7	59.31	$\pm$ 1.79	$\pm$ 3.39	0.545	81.5	36.25	$\pm$ 1.42	$\pm$ 2.67		
0.50–0.60	0.546	67.0	33.85	$\pm$ 1.25	$\pm$ 2.64	0.653	81.7	23.33	$\pm$ 1.06	$\pm$ 2.31		
0.60–0.72	0.794	67.3	14.89	$\pm$ 0.68	$\pm$ 1.60	0.794	81.3	7.00	$\pm$ 0.45	$\pm$ 0.91		
0.72–0.90	1.019	67.3	2.92	$\pm$ 0.19	$\pm$ 0.47	1.021	81.3	1.02	$\pm$ 0.10	$\pm$ 0.21		
$p_T$	90 < $\theta$ < 105						105 < $\theta$ < 125					
	$\langle p_T \rangle$	$\langle \theta \rangle$	$d^2\sigma/dpd\Omega$				$\langle p_T \rangle$	$\langle \theta \rangle$	$d^2\sigma/dpd\Omega$			
			359.27	$\pm$ 11.35	$\pm$ 40.79	0.145	114.5	272.87	$\pm$ 7.41	$\pm$ 16.61		
0.13–0.16	0.145	97.7	249.79	$\pm$ 6.47	$\pm$ 13.88	0.178	114.1	161.15	$\pm$ 4.21	$\pm$ 5.63		
0.16–0.20	0.219	97.1	169.80	$\pm$ 4.97	$\pm$ 6.70	0.219	113.6	100.76	$\pm$ 3.19	$\pm$ 3.48		
0.20–0.24	0.267	97.2	104.55	$\pm$ 3.10	$\pm$ 3.71	0.266	113.5	61.13	$\pm$ 2.06	$\pm$ 2.67		
0.30–0.36	0.329	97.0	62.96	$\pm$ 2.40	$\pm$ 2.77	0.328	113.6	39.06	$\pm$ 1.64	$\pm$ 2.38		
0.36–0.42	0.387	96.8	50.51	$\pm$ 2.18	$\pm$ 3.03	0.387	114.0	26.99	$\pm$ 1.37	$\pm$ 2.19		
0.42–0.50	0.457	97.0	34.63	$\pm$ 1.57	$\pm$ 2.73	0.457	112.9	18.02	$\pm$ 0.98	$\pm$ 1.90		
0.50–0.60	0.542	96.9	20.91	$\pm$ 1.11	$\pm$ 2.22	0.542	112.2	6.31	$\pm$ 0.49	$\pm$ 0.87		
0.60–0.72	0.652	96.4	9.41	$\pm$ 0.65	$\pm$ 1.28	0.647	112.1	1.57	$\pm$ 0.20	$\pm$ 0.30		
0.72–0.90	0.784	95.6	2.28	$\pm$ 0.23	$\pm$ 0.43	0.791	110.9	0.30	$\pm$ 0.06	$\pm$ 0.08		
0.90–1.25	1.013	96.5	0.29	$\pm$ 0.05	$\pm$ 0.09							

Table A.19: Double-differential inclusive cross-section  $d^2\sigma/dpd\Omega$  [mb/(GeV/c sr)] of the production of protons in  $p + \text{Sn} \rightarrow p + X$  interactions with  $+8.0$  GeV/c beam momentum; the first error is statistical, the second systematic;  $p_T$  in GeV/c, polar angle  $\theta$  in degrees.

$p_T$	20 < $\theta$ < 30						30 < $\theta$ < 40					
	$\langle p_T \rangle$		$\langle \theta \rangle$		$d^2\sigma/dpd\Omega$		$\langle p_T \rangle$		$\langle \theta \rangle$		$d^2\sigma/dpd\Omega$	
	$\langle p_T \rangle$	$\langle \theta \rangle$	$\langle p_T \rangle$	$\langle \theta \rangle$	$d^2\sigma/dpd\Omega$	$d^2\sigma/dpd\Omega$	$\langle p_T \rangle$	$\langle \theta \rangle$	$\langle p_T \rangle$	$\langle \theta \rangle$	$d^2\sigma/dpd\Omega$	$d^2\sigma/dpd\Omega$
0.20–0.24	0.220	25.2	1077.13	$\pm$ 19.91	$\pm$ 52.82		0.271	34.9	1119.41	$\pm$ 16.15	$\pm$ 45.29	
0.24–0.30	0.270	25.2	936.52	$\pm$ 14.82	$\pm$ 41.87		0.330	35.1	921.88	$\pm$ 14.36	$\pm$ 33.02	
0.30–0.36	0.330	25.3	769.04	$\pm$ 13.93	$\pm$ 35.26		0.390	35.1	726.06	$\pm$ 13.18	$\pm$ 28.07	
0.36–0.42	0.390	25.3	617.32	$\pm$ 12.59	$\pm$ 30.30		0.461	35.1	554.91	$\pm$ 10.32	$\pm$ 25.42	
0.42–0.50	0.460	25.2	455.42	$\pm$ 9.34	$\pm$ 23.89		0.550	35.1	399.43	$\pm$ 7.99	$\pm$ 22.80	
0.50–0.60	0.550	25.3	333.10	$\pm$ 7.20	$\pm$ 19.02		0.658	35.0	258.64	$\pm$ 5.86	$\pm$ 16.75	
0.60–0.72	0.659	25.2	221.89	$\pm$ 5.35	$\pm$ 14.72		0.803	35.0	134.81	$\pm$ 3.58	$\pm$ 12.46	
0.72–0.90												
40 < $\theta$ < 50												
$p_T$	$\langle p_T \rangle$		$\langle \theta \rangle$		$d^2\sigma/dpd\Omega$		$\langle p_T \rangle$	$\langle \theta \rangle$	50 < $\theta$ < 60			
	$\langle p_T \rangle$	$\langle \theta \rangle$	$\langle p_T \rangle$	$\langle \theta \rangle$	$d^2\sigma/dpd\Omega$	$d^2\sigma/dpd\Omega$			$d^2\sigma/dpd\Omega$	$d^2\sigma/dpd\Omega$	$d^2\sigma/dpd\Omega$	$d^2\sigma/dpd\Omega$
0.30–0.36	0.330	45.0	1055.32	$\pm$ 15.99	$\pm$ 31.86		0.391	55.1	887.42	$\pm$ 13.40	$\pm$ 25.37	
0.36–0.42	0.391	45.1	869.34	$\pm$ 13.79	$\pm$ 24.46		0.461	55.0	714.99	$\pm$ 10.87	$\pm$ 20.21	
0.42–0.50	0.460	45.1	640.08	$\pm$ 10.62	$\pm$ 22.21		0.550	55.0	473.04	$\pm$ 8.26	$\pm$ 19.90	
0.50–0.60	0.550	45.1	448.55	$\pm$ 8.41	$\pm$ 23.40		0.660	55.0	273.18	$\pm$ 6.21	$\pm$ 19.57	
0.60–0.72	0.660	45.1	286.62	$\pm$ 6.40	$\pm$ 19.88		0.807	55.0	130.37	$\pm$ 3.65	$\pm$ 13.02	
0.72–0.90	0.807	45.1	146.62	$\pm$ 3.81	$\pm$ 13.30							
0.90–1.25	1.044	45.0	40.58	$\pm$ 1.41	$\pm$ 5.29							
60 < $\theta$ < 75												
$p_T$	$\langle p_T \rangle$		$\langle \theta \rangle$		$d^2\sigma/dpd\Omega$		$\langle p_T \rangle$	$\langle \theta \rangle$	75 < $\theta$ < 90			
	$\langle p_T \rangle$	$\langle \theta \rangle$	$\langle p_T \rangle$	$\langle \theta \rangle$	$d^2\sigma/dpd\Omega$	$d^2\sigma/dpd\Omega$			$d^2\sigma/dpd\Omega$	$d^2\sigma/dpd\Omega$	$d^2\sigma/dpd\Omega$	$d^2\sigma/dpd\Omega$
0.50–0.60	0.552	67.4	439.24	$\pm$ 6.04	$\pm$ 16.89		0.551	82.0	366.56	$\pm$ 5.43	$\pm$ 17.40	
0.60–0.72	0.664	67.4	255.24	$\pm$ 4.67	$\pm$ 16.57		0.661	81.8	196.61	$\pm$ 3.85	$\pm$ 12.86	
0.72–0.90	0.809	67.1	100.25	$\pm$ 2.61	$\pm$ 11.59		0.810	81.8	63.52	$\pm$ 2.17	$\pm$ 8.86	
0.90–1.25	1.049	67.2	27.80	$\pm$ 1.03	$\pm$ 4.61							
90 < $\theta$ < 105												
$p_T$	$\langle p_T \rangle$		$\langle \theta \rangle$		$d^2\sigma/dpd\Omega$		$\langle p_T \rangle$	$\langle \theta \rangle$	105 < $\theta$ < 125			
	$\langle p_T \rangle$	$\langle \theta \rangle$	$\langle p_T \rangle$	$\langle \theta \rangle$	$d^2\sigma/dpd\Omega$	$d^2\sigma/dpd\Omega$			$d^2\sigma/dpd\Omega$	$d^2\sigma/dpd\Omega$	$d^2\sigma/dpd\Omega$	$d^2\sigma/dpd\Omega$
0.42–0.50	0.460	113.4	212.12	$\pm$ 3.78	$\pm$ 13.09		0.549	113.1	97.01	$\pm$ 2.49	$\pm$ 8.56	
0.50–0.60	0.550	96.9	244.41	$\pm$ 4.42	$\pm$ 15.64		0.659	112.6	34.05	$\pm$ 1.58	$\pm$ 5.00	
0.60–0.72	0.661	96.6	115.66	$\pm$ 3.05	$\pm$ 9.56							

Table A.20: Double-differential inclusive cross-section  $d^2\sigma/dpd\Omega$  [mb/(GeV/c sr)] of the production of  $\pi^+$ 's in  $p + \text{Sn} \rightarrow \pi^+ + \text{X}$  interactions with +8.0 GeV/c beam momentum; the first error is statistical, the second systematic;  $p_T$  in GeV/c, polar angle  $\theta$  in degrees.

$p_T$	20 < $\theta$ < 30						30 < $\theta$ < 40							
	$\langle p_T \rangle$	$\langle \theta \rangle$	$d^2\sigma/dpd\Omega$				$\langle p_T \rangle$	$\langle \theta \rangle$	$d^2\sigma/dpd\Omega$					
			394.60	$\pm$	15.57	$\pm$	27.53	325.31	$\pm$	13.98	$\pm$	23.72		
0.10–0.13	0.115	24.9	394.60	$\pm$	15.57	$\pm$	27.53	0.116	34.8	325.31	$\pm$	13.98	$\pm$	23.72
0.13–0.16	0.146	24.9	425.49	$\pm$	14.87	$\pm$	23.19	0.145	34.8	364.19	$\pm$	13.53	$\pm$	20.04
0.16–0.20	0.180	24.8	476.18	$\pm$	13.23	$\pm$	22.57	0.181	34.7	357.59	$\pm$	11.09	$\pm$	16.40
0.20–0.24	0.220	24.8	512.53	$\pm$	13.40	$\pm$	20.78	0.220	34.8	396.97	$\pm$	11.93	$\pm$	16.38
0.24–0.30	0.270	24.9	447.66	$\pm$	10.21	$\pm$	15.65	0.270	34.8	358.23	$\pm$	9.14	$\pm$	12.26
0.30–0.36	0.329	24.7	362.86	$\pm$	9.10	$\pm$	11.56	0.331	34.8	282.79	$\pm$	8.10	$\pm$	8.66
0.36–0.42	0.390	25.0	285.66	$\pm$	7.95	$\pm$	8.92	0.390	34.7	230.18	$\pm$	7.19	$\pm$	6.96
0.42–0.50	0.460	24.9	218.84	$\pm$	5.91	$\pm$	8.29	0.459	34.9	188.99	$\pm$	5.65	$\pm$	6.46
0.50–0.60	0.550	24.9	140.99	$\pm$	3.98	$\pm$	7.15	0.549	34.8	120.47	$\pm$	3.85	$\pm$	5.55
0.60–0.72	0.660	24.9	79.04	$\pm$	2.54	$\pm$	5.92	0.660	34.8	64.43	$\pm$	2.36	$\pm$	4.36
0.72–0.90								0.802	34.8	32.76	$\pm$	1.24	$\pm$	3.49
$p_T$	40 < $\theta$ < 50						50 < $\theta$ < 60							
	$\langle p_T \rangle$	$\langle \theta \rangle$	$d^2\sigma/dpd\Omega$				$\langle p_T \rangle$	$\langle \theta \rangle$	$d^2\sigma/dpd\Omega$					
			274.64	$\pm$	12.82	$\pm$	19.89	0.146	55.0	258.66	$\pm$	11.38	$\pm$	15.09
0.10–0.13	0.115	44.9	320.61	$\pm$	12.30	$\pm$	17.76	0.180	54.9	273.38	$\pm$	9.51	$\pm$	12.62
0.13–0.16	0.145	44.9	324.57	$\pm$	10.66	$\pm$	15.00	0.220	54.9	245.05	$\pm$	9.14	$\pm$	9.70
0.16–0.20	0.180	45.0	301.68	$\pm$	10.26	$\pm$	12.19	0.270	54.8	215.26	$\pm$	7.08	$\pm$	7.36
0.20–0.24	0.220	44.9	269.56	$\pm$	7.93	$\pm$	9.32	0.331	54.7	189.88	$\pm$	6.73	$\pm$	6.40
0.24–0.30	0.270	44.8	249.90	$\pm$	7.66	$\pm$	7.86	0.391	54.6	145.40	$\pm$	5.76	$\pm$	4.66
0.30–0.36	0.330	44.7	194.52	$\pm$	6.78	$\pm$	6.34	0.457	54.7	109.43	$\pm$	4.34	$\pm$	4.05
0.36–0.42	0.391	44.7	137.30	$\pm$	4.85	$\pm$	4.74	0.549	54.9	65.01	$\pm$	2.90	$\pm$	3.14
0.42–0.50	0.458	44.7	92.74	$\pm$	3.40	$\pm$	4.16	0.663	54.5	38.20	$\pm$	1.96	$\pm$	2.55
0.50–0.60	0.549	44.5	56.97	$\pm$	2.31	$\pm$	3.56	0.796	54.5	18.16	$\pm$	1.03	$\pm$	1.71
0.60–0.72	0.659	44.7	27.89	$\pm$	1.24	$\pm$	2.65	1.035	54.4	3.92	$\pm$	0.26	$\pm$	0.63
$p_T$	60 < $\theta$ < 75						75 < $\theta$ < 90							
	$\langle p_T \rangle$	$\langle \theta \rangle$	$d^2\sigma/dpd\Omega$				$\langle p_T \rangle$	$\langle \theta \rangle$	$d^2\sigma/dpd\Omega$					
			228.36	$\pm$	9.03	$\pm$	13.44	0.147	82.2	158.62	$\pm$	7.86	$\pm$	9.58
0.13–0.16	0.146	67.1	228.48	$\pm$	7.10	$\pm$	10.47	0.181	82.1	188.35	$\pm$	6.45	$\pm$	8.41
0.16–0.20	0.180	67.0	220.16	$\pm$	7.01	$\pm$	8.42	0.220	82.2	170.74	$\pm$	6.13	$\pm$	6.30
0.20–0.24	0.220	67.2	175.59	$\pm$	5.23	$\pm$	5.82	0.270	82.0	130.22	$\pm$	4.53	$\pm$	4.48
0.24–0.30	0.270	67.1	129.57	$\pm$	4.52	$\pm$	4.16	0.332	82.0	86.15	$\pm$	3.73	$\pm$	3.21
0.30–0.36	0.331	67.0	100.63	$\pm$	3.97	$\pm$	3.51	0.391	82.0	59.10	$\pm$	3.09	$\pm$	2.58
0.36–0.42	0.391	67.0	74.53	$\pm$	2.96	$\pm$	3.16	0.463	81.7	41.13	$\pm$	2.20	$\pm$	2.16
0.42–0.50	0.462	66.8	44.30	$\pm$	1.96	$\pm$	2.48	0.555	81.7	26.19	$\pm$	1.51	$\pm$	1.82
0.50–0.60	0.552	66.5	25.03	$\pm$	1.29	$\pm$	1.92	0.661	81.6	12.86	$\pm$	0.96	$\pm$	1.20
0.60–0.72	0.664	66.8	8.68	$\pm$	0.58	$\pm$	0.95	0.815	81.2	4.55	$\pm$	0.42	$\pm$	0.59
0.72–0.90	0.803	66.6	1.86	$\pm$	0.15	$\pm$	0.34	1.020	81.6	0.74	$\pm$	0.10	$\pm$	0.15
$p_T$	90 < $\theta$ < 105						105 < $\theta$ < 125							
	$\langle p_T \rangle$	$\langle \theta \rangle$	$d^2\sigma/dpd\Omega$				$\langle p_T \rangle$	$\langle \theta \rangle$	$d^2\sigma/dpd\Omega$					
			177.91	$\pm$	8.64	$\pm$	10.84	0.145	114.1	141.54	$\pm$	5.92	$\pm$	7.46
0.13–0.16	0.146	97.1	167.22	$\pm$	6.16	$\pm$	7.15	0.180	114.2	121.03	$\pm$	4.49	$\pm$	4.62
0.16–0.20	0.181	97.7	135.44	$\pm$	5.53	$\pm$	4.85	0.220	114.1	85.55	$\pm$	3.82	$\pm$	3.02
0.20–0.24	0.221	97.4	88.48	$\pm$	3.75	$\pm$	3.15	0.267	113.5	49.70	$\pm$	2.46	$\pm$	2.06
0.24–0.30	0.269	97.0	57.27	$\pm$	3.10	$\pm$	2.67	0.330	113.9	27.59	$\pm$	1.80	$\pm$	1.56
0.30–0.36	0.331	96.7	39.86	$\pm$	2.52	$\pm$	2.29	0.391	112.9	18.65	$\pm$	1.49	$\pm$	1.42
0.36–0.42	0.393	97.0	24.50	$\pm$	1.66	$\pm$	1.79	0.460	112.9	10.02	$\pm$	0.93	$\pm$	0.99
0.42–0.50	0.461	96.4	12.69	$\pm$	1.07	$\pm$	1.24	0.550	113.2	4.62	$\pm$	0.54	$\pm$	0.61
0.50–0.60	0.553	96.8	5.31	$\pm$	0.59	$\pm$	0.71	0.660	112.0	1.10	$\pm$	0.22	$\pm$	0.20
0.60–0.72	0.660	95.1	1.33	$\pm$	0.22	$\pm$	0.24	0.787	110.7	0.23	$\pm$	0.07	$\pm$	0.06
0.72–0.90	1.046	96.3	0.30	$\pm$	0.06	$\pm$	0.09	1.061	113.4	0.03	$\pm$	0.02	$\pm$	0.02

Table A.21: Double-differential inclusive cross-section  $d^2\sigma/dpd\Omega$  [mb/(GeV/c sr)] of the production of  $\pi^-$ 's in  $p + \text{Sn} \rightarrow \pi^- + X$  interactions with +8.0 GeV/c beam momentum; the first error is statistical, the second systematic;  $p_T$  in GeV/c, polar angle  $\theta$  in degrees.

$p_T$	20 < $\theta$ < 30						30 < $\theta$ < 40						
	$\langle p_T \rangle$	$\langle \theta \rangle$	$d^2\sigma/dpd\Omega$				$\langle p_T \rangle$	$\langle \theta \rangle$	$d^2\sigma/dpd\Omega$				
			$\langle p_T \rangle$	$\langle \theta \rangle$	$d^2\sigma/dpd\Omega$	$d^2\sigma/dpd\Omega$			$\langle p_T \rangle$	$\langle \theta \rangle$	$d^2\sigma/dpd\Omega$	$d^2\sigma/dpd\Omega$	
0.10–0.13	0.115	25.0	441.82	$\pm$ 16.13	$\pm$ 30.83	0.115	34.8	414.89	$\pm$ 15.27	$\pm$ 29.72			
0.13–0.16	0.145	24.9	473.85	$\pm$ 15.39	$\pm$ 26.26	0.145	34.9	427.50	$\pm$ 14.29	$\pm$ 23.79			
0.16–0.20	0.179	24.8	473.97	$\pm$ 12.85	$\pm$ 22.15	0.179	34.6	408.75	$\pm$ 11.80	$\pm$ 18.97			
0.20–0.24	0.219	24.9	425.82	$\pm$ 12.00	$\pm$ 16.81	0.219	34.8	366.64	$\pm$ 11.11	$\pm$ 14.51			
0.24–0.30	0.268	25.0	358.65	$\pm$ 8.97	$\pm$ 11.75	0.268	34.7	321.43	$\pm$ 8.52	$\pm$ 10.65			
0.30–0.36	0.327	25.1	279.16	$\pm$ 7.90	$\pm$ 8.25	0.328	35.0	268.70	$\pm$ 7.79	$\pm$ 7.82			
0.36–0.42	0.386	25.0	197.30	$\pm$ 6.58	$\pm$ 5.97	0.387	34.7	212.93	$\pm$ 6.92	$\pm$ 6.36			
0.42–0.50	0.455	24.9	152.75	$\pm$ 4.97	$\pm$ 5.48	0.455	34.9	121.69	$\pm$ 4.43	$\pm$ 4.27			
0.50–0.60	0.542	25.2	97.10	$\pm$ 3.54	$\pm$ 4.67	0.544	34.7	85.33	$\pm$ 3.36	$\pm$ 3.97			
0.60–0.72	0.650	25.1	47.25	$\pm$ 2.24	$\pm$ 3.14	0.647	34.9	44.24	$\pm$ 2.09	$\pm$ 2.91			
0.72–0.90						0.788	34.6	20.60	$\pm$ 1.15	$\pm$ 1.88			
$p_T$	40 < $\theta$ < 50						50 < $\theta$ < 60						
	$\langle p_T \rangle$	$\langle \theta \rangle$	$d^2\sigma/dpd\Omega$				$\langle p_T \rangle$	$\langle \theta \rangle$	$d^2\sigma/dpd\Omega$				
			$\langle p_T \rangle$	$\langle \theta \rangle$	$d^2\sigma/dpd\Omega$	$d^2\sigma/dpd\Omega$			$\langle p_T \rangle$	$\langle \theta \rangle$	$d^2\sigma/dpd\Omega$	$d^2\sigma/dpd\Omega$	
0.10–0.13	0.115	45.0	328.34	$\pm$ 13.85	$\pm$ 24.24		0.145	54.9	312.44	$\pm$ 12.28	$\pm$ 18.39		
0.13–0.16	0.145	44.9	371.69	$\pm$ 13.34	$\pm$ 21.03		0.179	54.8	303.47	$\pm$ 10.04	$\pm$ 14.21		
0.16–0.20	0.179	45.1	328.79	$\pm$ 10.44	$\pm$ 15.39		0.219	54.9	280.01	$\pm$ 9.72	$\pm$ 11.09		
0.20–0.24	0.220	44.8	292.71	$\pm$ 9.77	$\pm$ 11.80		0.268	54.9	226.34	$\pm$ 7.19	$\pm$ 7.68		
0.24–0.30	0.268	44.8	260.48	$\pm$ 7.74	$\pm$ 8.88		0.327	54.9	178.74	$\pm$ 6.53	$\pm$ 6.28		
0.30–0.36	0.328	44.9	208.92	$\pm$ 6.86	$\pm$ 6.16		0.387	54.6	126.91	$\pm$ 5.33	$\pm$ 4.14		
0.36–0.42	0.387	44.8	171.20	$\pm$ 6.18	$\pm$ 5.30		0.454	54.8	96.66	$\pm$ 4.08	$\pm$ 3.90		
0.42–0.50	0.456	44.9	121.98	$\pm$ 4.50	$\pm$ 4.47		0.544	54.8	54.11	$\pm$ 2.62	$\pm$ 2.81		
0.50–0.60	0.544	44.8	76.48	$\pm$ 3.16	$\pm$ 3.77		0.649	55.0	35.05	$\pm$ 1.96	$\pm$ 2.48		
0.60–0.72	0.649	44.8	41.88	$\pm$ 2.10	$\pm$ 2.85		0.790	54.9	12.20	$\pm$ 0.90	$\pm$ 1.21		
0.72–0.90						1.006	54.5	2.61	$\pm$ 0.26	$\pm$ 0.42			
$p_T$	60 < $\theta$ < 75						75 < $\theta$ < 90						
	$\langle p_T \rangle$	$\langle \theta \rangle$	$d^2\sigma/dpd\Omega$				$\langle p_T \rangle$	$\langle \theta \rangle$	$d^2\sigma/dpd\Omega$				
			$\langle p_T \rangle$	$\langle \theta \rangle$	$d^2\sigma/dpd\Omega$	$d^2\sigma/dpd\Omega$			$\langle p_T \rangle$	$\langle \theta \rangle$	$d^2\sigma/dpd\Omega$	$d^2\sigma/dpd\Omega$	
0.13–0.16	0.145	67.1	273.18	$\pm$ 9.88	$\pm$ 15.43	0.145	82.8	257.48	$\pm$ 15.20	$\pm$ 14.85			
0.16–0.20	0.178	67.6	256.48	$\pm$ 7.54	$\pm$ 11.29	0.178	82.3	223.93	$\pm$ 7.13	$\pm$ 9.65			
0.20–0.24	0.219	67.0	218.89	$\pm$ 7.02	$\pm$ 8.07	0.218	82.0	173.49	$\pm$ 6.22	$\pm$ 6.21			
0.24–0.30	0.267	67.2	168.39	$\pm$ 5.08	$\pm$ 5.40	0.266	82.2	126.42	$\pm$ 4.48	$\pm$ 4.50			
0.30–0.36	0.327	67.0	124.49	$\pm$ 4.41	$\pm$ 4.26	0.326	82.1	83.89	$\pm$ 3.64	$\pm$ 3.21			
0.36–0.42	0.385	66.9	95.46	$\pm$ 3.87	$\pm$ 3.67	0.385	81.8	65.49	$\pm$ 3.22	$\pm$ 3.04			
0.42–0.50	0.452	67.2	59.86	$\pm$ 2.56	$\pm$ 2.61	0.450	81.5	37.74	$\pm$ 2.07	$\pm$ 2.11			
0.50–0.60	0.539	66.3	37.22	$\pm$ 1.80	$\pm$ 2.18	0.537	81.8	21.38	$\pm$ 1.35	$\pm$ 1.61			
0.60–0.72	0.644	66.5	21.50	$\pm$ 1.21	$\pm$ 1.71	0.641	81.5	10.57	$\pm$ 0.86	$\pm$ 1.07			
0.72–0.90	0.784	67.1	8.22	$\pm$ 0.59	$\pm$ 0.91	0.770	81.1	2.81	$\pm$ 0.36	$\pm$ 0.38			
0.90–1.25	1.008	66.7	1.58	$\pm$ 0.17	$\pm$ 0.27	1.003	80.7	0.61	$\pm$ 0.09	$\pm$ 0.13			
$p_T$	90 < $\theta$ < 105						105 < $\theta$ < 125						
	$\langle p_T \rangle$	$\langle \theta \rangle$	$d^2\sigma/dpd\Omega$				$\langle p_T \rangle$	$\langle \theta \rangle$	$d^2\sigma/dpd\Omega$				
			$\langle p_T \rangle$	$\langle \theta \rangle$	$d^2\sigma/dpd\Omega$	$d^2\sigma/dpd\Omega$			$\langle p_T \rangle$	$\langle \theta \rangle$	$d^2\sigma/dpd\Omega$	$d^2\sigma/dpd\Omega$	
0.13–0.16	0.145	97.4	232.42	$\pm$ 9.82	$\pm$ 13.46	0.144	114.4	169.91	$\pm$ 6.64	$\pm$ 8.48			
0.16–0.20	0.178	97.1	179.56	$\pm$ 6.42	$\pm$ 7.56	0.178	113.6	124.68	$\pm$ 4.57	$\pm$ 4.79			
0.20–0.24	0.218	97.0	137.02	$\pm$ 5.65	$\pm$ 4.92	0.218	113.5	85.80	$\pm$ 3.88	$\pm$ 3.20			
0.24–0.30	0.266	97.1	98.42	$\pm$ 4.01	$\pm$ 3.95	0.264	113.5	46.59	$\pm$ 2.34	$\pm$ 2.12			
0.30–0.36	0.326	97.3	53.86	$\pm$ 2.92	$\pm$ 2.49	0.324	114.0	26.88	$\pm$ 1.76	$\pm$ 1.73			
0.36–0.42	0.386	97.1	37.22	$\pm$ 2.36	$\pm$ 2.23	0.384	113.4	18.58	$\pm$ 1.46	$\pm$ 1.61			
0.42–0.50	0.450	96.2	23.01	$\pm$ 1.60	$\pm$ 1.82	0.451	112.4	8.30	$\pm$ 0.80	$\pm$ 0.94			
0.50–0.60	0.540	96.4	11.38	$\pm$ 0.98	$\pm$ 1.22	0.544	112.0	3.30	$\pm$ 0.46	$\pm$ 0.49			
0.60–0.72	0.643	96.3	6.00	$\pm$ 0.65	$\pm$ 0.86	0.637	110.3	1.22	$\pm$ 0.25	$\pm$ 0.24			
0.72–0.90	0.768	95.8	1.20	$\pm$ 0.22	$\pm$ 0.24	0.782	110.1	0.42	$\pm$ 0.11	$\pm$ 0.12			
0.90–1.25	0.986	95.1	0.23	$\pm$ 0.06	$\pm$ 0.07	0.995	111.6	0.03	$\pm$ 0.02	$\pm$ 0.02			

Table A.22: Double-differential inclusive cross-section  $d^2\sigma/dpd\Omega$  [mb/(GeV/c sr)] of the production of protons in  $\pi^+ + \text{Sn} \rightarrow p + X$  interactions with +8.0 GeV/c beam momentum; the first error is statistical, the second systematic;  $p_T$  in GeV/c, polar angle  $\theta$  in degrees.

$p_T$	20 < $\theta$ < 30			30 < $\theta$ < 40				
	$\langle p_T \rangle$	$\langle \theta \rangle$	$d^2\sigma/dpd\Omega$		$\langle p_T \rangle$	$\langle \theta \rangle$	$d^2\sigma/dpd\Omega$	
			$d^2\sigma/dpd\Omega$	$d^2\sigma/dpd\Omega$			$d^2\sigma/dpd\Omega$	$d^2\sigma/dpd\Omega$
0.20–0.24	0.221	25.1	968.92 ± 26.83 ± 48.03		0.271	35.1	934.23 ± 21.41 ± 38.39	
0.24–0.30	0.270	25.2	804.14 ± 19.56 ± 36.41		0.330	35.1	800.24 ± 18.97 ± 29.16	
0.30–0.36	0.330	25.3	647.89 ± 18.11 ± 30.05		0.390	35.1	630.67 ± 17.40 ± 24.63	
0.36–0.42	0.390	25.2	495.15 ± 15.87 ± 24.65		0.460	35.2	490.41 ± 13.76 ± 22.74	
0.42–0.50	0.461	25.3	356.07 ± 11.59 ± 18.94		0.551	35.1	325.81 ± 10.18 ± 18.86	
0.50–0.60	0.551	25.3	260.85 ± 8.88 ± 15.14		0.658	35.1	207.80 ± 7.35 ± 13.58	
0.60–0.72	0.659	25.2	165.90 ± 6.40 ± 11.15		0.806	35.1	108.66 ± 4.49 ± 10.10	
0.72–0.90								
40 < $\theta$ < 50								
$p_T$	$\langle p_T \rangle$	$\langle \theta \rangle$	$d^2\sigma/dpd\Omega$		$\langle p_T \rangle$	$\langle \theta \rangle$	$d^2\sigma/dpd\Omega$	
			$d^2\sigma/dpd\Omega$	$d^2\sigma/dpd\Omega$			$d^2\sigma/dpd\Omega$	$d^2\sigma/dpd\Omega$
0.30–0.36	0.331	45.1	947.06 ± 20.40 ± 29.34		0.390	55.1	775.51 ± 17.68 ± 24.06	
0.36–0.42	0.390	45.1	733.04 ± 17.97 ± 21.24		0.460	55.3	625.31 ± 14.49 ± 18.28	
0.42–0.50	0.460	45.1	551.11 ± 14.01 ± 19.68		0.548	55.2	412.28 ± 11.01 ± 17.88	
0.50–0.60	0.550	45.1	369.22 ± 10.85 ± 19.77		0.657	54.9	222.67 ± 7.99 ± 16.26	
0.60–0.72	0.658	45.1	230.27 ± 8.13 ± 16.17		0.806	55.0	104.25 ± 4.63 ± 10.48	
0.72–0.90	0.805	44.9	116.44 ± 4.78 ± 10.63					
0.90–1.25	1.039	45.0	31.77 ± 1.76 ± 4.15					
60 < $\theta$ < 75								
$p_T$	$\langle p_T \rangle$	$\langle \theta \rangle$	$d^2\sigma/dpd\Omega$		$\langle p_T \rangle$	$\langle \theta \rangle$	$d^2\sigma/dpd\Omega$	
			$d^2\sigma/dpd\Omega$	$d^2\sigma/dpd\Omega$			$d^2\sigma/dpd\Omega$	$d^2\sigma/dpd\Omega$
0.50–0.60	0.552	67.3	390.54 ± 8.11 ± 15.31		0.553	82.1	334.08 ± 7.38 ± 16.04	
0.60–0.72	0.664	67.3	207.70 ± 5.99 ± 13.65		0.663	82.0	173.73 ± 5.15 ± 11.40	
0.72–0.90	0.810	67.2	92.17 ± 3.56 ± 10.65		0.808	81.7	55.63 ± 2.87 ± 7.65	
0.90–1.25	1.048	66.9	22.34 ± 1.30 ± 3.70					
90 < $\theta$ < 105								
$p_T$	$\langle p_T \rangle$	$\langle \theta \rangle$	$d^2\sigma/dpd\Omega$		$\langle p_T \rangle$	$\langle \theta \rangle$	$d^2\sigma/dpd\Omega$	
			$d^2\sigma/dpd\Omega$	$d^2\sigma/dpd\Omega$			$d^2\sigma/dpd\Omega$	$d^2\sigma/dpd\Omega$
0.42–0.50					0.461	113.4	220.62 ± 5.50 ± 13.53	
0.50–0.60	0.551	97.3	234.98 ± 6.17 ± 15.09		0.549	113.1	102.93 ± 3.67 ± 9.11	
0.60–0.72	0.663	96.7	111.59 ± 4.25 ± 9.22		0.655	112.5	34.97 ± 2.27 ± 5.12	

Table A.23: Double-differential inclusive cross-section  $d^2\sigma/dpd\Omega$  [mb/(GeV/c sr)] of the production of  $\pi^+$ 's in  $\pi^+ + \text{Sn} \rightarrow \pi^+ + \text{X}$  interactions with +8.0 GeV/c beam momentum; the first error is statistical, the second systematic;  $p_T$  in GeV/c, polar angle  $\theta$  in degrees.

$p_T$	20 < $\theta$ < 30					30 < $\theta$ < 40				
	$\langle p_T \rangle$	$\langle \theta \rangle$	$d^2\sigma/dpd\Omega$			$\langle p_T \rangle$	$\langle \theta \rangle$	$d^2\sigma/dpd\Omega$		
			20.13	24.8	35.16			34.9	451.36	21.65
0.10–0.13	0.116	24.8	460.25	$\pm$ 24.77	$\pm$ 35.16	0.116	35.0	403.71	$\pm$ 22.54	$\pm$ 30.32
0.13–0.16	0.145	24.8	496.03	$\pm$ 23.05	$\pm$ 27.72	0.146	34.9	451.36	$\pm$ 21.65	$\pm$ 25.21
0.16–0.20	0.181	24.8	589.13	$\pm$ 21.02	$\pm$ 28.51	0.181	34.9	429.22	$\pm$ 17.22	$\pm$ 19.75
0.20–0.24	0.221	24.7	600.45	$\pm$ 20.51	$\pm$ 24.50	0.220	35.0	486.78	$\pm$ 18.81	$\pm$ 20.16
0.24–0.30	0.270	24.9	569.71	$\pm$ 16.37	$\pm$ 20.20	0.270	34.7	436.28	$\pm$ 14.32	$\pm$ 15.02
0.30–0.36	0.330	24.8	511.09	$\pm$ 15.47	$\pm$ 16.47	0.331	34.8	388.41	$\pm$ 13.52	$\pm$ 11.93
0.36–0.42	0.390	24.7	419.91	$\pm$ 13.70	$\pm$ 13.13	0.390	34.6	318.29	$\pm$ 12.06	$\pm$ 9.56
0.42–0.50	0.462	24.8	302.33	$\pm$ 9.95	$\pm$ 11.47	0.461	34.9	256.29	$\pm$ 9.42	$\pm$ 8.71
0.50–0.60	0.549	24.7	213.12	$\pm$ 7.08	$\pm$ 10.74	0.549	34.7	161.98	$\pm$ 6.43	$\pm$ 7.41
0.60–0.72	0.659	24.8	131.29	$\pm$ 4.94	$\pm$ 9.77	0.659	34.9	95.77	$\pm$ 4.19	$\pm$ 6.42
0.72–0.90						0.805	34.9	46.51	$\pm$ 2.21	$\pm$ 4.92
$p_T$	40 < $\theta$ < 50					50 < $\theta$ < 60				
	$\langle p_T \rangle$	$\langle \theta \rangle$	$d^2\sigma/dpd\Omega$			$\langle p_T \rangle$	$\langle \theta \rangle$	$d^2\sigma/dpd\Omega$		
			40.13	44.9	24.36			50.16	54.8	18.16
0.10–0.13	0.115	44.9	333.87	$\pm$ 20.30	$\pm$ 24.36	0.145	54.8	311.75	$\pm$ 17.85	$\pm$ 18.16
0.13–0.16	0.146	44.7	303.91	$\pm$ 16.83	$\pm$ 16.79	0.180	54.8	294.62	$\pm$ 13.92	$\pm$ 13.62
0.16–0.20	0.181	44.5	368.61	$\pm$ 16.08	$\pm$ 17.03	0.220	54.9	304.67	$\pm$ 14.50	$\pm$ 12.08
0.20–0.24	0.219	44.8	397.74	$\pm$ 16.72	$\pm$ 16.04	0.271	54.8	261.19	$\pm$ 11.11	$\pm$ 9.09
0.24–0.30	0.271	44.7	323.73	$\pm$ 12.34	$\pm$ 11.22	0.330	54.6	220.08	$\pm$ 10.29	$\pm$ 7.48
0.30–0.36	0.331	44.9	276.26	$\pm$ 11.45	$\pm$ 8.67	0.390	54.6	171.50	$\pm$ 8.92	$\pm$ 5.44
0.36–0.42	0.391	44.7	230.83	$\pm$ 10.50	$\pm$ 7.46	0.461	54.6	143.27	$\pm$ 7.07	$\pm$ 5.26
0.42–0.50	0.461	44.7	182.80	$\pm$ 8.02	$\pm$ 6.26	0.549	54.5	91.31	$\pm$ 4.91	$\pm$ 4.35
0.50–0.60	0.551	44.7	121.30	$\pm$ 5.58	$\pm$ 5.39	0.657	54.9	51.95	$\pm$ 3.34	$\pm$ 3.42
0.60–0.72	0.656	44.5	70.07	$\pm$ 3.70	$\pm$ 4.33	0.804	54.7	21.43	$\pm$ 1.62	$\pm$ 2.00
0.72–0.90	0.796	44.2	34.12	$\pm$ 2.00	$\pm$ 3.21	1.033	54.7	4.95	$\pm$ 0.43	$\pm$ 0.80
$p_T$	60 < $\theta$ < 75					75 < $\theta$ < 90				
	$\langle p_T \rangle$	$\langle \theta \rangle$	$d^2\sigma/dpd\Omega$			$\langle p_T \rangle$	$\langle \theta \rangle$	$d^2\sigma/dpd\Omega$		
			60.16	66.4	22.67			75.13	82.3	11.23
0.13–0.16	0.140	69.4	384.94	$\pm$ 143.25	$\pm$ 22.67	0.147	82.3	188.46	$\pm$ 12.13	$\pm$ 11.23
0.16–0.20	0.181	67.5	253.06	$\pm$ 10.71	$\pm$ 11.67	0.180	82.0	212.41	$\pm$ 9.86	$\pm$ 9.52
0.20–0.24	0.221	67.1	232.87	$\pm$ 10.31	$\pm$ 8.98	0.220	82.2	177.26	$\pm$ 8.89	$\pm$ 6.55
0.24–0.30	0.270	67.0	189.28	$\pm$ 7.74	$\pm$ 6.57	0.269	82.1	144.84	$\pm$ 6.83	$\pm$ 5.10
0.30–0.36	0.331	66.7	152.21	$\pm$ 6.97	$\pm$ 5.07	0.330	81.7	100.81	$\pm$ 5.76	$\pm$ 3.73
0.36–0.42	0.392	66.8	120.98	$\pm$ 6.18	$\pm$ 4.27	0.392	81.9	80.84	$\pm$ 5.14	$\pm$ 3.48
0.42–0.50	0.461	66.9	95.77	$\pm$ 4.80	$\pm$ 4.06	0.461	81.8	52.83	$\pm$ 3.56	$\pm$ 2.73
0.50–0.60	0.553	66.6	55.44	$\pm$ 3.13	$\pm$ 3.08	0.552	81.3	33.85	$\pm$ 2.46	$\pm$ 2.32
0.60–0.72	0.662	66.8	29.89	$\pm$ 2.01	$\pm$ 2.27	0.664	81.7	18.72	$\pm$ 1.67	$\pm$ 1.73
0.72–0.90	0.807	66.4	14.04	$\pm$ 1.09	$\pm$ 1.52	0.814	80.1	5.58	$\pm$ 0.67	$\pm$ 0.71
0.90–1.25	1.043	66.8	2.55	$\pm$ 0.25	$\pm$ 0.47	1.021	81.9	1.22	$\pm$ 0.18	$\pm$ 0.25
$p_T$	90 < $\theta$ < 105					105 < $\theta$ < 125				
	$\langle p_T \rangle$	$\langle \theta \rangle$	$d^2\sigma/dpd\Omega$			$\langle p_T \rangle$	$\langle \theta \rangle$	$d^2\sigma/dpd\Omega$		
			90.16	97.4	10.93			105.13	114.9	7.95
0.13–0.16	0.147	97.4	185.77	$\pm$ 12.48	$\pm$ 10.93	0.145	114.9	158.34	$\pm$ 9.23	$\pm$ 7.95
0.16–0.20	0.180	97.4	155.87	$\pm$ 8.35	$\pm$ 6.62	0.180	114.1	141.63	$\pm$ 6.98	$\pm$ 5.30
0.20–0.24	0.221	97.1	145.04	$\pm$ 8.10	$\pm$ 5.09	0.219	113.3	93.76	$\pm$ 5.71	$\pm$ 3.32
0.24–0.30	0.271	97.2	105.05	$\pm$ 5.76	$\pm$ 3.51	0.271	114.1	58.89	$\pm$ 3.85	$\pm$ 2.59
0.30–0.36	0.330	96.4	68.78	$\pm$ 4.79	$\pm$ 3.04	0.328	113.8	35.25	$\pm$ 2.93	$\pm$ 2.00
0.36–0.42	0.391	97.2	40.19	$\pm$ 3.58	$\pm$ 2.21	0.390	114.1	24.65	$\pm$ 2.42	$\pm$ 1.85
0.42–0.50	0.465	97.1	29.67	$\pm$ 2.60	$\pm$ 2.11	0.456	113.5	12.15	$\pm$ 1.46	$\pm$ 1.17
0.50–0.60	0.554	97.2	20.60	$\pm$ 1.95	$\pm$ 1.97	0.543	112.9	4.97	$\pm$ 0.79	$\pm$ 0.63
0.60–0.72	0.661	94.6	6.97	$\pm$ 0.98	$\pm$ 0.91	0.651	111.3	2.61	$\pm$ 0.50	$\pm$ 0.45
0.72–0.90	0.811	94.6	1.96	$\pm$ 0.38	$\pm$ 0.34	0.821	113.4	0.47	$\pm$ 0.15	$\pm$ 0.11
0.90–1.25	1.047	94.5	0.39	$\pm$ 0.09	$\pm$ 0.11					

Table A.24: Double-differential inclusive cross-section  $d^2\sigma/dpd\Omega$  [mb/(GeV/c sr)] of the production of  $\pi^-$ 's in  $\pi^+ + \text{Sn} \rightarrow \pi^- + \text{X}$  interactions with +8.0 GeV/c beam momentum; the first error is statistical, the second systematic;  $p_T$  in GeV/c, polar angle  $\theta$  in degrees.

$p_T$	20 < $\theta$ < 30				30 < $\theta$ < 40			
	$\langle p_T \rangle$	$\langle \theta \rangle$	$d^2\sigma/dpd\Omega$		$\langle p_T \rangle$	$\langle \theta \rangle$	$d^2\sigma/dpd\Omega$	
			$d^2\sigma/dpd\Omega$	$d^2\sigma/dpd\Omega$			$d^2\sigma/dpd\Omega$	$d^2\sigma/dpd\Omega$
0.10–0.13	0.115	24.8	457.93 ± 22.99	± 32.52	0.115	34.8	388.88 ± 21.14	± 28.35
0.13–0.16	0.145	24.7	538.69 ± 23.11	± 29.96	0.145	34.8	375.82 ± 18.98	± 21.02
0.16–0.20	0.179	24.8	515.69 ± 18.95	± 24.42	0.180	34.7	420.33 ± 17.05	± 19.70
0.20–0.24	0.220	24.7	522.61 ± 18.91	± 20.88	0.220	35.0	435.57 ± 17.20	± 17.37
0.24–0.30	0.268	24.9	441.84 ± 14.13	± 14.71	0.268	35.0	387.08 ± 13.32	± 12.99
0.30–0.36	0.328	25.1	356.16 ± 12.69	± 10.59	0.328	35.0	291.38 ± 11.51	± 8.49
0.36–0.42	0.387	24.9	278.63 ± 11.10	± 8.35	0.388	34.8	217.21 ± 9.90	± 6.45
0.42–0.50	0.455	24.9	211.19 ± 8.29	± 7.50	0.456	34.6	168.56 ± 7.37	± 5.88
0.50–0.60	0.541	24.9	134.32 ± 5.90	± 6.38	0.541	34.8	105.75 ± 5.31	± 4.90
0.60–0.72	0.650	24.9	78.75 ± 4.08	± 5.16	0.647	34.8	57.36 ± 3.38	± 3.74
0.72–0.90					0.789	34.7	25.06 ± 1.81	± 2.28
$p_T$	40 < $\theta$ < 50				50 < $\theta$ < 60			
	$\langle p_T \rangle$	$\langle \theta \rangle$	$d^2\sigma/dpd\Omega$		$\langle p_T \rangle$	$\langle \theta \rangle$	$d^2\sigma/dpd\Omega$	
			$d^2\sigma/dpd\Omega$	$d^2\sigma/dpd\Omega$			$d^2\sigma/dpd\Omega$	$d^2\sigma/dpd\Omega$
0.10–0.13	0.115	45.3	371.16 ± 22.41	± 29.03	0.145	55.0	315.90 ± 17.46	± 18.61
0.13–0.16	0.145	44.7	372.08 ± 18.91	± 21.12	0.180	55.1	294.22 ± 14.02	± 13.88
0.16–0.20	0.180	44.8	360.17 ± 15.61	± 17.02	0.220	54.9	293.94 ± 14.12	± 11.79
0.20–0.24	0.219	44.8	325.77 ± 14.72	± 13.25	0.270	54.7	227.62 ± 10.25	± 7.81
0.24–0.30	0.268	44.8	307.72 ± 11.91	± 10.56	0.329	54.8	197.66 ± 9.72	± 6.82
0.30–0.36	0.327	44.9	238.53 ± 10.37	± 7.05	0.387	54.5	131.35 ± 7.67	± 4.25
0.36–0.42	0.387	44.8	176.77 ± 8.91	± 5.45	0.458	54.8	96.54 ± 5.80	± 3.83
0.42–0.50	0.456	44.8	138.37 ± 6.79	± 5.07	0.541	54.7	77.47 ± 4.44	± 4.01
0.50–0.60	0.545	44.8	81.10 ± 4.61	± 4.00	0.647	55.0	41.64 ± 3.04	± 2.94
0.60–0.72	0.648	45.0	46.91 ± 3.16	± 3.20	0.797	54.4	14.03 ± 1.36	± 1.40
0.72–0.90	0.788	44.7	17.64 ± 1.45	± 1.80	1.004	54.4	3.25 ± 0.41	± 0.52
$p_T$	60 < $\theta$ < 75				75 < $\theta$ < 90			
	$\langle p_T \rangle$	$\langle \theta \rangle$	$d^2\sigma/dpd\Omega$		$\langle p_T \rangle$	$\langle \theta \rangle$	$d^2\sigma/dpd\Omega$	
			$d^2\sigma/dpd\Omega$	$d^2\sigma/dpd\Omega$			$d^2\sigma/dpd\Omega$	$d^2\sigma/dpd\Omega$
0.13–0.16	0.144	67.1	284.40 ± 14.83	± 16.11	0.145	81.9	253.06 ± 15.17	± 15.72
0.16–0.20	0.179	67.3	259.78 ± 10.76	± 11.53	0.178	82.3	195.50 ± 9.51	± 8.52
0.20–0.24	0.219	67.1	237.82 ± 10.42	± 8.89	0.218	81.9	169.22 ± 8.76	± 6.13
0.24–0.30	0.267	67.3	174.50 ± 7.35	± 5.79	0.266	82.2	125.88 ± 6.37	± 4.67
0.30–0.36	0.326	66.8	135.40 ± 6.53	± 4.70	0.329	81.9	85.35 ± 5.24	± 3.33
0.36–0.42	0.388	66.9	100.06 ± 5.62	± 3.80	0.385	82.1	61.64 ± 4.46	± 2.86
0.42–0.50	0.451	66.9	71.81 ± 3.95	± 3.10	0.454	82.1	48.75 ± 3.35	± 2.67
0.50–0.60	0.539	66.6	42.19 ± 2.73	± 2.45	0.540	81.7	27.64 ± 2.18	± 2.04
0.60–0.72	0.643	66.5	25.13 ± 1.85	± 1.98	0.640	81.5	15.25 ± 1.47	± 1.50
0.72–0.90	0.777	66.4	8.04 ± 0.83	± 0.88	0.773	81.7	5.30 ± 0.70	± 0.71
0.90–1.25	0.997	66.1	1.99 ± 0.27	± 0.34	0.992	82.1	0.57 ± 0.13	± 0.12
$p_T$	90 < $\theta$ < 105				105 < $\theta$ < 125			
	$\langle p_T \rangle$	$\langle \theta \rangle$	$d^2\sigma/dpd\Omega$		$\langle p_T \rangle$	$\langle \theta \rangle$	$d^2\sigma/dpd\Omega$	
			$d^2\sigma/dpd\Omega$	$d^2\sigma/dpd\Omega$			$d^2\sigma/dpd\Omega$	$d^2\sigma/dpd\Omega$
0.13–0.16	0.145	98.0	233.82 ± 13.93	± 13.59	0.144	114.6	170.70 ± 9.23	± 8.90
0.16–0.20	0.178	97.3	196.49 ± 9.65	± 8.39	0.178	113.7	120.67 ± 6.46	± 4.51
0.20–0.24	0.219	97.0	121.90 ± 7.58	± 4.48	0.216	113.6	80.58 ± 5.36	± 2.98
0.24–0.30	0.267	97.0	102.40 ± 5.80	± 4.11	0.265	113.7	50.95 ± 3.48	± 2.29
0.30–0.36	0.326	96.9	58.58 ± 4.33	± 2.73	0.326	114.1	32.59 ± 2.75	± 2.05
0.36–0.42	0.386	96.9	40.72 ± 3.51	± 2.42	0.386	112.5	20.70 ± 2.20	± 1.74
0.42–0.50	0.453	95.5	27.12 ± 2.48	± 2.12	0.446	112.3	12.41 ± 1.41	± 1.36
0.50–0.60	0.538	96.6	11.59 ± 1.42	± 1.22	0.543	111.5	4.72 ± 0.79	± 0.67
0.60–0.72	0.643	96.7	6.41 ± 0.96	± 0.90	0.656	112.7	1.21 ± 0.36	± 0.22
0.72–0.90	0.766	95.3	1.84 ± 0.38	± 0.36	0.778	110.7	0.24 ± 0.12	± 0.06
0.90–1.25	0.998	95.7	0.35 ± 0.11	± 0.10				

Table A.25: Double-differential inclusive cross-section  $d^2\sigma/dpd\Omega$  [mb/(GeV/c sr)] of the production of protons in  $\pi^- + \text{Sn} \rightarrow p + X$  interactions with  $-8.0$  GeV/c beam momentum; the first error is statistical, the second systematic;  $p_T$  in GeV/c, polar angle  $\theta$  in degrees.

$p_T$	20 < $\theta$ < 30				30 < $\theta$ < 40			
	$\langle p_T \rangle$	$\langle \theta \rangle$	$d^2\sigma/dpd\Omega$		$\langle p_T \rangle$	$\langle \theta \rangle$	$d^2\sigma/dpd\Omega$	
0.20–0.24	0.220	25.1	818.29	$\pm$ 14.61	814.20	$\pm$ 11.94	$\pm$ 33.48	
0.24–0.30	0.268	25.2	699.04	$\pm$ 10.78	697.42	$\pm$ 10.61	$\pm$ 25.42	
0.30–0.36	0.328	25.3	544.92	$\pm$ 9.92	532.10	$\pm$ 9.55	$\pm$ 21.33	
0.36–0.42	0.388	25.3	432.30	$\pm$ 8.93	399.66	$\pm$ 7.48	$\pm$ 20.45	
0.42–0.50	0.456	25.3	326.71	$\pm$ 6.77	351	$\pm$ 5.75	$\pm$ 17.00	
0.50–0.60	0.543	25.3	227.81	$\pm$ 5.10	286.15	$\pm$ 4.29	$\pm$ 13.54	
0.60–0.72	0.650	25.3	145.82	$\pm$ 3.69	186.38	$\pm$ 2.62	$\pm$ 9.17	
0.72–0.90								
$p_T$	40 < $\theta$ < 50				50 < $\theta$ < 60			
	$\langle p_T \rangle$	$\langle \theta \rangle$	$d^2\sigma/dpd\Omega$		$\langle p_T \rangle$	$\langle \theta \rangle$	$d^2\sigma/dpd\Omega$	
0.30–0.36	0.328	45.1	797.85	$\pm$ 11.18	806.72	$\pm$ 111.04	$\pm$ 23.00	
0.36–0.42	0.386	45.1	619.69	$\pm$ 9.81	517.11	$\pm$ 7.76	$\pm$ 15.27	
0.42–0.50	0.454	45.1	473.55	$\pm$ 7.74	359.07	$\pm$ 6.17	$\pm$ 16.09	
0.50–0.60	0.541	45.1	318.83	$\pm$ 6.05	200.11	$\pm$ 4.54	$\pm$ 14.98	
0.60–0.72	0.647	45.0	201.03	$\pm$ 4.54	166.83	$\pm$ 3.02	$\pm$ 11.09	
0.72–0.90	0.786	44.9	109.34	$\pm$ 2.83	98.91	$\pm$ 2.72	$\pm$ 10.63	
0.90–1.25	1.011	44.8	29.79	$\pm$ 1.06	27.27	$\pm$ 1.06	$\pm$ 10.63	
$p_T$	60 < $\theta$ < 75				75 < $\theta$ < 90			
	$\langle p_T \rangle$	$\langle \theta \rangle$	$d^2\sigma/dpd\Omega$		$\langle p_T \rangle$	$\langle \theta \rangle$	$d^2\sigma/dpd\Omega$	
0.50–0.60	0.534	67.4	361.16	$\pm$ 4.68	318.21	$\pm$ 4.29	$\pm$ 15.17	
0.60–0.72	0.637	67.3	188.78	$\pm$ 3.41	166.83	$\pm$ 3.02	$\pm$ 11.09	
0.72–0.90	0.771	67.3	78.71	$\pm$ 2.00	96.33	$\pm$ 1.96	$\pm$ 11.09	
$p_T$	90 < $\theta$ < 105				105 < $\theta$ < 125			
	$\langle p_T \rangle$	$\langle \theta \rangle$	$d^2\sigma/dpd\Omega$		$\langle p_T \rangle$	$\langle \theta \rangle$	$d^2\sigma/dpd\Omega$	
0.42–0.50	0.533	97.2	230.63	$\pm$ 3.63	204.92	$\pm$ 3.15	$\pm$ 12.78	
0.50–0.60	0.635	97.0	104.16	$\pm$ 2.44	99.26	$\pm$ 2.15	$\pm$ 8.66	
0.60–0.72					30.40	$\pm$ 1.29	$\pm$ 4.87	

Table A.26: Double-differential inclusive cross-section  $d^2\sigma/dpd\Omega$  [mb/(GeV/c sr)] of the production of  $\pi^+$ 's in  $\pi^- + \text{Sn} \rightarrow \pi^+ + \text{X}$  interactions with  $-8.0$  GeV/c beam momentum; the first error is statistical, the second systematic;  $p_T$  in GeV/c, polar angle  $\theta$  in degrees.

$p_T$	20 < $\theta$ < 30			30 < $\theta$ < 40				
	$\langle p_T \rangle$	$\langle \theta \rangle$	$d^2\sigma/dpd\Omega$		$\langle p_T \rangle$	$\langle \theta \rangle$	$d^2\sigma/dpd\Omega$	
			$d^2\sigma/dpd\Omega$	$d^2\sigma/dpd\Omega$			$d^2\sigma/dpd\Omega$	$d^2\sigma/dpd\Omega$
0.10–0.13	0.116	24.9	389.60 ± 12.55 ± 27.25	0.115	35.0	347.16 ± 12.04 ± 25.48		
0.13–0.16	0.145	24.8	426.26 ± 12.13 ± 23.45	0.145	34.9	349.53 ± 10.68 ± 18.97		
0.16–0.20	0.180	24.9	463.95 ± 10.61 ± 21.59	0.180	34.8	373.26 ± 9.52 ± 17.01		
0.20–0.24	0.219	24.8	467.16 ± 10.46 ± 18.64	0.219	34.8	372.43 ± 9.37 ± 14.73		
0.24–0.30	0.269	24.9	422.98 ± 8.10 ± 14.40	0.269	34.8	344.87 ± 7.40 ± 11.59		
0.30–0.36	0.329	24.9	374.50 ± 7.62 ± 11.52	0.329	34.7	301.24 ± 6.94 ± 9.30		
0.36–0.42	0.388	24.8	303.18 ± 6.77 ± 9.35	0.387	34.7	252.16 ± 6.33 ± 7.63		
0.42–0.50	0.456	24.8	202.15 ± 4.56 ± 7.22	0.456	34.9	185.01 ± 4.62 ± 6.09		
0.50–0.60	0.544	24.8	145.18 ± 3.36 ± 7.26	0.544	34.7	113.33 ± 3.02 ± 5.07		
0.60–0.72	0.651	24.8	78.67 ± 2.09 ± 5.84	0.652	34.8	62.05 ± 1.90 ± 4.13		
0.72–0.90				0.787	34.9	31.43 ± 1.06 ± 3.31		
$p_T$	40 < $\theta$ < 50			50 < $\theta$ < 60				
	$\langle p_T \rangle$	$\langle \theta \rangle$	$d^2\sigma/dpd\Omega$		$\langle p_T \rangle$	$\langle \theta \rangle$	$d^2\sigma/dpd\Omega$	
			$d^2\sigma/dpd\Omega$	$d^2\sigma/dpd\Omega$			$d^2\sigma/dpd\Omega$	$d^2\sigma/dpd\Omega$
0.10–0.13	0.115	44.9	247.56 ± 10.33 ± 17.97	0.146	54.9	255.05 ± 9.31 ± 14.87		
0.13–0.16	0.145	44.8	318.75 ± 10.47 ± 17.60	0.179	55.0	268.45 ± 7.95 ± 12.40		
0.16–0.20	0.179	44.9	316.57 ± 8.62 ± 14.61	0.218	54.9	247.95 ± 7.63 ± 9.76		
0.20–0.24	0.219	44.8	299.99 ± 8.42 ± 11.96	0.268	54.7	225.17 ± 6.00 ± 7.49		
0.24–0.30	0.268	44.9	290.10 ± 6.90 ± 10.76	0.326	54.8	184.80 ± 5.53 ± 6.30		
0.30–0.36	0.326	44.9	232.81 ± 6.06 ± 6.95	0.386	54.8	138.78 ± 4.66 ± 4.33		
0.36–0.42	0.385	44.8	189.72 ± 5.54 ± 6.09	0.455	54.5	106.78 ± 3.56 ± 3.90		
0.42–0.50	0.454	44.8	140.06 ± 3.97 ± 4.63	0.541	54.6	68.61 ± 2.43 ± 3.21		
0.50–0.60	0.541	44.8	93.30 ± 2.84 ± 4.03	0.646	54.6	41.49 ± 1.69 ± 2.67		
0.60–0.72	0.649	44.6	52.33 ± 1.85 ± 3.19	0.784	54.7	18.33 ± 0.86 ± 1.69		
0.72–0.90	0.783	44.6	24.53 ± 0.97 ± 2.29	1.011	54.6	3.34 ± 0.20 ± 0.54		
$p_T$	60 < $\theta$ < 75			75 < $\theta$ < 90				
	$\langle p_T \rangle$	$\langle \theta \rangle$	$d^2\sigma/dpd\Omega$		$\langle p_T \rangle$	$\langle \theta \rangle$	$d^2\sigma/dpd\Omega$	
			$d^2\sigma/dpd\Omega$	$d^2\sigma/dpd\Omega$			$d^2\sigma/dpd\Omega$	$d^2\sigma/dpd\Omega$
0.13–0.16	0.145	67.0	203.11 ± 7.18 ± 11.96	0.145	82.3	150.13 ± 6.85 ± 9.05		
0.16–0.20	0.178	67.3	205.36 ± 5.58 ± 9.47	0.178	82.3	158.80 ± 5.02 ± 7.14		
0.20–0.24	0.218	67.2	204.04 ± 5.66 ± 7.84	0.217	82.3	154.91 ± 4.93 ± 5.73		
0.24–0.30	0.265	67.1	166.52 ± 4.20 ± 5.32	0.265	82.0	128.92 ± 3.79 ± 4.66		
0.30–0.36	0.324	66.9	125.91 ± 3.70 ± 4.05	0.324	81.7	83.24 ± 3.07 ± 3.29		
0.36–0.42	0.383	66.9	100.49 ± 3.34 ± 3.92	0.382	81.7	66.11 ± 2.68 ± 2.72		
0.42–0.50	0.449	66.9	75.77 ± 2.43 ± 3.05	0.449	82.3	46.89 ± 1.93 ± 2.38		
0.50–0.60	0.536	66.6	50.13 ± 1.75 ± 2.73	0.533	81.4	26.94 ± 1.27 ± 1.83		
0.60–0.72	0.638	66.8	25.20 ± 1.07 ± 1.90	0.638	81.2	14.92 ± 0.81 ± 1.37		
0.72–0.90	0.771	66.7	10.80 ± 0.54 ± 1.15	0.769	80.9	6.16 ± 0.42 ± 0.78		
0.90–1.25	0.998	66.3	2.26 ± 0.13 ± 0.41	0.988	81.3	1.02 ± 0.09 ± 0.21		
$p_T$	90 < $\theta$ < 105			105 < $\theta$ < 125				
	$\langle p_T \rangle$	$\langle \theta \rangle$	$d^2\sigma/dpd\Omega$		$\langle p_T \rangle$	$\langle \theta \rangle$	$d^2\sigma/dpd\Omega$	
			$d^2\sigma/dpd\Omega$	$d^2\sigma/dpd\Omega$			$d^2\sigma/dpd\Omega$	$d^2\sigma/dpd\Omega$
0.13–0.16	0.145	97.6	158.08 ± 7.06 ± 9.53	0.144	114.7	141.30 ± 5.38 ± 7.18		
0.16–0.20	0.178	97.3	147.08 ± 4.86 ± 6.32	0.178	114.5	110.52 ± 3.59 ± 4.36		
0.20–0.24	0.217	97.1	119.62 ± 4.40 ± 4.25	0.216	113.8	81.52 ± 3.15 ± 2.89		
0.24–0.30	0.264	97.0	92.61 ± 3.23 ± 3.36	0.263	113.7	46.76 ± 1.98 ± 1.91		
0.30–0.36	0.324	96.7	56.81 ± 2.56 ± 2.62	0.324	114.1	27.33 ± 1.48 ± 1.53		
0.36–0.42	0.383	97.2	35.16 ± 1.94 ± 1.91	0.382	113.3	17.90 ± 1.17 ± 1.35		
0.42–0.50	0.449	96.9	27.32 ± 1.47 ± 1.96	0.447	114.2	9.69 ± 0.74 ± 0.94		
0.50–0.60	0.532	96.7	13.24 ± 0.88 ± 1.27	0.533	112.8	5.26 ± 0.47 ± 0.67		
0.60–0.72	0.631	95.7	5.98 ± 0.52 ± 0.77	0.631	112.2	1.58 ± 0.23 ± 0.27		
0.72–0.90	0.775	95.3	2.33 ± 0.26 ± 0.40	0.766	109.6	0.30 ± 0.07 ± 0.07		
0.90–1.25	0.997	95.6	0.28 ± 0.05 ± 0.08					

Table A.27: Double-differential inclusive cross-section  $d^2\sigma/dpd\Omega$  [mb/(GeV/c sr)] of the production of  $\pi^-$ 's in  $\pi^- + \text{Sn} \rightarrow \pi^- + \text{X}$  interactions with  $-8.0 \text{ GeV}/c$  beam momentum; the first error is statistical, the second systematic;  $p_T$  in  $\text{GeV}/c$ , polar angle  $\theta$  in degrees.

$p_T$	20 < $\theta$ < 30						30 < $\theta$ < 40					
	$\langle p_T \rangle$	$\langle \theta \rangle$	$d^2\sigma/dpd\Omega$			$\langle p_T \rangle$	$\langle \theta \rangle$	$d^2\sigma/dpd\Omega$			$\langle p_T \rangle$	$\langle \theta \rangle$
			$\langle p_T \rangle$	$\langle \theta \rangle$	$d^2\sigma/dpd\Omega$			$\langle p_T \rangle$	$\langle \theta \rangle$	$d^2\sigma/dpd\Omega$		
0.10–0.13	0.116	24.9	573.72	$\pm$ 15.50	$\pm$ 38.78	0.116	34.9	469.04	$\pm$ 13.66	$\pm$ 33.35	0.116	34.9
0.13–0.16	0.145	24.9	625.54	$\pm$ 15.05	$\pm$ 34.28	0.146	35.0	520.47	$\pm$ 13.78	$\pm$ 29.32	0.146	35.0
0.16–0.20	0.181	24.7	680.77	$\pm$ 13.18	$\pm$ 31.70	0.181	34.9	562.05	$\pm$ 12.06	$\pm$ 26.68	0.181	34.9
0.20–0.24	0.220	24.8	682.98	$\pm$ 13.08	$\pm$ 27.47	0.221	34.7	490.34	$\pm$ 10.92	$\pm$ 19.21	0.221	34.7
0.24–0.30	0.270	24.8	618.16	$\pm$ 10.09	$\pm$ 20.53	0.271	34.8	484.51	$\pm$ 8.93	$\pm$ 16.00	0.271	34.8
0.30–0.36	0.330	24.8	490.20	$\pm$ 8.88	$\pm$ 13.93	0.331	34.7	385.44	$\pm$ 7.95	$\pm$ 11.16	0.331	34.7
0.36–0.42	0.390	24.9	379.37	$\pm$ 7.72	$\pm$ 11.01	0.390	34.8	313.84	$\pm$ 7.07	$\pm$ 9.08	0.390	34.8
0.42–0.50	0.460	25.0	300.40	$\pm$ 6.06	$\pm$ 10.67	0.460	34.9	229.96	$\pm$ 5.27	$\pm$ 7.80	0.460	34.9
0.50–0.60	0.550	24.8	203.50	$\pm$ 4.41	$\pm$ 9.50	0.549	34.7	161.56	$\pm$ 3.92	$\pm$ 7.33	0.549	34.7
0.60–0.72	0.658	24.8	115.48	$\pm$ 2.93	$\pm$ 7.45	0.659	34.7	87.24	$\pm$ 2.53	$\pm$ 5.46	0.659	34.7
0.72–0.90						0.806	34.7	39.42	$\pm$ 1.39	$\pm$ 3.46	0.806	34.7
$p_T$	40 < $\theta$ < 50						50 < $\theta$ < 60					
	$\langle p_T \rangle$	$\langle \theta \rangle$	$d^2\sigma/dpd\Omega$			$\langle p_T \rangle$	$\langle \theta \rangle$	$d^2\sigma/dpd\Omega$			$\langle p_T \rangle$	$\langle \theta \rangle$
			$\langle p_T \rangle$	$\langle \theta \rangle$	$d^2\sigma/dpd\Omega$			$\langle p_T \rangle$	$\langle \theta \rangle$	$d^2\sigma/dpd\Omega$		
0.10–0.13	0.115	45.1	439.06	$\pm$ 14.06	$\pm$ 32.28	0.145	54.8	368.77	$\pm$ 11.56	$\pm$ 21.59	0.145	54.8
0.13–0.16	0.145	44.9	435.29	$\pm$ 12.46	$\pm$ 24.51	0.181	54.9	347.86	$\pm$ 9.23	$\pm$ 16.24	0.181	54.9
0.16–0.20	0.181	44.8	432.99	$\pm$ 10.39	$\pm$ 20.19	0.221	54.8	320.65	$\pm$ 8.85	$\pm$ 12.55	0.221	54.8
0.20–0.24	0.221	44.9	394.58	$\pm$ 9.79	$\pm$ 15.73	0.270	54.7	271.25	$\pm$ 6.71	$\pm$ 9.19	0.270	54.7
0.24–0.30	0.271	44.8	360.75	$\pm$ 7.79	$\pm$ 12.61	0.331	54.8	240.90	$\pm$ 6.44	$\pm$ 8.37	0.331	54.8
0.30–0.36	0.332	44.7	296.66	$\pm$ 6.99	$\pm$ 8.79	0.392	54.8	185.00	$\pm$ 5.54	$\pm$ 6.07	0.392	54.8
0.36–0.42	0.392	44.7	252.59	$\pm$ 6.41	$\pm$ 7.62	0.462	54.9	126.93	$\pm$ 3.90	$\pm$ 4.77	0.462	54.9
0.42–0.50	0.462	44.8	184.67	$\pm$ 4.73	$\pm$ 6.60	0.552	54.9	92.85	$\pm$ 2.99	$\pm$ 4.65	0.552	54.9
0.50–0.60	0.552	44.6	107.40	$\pm$ 3.14	$\pm$ 5.16	0.661	54.6	50.92	$\pm$ 1.99	$\pm$ 3.49	0.661	54.6
0.60–0.72	0.663	44.8	65.54	$\pm$ 2.25	$\pm$ 4.34	0.807	55.0	21.69	$\pm$ 1.04	$\pm$ 2.06	0.807	55.0
0.72–0.90	0.815	45.0	28.85	$\pm$ 1.19	$\pm$ 2.69	1.055	54.9	4.91	$\pm$ 0.31	$\pm$ 0.76	1.055	54.9
$p_T$	60 < $\theta$ < 75						75 < $\theta$ < 90					
	$\langle p_T \rangle$	$\langle \theta \rangle$	$d^2\sigma/dpd\Omega$			$\langle p_T \rangle$	$\langle \theta \rangle$	$d^2\sigma/dpd\Omega$			$\langle p_T \rangle$	$\langle \theta \rangle$
			$\langle p_T \rangle$	$\langle \theta \rangle$	$d^2\sigma/dpd\Omega$			$\langle p_T \rangle$	$\langle \theta \rangle$	$d^2\sigma/dpd\Omega$		
0.13–0.16	0.146	67.3	315.83	$\pm$ 8.82	$\pm$ 17.77	0.144	83.8	321.02	$\pm$ 60.95	$\pm$ 18.41	0.144	83.8
0.16–0.20	0.181	67.3	284.77	$\pm$ 6.77	$\pm$ 12.51	0.181	82.1	248.78	$\pm$ 6.48	$\pm$ 10.68	0.181	82.1
0.20–0.24	0.222	67.4	266.16	$\pm$ 6.59	$\pm$ 9.75	0.221	81.8	209.78	$\pm$ 5.92	$\pm$ 7.43	0.221	81.8
0.24–0.30	0.272	67.0	207.03	$\pm$ 4.80	$\pm$ 6.67	0.271	82.0	155.04	$\pm$ 4.23	$\pm$ 5.57	0.271	82.0
0.30–0.36	0.333	66.9	158.63	$\pm$ 4.24	$\pm$ 5.33	0.333	82.0	99.25	$\pm$ 3.34	$\pm$ 3.58	0.333	82.0
0.36–0.42	0.395	66.6	122.87	$\pm$ 3.69	$\pm$ 4.34	0.395	81.8	83.17	$\pm$ 3.09	$\pm$ 3.84	0.395	81.8
0.42–0.50	0.466	66.9	92.63	$\pm$ 2.76	$\pm$ 3.95	0.466	81.5	51.12	$\pm$ 2.03	$\pm$ 2.75	0.466	81.5
0.50–0.60	0.559	66.9	60.17	$\pm$ 1.96	$\pm$ 3.41	0.558	81.7	32.79	$\pm$ 1.44	$\pm$ 2.38	0.558	81.7
0.60–0.72	0.672	66.6	32.80	$\pm$ 1.29	$\pm$ 2.52	0.670	81.6	15.73	$\pm$ 0.90	$\pm$ 1.53	0.670	81.6
0.72–0.90	0.817	66.8	12.02	$\pm$ 0.61	$\pm$ 1.29	0.818	81.4	5.90	$\pm$ 0.42	$\pm$ 0.79	0.818	81.4
0.90–1.25	1.061	66.3	3.01	$\pm$ 0.21	$\pm$ 0.49	1.048	80.7	0.96	$\pm$ 0.11	$\pm$ 0.20	1.048	80.7
$p_T$	90 < $\theta$ < 105						105 < $\theta$ < 125					
	$\langle p_T \rangle$	$\langle \theta \rangle$	$d^2\sigma/dpd\Omega$			$\langle p_T \rangle$	$\langle \theta \rangle$	$d^2\sigma/dpd\Omega$			$\langle p_T \rangle$	$\langle \theta \rangle$
			$\langle p_T \rangle$	$\langle \theta \rangle$	$d^2\sigma/dpd\Omega$			$\langle p_T \rangle$	$\langle \theta \rangle$	$d^2\sigma/dpd\Omega$		
0.13–0.16	0.146	97.5	227.59	$\pm$ 8.28	$\pm$ 13.11	0.145	114.2	193.60	$\pm$ 5.92	$\pm$ 10.02	0.145	114.2
0.16–0.20	0.181	97.4	204.17	$\pm$ 5.92	$\pm$ 8.54	0.180	114.2	135.73	$\pm$ 4.11	$\pm$ 4.90	0.180	114.2
0.20–0.24	0.221	97.0	165.64	$\pm$ 5.34	$\pm$ 6.01	0.220	113.7	99.70	$\pm$ 3.58	$\pm$ 3.55	0.220	113.7
0.24–0.30	0.270	97.2	107.20	$\pm$ 3.54	$\pm$ 4.16	0.270	113.9	59.24	$\pm$ 2.27	$\pm$ 2.69	0.270	113.9
0.30–0.36	0.332	97.0	68.83	$\pm$ 2.85	$\pm$ 3.36	0.332	113.9	37.58	$\pm$ 1.77	$\pm$ 2.31	0.332	113.9
0.36–0.42	0.394	96.7	47.51	$\pm$ 2.31	$\pm$ 2.78	0.395	114.5	25.18	$\pm$ 1.41	$\pm$ 2.07	0.395	114.5
0.42–0.50	0.466	96.8	33.97	$\pm$ 1.68	$\pm$ 2.60	0.465	113.3	14.76	$\pm$ 0.94	$\pm$ 1.57	0.465	113.3
0.50–0.60	0.558	96.3	19.46	$\pm$ 1.11	$\pm$ 2.00	0.549	113.0	6.26	$\pm$ 0.53	$\pm$ 0.87	0.549	113.0
0.60–0.72	0.665	96.4	7.74	$\pm$ 0.63	$\pm$ 1.06	0.670	110.4	2.25	$\pm$ 0.28	$\pm$ 0.42	0.670	110.4
0.72–0.90	0.813	95.5	2.35	$\pm$ 0.26	$\pm$ 0.44	0.792	111.9	0.27	$\pm$ 0.08	$\pm$ 0.07	0.792	111.9
0.90–1.25	1.068	97.5	0.19	$\pm$ 0.04	$\pm$ 0.06							

Table A.28: Double-differential inclusive cross-section  $d^2\sigma/dpd\Omega$  [mb/(GeV/c sr)] of the production of protons in  $p + \text{Sn} \rightarrow p + X$  interactions with  $+12.0 \text{ GeV}/c$  beam momentum; the first error is statistical, the second systematic;  $p_T$  in  $\text{GeV}/c$ , polar angle  $\theta$  in degrees.

$p_T$	20 < $\theta$ < 30				30 < $\theta$ < 40					
	$\langle p_T \rangle$	$\langle \theta \rangle$	$d^2\sigma/dpd\Omega$		$\langle p_T \rangle$	$\langle \theta \rangle$	$d^2\sigma/dpd\Omega$			
0.20–0.24	0.221	25.1	1102.76	$\pm$ 15.70	$\pm$ 53.69	0.273	35.0	1103.56	$\pm$ 12.09	$\pm$ 44.39
0.24–0.30	0.271	25.2	960.88	$\pm$ 11.37	$\pm$ 43.03	0.333	35.2	956.92	$\pm$ 11.04	$\pm$ 33.87
0.30–0.36	0.333	25.2	794.88	$\pm$ 10.66	$\pm$ 36.77	0.394	35.1	771.17	$\pm$ 10.31	$\pm$ 29.82
0.36–0.42	0.394	25.2	632.81	$\pm$ 9.68	$\pm$ 32.44	0.465	35.1	604.16	$\pm$ 8.20	$\pm$ 28.44
0.42–0.50	0.465	25.3	506.37	$\pm$ 7.48	$\pm$ 27.17	0.557	35.1	455.94	$\pm$ 6.49	$\pm$ 25.60
0.50–0.60	0.556	25.2	381.29	$\pm$ 5.81	$\pm$ 22.60	0.669	35.1	300.91	$\pm$ 4.86	$\pm$ 21.33
0.60–0.72	0.669	25.1	256.64	$\pm$ 4.29	$\pm$ 17.16	0.821	35.1	164.43	$\pm$ 3.00	$\pm$ 15.50
0.72–0.90										
$p_T$	40 < $\theta$ < 50				50 < $\theta$ < 60					
	$\langle p_T \rangle$	$\langle \theta \rangle$	$d^2\sigma/dpd\Omega$		$\langle p_T \rangle$	$\langle \theta \rangle$	$d^2\sigma/dpd\Omega$			
0.30–0.36	0.330	45.1	1033.68	$\pm$ 11.29	$\pm$ 30.86	0.389	55.0	917.82	$\pm$ 10.34	$\pm$ 25.21
0.36–0.42	0.389	45.1	883.18	$\pm$ 10.54	$\pm$ 24.75	0.458	55.0	723.16	$\pm$ 8.18	$\pm$ 20.15
0.42–0.50	0.458	45.0	682.74	$\pm$ 8.35	$\pm$ 23.31	0.547	55.1	504.66	$\pm$ 6.51	$\pm$ 21.15
0.50–0.60	0.548	45.1	468.34	$\pm$ 6.52	$\pm$ 24.68	0.655	55.0	291.52	$\pm$ 4.85	$\pm$ 20.92
0.60–0.72	0.655	45.1	317.11	$\pm$ 5.06	$\pm$ 21.56	0.799	55.0	152.11	$\pm$ 2.99	$\pm$ 15.50
0.72–0.90	0.800	45.0	168.48	$\pm$ 3.11	$\pm$ 16.14					
0.90–1.25	1.036	44.8	51.24	$\pm$ 1.22	$\pm$ 7.31					
$p_T$	60 < $\theta$ < 75				75 < $\theta$ < 90					
	$\langle p_T \rangle$	$\langle \theta \rangle$	$d^2\sigma/dpd\Omega$		$\langle p_T \rangle$	$\langle \theta \rangle$	$d^2\sigma/dpd\Omega$			
0.50–0.60	0.538	67.4	471.30	$\pm$ 4.75	$\pm$ 17.71	0.537	82.0	394.28	$\pm$ 4.27	$\pm$ 18.45
0.60–0.72	0.642	67.3	279.41	$\pm$ 3.67	$\pm$ 18.30	0.641	81.9	222.21	$\pm$ 3.13	$\pm$ 14.48
0.72–0.90	0.779	67.0	128.05	$\pm$ 2.26	$\pm$ 14.89	0.778	81.7	79.82	$\pm$ 1.82	$\pm$ 10.74
$p_T$	90 < $\theta$ < 105				105 < $\theta$ < 125					
	$\langle p_T \rangle$	$\langle \theta \rangle$	$d^2\sigma/dpd\Omega$		$\langle p_T \rangle$	$\langle \theta \rangle$	$d^2\sigma/dpd\Omega$			
0.42–0.50					0.451	113.3	244.36	$\pm$ 4.09	$\pm$ 15.27	
0.50–0.60	0.535	97.2	280.48	$\pm$ 3.59	$\pm$ 17.82	0.535	113.2	117.37	$\pm$ 2.06	$\pm$ 10.12
0.60–0.72	0.640	96.9	133.90	$\pm$ 2.45	$\pm$ 10.94	0.637	112.6	39.81	$\pm$ 1.32	$\pm$ 6.08

Table A.29: Double-differential inclusive cross-section  $d^2\sigma/dpd\Omega$  [mb/(GeV/c sr)] of the production of  $\pi^+$ 's in  $p + \text{Sn} \rightarrow \pi^+ + \text{X}$  interactions with +12.0 GeV/c beam momentum; the first error is statistical, the second systematic;  $p_T$  in GeV/c, polar angle  $\theta$  in degrees.

$p_T$	20 < $\theta$ < 30						30 < $\theta$ < 40					
	$\langle p_T \rangle$	$\langle \theta \rangle$	$d^2\sigma/dpd\Omega$				$\langle p_T \rangle$	$\langle \theta \rangle$	$d^2\sigma/dpd\Omega$			
			$\langle p_T \rangle$	$\langle \theta \rangle$	$d^2\sigma/dpd\Omega$	$d^2\sigma/dpd\Omega$			$\langle p_T \rangle$	$\langle \theta \rangle$	$d^2\sigma/dpd\Omega$	$d^2\sigma/dpd\Omega$
0.10–0.13	0.116	24.9	491.66	$\pm$ 12.99	$\pm$ 33.68	0.116	34.8	428.70	$\pm$ 11.83	$\pm$ 29.70		
0.13–0.16	0.146	24.8	551.04	$\pm$ 12.73	$\pm$ 30.12	0.146	34.7	453.34	$\pm$ 11.12	$\pm$ 24.09		
0.16–0.20	0.181	24.9	620.52	$\pm$ 11.35	$\pm$ 28.96	0.182	34.8	489.35	$\pm$ 9.97	$\pm$ 22.06		
0.20–0.24	0.221	24.8	629.39	$\pm$ 11.17	$\pm$ 24.95	0.221	34.8	491.67	$\pm$ 9.80	$\pm$ 19.10		
0.24–0.30	0.272	24.8	593.26	$\pm$ 8.81	$\pm$ 20.12	0.271	34.9	449.79	$\pm$ 7.71	$\pm$ 14.98		
0.30–0.36	0.332	24.7	493.58	$\pm$ 7.90	$\pm$ 14.67	0.332	34.8	390.29	$\pm$ 7.13	$\pm$ 11.41		
0.36–0.42	0.393	24.8	416.51	$\pm$ 7.18	$\pm$ 12.24	0.394	34.8	316.60	$\pm$ 6.45	$\pm$ 9.17		
0.42–0.50	0.465	24.9	295.23	$\pm$ 5.10	$\pm$ 10.34	0.463	34.7	229.10	$\pm$ 4.60	$\pm$ 7.47		
0.50–0.60	0.556	24.8	203.36	$\pm$ 3.65	$\pm$ 10.03	0.554	34.8	152.35	$\pm$ 3.21	$\pm$ 6.87		
0.60–0.72	0.668	24.7	125.91	$\pm$ 2.45	$\pm$ 9.28	0.667	34.7	93.05	$\pm$ 2.19	$\pm$ 6.18		
0.72–0.90						0.815	34.7	42.56	$\pm$ 1.04	$\pm$ 4.49		
$p_T$	40 < $\theta$ < 50						50 < $\theta$ < 60					
	$\langle p_T \rangle$	$\langle \theta \rangle$	$d^2\sigma/dpd\Omega$				$\langle p_T \rangle$	$\langle \theta \rangle$	$d^2\sigma/dpd\Omega$			
			$\langle p_T \rangle$	$\langle \theta \rangle$	$d^2\sigma/dpd\Omega$	$d^2\sigma/dpd\Omega$			$\langle p_T \rangle$	$\langle \theta \rangle$	$d^2\sigma/dpd\Omega$	$d^2\sigma/dpd\Omega$
0.10–0.13	0.116	44.9	334.88	$\pm$ 10.71	$\pm$ 23.66	0.145	55.0	321.67	$\pm$ 9.58	$\pm$ 18.20		
0.13–0.16	0.145	45.0	381.07	$\pm$ 10.14	$\pm$ 20.48	0.180	54.8	339.67	$\pm$ 8.05	$\pm$ 15.21		
0.16–0.20	0.180	44.9	391.58	$\pm$ 8.63	$\pm$ 17.57	0.220	54.8	323.23	$\pm$ 7.89	$\pm$ 12.22		
0.20–0.24	0.220	44.8	384.17	$\pm$ 8.71	$\pm$ 14.93	0.270	54.8	273.84	$\pm$ 6.02	$\pm$ 8.95		
0.24–0.30	0.269	44.9	357.47	$\pm$ 6.91	$\pm$ 11.88	0.329	54.9	228.19	$\pm$ 5.54	$\pm$ 6.99		
0.30–0.36	0.329	44.8	308.42	$\pm$ 6.41	$\pm$ 9.04	0.390	54.7	183.00	$\pm$ 4.93	$\pm$ 5.55		
0.36–0.42	0.389	44.7	238.41	$\pm$ 5.61	$\pm$ 6.92	0.458	54.6	133.76	$\pm$ 3.60	$\pm$ 4.70		
0.42–0.50	0.459	44.7	166.01	$\pm$ 3.97	$\pm$ 5.53	0.546	54.6	84.33	$\pm$ 2.50	$\pm$ 3.92		
0.50–0.60	0.547	44.6	120.46	$\pm$ 2.97	$\pm$ 5.20	0.654	54.6	48.48	$\pm$ 1.68	$\pm$ 3.12		
0.60–0.72	0.655	44.7	71.47	$\pm$ 2.00	$\pm$ 4.39	0.794	54.8	21.69	$\pm$ 0.82	$\pm$ 2.05		
0.72–0.90	0.796	44.5	30.84	$\pm$ 0.94	$\pm$ 2.95	1.022	54.4	4.57	$\pm$ 0.21	$\pm$ 0.73		
$p_T$	60 < $\theta$ < 75						75 < $\theta$ < 90					
	$\langle p_T \rangle$	$\langle \theta \rangle$	$d^2\sigma/dpd\Omega$				$\langle p_T \rangle$	$\langle \theta \rangle$	$d^2\sigma/dpd\Omega$			
			$\langle p_T \rangle$	$\langle \theta \rangle$	$d^2\sigma/dpd\Omega$	$d^2\sigma/dpd\Omega$			$\langle p_T \rangle$	$\langle \theta \rangle$	$d^2\sigma/dpd\Omega$	$d^2\sigma/dpd\Omega$
0.13–0.16	0.146	67.2	250.64	$\pm$ 7.03	$\pm$ 14.39	0.145	82.4	187.23	$\pm$ 6.64	$\pm$ 11.19		
0.16–0.20	0.179	67.2	269.69	$\pm$ 5.77	$\pm$ 12.10	0.179	82.3	205.92	$\pm$ 5.11	$\pm$ 8.93		
0.20–0.24	0.219	67.1	250.63	$\pm$ 5.62	$\pm$ 9.26	0.218	82.3	189.76	$\pm$ 4.83	$\pm$ 6.64		
0.24–0.30	0.266	67.0	205.87	$\pm$ 4.25	$\pm$ 6.47	0.266	82.0	143.60	$\pm$ 3.55	$\pm$ 4.37		
0.30–0.36	0.325	67.0	156.30	$\pm$ 3.78	$\pm$ 5.09	0.326	81.9	101.54	$\pm$ 3.08	$\pm$ 3.71		
0.36–0.42	0.384	66.9	118.97	$\pm$ 3.24	$\pm$ 3.80	0.383	82.1	69.04	$\pm$ 2.50	$\pm$ 2.74		
0.42–0.50	0.452	66.7	88.54	$\pm$ 2.39	$\pm$ 3.50	0.451	81.6	49.72	$\pm$ 1.80	$\pm$ 2.44		
0.50–0.60	0.538	66.5	55.91	$\pm$ 1.68	$\pm$ 3.05	0.537	81.8	31.67	$\pm$ 1.27	$\pm$ 2.12		
0.60–0.72	0.641	66.6	30.82	$\pm$ 1.11	$\pm$ 2.34	0.638	81.4	15.06	$\pm$ 0.79	$\pm$ 1.38		
0.72–0.90	0.777	66.3	11.91	$\pm$ 0.50	$\pm$ 1.32	0.777	81.6	6.43	$\pm$ 0.38	$\pm$ 0.83		
0.90–1.25	1.005	66.2	2.56	$\pm$ 0.13	$\pm$ 0.47	0.993	82.1	1.02	$\pm$ 0.08	$\pm$ 0.22		
$p_T$	90 < $\theta$ < 105						105 < $\theta$ < 125					
	$\langle p_T \rangle$	$\langle \theta \rangle$	$d^2\sigma/dpd\Omega$				$\langle p_T \rangle$	$\langle \theta \rangle$	$d^2\sigma/dpd\Omega$			
			$\langle p_T \rangle$	$\langle \theta \rangle$	$d^2\sigma/dpd\Omega$	$d^2\sigma/dpd\Omega$			$\langle p_T \rangle$	$\langle \theta \rangle$	$d^2\sigma/dpd\Omega$	$d^2\sigma/dpd\Omega$
0.13–0.16	0.146	97.5	181.45	$\pm$ 6.61	$\pm$ 10.27	0.144	114.6	160.79	$\pm$ 4.77	$\pm$ 8.08		
0.16–0.20	0.179	97.4	175.20	$\pm$ 4.70	$\pm$ 7.15	0.178	114.3	132.06	$\pm$ 3.52	$\pm$ 4.90		
0.20–0.24	0.218	97.0	149.48	$\pm$ 4.33	$\pm$ 4.88	0.217	114.1	97.15	$\pm$ 3.11	$\pm$ 3.15		
0.24–0.30	0.265	97.0	107.27	$\pm$ 3.09	$\pm$ 3.35	0.265	113.7	55.27	$\pm$ 1.93	$\pm$ 2.11		
0.30–0.36	0.325	96.8	65.36	$\pm$ 2.45	$\pm$ 2.64	0.323	113.7	33.08	$\pm$ 1.48	$\pm$ 1.78		
0.36–0.42	0.384	96.9	42.93	$\pm$ 1.96	$\pm$ 2.25	0.383	112.9	18.30	$\pm$ 1.10	$\pm$ 1.33		
0.42–0.50	0.452	96.7	28.53	$\pm$ 1.36	$\pm$ 1.99	0.449	113.4	13.57	$\pm$ 0.81	$\pm$ 1.29		
0.50–0.60	0.536	96.1	15.62	$\pm$ 0.89	$\pm$ 1.47	0.534	112.8	4.92	$\pm$ 0.41	$\pm$ 0.64		
0.60–0.72	0.639	95.4	7.25	$\pm$ 0.52	$\pm$ 0.93	0.638	112.8	1.94	$\pm$ 0.24	$\pm$ 0.33		
0.72–0.90	0.780	96.4	2.19	$\pm$ 0.22	$\pm$ 0.38	0.776	111.7	0.43	$\pm$ 0.08	$\pm$ 0.10		
0.90–1.25	0.996	95.8	0.27	$\pm$ 0.04	$\pm$ 0.08	0.987	109.5	0.03	$\pm$ 0.01	$\pm$ 0.02		

Table A.30: Double-differential inclusive cross-section  $d^2\sigma/dpd\Omega$  [mb/(GeV/c sr)] of the production of  $\pi^-$ 's in  $p + \text{Sn} \rightarrow \pi^- + \text{X}$  interactions with +12.0 GeV/c beam momentum; the first error is statistical, the second systematic;  $p_T$  in GeV/c, polar angle  $\theta$  in degrees.

$p_T$	20 < $\theta$ < 30				30 < $\theta$ < 40			
	$\langle p_T \rangle$	$\langle \theta \rangle$	$d^2\sigma/dpd\Omega$		$\langle p_T \rangle$	$\langle \theta \rangle$	$d^2\sigma/dpd\Omega$	
			$d^2\sigma/dpd\Omega$	$d^2\sigma/dpd\Omega$			$d^2\sigma/dpd\Omega$	$d^2\sigma/dpd\Omega$
0.10–0.13	0.115	24.8	578.17 ± 13.58 ± 38.93	0.115	34.9	505.64 ± 12.67 ± 35.61		
0.13–0.16	0.145	24.9	644.02 ± 13.43 ± 35.19	0.145	34.9	537.48 ± 11.94 ± 29.26		
0.16–0.20	0.179	24.9	644.19 ± 11.25 ± 29.01	0.179	34.7	521.61 ± 10.02 ± 23.65		
0.20–0.24	0.218	24.9	614.37 ± 10.77 ± 23.36	0.219	34.8	514.19 ± 9.90 ± 19.65		
0.24–0.30	0.267	24.8	535.39 ± 8.15 ± 16.83	0.267	34.7	456.81 ± 7.65 ± 14.39		
0.30–0.36	0.326	24.9	435.85 ± 7.41 ± 11.94	0.326	34.8	353.15 ± 6.62 ± 9.64		
0.36–0.42	0.384	24.9	334.21 ± 6.45 ± 9.35	0.384	34.7	287.81 ± 6.05 ± 7.97		
0.42–0.50	0.451	25.0	236.32 ± 4.70 ± 7.99	0.451	34.9	187.91 ± 4.11 ± 6.19		
0.50–0.60	0.537	24.9	155.25 ± 3.37 ± 7.14	0.538	34.9	122.51 ± 2.97 ± 5.47		
0.60–0.72	0.642	24.8	83.85 ± 2.23 ± 5.37	0.642	34.9	66.69 ± 1.94 ± 4.20		
0.72–0.90				0.780	34.9	29.59 ± 1.03 ± 2.68		
$p_T$	40 < $\theta$ < 50				50 < $\theta$ < 60			
	$\langle p_T \rangle$	$\langle \theta \rangle$	$d^2\sigma/dpd\Omega$		$\langle p_T \rangle$	$\langle \theta \rangle$	$d^2\sigma/dpd\Omega$	
			$d^2\sigma/dpd\Omega$	$d^2\sigma/dpd\Omega$			$d^2\sigma/dpd\Omega$	$d^2\sigma/dpd\Omega$
0.10–0.13	0.115	44.8	447.30 ± 12.25 ± 32.40	0.145	54.8	365.67 ± 9.98 ± 21.02		
0.13–0.16	0.145	44.9	467.77 ± 11.25 ± 25.85	0.180	54.8	383.93 ± 8.54 ± 17.50		
0.16–0.20	0.180	44.8	418.14 ± 8.80 ± 19.09	0.220	55.0	328.75 ± 7.94 ± 12.46		
0.20–0.24	0.220	44.9	411.26 ± 8.88 ± 15.94	0.269	54.7	281.20 ± 6.08 ± 9.34		
0.24–0.30	0.270	44.8	356.04 ± 6.75 ± 11.26	0.329	54.8	221.17 ± 5.37 ± 6.42		
0.30–0.36	0.329	44.8	288.51 ± 6.13 ± 8.33	0.388	54.8	176.23 ± 4.81 ± 5.46		
0.36–0.42	0.389	44.7	217.36 ± 5.20 ± 6.22	0.457	54.8	123.81 ± 3.40 ± 4.51		
0.42–0.50	0.458	44.8	165.76 ± 3.95 ± 5.73	0.547	54.8	76.46 ± 2.36 ± 3.77		
0.50–0.60	0.545	44.9	98.43 ± 2.66 ± 4.65	0.655	54.6	42.06 ± 1.58 ± 2.85		
0.60–0.72	0.653	44.8	49.81 ± 1.68 ± 3.35	0.797	54.8	16.45 ± 0.76 ± 1.64		
0.72–0.90	0.796	44.9	24.10 ± 0.93 ± 2.29	1.018	54.3	3.21 ± 0.21 ± 0.52		
$p_T$	60 < $\theta$ < 75				75 < $\theta$ < 90			
	$\langle p_T \rangle$	$\langle \theta \rangle$	$d^2\sigma/dpd\Omega$		$\langle p_T \rangle$	$\langle \theta \rangle$	$d^2\sigma/dpd\Omega$	
			$d^2\sigma/dpd\Omega$	$d^2\sigma/dpd\Omega$			$d^2\sigma/dpd\Omega$	$d^2\sigma/dpd\Omega$
0.13–0.16	0.145	67.4	341.79 ± 11.29 ± 18.90	0.146	82.5	277.68 ± 7.85 ± 15.59		
0.16–0.20	0.180	67.2	307.85 ± 6.15 ± 13.22	0.180	82.3	251.88 ± 5.68 ± 10.53		
0.20–0.24	0.221	67.2	265.52 ± 5.78 ± 9.41	0.221	82.3	206.77 ± 5.07 ± 6.98		
0.24–0.30	0.271	67.0	209.75 ± 4.27 ± 6.57	0.270	82.0	148.32 ± 3.61 ± 4.71		
0.30–0.36	0.331	67.0	155.26 ± 3.70 ± 4.71	0.332	82.0	100.90 ± 3.00 ± 3.48		
0.36–0.42	0.393	66.9	122.69 ± 3.28 ± 4.12	0.393	81.7	73.39 ± 2.57 ± 3.17		
0.42–0.50	0.465	66.9	83.76 ± 2.29 ± 3.45	0.464	81.4	47.88 ± 1.76 ± 2.52		
0.50–0.60	0.553	66.8	47.30 ± 1.50 ± 2.65	0.555	81.8	27.07 ± 1.14 ± 1.94		
0.60–0.72	0.665	66.7	23.13 ± 0.93 ± 1.80	0.665	81.2	11.62 ± 0.67 ± 1.13		
0.72–0.90	0.811	66.8	8.86 ± 0.47 ± 0.95	0.806	81.2	3.51 ± 0.29 ± 0.47		
0.90–1.25	1.063	66.7	1.50 ± 0.11 ± 0.27	1.054	81.2	0.54 ± 0.07 ± 0.12		
$p_T$	90 < $\theta$ < 105				105 < $\theta$ < 125			
	$\langle p_T \rangle$	$\langle \theta \rangle$	$d^2\sigma/dpd\Omega$		$\langle p_T \rangle$	$\langle \theta \rangle$	$d^2\sigma/dpd\Omega$	
			$d^2\sigma/dpd\Omega$	$d^2\sigma/dpd\Omega$			$d^2\sigma/dpd\Omega$	$d^2\sigma/dpd\Omega$
0.13–0.16	0.145	97.2	272.21 ± 20.29 ± 15.31	0.145	114.4	199.85 ± 5.25 ± 10.28		
0.16–0.20	0.180	97.4	212.25 ± 5.22 ± 8.58	0.179	114.3	145.79 ± 3.71 ± 5.21		
0.20–0.24	0.220	97.2	165.13 ± 4.65 ± 5.38	0.220	113.7	93.76 ± 3.02 ± 3.19		
0.24–0.30	0.270	97.0	110.16 ± 3.15 ± 3.81	0.269	113.5	57.78 ± 1.96 ± 2.46		
0.30–0.36	0.330	97.1	63.95 ± 2.42 ± 2.91	0.331	113.3	32.20 ± 1.46 ± 1.95		
0.36–0.42	0.393	96.5	42.00 ± 1.95 ± 2.44	0.393	112.9	18.61 ± 1.07 ± 1.52		
0.42–0.50	0.463	96.8	27.50 ± 1.31 ± 2.08	0.461	112.9	10.36 ± 0.71 ± 1.10		
0.50–0.60	0.552	97.0	12.91 ± 0.79 ± 1.33	0.550	112.3	4.41 ± 0.40 ± 0.62		
0.60–0.72	0.666	96.1	5.43 ± 0.45 ± 0.76	0.657	112.2	1.53 ± 0.21 ± 0.28		
0.72–0.90	0.806	95.9	1.44 ± 0.18 ± 0.27	0.803	112.4	0.35 ± 0.07 ± 0.09		
0.90–1.25	1.063	97.4	0.12 ± 0.03 ± 0.04					

Table A.31: Double-differential inclusive cross-section  $d^2\sigma/dpd\Omega$  [mb/(GeV/c sr)] of the production of protons in  $\pi^+ + \text{Sn} \rightarrow p + X$  interactions with  $+12.0$  GeV/c beam momentum; the first error is statistical, the second systematic;  $p_T$  in GeV/c, polar angle  $\theta$  in degrees.

$p_T$	20 < $\theta$ < 30				30 < $\theta$ < 40			
	$\langle p_T \rangle$	$\langle \theta \rangle$	$d^2\sigma/dpd\Omega$		$\langle p_T \rangle$	$\langle \theta \rangle$	$d^2\sigma/dpd\Omega$	
			$d^2\sigma/dpd\Omega$	$d^2\sigma/dpd\Omega$			$d^2\sigma/dpd\Omega$	$d^2\sigma/dpd\Omega$
0.20–0.24	0.222	25.2	919.71 $\pm$ 46.41 $\pm$ 45.43		0.273	35.1	917.12 $\pm$ 37.23 $\pm$ 37.62	
0.24–0.30	0.271	25.3	733.77 $\pm$ 33.61 $\pm$ 33.35		0.333	35.1	798.58 $\pm$ 33.97 $\pm$ 28.94	
0.30–0.36	0.333	25.2	625.48 $\pm$ 31.60 $\pm$ 28.93		0.393	35.2	636.82 $\pm$ 31.44 $\pm$ 24.75	
0.36–0.42	0.393	25.3	488.37 $\pm$ 28.43 $\pm$ 25.06		0.465	35.2	526.73 $\pm$ 25.67 $\pm$ 24.99	
0.42–0.50	0.465	25.3	345.35 $\pm$ 20.53 $\pm$ 18.68		0.554	35.3	351.22 $\pm$ 19.09 $\pm$ 20.08	
0.50–0.60	0.557	25.4	260.85 $\pm$ 15.97 $\pm$ 15.59		0.670	35.2	205.62 $\pm$ 13.37 $\pm$ 14.76	
0.60–0.72	0.668	25.3	181.58 $\pm$ 11.88 $\pm$ 12.33		0.818	35.2	123.69 $\pm$ 8.58 $\pm$ 11.76	
0.72–0.90								
$p_T$	40 < $\theta$ < 50				50 < $\theta$ < 60			
	$\langle p_T \rangle$	$\langle \theta \rangle$	$d^2\sigma/dpd\Omega$		$\langle p_T \rangle$	$\langle \theta \rangle$	$d^2\sigma/dpd\Omega$	
			$d^2\sigma/dpd\Omega$	$d^2\sigma/dpd\Omega$			$d^2\sigma/dpd\Omega$	$d^2\sigma/dpd\Omega$
0.30–0.36	0.330	45.0	906.65 $\pm$ 35.61 $\pm$ 28.02		0.388	55.0	768.38 $\pm$ 31.90 $\pm$ 22.26	
0.36–0.42	0.388	45.1	703.00 $\pm$ 31.64 $\pm$ 20.48		0.458	54.9	623.62 $\pm$ 25.64 $\pm$ 18.10	
0.42–0.50	0.458	45.0	538.70 $\pm$ 24.93 $\pm$ 18.88		0.547	55.0	385.02 $\pm$ 19.20 $\pm$ 16.59	
0.50–0.60	0.548	45.1	392.94 $\pm$ 20.12 $\pm$ 21.17		0.655	55.1	231.25 $\pm$ 14.59 $\pm$ 16.98	
0.60–0.72	0.657	45.0	268.88 $\pm$ 15.68 $\pm$ 18.62		0.805	54.9	108.90 $\pm$ 8.54 $\pm$ 11.25	
0.72–0.90	0.794	44.9	128.08 $\pm$ 9.08 $\pm$ 12.40					
0.90–1.25	1.036	44.7	35.27 $\pm$ 3.38 $\pm$ 5.04					
$p_T$	60 < $\theta$ < 75				75 < $\theta$ < 90			
	$\langle p_T \rangle$	$\langle \theta \rangle$	$d^2\sigma/dpd\Omega$		$\langle p_T \rangle$	$\langle \theta \rangle$	$d^2\sigma/dpd\Omega$	
			$d^2\sigma/dpd\Omega$	$d^2\sigma/dpd\Omega$			$d^2\sigma/dpd\Omega$	$d^2\sigma/dpd\Omega$
0.50–0.60	0.537	67.5	400.56 $\pm$ 14.80 $\pm$ 15.51		0.537	82.3	339.94 $\pm$ 13.39 $\pm$ 16.19	
0.60–0.72	0.641	67.5	222.32 $\pm$ 11.09 $\pm$ 14.83		0.639	82.1	182.16 $\pm$ 9.53 $\pm$ 11.96	
0.72–0.90	0.780	67.0	99.99 $\pm$ 6.75 $\pm$ 11.78		0.775	81.6	64.88 $\pm$ 5.51 $\pm$ 8.80	
$p_T$	90 < $\theta$ < 105				105 < $\theta$ < 125			
	$\langle p_T \rangle$	$\langle \theta \rangle$	$d^2\sigma/dpd\Omega$		$\langle p_T \rangle$	$\langle \theta \rangle$	$d^2\sigma/dpd\Omega$	
			$d^2\sigma/dpd\Omega$	$d^2\sigma/dpd\Omega$			$d^2\sigma/dpd\Omega$	$d^2\sigma/dpd\Omega$
0.42–0.50	0.535	97.2	253.36 $\pm$ 11.53 $\pm$ 16.17		0.449	113.7	238.21 $\pm$ 10.22 $\pm$ 14.70	
0.50–0.60	0.641	96.8	119.91 $\pm$ 7.82 $\pm$ 9.83		0.537	112.8	113.13 $\pm$ 6.87 $\pm$ 9.72	
0.60–0.72					0.642	112.4	41.03 $\pm$ 4.49 $\pm$ 6.16	

Table A.32: Double-differential inclusive cross-section  $d^2\sigma/dpd\Omega$  [mb/(GeV/c sr)] of the production of  $\pi^+$ 's in  $\pi^+ + \text{Sn} \rightarrow \pi^+ + \text{X}$  interactions with +12.0 GeV/c beam momentum; the first error is statistical, the second systematic;  $p_T$  in GeV/c, polar angle  $\theta$  in degrees.

			20 < $\theta$ < 30				30 < $\theta$ < 40					
$p_T$	$\langle p_T \rangle$	$\langle \theta \rangle$	$d^2\sigma/dpd\Omega$				$\langle p_T \rangle$	$\langle \theta \rangle$	$d^2\sigma/dpd\Omega$			
0.10–0.13	0.116	24.6	511.20	± 45.97	± 40.33		0.117	34.9	354.18	± 38.23	± 28.56	
0.13–0.16	0.146	25.3	507.21	± 40.99	± 28.29		0.147	34.8	381.29	± 34.15	± 20.48	
0.16–0.20	0.182	25.0	624.86	± 38.64	± 29.65		0.180	35.0	459.24	± 32.09	± 21.07	
0.20–0.24	0.221	24.5	624.61	± 36.85	± 25.22		0.220	34.9	459.84	± 31.99	± 18.24	
0.24–0.30	0.271	24.7	671.06	± 31.49	± 23.56		0.273	34.5	416.32	± 24.65	± 14.23	
0.30–0.36	0.331	24.9	529.34	± 27.61	± 16.20		0.333	34.8	408.85	± 24.57	± 12.33	
0.36–0.42	0.395	24.6	446.04	± 25.05	± 13.47		0.395	34.9	365.53	± 23.43	± 10.96	
0.42–0.50	0.466	24.7	321.95	± 18.04	± 11.49		0.467	34.5	251.33	± 16.26	± 8.37	
0.50–0.60	0.556	24.5	219.00	± 12.85	± 10.90		0.555	34.8	171.68	± 11.63	± 7.82	
0.60–0.72	0.668	24.7	160.15	± 9.71	± 11.84		0.669	34.8	112.33	± 8.41	± 7.48	
0.72–0.90							0.822	34.5	52.07	± 4.02	± 5.49	
			40 < $\theta$ < 50				50 < $\theta$ < 60					
$p_T$	$\langle p_T \rangle$	$\langle \theta \rangle$	$d^2\sigma/dpd\Omega$				$\langle p_T \rangle$	$\langle \theta \rangle$	$d^2\sigma/dpd\Omega$			
0.10–0.13	0.118	45.6	342.26	± 39.82	± 30.96		0.146	54.6	378.23	± 34.61	± 21.58	
0.13–0.16	0.146	44.7	357.96	± 32.41	± 19.42		0.181	54.9	310.44	± 25.59	± 14.08	
0.16–0.20	0.180	44.6	417.26	± 30.08	± 19.00		0.220	54.8	299.22	± 25.53	± 11.53	
0.20–0.24	0.221	44.9	392.62	± 29.61	± 15.57		0.269	55.0	280.65	± 20.47	± 9.43	
0.24–0.30	0.269	44.7	338.13	± 22.48	± 11.65		0.328	54.7	219.89	± 18.20	± 6.85	
0.30–0.36	0.331	44.5	279.34	± 20.31	± 8.46		0.389	54.4	181.55	± 16.46	± 5.57	
0.36–0.42	0.386	44.8	233.06	± 18.75	± 6.94		0.459	54.3	151.77	± 12.89	± 5.41	
0.42–0.50	0.458	44.9	204.14	± 14.81	± 6.92		0.547	54.7	103.70	± 9.39	± 4.85	
0.50–0.60	0.546	44.6	139.97	± 10.87	± 6.11		0.652	54.6	51.10	± 5.82	± 3.29	
0.60–0.72	0.659	44.9	74.66	± 7.01	± 4.60		0.801	54.1	20.47	± 2.74	± 1.94	
0.72–0.90	0.808	44.3	26.65	± 2.88	± 2.55		0.996	55.0	4.88	± 0.76	± 0.78	
			60 < $\theta$ < 75				75 < $\theta$ < 90					
$p_T$	$\langle p_T \rangle$	$\langle \theta \rangle$	$d^2\sigma/dpd\Omega$				$\langle p_T \rangle$	$\langle \theta \rangle$	$d^2\sigma/dpd\Omega$			
0.13–0.16	0.144	67.5	218.26	± 22.22	± 12.62		0.145	81.6	189.32	± 22.05	± 11.02	
0.16–0.20	0.178	67.5	211.86	± 17.05	± 9.64		0.178	83.1	202.65	± 17.25	± 8.93	
0.20–0.24	0.220	66.2	272.23	± 19.58	± 10.26		0.219	83.2	156.73	± 14.81	± 5.62	
0.24–0.30	0.267	67.0	199.13	± 13.99	± 6.43		0.264	82.1	143.30	± 11.87	± 4.54	
0.30–0.36	0.326	67.7	172.37	± 13.34	± 5.61		0.324	82.5	89.71	± 9.65	± 3.26	
0.36–0.42	0.384	67.6	130.09	± 11.31	± 4.16		0.382	81.5	76.75	± 8.92	± 3.01	
0.42–0.50	0.452	66.9	77.09	± 7.50	± 3.08		0.449	81.5	57.66	± 6.55	± 2.84	
0.50–0.60	0.539	66.6	56.64	± 5.70	± 3.10		0.543	80.9	33.74	± 4.41	± 2.27	
0.60–0.72	0.649	66.7	36.05	± 4.08	± 2.74		0.644	81.7	17.06	± 2.82	± 1.56	
0.72–0.90	0.773	66.4	12.85	± 1.77	± 1.43		0.778	81.4	7.54	± 1.38	± 0.98	
0.90–1.25	0.994	65.4	3.10	± 0.49	± 0.56		0.989	81.1	1.19	± 0.32	± 0.25	
			90 < $\theta$ < 105				105 < $\theta$ < 125					
$p_T$	$\langle p_T \rangle$	$\langle \theta \rangle$	$d^2\sigma/dpd\Omega$				$\langle p_T \rangle$	$\langle \theta \rangle$	$d^2\sigma/dpd\Omega$			
0.13–0.16	0.144	97.8	175.96	± 21.21	± 9.98		0.146	114.8	131.72	± 15.30	± 6.44	
0.16–0.20	0.180	97.1	172.49	± 15.78	± 7.17		0.178	114.4	108.41	± 10.67	± 4.12	
0.20–0.24	0.217	97.2	145.56	± 14.44	± 4.89		0.217	113.4	97.90	± 10.43	± 3.22	
0.24–0.30	0.266	97.4	82.15	± 9.14	± 2.72		0.263	113.0	63.96	± 7.01	± 2.47	
0.30–0.36	0.323	97.6	70.81	± 8.53	± 2.90		0.322	113.6	35.74	± 5.22	± 1.91	
0.36–0.42	0.386	97.4	47.20	± 6.88	± 2.46		0.382	114.0	26.49	± 4.41	± 1.91	
0.42–0.50	0.452	96.7	32.21	± 4.81	± 2.24		0.447	111.1	13.83	± 2.78	± 1.30	
0.50–0.60	0.537	97.1	14.41	± 2.85	± 1.35		0.541	113.9	7.59	± 1.71	± 0.96	
0.60–0.72	0.633	97.1	5.56	± 1.50	± 0.71		0.636	113.6	3.11	± 1.01	± 0.51	
0.72–0.90	0.758	96.6	1.76	± 0.63	± 0.31		0.770	109.8	0.62	± 0.31	± 0.14	
0.90–1.25	1.012	94.9	0.24	± 0.11	± 0.07							

Table A.33: Double-differential inclusive cross-section  $d^2\sigma/dpd\Omega$  [mb/(GeV/c sr)] of the production of  $\pi^-$ 's in  $\pi^+ + \text{Sn} \rightarrow \pi^- + \text{X}$  interactions with +12.0 GeV/c beam momentum; the first error is statistical, the second systematic;  $p_T$  in GeV/c, polar angle  $\theta$  in degrees.

$p_T$	20 < $\theta$ < 30						30 < $\theta$ < 40						
	$\langle p_T \rangle$	$\langle \theta \rangle$	$d^2\sigma/dpd\Omega$				$\langle p_T \rangle$	$\langle \theta \rangle$	$d^2\sigma/dpd\Omega$				
			518.81	$\pm$	44.83	$\pm$	39.22	546.33	$\pm$	46.89	$\pm$	43.97	
0.10–0.13	0.115	24.9	518.81	$\pm$	44.83	$\pm$	39.22	0.114	34.6	546.33	$\pm$	46.89	
0.13–0.16	0.144	25.0	693.78	$\pm$	47.31	$\pm$	38.89	0.145	34.5	530.26	$\pm$	39.72	
0.16–0.20	0.178	24.6	655.77	$\pm$	38.24	$\pm$	29.99	0.179	34.8	441.05	$\pm$	31.00	
0.20–0.24	0.217	24.5	615.46	$\pm$	36.02	$\pm$	23.85	0.218	34.9	458.40	$\pm$	31.40	
0.24–0.30	0.269	24.7	554.15	$\pm$	27.73	$\pm$	17.92	0.268	34.7	503.05	$\pm$	26.99	
0.30–0.36	0.324	25.0	461.58	$\pm$	25.77	$\pm$	13.10	0.325	35.1	317.46	$\pm$	21.28	
0.36–0.42	0.383	24.9	374.84	$\pm$	23.03	$\pm$	10.82	0.385	35.0	299.25	$\pm$	20.93	
0.42–0.50	0.450	25.0	268.11	$\pm$	16.89	$\pm$	9.27	0.452	34.7	183.11	$\pm$	13.72	
0.50–0.60	0.539	24.9	151.49	$\pm$	11.18	$\pm$	7.04	0.537	34.7	133.11	$\pm$	10.39	
0.60–0.72	0.647	24.7	94.60	$\pm$	7.94	$\pm$	6.08	0.644	35.2	75.12	$\pm$	7.01	
0.72–0.90								0.776	34.7	28.42	$\pm$	4.74	
										3.40	$\pm$	2.57	
$p_T$	40 < $\theta$ < 50						50 < $\theta$ < 60						
	$\langle p_T \rangle$	$\langle \theta \rangle$	$d^2\sigma/dpd\Omega$				$\langle p_T \rangle$	$\langle \theta \rangle$	$d^2\sigma/dpd\Omega$				
			411.10	$\pm$	43.46	$\pm$	33.84	0.145	54.6	262.93	$\pm$	27.94	15.26
0.10–0.13	0.114	45.1	403.18	$\pm$	34.38	$\pm$	22.50	0.181	55.0	278.73	$\pm$	24.20	12.89
0.13–0.16	0.146	45.0	393.14	$\pm$	28.81	$\pm$	18.20	0.219	55.1	288.63	$\pm$	24.96	11.17
0.16–0.20	0.179	44.8	466.84	$\pm$	31.80	$\pm$	18.43	0.270	54.9	268.01	$\pm$	20.03	9.24
0.20–0.24	0.220	45.0	325.87	$\pm$	21.66	$\pm$	10.59	0.330	54.8	219.86	$\pm$	17.99	6.56
0.24–0.30	0.269	44.6	259.82	$\pm$	19.49	$\pm$	7.70	0.387	54.9	149.78	$\pm$	14.87	4.70
0.30–0.36	0.330	44.5	215.07	$\pm$	17.35	$\pm$	6.32	0.460	55.1	129.12	$\pm$	11.67	4.78
0.36–0.42	0.389	44.5	160.68	$\pm$	13.12	$\pm$	5.66	0.545	54.9	79.43	$\pm$	8.09	3.95
0.42–0.50	0.455	45.1	96.93	$\pm$	8.87	$\pm$	4.62	0.651	54.6	42.24	$\pm$	5.34	2.88
0.50–0.60	0.653	45.3	53.66	$\pm$	5.89	$\pm$	3.63	0.791	54.9	21.08	$\pm$	2.88	2.10
0.60–0.72	0.794	45.2	29.35	$\pm$	3.48	$\pm$	2.80	1.033	54.0	3.76	$\pm$	0.75	0.61
$p_T$	60 < $\theta$ < 75						75 < $\theta$ < 90						
	$\langle p_T \rangle$	$\langle \theta \rangle$	$d^2\sigma/dpd\Omega$				$\langle p_T \rangle$	$\langle \theta \rangle$	$d^2\sigma/dpd\Omega$				
			275.33	$\pm$	24.62	$\pm$	15.39	0.147	82.7	225.60	$\pm$	23.64	12.77
0.13–0.16	0.147	67.8	289.45	$\pm$	20.08	$\pm$	12.65	0.180	82.3	177.46	$\pm$	16.03	7.56
0.16–0.20	0.182	66.4	251.18	$\pm$	18.97	$\pm$	9.14	0.220	82.9	171.48	$\pm$	15.64	5.96
0.20–0.24	0.220	66.9	172.22	$\pm$	13.03	$\pm$	5.77	0.273	81.7	141.49	$\pm$	11.86	4.80
0.24–0.30	0.271	67.0	140.84	$\pm$	11.84	$\pm$	4.52	0.335	81.7	92.31	$\pm$	9.65	3.32
0.30–0.36	0.331	66.9	82.48	$\pm$	8.99	$\pm$	2.86	0.395	82.6	77.68	$\pm$	8.91	3.40
0.36–0.42	0.394	66.3	91.98	$\pm$	8.09	$\pm$	3.85	0.469	82.1	49.81	$\pm$	6.05	2.64
0.42–0.50	0.462	66.4	39.91	$\pm$	4.62	$\pm$	2.26	0.547	81.0	28.22	$\pm$	3.92	2.03
0.50–0.60	0.658	66.9	25.49	$\pm$	3.29	$\pm$	2.00	0.657	80.1	11.09	$\pm$	2.22	1.08
0.60–0.72	0.818	66.7	9.83	$\pm$	1.66	$\pm$	1.05	0.834	81.5	2.94	$\pm$	0.89	0.40
0.72–0.90	1.066	64.4	1.46	$\pm$	0.37	$\pm$	0.26	1.031	84.0	0.38	$\pm$	0.19	0.08
$p_T$	90 < $\theta$ < 105						105 < $\theta$ < 125						
	$\langle p_T \rangle$	$\langle \theta \rangle$	$d^2\sigma/dpd\Omega$				$\langle p_T \rangle$	$\langle \theta \rangle$	$d^2\sigma/dpd\Omega$				
			224.88	$\pm$	23.27	$\pm$	12.73	0.145	114.7	196.46	$\pm$	17.92	9.57
0.13–0.16	0.146	97.5	190.47	$\pm$	16.63	$\pm$	7.85	0.180	114.4	136.53	$\pm$	12.08	4.86
0.16–0.20	0.220	97.1	159.67	$\pm$	15.35	$\pm$	5.34	0.219	114.0	95.72	$\pm$	10.27	3.31
0.20–0.24	0.270	96.7	94.43	$\pm$	9.88	$\pm$	3.26	0.269	113.9	56.84	$\pm$	6.53	2.44
0.24–0.30	0.331	97.5	68.90	$\pm$	8.46	$\pm$	3.03	0.333	113.1	27.43	$\pm$	4.52	1.67
0.30–0.36	0.393	96.4	44.81	$\pm$	6.68	$\pm$	2.55	0.389	113.5	15.96	$\pm$	3.33	1.30
0.36–0.42	0.463	97.2	30.58	$\pm$	4.63	$\pm$	2.30	0.465	113.7	12.55	$\pm$	2.62	1.32
0.42–0.50	0.555	96.9	14.90	$\pm$	2.87	$\pm$	1.52	0.562	115.2	3.14	$\pm$	1.11	0.43
0.50–0.60	0.663	96.7	6.23	$\pm$	1.61	$\pm$	0.86	0.645	113.9	1.72	$\pm$	0.72	0.31
0.60–0.72	0.830	98.1	1.51	$\pm$	0.62	$\pm$	0.28						

Table A.34: Double-differential inclusive cross-section  $d^2\sigma/dpd\Omega$  [mb/(GeV/c sr)] of the production of protons in  $\pi^- + \text{Sn} \rightarrow p + X$  interactions with  $-12.0 \text{ GeV}/c$  beam momentum; the first error is statistical, the second systematic;  $p_T$  in  $\text{GeV}/c$ , polar angle  $\theta$  in degrees.

$p_T$	20 < $\theta$ < 30			30 < $\theta$ < 40		
	$\langle p_T \rangle$	$\langle \theta \rangle$	$d^2\sigma/dpd\Omega$	$\langle p_T \rangle$	$\langle \theta \rangle$	$d^2\sigma/dpd\Omega$
0.20–0.24	0.219	25.1	846.19 $\pm$ 15.79 $\pm$ 42.10	0.270	35.0	836.56 $\pm$ 12.62 $\pm$ 34.56
0.24–0.30	0.268	25.1	709.25 $\pm$ 11.06 $\pm$ 32.66	0.328	35.3	726.76 $\pm$ 11.00 $\pm$ 26.83
0.30–0.36	0.328	25.2	553.42 $\pm$ 10.16 $\pm$ 28.09	0.388	35.1	558.40 $\pm$ 9.95 $\pm$ 22.84
0.36–0.42	0.387	25.3	455.19 $\pm$ 9.39 $\pm$ 25.02	0.456	35.2	416.93 $\pm$ 7.69 $\pm$ 20.89
0.42–0.50	0.456	25.3	345.05 $\pm$ 7.05 $\pm$ 21.04	0.544	35.1	306.15 $\pm$ 5.97 $\pm$ 17.39
0.50–0.60	0.544	25.3	249.70 $\pm$ 5.36 $\pm$ 16.30	0.651	35.1	186.31 $\pm$ 4.28 $\pm$ 14.42
0.60–0.72	0.652	25.1	166.30 $\pm$ 3.90 $\pm$ 11.83	0.792	35.0	96.22 $\pm$ 2.53 $\pm$ 8.93
0.72–0.90						
40 < $\theta$ < 50						
$p_T$	$\langle p_T \rangle$	$\langle \theta \rangle$	$d^2\sigma/dpd\Omega$	$\langle p_T \rangle$	$\langle \theta \rangle$	$d^2\sigma/dpd\Omega$
0.30–0.36	0.327	45.1	796.44 $\pm$ 11.53 $\pm$ 24.95	0.386	55.1	700.78 $\pm$ 10.21 $\pm$ 21.29
0.36–0.42	0.386	45.1	661.57 $\pm$ 10.28 $\pm$ 19.47	0.454	55.0	543.26 $\pm$ 8.08 $\pm$ 16.49
0.42–0.50	0.454	45.1	489.88 $\pm$ 8.03 $\pm$ 18.02	0.541	55.0	349.27 $\pm$ 6.11 $\pm$ 16.02
0.50–0.60	0.540	45.1	336.29 $\pm$ 6.27 $\pm$ 18.68	0.646	54.9	200.53 $\pm$ 4.63 $\pm$ 15.58
0.60–0.72	0.647	45.1	208.45 $\pm$ 4.67 $\pm$ 15.18	0.785	54.9	97.78 $\pm$ 2.79 $\pm$ 10.82
0.72–0.90	0.784	45.0	102.58 $\pm$ 2.76 $\pm$ 10.57			
60 < $\theta$ < 75						
$p_T$	$\langle p_T \rangle$	$\langle \theta \rangle$	$d^2\sigma/dpd\Omega$	$\langle p_T \rangle$	$\langle \theta \rangle$	$d^2\sigma/dpd\Omega$
0.50–0.60	0.543	67.5	349.60 $\pm$ 4.66 $\pm$ 13.54	0.542	82.0	304.85 $\pm$ 4.25 $\pm$ 14.63
0.60–0.72	0.650	67.4	189.70 $\pm$ 3.46 $\pm$ 13.25	0.649	82.0	157.13 $\pm$ 2.98 $\pm$ 10.45
0.72–0.90	0.790	67.2	79.57 $\pm$ 2.01 $\pm$ 9.45	0.788	82.1	53.89 $\pm$ 1.75 $\pm$ 7.88
90 < $\theta$ < 105						
$p_T$	$\langle p_T \rangle$	$\langle \theta \rangle$	$d^2\sigma/dpd\Omega$	$\langle p_T \rangle$	$\langle \theta \rangle$	$d^2\sigma/dpd\Omega$
0.42–0.50				0.454	113.2	204.95 $\pm$ 3.20 $\pm$ 12.60
0.50–0.60	0.541	97.0	212.82 $\pm$ 3.56 $\pm$ 13.66	0.540	112.8	90.66 $\pm$ 2.09 $\pm$ 7.90
0.60–0.72	0.648	96.8	91.61 $\pm$ 2.31 $\pm$ 7.75	0.647	112.7	30.03 $\pm$ 1.26 $\pm$ 4.40

Table A.35: Double-differential inclusive cross-section  $d^2\sigma/dpd\Omega$  [mb/(GeV/c sr)] of the production of  $\pi^+$ 's in  $\pi^- + \text{Sn} \rightarrow \pi^+ + \text{X}$  interactions with  $-12.0$  GeV/c beam momentum; the first error is statistical, the second systematic;  $p_T$  in GeV/c, polar angle  $\theta$  in degrees.

$p_T$	20 < $\theta$ < 30						30 < $\theta$ < 40					
	$\langle p_T \rangle$	$\langle \theta \rangle$	$d^2\sigma/dpd\Omega$				$\langle p_T \rangle$	$\langle \theta \rangle$	$d^2\sigma/dpd\Omega$			
			$\langle p_T \rangle$	$\langle \theta \rangle$	$d^2\sigma/dpd\Omega$	$d^2\sigma/dpd\Omega$			$\langle p_T \rangle$	$\langle \theta \rangle$	$d^2\sigma/dpd\Omega$	$d^2\sigma/dpd\Omega$
0.10–0.13	0.116	25.0	462.27	$\pm$ 13.91	$\pm$ 31.68	0.115	34.8	386.69	$\pm$ 12.56	$\pm$ 27.54		
0.13–0.16	0.145	24.8	548.42	$\pm$ 13.83	$\pm$ 29.63	0.145	34.9	442.69	$\pm$ 12.33	$\pm$ 24.02		
0.16–0.20	0.180	24.7	591.05	$\pm$ 12.09	$\pm$ 27.14	0.180	34.8	450.75	$\pm$ 10.43	$\pm$ 20.52		
0.20–0.24	0.219	24.8	603.62	$\pm$ 12.05	$\pm$ 24.34	0.219	34.7	434.09	$\pm$ 10.16	$\pm$ 17.13		
0.24–0.30	0.268	24.8	563.43	$\pm$ 9.34	$\pm$ 19.22	0.269	34.8	442.45	$\pm$ 8.53	$\pm$ 15.11		
0.30–0.36	0.327	24.8	493.56	$\pm$ 8.96	$\pm$ 16.36	0.327	34.8	380.94	$\pm$ 7.89	$\pm$ 11.53		
0.36–0.42	0.387	24.8	360.45	$\pm$ 7.36	$\pm$ 10.86	0.387	34.8	297.25	$\pm$ 6.84	$\pm$ 8.64		
0.42–0.50	0.456	24.8	296.26	$\pm$ 5.75	$\pm$ 10.53	0.456	34.8	217.70	$\pm$ 4.94	$\pm$ 7.11		
0.50–0.60	0.544	24.8	190.84	$\pm$ 3.95	$\pm$ 9.50	0.544	34.8	147.35	$\pm$ 3.51	$\pm$ 6.57		
0.60–0.72	0.652	24.8	107.06	$\pm$ 2.48	$\pm$ 7.93	0.651	34.8	90.14	$\pm$ 2.38	$\pm$ 5.94		
0.72–0.90						0.788	34.8	40.66	$\pm$ 1.16	$\pm$ 4.37		
$p_T$	40 < $\theta$ < 50						50 < $\theta$ < 60					
	$\langle p_T \rangle$	$\langle \theta \rangle$	$d^2\sigma/dpd\Omega$				$\langle p_T \rangle$	$\langle \theta \rangle$	$d^2\sigma/dpd\Omega$			
			$\langle p_T \rangle$	$\langle \theta \rangle$	$d^2\sigma/dpd\Omega$	$d^2\sigma/dpd\Omega$			$\langle p_T \rangle$	$\langle \theta \rangle$	$d^2\sigma/dpd\Omega$	$d^2\sigma/dpd\Omega$
0.10–0.13	0.115	45.2	331.67	$\pm$ 12.15	$\pm$ 23.86	0.145	54.7	291.28	$\pm$ 10.32	$\pm$ 16.97		
0.13–0.16	0.145	45.0	362.90	$\pm$ 11.18	$\pm$ 20.05	0.179	54.8	293.68	$\pm$ 8.37	$\pm$ 13.61		
0.16–0.20	0.179	44.8	372.22	$\pm$ 9.50	$\pm$ 17.17	0.219	54.8	286.47	$\pm$ 8.35	$\pm$ 11.30		
0.20–0.24	0.219	44.8	329.19	$\pm$ 8.85	$\pm$ 13.10	0.268	54.6	252.61	$\pm$ 6.40	$\pm$ 8.49		
0.24–0.30	0.268	44.8	334.56	$\pm$ 7.34	$\pm$ 11.26	0.327	54.7	214.99	$\pm$ 6.05	$\pm$ 7.47		
0.30–0.36	0.327	44.7	275.04	$\pm$ 6.72	$\pm$ 8.67	0.386	54.6	166.22	$\pm$ 5.25	$\pm$ 5.74		
0.36–0.42	0.386	44.7	221.23	$\pm$ 5.94	$\pm$ 6.57	0.453	54.6	131.32	$\pm$ 3.97	$\pm$ 4.69		
0.42–0.50	0.453	44.7	168.73	$\pm$ 4.43	$\pm$ 5.57	0.540	54.4	75.82	$\pm$ 2.55	$\pm$ 3.52		
0.50–0.60	0.540	44.8	109.79	$\pm$ 3.10	$\pm$ 4.70	0.648	66.71	49.58	$\pm$ 1.88	$\pm$ 3.17		
0.60–0.72	0.648	44.6	66.71	$\pm$ 2.08	$\pm$ 4.04	0.72–0.90	33.48	22.69	$\pm$ 0.96	$\pm$ 2.09		
0.72–0.90	0.786	44.6	33.48	$\pm$ 1.15	$\pm$ 3.10	0.90–1.25	54.7	5.19	$\pm$ 0.26	$\pm$ 0.83		
$p_T$	60 < $\theta$ < 75						75 < $\theta$ < 90					
	$\langle p_T \rangle$	$\langle \theta \rangle$	$d^2\sigma/dpd\Omega$				$\langle p_T \rangle$	$\langle \theta \rangle$	$d^2\sigma/dpd\Omega$			
			$\langle p_T \rangle$	$\langle \theta \rangle$	$d^2\sigma/dpd\Omega$	$d^2\sigma/dpd\Omega$			$\langle p_T \rangle$	$\langle \theta \rangle$	$d^2\sigma/dpd\Omega$	$d^2\sigma/dpd\Omega$
0.13–0.16	0.145	67.2	227.29	$\pm$ 7.72	$\pm$ 13.39	0.146	82.5	174.15	$\pm$ 7.38	$\pm$ 10.83		
0.16–0.20	0.179	67.2	241.71	$\pm$ 6.12	$\pm$ 11.21	0.180	82.4	186.41	$\pm$ 5.48	$\pm$ 8.40		
0.20–0.24	0.219	67.4	211.90	$\pm$ 5.77	$\pm$ 8.19	0.219	82.1	163.59	$\pm$ 5.12	$\pm$ 6.08		
0.24–0.30	0.268	67.3	185.77	$\pm$ 4.53	$\pm$ 6.24	0.268	82.1	124.58	$\pm$ 3.67	$\pm$ 3.94		
0.30–0.36	0.327	66.8	147.18	$\pm$ 4.04	$\pm$ 4.78	0.329	81.7	95.18	$\pm$ 3.31	$\pm$ 3.62		
0.36–0.42	0.387	67.0	114.15	$\pm$ 3.56	$\pm$ 3.97	0.388	81.7	67.80	$\pm$ 2.76	$\pm$ 2.85		
0.42–0.50	0.456	66.8	83.77	$\pm$ 2.58	$\pm$ 3.39	0.458	82.2	43.81	$\pm$ 1.88	$\pm$ 2.20		
0.50–0.60	0.544	66.8	54.93	$\pm$ 1.84	$\pm$ 3.00	0.544	82.0	27.92	$\pm$ 1.31	$\pm$ 1.90		
0.60–0.72	0.651	67.1	30.28	$\pm$ 1.20	$\pm$ 2.28	0.651	81.7	14.28	$\pm$ 0.81	$\pm$ 1.31		
0.72–0.90	0.787	66.6	10.93	$\pm$ 0.53	$\pm$ 1.19	0.789	81.5	5.24	$\pm$ 0.37	$\pm$ 0.68		
0.90–1.25	1.025	66.2	2.33	$\pm$ 0.13	$\pm$ 0.43	1.016	81.4	0.82	$\pm$ 0.08	$\pm$ 0.18		
$p_T$	90 < $\theta$ < 105						105 < $\theta$ < 125					
	$\langle p_T \rangle$	$\langle \theta \rangle$	$d^2\sigma/dpd\Omega$				$\langle p_T \rangle$	$\langle \theta \rangle$	$d^2\sigma/dpd\Omega$			
			$\langle p_T \rangle$	$\langle \theta \rangle$	$d^2\sigma/dpd\Omega$	$d^2\sigma/dpd\Omega$			$\langle p_T \rangle$	$\langle \theta \rangle$	$d^2\sigma/dpd\Omega$	$d^2\sigma/dpd\Omega$
0.13–0.16	0.145	97.5	169.12	$\pm$ 7.19	$\pm$ 9.95	0.145	114.2	139.16	$\pm$ 5.04	$\pm$ 7.19		
0.16–0.20	0.179	97.4	165.36	$\pm$ 5.14	$\pm$ 7.06	0.178	114.1	115.53	$\pm$ 3.65	$\pm$ 4.86		
0.20–0.24	0.219	97.1	132.12	$\pm$ 4.56	$\pm$ 4.71	0.218	113.7	88.74	$\pm$ 3.34	$\pm$ 3.16		
0.24–0.30	0.266	97.2	100.56	$\pm$ 3.44	$\pm$ 3.92	0.266	113.4	48.97	$\pm$ 2.03	$\pm$ 1.99		
0.30–0.36	0.328	97.2	65.78	$\pm$ 2.74	$\pm$ 2.84	0.327	113.7	28.84	$\pm$ 1.53	$\pm$ 1.62		
0.36–0.42	0.388	97.1	39.39	$\pm$ 2.04	$\pm$ 2.14	0.387	113.2	20.75	$\pm$ 1.29	$\pm$ 1.56		
0.42–0.50	0.457	96.9	25.63	$\pm$ 1.41	$\pm$ 1.82	0.454	113.4	10.09	$\pm$ 0.75	$\pm$ 0.99		
0.50–0.60	0.538	96.6	16.58	$\pm$ 1.02	$\pm$ 1.59	0.536	112.9	4.95	$\pm$ 0.47	$\pm$ 0.64		
0.60–0.72	0.648	96.3	5.71	$\pm$ 0.49	$\pm$ 0.75	0.640	112.0	1.39	$\pm$ 0.20	$\pm$ 0.25		
0.72–0.90	0.791	96.2	2.04	$\pm$ 0.22	$\pm$ 0.37	0.790	112.0	0.30	$\pm$ 0.07	$\pm$ 0.08		
0.90–1.25	1.019	95.5	0.26	$\pm$ 0.04	$\pm$ 0.07	0.948	108.3	0.04	$\pm$ 0.02	$\pm$ 0.02		

Table A.36: Double-differential inclusive cross-section  $d^2\sigma/dpd\Omega$  [mb/(GeV/c sr)] of the production of  $\pi^-$ 's in  $\pi^- + \text{Sn} \rightarrow \pi^- + \text{X}$  interactions with  $-12.0$  GeV/c beam momentum; the first error is statistical, the second systematic;  $p_T$  in GeV/c, polar angle  $\theta$  in degrees.

$p_T$	20 < $\theta$ < 30						30 < $\theta$ < 40							
	$\langle p_T \rangle$	$\langle \theta \rangle$	$d^2\sigma/dpd\Omega$				$\langle p_T \rangle$	$\langle \theta \rangle$	$d^2\sigma/dpd\Omega$					
			645.19	$\pm$	16.67	$\pm$	44.24	519.70	$\pm$	14.83	$\pm$	37.00		
0.10–0.13	0.115	24.9	645.19	$\pm$	16.67	$\pm$	44.24	0.115	34.9	519.70	$\pm$	14.83	$\pm$	37.00
0.13–0.16	0.146	24.8	745.73	$\pm$	16.62	$\pm$	41.54	0.145	34.8	560.92	$\pm$	14.11	$\pm$	31.04
0.16–0.20	0.180	24.8	772.10	$\pm$	14.06	$\pm$	35.44	0.180	34.7	585.13	$\pm$	12.15	$\pm$	27.07
0.20–0.24	0.221	24.8	763.41	$\pm$	13.72	$\pm$	29.78	0.220	34.6	570.23	$\pm$	11.76	$\pm$	22.43
0.24–0.30	0.270	24.8	720.07	$\pm$	10.87	$\pm$	23.42	0.271	34.7	532.89	$\pm$	9.40	$\pm$	17.45
0.30–0.36	0.331	24.7	579.49	$\pm$	9.73	$\pm$	16.60	0.330	34.7	427.39	$\pm$	8.40	$\pm$	12.26
0.36–0.42	0.390	24.8	471.70	$\pm$	8.75	$\pm$	13.77	0.391	34.7	345.20	$\pm$	7.47	$\pm$	10.05
0.42–0.50	0.460	24.8	351.72	$\pm$	6.60	$\pm$	12.38	0.460	34.8	260.92	$\pm$	5.63	$\pm$	8.89
0.50–0.60	0.549	24.7	227.74	$\pm$	4.59	$\pm$	10.63	0.549	34.8	166.78	$\pm$	3.95	$\pm$	7.57
0.60–0.72	0.659	24.7	136.79	$\pm$	3.25	$\pm$	8.81	0.659	34.9	103.28	$\pm$	2.87	$\pm$	6.45
0.72–0.90								0.801	34.7	48.95	$\pm$	1.54	$\pm$	4.34
$p_T$	40 < $\theta$ < 50						50 < $\theta$ < 60							
	$\langle p_T \rangle$	$\langle \theta \rangle$	$d^2\sigma/dpd\Omega$				$\langle p_T \rangle$	$\langle \theta \rangle$	$d^2\sigma/dpd\Omega$					
			441.14	$\pm$	14.03	$\pm$	32.36	0.145	55.0	361.64	$\pm$	11.66	$\pm$	21.23
0.10–0.13	0.116	45.0	485.30	$\pm$	13.15	$\pm$	27.33	0.181	54.8	377.72	$\pm$	9.72	$\pm$	17.66
0.13–0.16	0.146	45.0	454.58	$\pm$	10.69	$\pm$	21.22	0.221	54.8	358.79	$\pm$	9.43	$\pm$	14.11
0.16–0.20	0.181	44.9	421.56	$\pm$	10.26	$\pm$	16.96	0.270	54.8	307.41	$\pm$	7.22	$\pm$	10.75
0.20–0.24	0.221	44.6	398.51	$\pm$	8.18	$\pm$	13.32	0.332	54.7	245.23	$\pm$	6.52	$\pm$	8.15
0.24–0.30	0.271	44.7	317.97	$\pm$	7.25	$\pm$	9.26	0.391	54.6	190.40	$\pm$	5.70	$\pm$	6.33
0.30–0.36	0.332	44.6	186.93	$\pm$	4.71	$\pm$	6.70	0.461	54.8	141.62	$\pm$	4.12	$\pm$	5.35
0.36–0.42	0.392	44.9	128.69	$\pm$	3.45	$\pm$	6.20	0.553	54.8	95.11	$\pm$	3.05	$\pm$	4.77
0.42–0.50	0.662	45.0	67.01	$\pm$	2.21	$\pm$	4.51	0.661	54.7	51.64	$\pm$	1.95	$\pm$	3.60
0.50–0.60	0.805	44.6	37.02	$\pm$	1.39	$\pm$	3.44	0.809	54.8	27.22	$\pm$	1.21	$\pm$	2.59
0.72–0.90								1.064	55.1	5.40	$\pm$	0.31	$\pm$	0.86
$p_T$	60 < $\theta$ < 75						75 < $\theta$ < 90							
	$\langle p_T \rangle$	$\langle \theta \rangle$	$d^2\sigma/dpd\Omega$				$\langle p_T \rangle$	$\langle \theta \rangle$	$d^2\sigma/dpd\Omega$					
			347.66	$\pm$	9.93	$\pm$	20.31	0.146	82.1	259.95	$\pm$	8.77	$\pm$	15.00
0.13–0.16	0.145	67.4	306.14	$\pm$	7.08	$\pm$	13.53	0.180	82.3	245.38	$\pm$	6.45	$\pm$	10.60
0.16–0.20	0.220	67.1	280.95	$\pm$	6.75	$\pm$	10.39	0.220	82.4	199.85	$\pm$	5.73	$\pm$	7.10
0.20–0.24	0.270	67.2	237.77	$\pm$	5.21	$\pm$	8.04	0.269	82.0	149.01	$\pm$	4.15	$\pm$	5.10
0.24–0.30	0.331	67.0	170.52	$\pm$	4.42	$\pm$	5.66	0.329	81.8	114.47	$\pm$	3.66	$\pm$	4.48
0.30–0.36	0.389	66.9	135.75	$\pm$	3.94	$\pm$	4.86	0.390	82.0	79.11	$\pm$	3.04	$\pm$	3.57
0.36–0.42	0.460	66.7	105.54	$\pm$	3.01	$\pm$	4.63	0.460	81.6	60.32	$\pm$	2.27	$\pm$	3.31
0.42–0.50	0.549	66.6	61.98	$\pm$	1.97	$\pm$	3.53	0.548	81.7	32.27	$\pm$	1.45	$\pm$	2.34
0.50–0.60	0.658	67.1	33.00	$\pm$	1.30	$\pm$	2.55	0.658	81.8	16.29	$\pm$	0.93	$\pm$	1.59
0.60–0.72	0.803	67.2	13.16	$\pm$	0.65	$\pm$	1.42	0.802	80.9	5.18	$\pm$	0.39	$\pm$	0.71
0.72–0.90								1.038	81.6	0.93	$\pm$	0.11	$\pm$	0.19
$p_T$	90 < $\theta$ < 105						105 < $\theta$ < 125							
	$\langle p_T \rangle$	$\langle \theta \rangle$	$d^2\sigma/dpd\Omega$				$\langle p_T \rangle$	$\langle \theta \rangle$	$d^2\sigma/dpd\Omega$					
			236.15	$\pm$	9.45	$\pm$	13.64	0.145	114.2	194.55	$\pm$	6.00	$\pm$	10.17
0.13–0.16	0.145	97.3	221.14	$\pm$	6.13	$\pm$	9.29	0.179	114.0	144.24	$\pm$	4.22	$\pm$	5.43
0.16–0.20	0.219	97.2	168.27	$\pm$	5.32	$\pm$	5.85	0.219	113.6	98.13	$\pm$	3.54	$\pm$	3.58
0.20–0.24	0.268	96.9	108.36	$\pm$	3.52	$\pm$	3.73	0.269	113.2	57.87	$\pm$	2.23	$\pm$	2.58
0.24–0.30	0.329	96.8	73.55	$\pm$	2.92	$\pm$	3.28	0.329	113.8	37.34	$\pm$	1.79	$\pm$	2.32
0.30–0.36	0.389	97.0	53.82	$\pm$	2.52	$\pm$	3.23	0.390	113.2	24.62	$\pm$	1.40	$\pm$	2.04
0.36–0.42	0.459	97.0	35.67	$\pm$	1.71	$\pm$	2.73	0.458	112.8	14.86	$\pm$	0.95	$\pm$	1.59
0.42–0.50	0.549	96.7	18.38	$\pm$	1.08	$\pm$	1.90	0.546	112.8	6.27	$\pm$	0.53	$\pm$	0.88
0.50–0.60	0.655	96.7	7.98	$\pm$	0.63	$\pm$	1.10	0.653	111.5	2.77	$\pm$	0.33	$\pm$	0.51
0.60–0.72	0.798	97.2	2.29	$\pm$	0.27	$\pm$	0.43	0.802	110.6	0.53	$\pm$	0.10	$\pm$	0.13
0.72–0.90								0.983	111.8	0.03	$\pm$	0.02	$\pm$	0.02

Table A.37: Double-differential inclusive cross-section  $d^2\sigma/dpd\Omega$  [mb/(GeV/c sr)] of the production of protons in  $p + \text{Sn} \rightarrow p + X$  interactions with  $+15.0$  GeV/c beam momentum; the first error is statistical, the second systematic;  $p_T$  in GeV/c, polar angle  $\theta$  in degrees.

$p_T$	20 < $\theta$ < 30						30 < $\theta$ < 40							
	$\langle p_T \rangle$		$\langle \theta \rangle$		$d^2\sigma/dpd\Omega$		$\langle p_T \rangle$		$\langle \theta \rangle$		$d^2\sigma/dpd\Omega$			
0.20–0.24	0.221	25.2	1209.87	$\pm$	35.14	$\pm$	59.49							
0.24–0.30	0.272	25.2	992.50	$\pm$	22.37	$\pm$	44.59	0.272	34.9	1177.85	$\pm$	24.00	$\pm$	47.78
0.30–0.36	0.333	25.2	882.21	$\pm$	21.97	$\pm$	42.51	0.333	35.2	1007.15	$\pm$	21.98	$\pm$	35.96
0.36–0.42	0.394	25.2	680.87	$\pm$	19.01	$\pm$	33.21	0.393	35.1	802.70	$\pm$	20.31	$\pm$	31.06
0.42–0.50	0.465	25.2	533.58	$\pm$	14.70	$\pm$	29.12	0.465	35.1	605.20	$\pm$	15.62	$\pm$	28.70
0.50–0.60	0.555	25.2	387.26	$\pm$	11.03	$\pm$	23.09	0.556	35.1	442.63	$\pm$	12.35	$\pm$	25.59
0.60–0.72	0.668	25.2	269.94	$\pm$	8.49	$\pm$	17.78	0.668	35.1	292.30	$\pm$	9.21	$\pm$	20.90
0.72–0.90								0.818	35.1	159.21	$\pm$	5.63	$\pm$	15.09
40 < $\theta$ < 50														
$p_T$	$\langle p_T \rangle$		$\langle \theta \rangle$		$d^2\sigma/dpd\Omega$		$\langle p_T \rangle$	$\langle \theta \rangle$	50 < $\theta$ < 60					
	0.30–0.36	0.329	45.0	1070.68	$\pm$	22.70	$\pm$	32.50	0.389	55.0	918.76	$\pm$	20.12	$\pm$
0.36–0.42	0.389	45.1	927.78	$\pm$	20.80	$\pm$	26.30	0.458	55.0	709.56	$\pm$	15.76	$\pm$	20.12
0.42–0.50	0.458	45.1	716.70	$\pm$	16.59	$\pm$	24.09	0.547	55.0	478.43	$\pm$	12.26	$\pm$	21.15
0.50–0.60	0.545	45.0	497.25	$\pm$	13.04	$\pm$	26.15	0.655	54.9	308.66	$\pm$	9.64	$\pm$	21.57
0.60–0.72	0.656	45.0	331.91	$\pm$	10.07	$\pm$	23.05	0.797	55.0	151.42	$\pm$	5.82	$\pm$	15.48
0.72–0.90	0.800	45.0	159.99	$\pm$	5.78	$\pm$	15.21							
0.90–1.25	1.035	45.1	50.03	$\pm$	2.35	$\pm$	7.01	0.797	55.0	151.42	$\pm$	5.82	$\pm$	15.48
60 < $\theta$ < 75														
$p_T$	$\langle p_T \rangle$		$\langle \theta \rangle$		$d^2\sigma/dpd\Omega$		$\langle p_T \rangle$	$\langle \theta \rangle$	75 < $\theta$ < 90					
	0.50–0.60	0.547	67.4	480.70	$\pm$	9.31	$\pm$	18.13	0.546	82.0	411.50	$\pm$	8.44	$\pm$
0.60–0.72	0.656	67.1	281.64	$\pm$	7.08	$\pm$	17.73	0.655	81.9	230.18	$\pm$	6.14	$\pm$	15.07
0.72–0.90	0.796	67.2	128.08	$\pm$	4.35	$\pm$	14.55	0.797	81.9	74.54	$\pm$	3.43	$\pm$	9.99
90 < $\theta$ < 105														
$p_T$	$\langle p_T \rangle$		$\langle \theta \rangle$		$d^2\sigma/dpd\Omega$		$\langle p_T \rangle$	$\langle \theta \rangle$	105 < $\theta$ < 125					
	0.42–0.50	0.544	97.0	278.29	$\pm$	6.95	$\pm$	17.75	0.456	113.3	270.46	$\pm$	6.30	$\pm$
0.50–0.60	0.650	96.5	132.25	$\pm$	4.70	$\pm$	10.80	0.541	112.9	115.05	$\pm$	4.01	$\pm$	10.01
0.60–0.72								0.650	112.7	38.31	$\pm$	2.48	$\pm$	5.90

Table A.38: Double-differential inclusive cross-section  $d^2\sigma/dpd\Omega$  [mb/(GeV/c sr)] of the production of  $\pi^+$ 's in  $p + \text{Sn} \rightarrow \pi^+ + \text{X}$  interactions with +15.0 GeV/c beam momentum; the first error is statistical, the second systematic;  $p_T$  in GeV/c, polar angle  $\theta$  in degrees.

$p_T$	20 < $\theta$ < 30				30 < $\theta$ < 40			
	$\langle p_T \rangle$	$\langle \theta \rangle$	$d^2\sigma/dpd\Omega$		$\langle p_T \rangle$	$\langle \theta \rangle$	$d^2\sigma/dpd\Omega$	
			$d^2\sigma/dpd\Omega$	$d^2\sigma/dpd\Omega$			$d^2\sigma/dpd\Omega$	$d^2\sigma/dpd\Omega$
0.10–0.13	0.116	25.0	581.39 $\pm$ 27.08 $\pm$ 40.60	0.116	34.5	475.93 $\pm$ 24.05 $\pm$ 33.78		
0.13–0.16	0.146	24.7	636.36 $\pm$ 25.88 $\pm$ 34.27	0.146	34.7	516.05 $\pm$ 22.82 $\pm$ 27.92		
0.16–0.20	0.181	24.8	755.45 $\pm$ 23.91 $\pm$ 35.33	0.182	34.8	572.91 $\pm$ 20.76 $\pm$ 26.06		
0.20–0.24	0.221	24.8	752.24 $\pm$ 23.54 $\pm$ 30.35	0.221	34.9	590.67 $\pm$ 20.91 $\pm$ 23.64		
0.24–0.30	0.271	24.7	697.74 $\pm$ 18.43 $\pm$ 23.95	0.271	34.8	532.92 $\pm$ 16.10 $\pm$ 18.04		
0.30–0.36	0.333	24.8	581.43 $\pm$ 16.72 $\pm$ 18.03	0.333	34.8	442.30 $\pm$ 14.83 $\pm$ 13.52		
0.36–0.42	0.393	24.8	487.52 $\pm$ 14.95 $\pm$ 14.66	0.392	34.6	346.58 $\pm$ 13.02 $\pm$ 10.65		
0.42–0.50	0.464	24.7	367.50 $\pm$ 11.07 $\pm$ 13.05	0.464	34.7	272.64 $\pm$ 9.71 $\pm$ 9.27		
0.50–0.60	0.555	24.9	252.87 $\pm$ 7.78 $\pm$ 12.61	0.556	34.6	189.87 $\pm$ 7.07 $\pm$ 8.59		
0.60–0.72	0.665	24.8	148.13 $\pm$ 5.07 $\pm$ 10.98	0.667	34.8	117.10 $\pm$ 4.71 $\pm$ 7.80		
0.72–0.90				0.817	34.8	53.93 $\pm$ 2.31 $\pm$ 5.69		
$p_T$	40 < $\theta$ < 50				50 < $\theta$ < 60			
	$\langle p_T \rangle$	$\langle \theta \rangle$	$d^2\sigma/dpd\Omega$		$\langle p_T \rangle$	$\langle \theta \rangle$	$d^2\sigma/dpd\Omega$	
			$d^2\sigma/dpd\Omega$	$d^2\sigma/dpd\Omega$			$d^2\sigma/dpd\Omega$	$d^2\sigma/dpd\Omega$
0.10–0.13	0.115	45.1	391.80 $\pm$ 22.85 $\pm$ 28.54	0.145	54.7	359.76 $\pm$ 19.50 $\pm$ 20.91		
0.13–0.16	0.145	44.9	495.49 $\pm$ 22.28 $\pm$ 27.30	0.181	54.8	359.29 $\pm$ 15.68 $\pm$ 16.54		
0.16–0.20	0.180	44.8	444.52 $\pm$ 17.89 $\pm$ 20.39	0.220	55.2	356.46 $\pm$ 16.30 $\pm$ 14.00		
0.20–0.24	0.220	44.5	438.37 $\pm$ 17.68 $\pm$ 17.56	0.270	54.6	295.05 $\pm$ 12.06 $\pm$ 9.81		
0.24–0.30	0.268	44.8	401.63 $\pm$ 14.23 $\pm$ 13.96	0.329	54.6	247.40 $\pm$ 11.16 $\pm$ 7.87		
0.30–0.36	0.329	44.8	309.08 $\pm$ 12.22 $\pm$ 9.42	0.387	54.9	202.32 $\pm$ 10.04 $\pm$ 6.49		
0.36–0.42	0.389	44.8	272.72 $\pm$ 11.69 $\pm$ 8.35	0.458	54.8	140.81 $\pm$ 7.23 $\pm$ 5.11		
0.42–0.50	0.460	44.5	192.84 $\pm$ 8.29 $\pm$ 6.67	0.548	54.7	91.01 $\pm$ 5.12 $\pm$ 4.38		
0.50–0.60	0.546	44.5	120.85 $\pm$ 5.75 $\pm$ 5.52	0.658	54.6	45.25 $\pm$ 3.03 $\pm$ 3.02		
0.60–0.72	0.654	44.5	78.42 $\pm$ 3.99 $\pm$ 4.92	0.799	54.7	20.59 $\pm$ 1.51 $\pm$ 2.03		
0.72–0.90	0.798	44.4	33.25 $\pm$ 1.85 $\pm$ 3.23	1.030	54.5	4.70 $\pm$ 0.41 $\pm$ 0.78		
$p_T$	60 < $\theta$ < 75				75 < $\theta$ < 90			
	$\langle p_T \rangle$	$\langle \theta \rangle$	$d^2\sigma/dpd\Omega$		$\langle p_T \rangle$	$\langle \theta \rangle$	$d^2\sigma/dpd\Omega$	
			$d^2\sigma/dpd\Omega$	$d^2\sigma/dpd\Omega$			$d^2\sigma/dpd\Omega$	$d^2\sigma/dpd\Omega$
0.13–0.16	0.145	67.2	277.20 $\pm$ 14.51 $\pm$ 16.25	0.146	82.6	216.91 $\pm$ 13.62 $\pm$ 12.90		
0.16–0.20	0.180	67.1	297.01 $\pm$ 11.61 $\pm$ 13.62	0.179	82.0	216.39 $\pm$ 9.91 $\pm$ 9.68		
0.20–0.24	0.220	66.9	276.91 $\pm$ 11.22 $\pm$ 10.57	0.220	82.5	202.12 $\pm$ 9.54 $\pm$ 7.44		
0.24–0.30	0.269	67.0	226.59 $\pm$ 8.61 $\pm$ 7.45	0.266	82.3	159.94 $\pm$ 7.27 $\pm$ 5.35		
0.30–0.36	0.328	67.1	168.27 $\pm$ 7.56 $\pm$ 5.55	0.328	82.0	111.95 $\pm$ 6.27 $\pm$ 4.39		
0.36–0.42	0.387	67.1	127.07 $\pm$ 6.51 $\pm$ 4.40	0.390	81.6	73.65 $\pm$ 4.95 $\pm$ 2.97		
0.42–0.50	0.459	66.9	90.21 $\pm$ 4.65 $\pm$ 3.72	0.458	81.5	57.06 $\pm$ 3.73 $\pm$ 2.89		
0.50–0.60	0.546	66.7	63.52 $\pm$ 3.51 $\pm$ 3.53	0.546	81.8	34.78 $\pm$ 2.58 $\pm$ 2.39		
0.60–0.72	0.657	66.5	31.72 $\pm$ 2.16 $\pm$ 2.44	0.651	82.0	17.83 $\pm$ 1.60 $\pm$ 1.67		
0.72–0.90	0.792	66.5	13.11 $\pm$ 1.00 $\pm$ 1.47	0.794	81.1	6.78 $\pm$ 0.73 $\pm$ 0.89		
0.90–1.25	1.032	66.4	2.35 $\pm$ 0.24 $\pm$ 0.44	1.002	81.2	0.66 $\pm$ 0.12 $\pm$ 0.15		
$p_T$	90 < $\theta$ < 105				105 < $\theta$ < 125			
	$\langle p_T \rangle$	$\langle \theta \rangle$	$d^2\sigma/dpd\Omega$		$\langle p_T \rangle$	$\langle \theta \rangle$	$d^2\sigma/dpd\Omega$	
			$d^2\sigma/dpd\Omega$	$d^2\sigma/dpd\Omega$			$d^2\sigma/dpd\Omega$	$d^2\sigma/dpd\Omega$
0.13–0.16	0.146	97.5	203.61 $\pm$ 13.13 $\pm$ 11.91	0.145	114.5	176.61 $\pm$ 9.55 $\pm$ 9.38		
0.16–0.20	0.180	97.2	215.75 $\pm$ 10.23 $\pm$ 9.24	0.180	114.1	138.48 $\pm$ 6.72 $\pm$ 5.90		
0.20–0.24	0.219	97.2	170.75 $\pm$ 8.93 $\pm$ 6.07	0.219	113.4	115.29 $\pm$ 6.47 $\pm$ 4.06		
0.24–0.30	0.267	96.5	115.66 $\pm$ 6.30 $\pm$ 4.23	0.267	113.7	61.72 $\pm$ 3.95 $\pm$ 2.52		
0.30–0.36	0.328	96.9	80.02 $\pm$ 5.28 $\pm$ 3.55	0.328	113.7	36.57 $\pm$ 3.03 $\pm$ 2.07		
0.36–0.42	0.389	96.7	48.20 $\pm$ 4.03 $\pm$ 2.68	0.387	112.3	20.41 $\pm$ 2.32 $\pm$ 1.56		
0.42–0.50	0.458	96.4	29.94 $\pm$ 2.68 $\pm$ 2.17	0.458	113.5	14.24 $\pm$ 1.58 $\pm$ 1.41		
0.50–0.60	0.543	97.0	16.11 $\pm$ 1.73 $\pm$ 1.56	0.551	113.3	3.92 $\pm$ 0.73 $\pm$ 0.51		
0.60–0.72	0.653	95.2	7.66 $\pm$ 1.06 $\pm$ 0.99	0.645	110.2	2.18 $\pm$ 0.49 $\pm$ 0.38		
0.72–0.90	0.794	95.4	3.16 $\pm$ 0.52 $\pm$ 0.56	0.786	111.7	0.34 $\pm$ 0.12 $\pm$ 0.08		
0.90–1.25	1.087	96.0	0.24 $\pm$ 0.06 $\pm$ 0.08					

Table A.39: Double-differential inclusive cross-section  $d^2\sigma/dpd\Omega$  [mb/(GeV/c sr)] of the production of  $\pi^-$ 's in  $p + \text{Sn} \rightarrow \pi^- + X$  interactions with +15.0 GeV/c beam momentum; the first error is statistical, the second systematic;  $p_T$  in GeV/c, polar angle  $\theta$  in degrees.

$p_T$	20 < $\theta$ < 30						30 < $\theta$ < 40							
	$\langle p_T \rangle$	$\langle \theta \rangle$	$d^2\sigma/dpd\Omega$				$\langle p_T \rangle$	$\langle \theta \rangle$	$d^2\sigma/dpd\Omega$					
			613.15	$\pm$	27.35	$\pm$	42.51	518.24	$\pm$	25.20	$\pm$	37.62		
0.10–0.13	0.116	24.7	613.15	$\pm$	27.35	$\pm$	42.51	0.115	34.7	518.24	$\pm$	25.20	$\pm$	37.62
0.13–0.16	0.145	24.8	655.87	$\pm$	25.97	$\pm$	35.57	0.145	34.9	580.06	$\pm$	24.13	$\pm$	32.08
0.16–0.20	0.179	24.8	738.50	$\pm$	23.27	$\pm$	33.82	0.178	34.8	546.59	$\pm$	19.82	$\pm$	25.17
0.20–0.24	0.218	24.6	729.37	$\pm$	22.84	$\pm$	28.36	0.218	34.9	599.28	$\pm$	20.75	$\pm$	23.39
0.24–0.30	0.267	24.8	632.24	$\pm$	17.16	$\pm$	20.14	0.266	34.8	490.73	$\pm$	15.32	$\pm$	15.80
0.30–0.36	0.325	24.9	527.59	$\pm$	15.56	$\pm$	14.75	0.326	34.9	438.16	$\pm$	14.39	$\pm$	12.33
0.36–0.42	0.385	24.7	421.10	$\pm$	14.16	$\pm$	12.40	0.385	34.9	328.68	$\pm$	12.46	$\pm$	9.42
0.42–0.50	0.451	25.1	314.70	$\pm$	10.43	$\pm$	10.80	0.452	34.8	248.51	$\pm$	9.36	$\pm$	8.37
0.50–0.60	0.535	24.8	185.52	$\pm$	7.12	$\pm$	8.62	0.538	34.8	152.25	$\pm$	6.30	$\pm$	6.91
0.60–0.72	0.642	24.7	114.03	$\pm$	5.00	$\pm$	7.34	0.642	34.8	79.20	$\pm$	4.03	$\pm$	5.17
0.72–0.90								0.779	34.5	41.35	$\pm$	2.37	$\pm$	3.72
$p_T$	40 < $\theta$ < 50						50 < $\theta$ < 60							
	$\langle p_T \rangle$	$\langle \theta \rangle$	$d^2\sigma/dpd\Omega$				$\langle p_T \rangle$	$\langle \theta \rangle$	$d^2\sigma/dpd\Omega$					
			479.18	$\pm$	25.58	$\pm$	36.85	0.145	54.9	355.82	$\pm$	19.16	$\pm$	20.93
0.10–0.13	0.116	45.1	504.88	$\pm$	22.48	$\pm$	28.49	0.180	54.8	382.99	$\pm$	16.36	$\pm$	17.95
0.13–0.16	0.145	45.1	450.53	$\pm$	17.79	$\pm$	21.01	0.220	55.1	364.36	$\pm$	16.03	$\pm$	14.42
0.16–0.20	0.180	45.0	473.66	$\pm$	18.60	$\pm$	19.07	0.269	55.0	314.49	$\pm$	12.49	$\pm$	10.95
0.20–0.24	0.219	44.8	391.33	$\pm$	13.68	$\pm$	12.77	0.329	54.7	259.92	$\pm$	11.44	$\pm$	8.75
0.24–0.30	0.269	44.7	314.32	$\pm$	12.25	$\pm$	9.02	0.388	54.4	183.62	$\pm$	9.29	$\pm$	5.79
0.30–0.36	0.329	44.9	249.08	$\pm$	10.85	$\pm$	7.45	0.455	54.6	136.10	$\pm$	6.87	$\pm$	5.15
0.36–0.42	0.388	44.6	186.12	$\pm$	8.05	$\pm$	6.65	0.549	54.5	91.13	$\pm$	5.06	$\pm$	4.62
0.42–0.50	0.457	44.7	108.17	$\pm$	5.29	$\pm$	5.28	0.650	54.7	41.73	$\pm$	2.96	$\pm$	2.96
0.50–0.60	0.544	44.6	74.62	$\pm$	4.11	$\pm$	4.98	0.794	54.9	22.40	$\pm$	1.77	$\pm$	2.20
0.60–0.72	0.653	44.8	25.97	$\pm$	1.81	$\pm$	2.60	1.039	54.5	4.06	$\pm$	0.45	$\pm$	0.67
$p_T$	60 < $\theta$ < 75						75 < $\theta$ < 90							
	$\langle p_T \rangle$	$\langle \theta \rangle$	$d^2\sigma/dpd\Omega$				$\langle p_T \rangle$	$\langle \theta \rangle$	$d^2\sigma/dpd\Omega$					
			339.20	$\pm$	15.77	$\pm$	19.18	0.146	81.9	319.80	$\pm$	16.38	$\pm$	18.48
0.13–0.16	0.144	67.4	295.51	$\pm$	11.66	$\pm$	13.01	0.180	82.0	261.51	$\pm$	11.07	$\pm$	11.30
0.16–0.20	0.179	67.0	295.14	$\pm$	11.72	$\pm$	10.86	0.220	82.0	217.26	$\pm$	10.12	$\pm$	7.73
0.20–0.24	0.219	66.9	234.02	$\pm$	8.67	$\pm$	7.31	0.269	82.0	160.17	$\pm$	7.30	$\pm$	5.40
0.24–0.30	0.267	66.9	179.61	$\pm$	7.74	$\pm$	6.01	0.327	81.7	109.58	$\pm$	6.15	$\pm$	4.28
0.30–0.36	0.329	66.7	132.36	$\pm$	6.62	$\pm$	4.63	0.389	81.8	72.01	$\pm$	4.84	$\pm$	3.05
0.36–0.42	0.389	66.7	90.36	$\pm$	4.61	$\pm$	3.84	0.462	82.0	56.16	$\pm$	3.70	$\pm$	3.08
0.42–0.50	0.457	66.7	59.02	$\pm$	3.31	$\pm$	3.38	0.547	81.8	29.21	$\pm$	2.32	$\pm$	2.15
0.50–0.60	0.654	66.8	34.68	$\pm$	2.24	$\pm$	2.72	0.655	81.7	13.96	$\pm$	1.47	$\pm$	1.38
0.60–0.72	0.794	66.0	12.62	$\pm$	1.06	$\pm$	1.39	0.798	81.2	3.95	$\pm$	0.59	$\pm$	0.54
0.72–0.90	1.030	66.3	2.63	$\pm$	0.30	$\pm$	0.46	1.010	81.5	0.62	$\pm$	0.13	$\pm$	0.14
$p_T$	90 < $\theta$ < 105						105 < $\theta$ < 125							
	$\langle p_T \rangle$	$\langle \theta \rangle$	$d^2\sigma/dpd\Omega$				$\langle p_T \rangle$	$\langle \theta \rangle$	$d^2\sigma/dpd\Omega$					
			273.89	$\pm$	16.49	$\pm$	16.68	0.144	114.5	184.72	$\pm$	9.72	$\pm$	10.44
0.13–0.16	0.146	97.3	205.97	$\pm$	9.93	$\pm$	8.74	0.178	114.4	134.13	$\pm$	6.91	$\pm$	4.98
0.16–0.20	0.179	97.1	168.31	$\pm$	8.97	$\pm$	6.05	0.219	113.5	102.57	$\pm$	6.05	$\pm$	3.85
0.20–0.24	0.219	97.0	113.35	$\pm$	6.30	$\pm$	4.91	0.269	113.7	62.14	$\pm$	3.96	$\pm$	2.82
0.24–0.30	0.328	97.0	76.38	$\pm$	5.09	$\pm$	3.58	0.329	113.8	33.83	$\pm$	2.86	$\pm$	2.14
0.30–0.36	0.388	96.8	40.91	$\pm$	3.62	$\pm$	2.43	0.389	114.0	23.38	$\pm$	2.39	$\pm$	1.98
0.36–0.42	0.456	97.0	32.54	$\pm$	2.79	$\pm$	2.56	0.459	112.2	10.77	$\pm$	1.35	$\pm$	1.18
0.42–0.50	0.543	96.3	18.75	$\pm$	1.83	$\pm$	2.00	0.546	112.6	6.02	$\pm$	0.90	$\pm$	0.86
0.50–0.60	0.647	95.6	7.90	$\pm$	1.06	$\pm$	1.13	0.644	111.5	1.43	$\pm$	0.37	$\pm$	0.28
0.60–0.72	0.792	96.2	1.82	$\pm$	0.38	$\pm$	0.36	0.781	108.1	0.60	$\pm$	0.19	$\pm$	0.16
0.72–0.90	0.997	96.3	0.20	$\pm$	0.07	$\pm$	0.06	1.088	108.5	0.05	$\pm$	0.02	$\pm$	0.02

Table A.40: Double-differential inclusive cross-section  $d^2\sigma/dpd\Omega$  [mb/(GeV/c sr)] of the production of protons in  $\pi^+ + \text{Sn} \rightarrow p + X$  interactions with  $+15.0 \text{ GeV}/c$  beam momentum; the first error is statistical, the second systematic;  $p_T$  in  $\text{GeV}/c$ , polar angle  $\theta$  in degrees.

$p_T$	20 < $\theta$ < 30			30 < $\theta$ < 40				
	$\langle p_T \rangle$	$\langle \theta \rangle$	$d^2\sigma/dpd\Omega$		$\langle p_T \rangle$	$\langle \theta \rangle$	$d^2\sigma/dpd\Omega$	
			$d^2\sigma/dpd\Omega$	$d^2\sigma/dpd\Omega$			$d^2\sigma/dpd\Omega$	$d^2\sigma/dpd\Omega$
0.20–0.24	0.213	25.3	484.11 $\pm$ 177.83 $\pm$ 28.23					
0.24–0.30	0.264	25.4	533.97 $\pm$ 143.79 $\pm$ 28.05					
0.30–0.36	0.321	24.7	471.11 $\pm$ 137.24 $\pm$ 25.93					
0.36–0.42	0.388	25.7	559.00 $\pm$ 152.36 $\pm$ 31.76					
0.42–0.50	0.471	25.3	410.33 $\pm$ 109.65 $\pm$ 25.32					
0.50–0.60	0.544	24.9	265.45 $\pm$ 76.23 $\pm$ 17.82					
0.60–0.72	0.666	25.3	99.80 $\pm$ 43.28 $\pm$ 7.35					
0.72–0.90					0.822	33.4	120.94 $\pm$ 42.70 $\pm$ 12.03	
40 < $\theta$ < 50								
$p_T$	$\langle p_T \rangle$	$\langle \theta \rangle$	$d^2\sigma/dpd\Omega$		$\langle p_T \rangle$	$\langle \theta \rangle$	$d^2\sigma/dpd\Omega$	
			$d^2\sigma/dpd\Omega$	$d^2\sigma/dpd\Omega$			$d^2\sigma/dpd\Omega$	$d^2\sigma/dpd\Omega$
0.30–0.36	0.324	44.8	742.29 $\pm$ 162.57 $\pm$ 30.68					
0.36–0.42	0.388	45.4	905.52 $\pm$ 179.42 $\pm$ 35.99					
0.42–0.50	0.457	44.6	694.54 $\pm$ 142.42 $\pm$ 30.27					
0.50–0.60	0.549	44.8	305.10 $\pm$ 88.79 $\pm$ 18.37					
0.60–0.72	0.649	44.7	266.05 $\pm$ 77.95 $\pm$ 20.12					
0.72–0.90	0.809	44.4	140.84 $\pm$ 47.05 $\pm$ 14.05					
0.90–1.25	1.005	44.8	38.01 $\pm$ 17.89 $\pm$ 5.44		0.814	56.6	133.00 $\pm$ 48.20 $\pm$ 14.16	
60 < $\theta$ < 75								
$p_T$	$\langle p_T \rangle$	$\langle \theta \rangle$	$d^2\sigma/dpd\Omega$		$\langle p_T \rangle$	$\langle \theta \rangle$	$d^2\sigma/dpd\Omega$	
			$d^2\sigma/dpd\Omega$	$d^2\sigma/dpd\Omega$			$d^2\sigma/dpd\Omega$	$d^2\sigma/dpd\Omega$
0.50–0.60	0.550	67.0	262.04 $\pm$ 60.65 $\pm$ 12.18		0.549	84.1	370.38 $\pm$ 70.95 $\pm$ 20.11	
0.60–0.72	0.660	68.2	260.72 $\pm$ 59.91 $\pm$ 17.70		0.641	82.5	230.99 $\pm$ 53.80 $\pm$ 16.33	
0.72–0.90	0.798	67.9	100.34 $\pm$ 33.77 $\pm$ 11.52		0.798	82.2	89.54 $\pm$ 31.98 $\pm$ 11.27	
90 < $\theta$ < 105								
$p_T$	$\langle p_T \rangle$	$\langle \theta \rangle$	$d^2\sigma/dpd\Omega$		$\langle p_T \rangle$	$\langle \theta \rangle$	$d^2\sigma/dpd\Omega$	
			$d^2\sigma/dpd\Omega$	$d^2\sigma/dpd\Omega$			$d^2\sigma/dpd\Omega$	$d^2\sigma/dpd\Omega$
0.42–0.50					0.453	114.1	257.92 $\pm$ 54.45 $\pm$ 16.72	
0.50–0.60	0.541	98.0	235.70 $\pm$ 56.85 $\pm$ 16.21		0.540	114.8	104.27 $\pm$ 33.71 $\pm$ 9.28	
0.60–0.72	0.642	96.5	102.22 $\pm$ 35.69 $\pm$ 8.70		0.611	113.5	19.24 $\pm$ 14.99 $\pm$ 2.76	
0.72–0.90	0.800	99.6	20.81 $\pm$ 16.11 $\pm$ 3.30					
105 < $\theta$ < 125								
$p_T$	$\langle p_T \rangle$	$\langle \theta \rangle$	$d^2\sigma/dpd\Omega$		$\langle p_T \rangle$	$\langle \theta \rangle$	$d^2\sigma/dpd\Omega$	
			$d^2\sigma/dpd\Omega$	$d^2\sigma/dpd\Omega$			$d^2\sigma/dpd\Omega$	$d^2\sigma/dpd\Omega$

Table A.41: Double-differential inclusive cross-section  $d^2\sigma/dpd\Omega$  [mb/(GeV/c sr)] of the production of  $\pi^+$ 's in  $\pi^+ + \text{Sn} \rightarrow \pi^+ + X$  interactions with +15.0 GeV/c beam momentum; the first error is statistical, the second systematic;  $p_T$  in GeV/c, polar angle  $\theta$  in degrees.

$p_T$	20 < $\theta$ < 30						30 < $\theta$ < 40					
	$\langle p_T \rangle$		$\langle \theta \rangle$		$d^2\sigma/dpd\Omega$		$\langle p_T \rangle$		$\langle \theta \rangle$		$d^2\sigma/dpd\Omega$	
	stat	syst	stat	syst	stat	syst	stat	syst	stat	syst	stat	syst
0.13–0.16	0.148	24.0	423.10	± 181.02	± 25.57		0.142	33.2	414.37	± 176.92	± 25.16	
0.20–0.24							0.224	35.5	437.16	± 162.00	± 21.21	
0.24–0.30	0.275	25.1	857.57	± 180.84	± 37.87		0.263	34.5	501.34	± 136.73	± 21.90	
0.30–0.36	0.336	24.2	784.91	± 170.35	± 32.43		0.326	35.1	383.45	± 121.33	± 15.80	
0.36–0.42	0.401	25.4	271.48	± 97.22	± 11.16		0.394	33.3	412.22	± 125.54	± 16.99	
0.42–0.50	0.461	24.1	452.45	± 106.92	± 20.43		0.480	35.1	114.94	± 54.46	± 5.09	
0.50–0.60	0.554	25.3	286.51	± 73.17	± 16.44		0.537	34.6	130.84	± 51.87	± 7.05	
0.60–0.72	0.665	24.8	183.51	± 54.18	± 14.60		0.685	35.1	79.05	± 33.60	± 5.79	
0.72–0.90							0.802	34.2	46.08	± 20.47	± 5.09	
40 < $\theta$ < 50												
$p_T$	$\langle p_T \rangle$		$\langle \theta \rangle$		$d^2\sigma/dpd\Omega$		$\langle p_T \rangle$		$\langle \theta \rangle$		$d^2\sigma/dpd\Omega$	
	stat	syst	stat	syst	stat	syst	stat	syst	stat	syst	stat	syst
0.10–0.13	0.111	44.8	195.47	± 142.03	± 15.07		0.141	54.2	366.95	± 178.12	± 23.59	
0.13–0.16	0.149	44.8	414.67	± 159.10	± 25.52		0.183	53.6	283.62	± 113.80	± 15.22	
0.16–0.20							0.221	55.0	507.11	± 161.70	± 24.32	
0.20–0.24	0.227	43.7	558.09	± 174.70	± 27.10		0.268	53.6	290.24	± 104.44	± 12.46	
0.24–0.30	0.268	46.5	440.47	± 131.34	± 19.21		0.326	54.3	182.30	± 84.84	± 7.43	
0.30–0.36	0.324	45.2	629.68	± 153.04	± 25.81		0.397	54.4	193.19	± 84.38	± 8.11	
0.36–0.42	0.392	44.3	144.18	± 74.28	± 5.94							
0.42–0.50	0.455	45.3	173.87	± 69.56	± 7.76		0.558	52.0	86.30	± 42.20	± 4.85	
0.50–0.60	0.549	44.4	157.86	± 57.95	± 8.56		0.651	55.0	62.58	± 31.92	± 4.71	
0.60–0.72	0.656	44.2	54.66	± 27.21	± 3.82		0.846	56.2	8.55	± 6.33	± 0.91	
0.72–0.90	0.759	46.2	43.99	± 19.89	± 4.55		1.043	53.2	4.01	± 2.64	± 0.70	
0.90–1.25												
60 < $\theta$ < 75												
$p_T$	$\langle p_T \rangle$		$\langle \theta \rangle$		$d^2\sigma/dpd\Omega$		$\langle p_T \rangle$		$\langle \theta \rangle$		$d^2\sigma/dpd\Omega$	
	stat	syst	stat	syst	stat	syst	stat	syst	stat	syst	stat	syst
0.13–0.16	0.143	66.0	293.08	± 131.78	± 19.05		0.146	80.7	404.09	± 165.02	± 26.63	
0.16–0.20	0.177	68.1	258.30	± 95.90	± 13.88		0.188	80.5	187.24	± 83.95	± 9.94	
0.20–0.24	0.221	68.7	308.95	± 110.13	± 14.56		0.213	82.7	152.70	± 73.87	± 7.07	
0.24–0.30	0.270	66.3	304.24	± 89.04	± 12.86		0.274	81.7	150.03	± 60.33	± 6.33	
0.30–0.36	0.334	65.5	206.95	± 72.32	± 8.51		0.317	82.5	75.73	± 45.24	± 3.40	
0.36–0.42	0.393	67.2	101.48	± 51.38	± 4.34		0.387	80.9	96.59	± 50.58	± 4.67	
0.42–0.50	0.472	64.3	67.09	± 35.26	± 3.34		0.476	83.9	36.95	± 26.43	± 2.15	
0.50–0.60	0.544	67.5	31.82	± 21.23	± 1.99		0.568	82.2	27.48	± 20.32	± 2.07	
0.60–0.72	0.639	67.6	22.22	± 16.44	± 1.85		0.626	82.5	29.11	± 17.68	± 2.94	
0.72–0.90	0.817	65.7	21.92	± 11.99	± 2.61		0.827	77.2	8.92	± 6.72	± 1.25	
0.90–1.25	1.133	67.1	2.12	± 1.43	± 0.41							
90 < $\theta$ < 105												
$p_T$	$\langle p_T \rangle$		$\langle \theta \rangle$		$d^2\sigma/dpd\Omega$		$\langle p_T \rangle$		$\langle \theta \rangle$		$d^2\sigma/dpd\Omega$	
	stat	syst	stat	syst	stat	syst	stat	syst	stat	syst	stat	syst
0.13–0.16	0.141	94.5	236.81	± 121.07	± 15.40		0.143	112.8	144.02	± 83.98	± 8.57	
0.16–0.20	0.182	97.1	257.19	± 99.19	± 13.40		0.213	112.4	154.51	± 65.31	± 7.75	
0.20–0.24	0.226	94.0	113.12	± 65.54	± 5.22		0.264	120.7	28.51	± 20.95	± 1.59	
0.24–0.30	0.261	98.5	126.56	± 57.37	± 5.70		0.342	113.3	5.14	± 4.54	± 0.38	
0.30–0.36	0.334	95.7	103.02	± 51.41	± 5.24							
0.36–0.42	0.376	96.9	47.20	± 35.21	± 2.98							
0.42–0.50	0.440	97.4	69.41	± 36.65	± 5.55							

Table A.42: Double-differential inclusive cross-section  $d^2\sigma/dpd\Omega$  [mb/(GeV/c sr)] of the production of  $\pi^-$ 's in  $\pi^+ + \text{Sn} \rightarrow \pi^- + \text{X}$  interactions with +15.0 GeV/c beam momentum; the first error is statistical, the second systematic;  $p_T$  in GeV/c, polar angle  $\theta$  in degrees.

$p_T$	20 < $\theta$ < 30			30 < $\theta$ < 40		
	$\langle p_T \rangle$	$\langle \theta \rangle$	$d^2\sigma/dpd\Omega$	$\langle p_T \rangle$	$\langle \theta \rangle$	$d^2\sigma/dpd\Omega$
0.10–0.13	0.119	23.8	394.50 ± 166.37 ± 28.99	0.118	35.8	199.23 ± 138.13 ± 15.05
0.13–0.16				0.139	33.9	474.97 ± 192.80 ± 29.11
0.16–0.20	0.179	24.7	682.15 ± 194.29 ± 36.61	0.212	33.8	558.48 ± 174.36 ± 26.55
0.20–0.24				0.266	34.7	567.51 ± 146.73 ± 24.05
0.24–0.30	0.268	25.4	900.15 ± 184.60 ± 37.95	0.334	35.4	493.14 ± 136.78 ± 19.52
0.30–0.36	0.324	24.7	977.76 ± 188.44 ± 38.51	0.380	33.6	288.38 ± 101.97 ± 11.63
0.36–0.42	0.385	25.9	358.45 ± 119.54 ± 14.53	0.442	32.5	246.44 ± 78.22 ± 10.96
0.42–0.50	0.446	24.5	313.65 ± 91.13 ± 13.92	0.538	35.5	99.71 ± 44.71 ± 5.52
0.50–0.60	0.535	24.9	239.16 ± 72.13 ± 13.03	0.653	34.4	80.61 ± 36.05 ± 5.90
0.60–0.72	0.640	25.6	232.21 ± 64.41 ± 16.40	0.753	37.2	22.84 ± 16.15 ± 2.23
0.72–0.90						
0.90–1.25						
$p_T$	40 < $\theta$ < 50			50 < $\theta$ < 60		
	$\langle p_T \rangle$	$\langle \theta \rangle$	$d^2\sigma/dpd\Omega$	$\langle p_T \rangle$	$\langle \theta \rangle$	$d^2\sigma/dpd\Omega$
0.10–0.13	0.116	46.3	211.03 ± 148.14 ± 16.35	0.145	55.6	357.87 ± 170.42 ± 23.29
0.13–0.16	0.151	44.7	248.86 ± 142.09 ± 15.51	0.180	53.4	462.05 ± 159.41 ± 25.20
0.16–0.20	0.183	43.8	492.38 ± 166.35 ± 26.57	0.218	53.6	177.44 ± 102.45 ± 8.57
0.20–0.24	0.213	45.3	333.89 ± 137.12 ± 16.12	0.268	53.7	496.66 ± 137.85 ± 21.71
0.24–0.30	0.259	44.4	204.80 ± 86.13 ± 8.74	0.316	54.5	245.56 ± 96.41 ± 10.41
0.30–0.36	0.330	45.5	262.53 ± 99.32 ± 10.51	0.396	54.3	242.79 ± 92.28 ± 10.44
0.36–0.42	0.386	46.4	340.60 ± 113.55 ± 14.12	0.462	56.8	110.91 ± 55.46 ± 5.41
0.42–0.50	0.461	43.4	238.27 ± 79.43 ± 11.09	0.560	53.2	127.42 ± 52.02 ± 7.79
0.50–0.60	0.557	44.7	40.73 ± 28.80 ± 2.39	0.667	56.3	33.96 ± 24.02 ± 2.78
0.60–0.72	0.645	44.7	70.92 ± 35.46 ± 5.38	0.758	51.7	21.00 ± 14.85 ± 2.33
0.72–0.90				1.001	56.5	8.24 ± 5.83 ± 1.54
0.90–1.25						
$p_T$	60 < $\theta$ < 75			75 < $\theta$ < 90		
	$\langle p_T \rangle$	$\langle \theta \rangle$	$d^2\sigma/dpd\Omega$	$\langle p_T \rangle$	$\langle \theta \rangle$	$d^2\sigma/dpd\Omega$
0.13–0.16	0.141	68.2	379.86 ± 161.65 ± 24.52	0.185	83.2	262.09 ± 100.03 ± 14.35
0.16–0.20	0.189	69.2	218.18 ± 91.27 ± 11.51	0.208	84.0	148.30 ± 75.69 ± 7.30
0.20–0.24	0.220	64.7	155.15 ± 77.73 ± 7.59	0.290	77.1	108.55 ± 54.31 ± 5.16
0.24–0.30	0.269	66.7	146.03 ± 60.23 ± 6.30	0.342	80.9	109.70 ± 54.85 ± 5.37
0.30–0.36	0.335	70.1	100.47 ± 50.80 ± 4.39	0.575	79.9	28.98 ± 20.49 ± 2.39
0.36–0.42	0.393	69.2	52.00 ± 36.77 ± 2.36			
0.50–0.60	0.543	67.0	99.98 ± 37.79 ± 6.71			
0.60–0.72	0.661	68.2	22.20 ± 15.70 ± 1.99			
0.72–0.90	0.767	64.4	11.83 ± 8.42 ± 1.46			
0.90–1.25	1.099	68.1	5.50 ± 3.89 ± 1.07			
$p_T$	90 < $\theta$ < 105			105 < $\theta$ < 125		
	$\langle p_T \rangle$	$\langle \theta \rangle$	$d^2\sigma/dpd\Omega$	$\langle p_T \rangle$	$\langle \theta \rangle$	$d^2\sigma/dpd\Omega$
0.13–0.16				0.146	112.1	212.86 ± 95.38 ± 12.35
0.16–0.20	0.179	93.6	211.58 ± 95.12 ± 10.71	0.178	108.5	122.22 ± 62.48 ± 5.43
0.20–0.24	0.222	97.2	159.82 ± 79.93 ± 7.07	0.223	110.1	59.08 ± 41.79 ± 2.56
0.24–0.30	0.257	97.6	109.32 ± 54.83 ± 5.25			
0.30–0.36	0.332	92.9	51.97 ± 36.77 ± 2.66			
0.36–0.42	0.396	91.8	50.60 ± 35.78 ± 3.23			
0.42–0.50	0.454	93.9	74.73 ± 37.37 ± 6.15	0.458	110.4	26.14 ± 18.48 ± 2.88
0.50–0.60	0.550	95.5	27.89 ± 19.72 ± 3.06			

Table A.43: Double-differential inclusive cross-section  $d^2\sigma/dpd\Omega$  [mb/(GeV/c sr)] of the production of protons in  $\pi^- + \text{Sn} \rightarrow p + X$  interactions with  $-15.0$  GeV/c beam momentum; the first error is statistical, the second systematic;  $p_T$  in GeV/c, polar angle  $\theta$  in degrees.

$p_T$	20 < $\theta$ < 30						30 < $\theta$ < 40							
	$\langle p_T \rangle$	$\langle \theta \rangle$	$d^2\sigma/dpd\Omega$				$\langle p_T \rangle$	$\langle \theta \rangle$	$d^2\sigma/dpd\Omega$					
			759.05	$\pm$	29.64	$\pm$	43.00	912.85	$\pm$	25.87	$\pm$	44.94		
0.20–0.24	0.222	25.0	759.05	$\pm$	29.64	$\pm$	43.00	0.274	34.9	912.85	$\pm$	25.87	$\pm$	44.94
0.24–0.30	0.272	25.1	719.38	$\pm$	22.71	$\pm$	38.06	0.332	35.2	735.85	$\pm$	22.45	$\pm$	33.33
0.30–0.36	0.333	25.2	584.49	$\pm$	21.01	$\pm$	31.63	0.395	35.1	583.07	$\pm$	20.76	$\pm$	28.04
0.36–0.42	0.395	25.3	470.85	$\pm$	19.37	$\pm$	27.39	0.465	35.1	434.65	$\pm$	15.97	$\pm$	23.89
0.42–0.50	0.467	25.2	355.96	$\pm$	14.40	$\pm$	22.34	0.559	35.1	299.54	$\pm$	12.14	$\pm$	19.13
0.50–0.60	0.559	25.1	250.83	$\pm$	10.80	$\pm$	17.76	0.671	35.0	186.39	$\pm$	8.81	$\pm$	14.33
0.60–0.72	0.671	25.3	148.72	$\pm$	7.38	$\pm$	11.54	0.825	35.1	81.47	$\pm$	4.80	$\pm$	8.32
40 < $\theta$ < 50														
$p_T$	$\langle p_T \rangle$	$\langle \theta \rangle$	$d^2\sigma/dpd\Omega$				$\langle p_T \rangle$	$\langle \theta \rangle$	$d^2\sigma/dpd\Omega$					
			808.76	$\pm$	23.31	$\pm$	33.34		669.99	$\pm$	20.60	$\pm$	27.07	
0.30–0.36	0.331	45.1	687.25	$\pm$	21.51	$\pm$	27.36	0.391	55.2	537.55	$\pm$	16.57	$\pm$	21.59
0.36–0.42	0.391	45.1	456.41	$\pm$	15.93	$\pm$	21.34	0.549	54.9	350.99	$\pm$	12.68	$\pm$	18.70
0.42–0.50	0.460	45.0	324.24	$\pm$	12.82	$\pm$	21.08	0.661	55.0	203.75	$\pm$	9.53	$\pm$	16.33
0.50–0.60	0.549	45.0	201.28	$\pm$	9.51	$\pm$	16.84	0.806	54.9	98.30	$\pm$	5.59	$\pm$	10.62
60 < $\theta$ < 75														
$p_T$	$\langle p_T \rangle$	$\langle \theta \rangle$	$d^2\sigma/dpd\Omega$				$\langle p_T \rangle$	$\langle \theta \rangle$	$d^2\sigma/dpd\Omega$					
			345.49	$\pm$	9.50	$\pm$	16.47		299.50	$\pm$	8.71	$\pm$	16.45	
0.50–0.60	0.549	67.2	189.02	$\pm$	7.11	$\pm$	13.69	0.659	82.0	152.76	$\pm$	6.05	$\pm$	10.86
0.60–0.72	0.659	67.3	81.32	$\pm$	4.20	$\pm$	9.80	0.803	82.1	52.31	$\pm$	3.50	$\pm$	7.62
90 < $\theta$ < 105														
$p_T$	$\langle p_T \rangle$	$\langle \theta \rangle$	$d^2\sigma/dpd\Omega$				$\langle p_T \rangle$	$\langle \theta \rangle$	$d^2\sigma/dpd\Omega$					
			203.22	$\pm$	7.09	$\pm$	14.34		189.91	$\pm$	6.33	$\pm$	13.01	
0.42–0.50	0.547	97.1	101.06	$\pm$	4.96	$\pm$	8.75	0.544	113.1	94.24	$\pm$	4.41	$\pm$	8.72
0.50–0.60	0.658	96.6						0.656	112.8	26.64	$\pm$	2.51	$\pm$	4.14

Table A.44: Double-differential inclusive cross-section  $d^2\sigma/dpd\Omega$  [mb/(GeV/c sr)] of the production of  $\pi^+$ 's in  $\pi^- + \text{Sn} \rightarrow \pi^+ + \text{X}$  interactions with  $-15.0$  GeV/c beam momentum; the first error is statistical, the second systematic;  $p_T$  in GeV/c, polar angle  $\theta$  in degrees.

$p_T$	20 < $\theta$ < 30						30 < $\theta$ < 40					
	$\langle p_T \rangle$	$\langle \theta \rangle$	$d^2\sigma/dpd\Omega$				$\langle p_T \rangle$	$\langle \theta \rangle$	$d^2\sigma/dpd\Omega$			
			527.24	$\pm$ 31.02	$\pm$ 41.18	414.47	$\pm$ 27.30	$\pm$ 32.30	482.45	$\pm$ 26.21	$\pm$ 29.19	
0.10–0.13	0.115	25.0	527.24	$\pm$ 31.02	$\pm$ 41.18	0.116	34.6	414.47	$\pm$ 27.30	$\pm$ 32.30		
0.13–0.16	0.147	24.4	534.20	$\pm$ 28.05	$\pm$ 32.71	0.146	34.6	482.45	$\pm$ 26.21	$\pm$ 29.19		
0.16–0.20	0.182	24.7	617.91	$\pm$ 25.08	$\pm$ 32.72	0.181	34.9	416.03	$\pm$ 20.46	$\pm$ 21.97		
0.20–0.24	0.222	24.8	647.96	$\pm$ 25.54	$\pm$ 31.28	0.222	34.9	491.87	$\pm$ 22.61	$\pm$ 24.05		
0.24–0.30	0.273	24.7	607.82	$\pm$ 20.31	$\pm$ 26.82	0.272	34.9	458.08	$\pm$ 17.44	$\pm$ 19.62		
0.30–0.36	0.334	24.8	556.92	$\pm$ 19.18	$\pm$ 22.46	0.332	34.7	392.40	$\pm$ 16.46	$\pm$ 15.80		
0.36–0.42	0.395	24.8	418.86	$\pm$ 16.43	$\pm$ 16.82	0.394	34.9	293.63	$\pm$ 13.83	$\pm$ 11.58		
0.42–0.50	0.465	24.7	316.54	$\pm$ 11.75	$\pm$ 14.04	0.465	34.7	233.78	$\pm$ 10.49	$\pm$ 9.83		
0.50–0.60	0.557	24.7	220.68	$\pm$ 8.82	$\pm$ 12.48	0.559	34.9	162.56	$\pm$ 7.62	$\pm$ 8.43		
0.60–0.72	0.670	24.9	127.35	$\pm$ 5.86	$\pm$ 10.00	0.672	34.6	97.05	$\pm$ 4.99	$\pm$ 6.90		
0.72–0.90						0.822	34.5	38.94	$\pm$ 2.29	$\pm$ 4.29		
$p_T$	40 < $\theta$ < 50						50 < $\theta$ < 60					
	$\langle p_T \rangle$	$\langle \theta \rangle$	$d^2\sigma/dpd\Omega$				$\langle p_T \rangle$	$\langle \theta \rangle$	$d^2\sigma/dpd\Omega$			
			316.46	$\pm$ 24.55	$\pm$ 24.65	0.145	55.2	314.49	$\pm$ 22.04	$\pm$ 20.17		
0.10–0.13	0.115	44.5	341.69	$\pm$ 22.22	$\pm$ 20.97	0.181	55.0	307.77	$\pm$ 17.62	$\pm$ 16.41		
0.13–0.16	0.145	44.7	338.22	$\pm$ 18.36	$\pm$ 18.02	0.220	54.5	307.09	$\pm$ 17.36	$\pm$ 14.62		
0.16–0.20	0.181	44.8	410.87	$\pm$ 20.60	$\pm$ 19.69	0.271	54.7	248.44	$\pm$ 13.09	$\pm$ 10.70		
0.20–0.24	0.220	44.6	345.26	$\pm$ 15.44	$\pm$ 15.17	0.328	54.7	201.56	$\pm$ 11.84	$\pm$ 8.25		
0.24–0.30	0.269	44.6	303.30	$\pm$ 14.60	$\pm$ 12.33	0.391	54.8	153.83	$\pm$ 10.22	$\pm$ 6.30		
0.30–0.36	0.332	45.0	228.75	$\pm$ 12.41	$\pm$ 9.09	0.458	54.9	130.89	$\pm$ 8.18	$\pm$ 5.82		
0.36–0.42	0.389	44.7	158.96	$\pm$ 8.73	$\pm$ 6.72	0.551	54.9	85.33	$\pm$ 5.66	$\pm$ 4.55		
0.42–0.50	0.459	44.6	122.01	$\pm$ 6.72	$\pm$ 6.14	0.655	54.6	52.44	$\pm$ 4.02	$\pm$ 3.62		
0.50–0.60	0.551	44.6	71.14	$\pm$ 4.33	$\pm$ 4.77	0.798	54.8	19.08	$\pm$ 1.75	$\pm$ 1.89		
0.60–0.72	0.658	44.1	32.20	$\pm$ 2.21	$\pm$ 3.21	1.052	54.9	5.39	$\pm$ 0.58	$\pm$ 0.83		
0.72–0.90	0.803	44.8										
0.90–1.25												
$p_T$	60 < $\theta$ < 75						75 < $\theta$ < 90					
	$\langle p_T \rangle$	$\langle \theta \rangle$	$d^2\sigma/dpd\Omega$				$\langle p_T \rangle$	$\langle \theta \rangle$	$d^2\sigma/dpd\Omega$			
			237.66	$\pm$ 16.47	$\pm$ 15.52	0.146	82.5	166.34	$\pm$ 14.68	$\pm$ 10.88		
0.13–0.16	0.147	67.1	247.93	$\pm$ 12.84	$\pm$ 13.23	0.179	82.1	181.82	$\pm$ 11.04	$\pm$ 9.54		
0.16–0.20	0.180	67.1	229.08	$\pm$ 12.38	$\pm$ 10.74	0.221	82.5	168.58	$\pm$ 10.51	$\pm$ 7.71		
0.20–0.24	0.219	67.1	186.16	$\pm$ 9.28	$\pm$ 7.87	0.269	82.3	125.80	$\pm$ 7.73	$\pm$ 5.47		
0.24–0.30	0.269	67.5	164.40	$\pm$ 8.86	$\pm$ 7.02	0.331	81.9	105.30	$\pm$ 7.17	$\pm$ 4.90		
0.30–0.36	0.328	66.8	126.98	$\pm$ 7.78	$\pm$ 5.65	0.390	81.6	62.37	$\pm$ 5.46	$\pm$ 3.08		
0.36–0.42	0.390	67.3	88.91	$\pm$ 5.46	$\pm$ 4.31	0.460	81.3	43.21	$\pm$ 3.80	$\pm$ 2.47		
0.42–0.50	0.460	66.5	57.41	$\pm$ 3.93	$\pm$ 3.48	0.547	81.6	28.95	$\pm$ 2.78	$\pm$ 2.11		
0.50–0.60	0.550	66.3	26.32	$\pm$ 2.27	$\pm$ 2.10	0.657	82.2	14.84	$\pm$ 1.73	$\pm$ 1.42		
0.60–0.72	0.654	66.4	12.68	$\pm$ 1.20	$\pm$ 1.42	0.795	83.0	5.98	$\pm$ 0.85	$\pm$ 0.78		
0.72–0.90	0.793	66.6	1.98	$\pm$ 0.25	$\pm$ 0.37	1.048	80.4	1.08	$\pm$ 0.20	$\pm$ 0.23		
0.90–1.25	1.009	66.0										
$p_T$	90 < $\theta$ < 105						105 < $\theta$ < 125					
	$\langle p_T \rangle$	$\langle \theta \rangle$	$d^2\sigma/dpd\Omega$				$\langle p_T \rangle$	$\langle \theta \rangle$	$d^2\sigma/dpd\Omega$			
			170.47	$\pm$ 13.74	$\pm$ 11.01	0.145	114.6	139.14	$\pm$ 10.27	$\pm$ 8.25		
0.13–0.16	0.146	97.4	179.30	$\pm$ 11.16	$\pm$ 9.09	0.181	114.2	110.04	$\pm$ 7.43	$\pm$ 5.34		
0.16–0.20	0.179	97.2	128.89	$\pm$ 9.36	$\pm$ 5.76	0.219	113.9	81.51	$\pm$ 6.58	$\pm$ 3.64		
0.20–0.24	0.220	97.3	88.01	$\pm$ 6.53	$\pm$ 3.85	0.268	114.4	52.84	$\pm$ 4.38	$\pm$ 2.61		
0.24–0.30	0.330	97.1	64.97	$\pm$ 5.54	$\pm$ 3.22	0.331	114.1	33.08	$\pm$ 3.39	$\pm$ 2.05		
0.30–0.36	0.390	96.5	36.66	$\pm$ 4.08	$\pm$ 2.20	0.390	114.3	19.32	$\pm$ 2.52	$\pm$ 1.55		
0.36–0.42	0.457	96.0	26.20	$\pm$ 2.94	$\pm$ 1.98	0.460	113.8	11.85	$\pm$ 1.66	$\pm$ 1.20		
0.42–0.50	0.548	96.2	13.72	$\pm$ 1.83	$\pm$ 1.36	0.549	113.0	4.10	$\pm$ 0.82	$\pm$ 0.55		
0.50–0.60	0.653	96.0	8.20	$\pm$ 1.32	$\pm$ 1.06	0.665	110.9	1.63	$\pm$ 0.48	$\pm$ 0.29		
0.60–0.72	0.822	96.4	1.87	$\pm$ 0.41	$\pm$ 0.34	0.782	112.4	0.25	$\pm$ 0.13	$\pm$ 0.06		
0.72–0.90	1.031	94.1	0.41	$\pm$ 0.11	$\pm$ 0.12							
0.90–1.25												

Table A.45: Double-differential inclusive cross-section  $d^2\sigma/dpd\Omega$  [mb/(GeV/c sr)] of the production of  $\pi^-$ 's in  $\pi^- + \text{Sn} \rightarrow \pi^- + \text{X}$  interactions with  $-15.0$  GeV/c beam momentum; the first error is statistical, the second systematic;  $p_T$  in GeV/c, polar angle  $\theta$  in degrees.

$p_T$	20 < $\theta$ < 30						30 < $\theta$ < 40						
	$\langle p_T \rangle$	$\langle \theta \rangle$	$d^2\sigma/dpd\Omega$				$\langle p_T \rangle$	$\langle \theta \rangle$	$d^2\sigma/dpd\Omega$				
			$\langle p_T \rangle$	$\langle \theta \rangle$	$d^2\sigma/dpd\Omega$	$d^2\sigma/dpd\Omega$			$\langle p_T \rangle$	$\langle \theta \rangle$	$d^2\sigma/dpd\Omega$	$d^2\sigma/dpd\Omega$	
0.10–0.13	0.115	24.9	706.38	$\pm$ 36.87	$\pm$ 55.60	0.115	35.0	527.16	$\pm$ 31.28	$\pm$ 40.67			
0.13–0.16	0.144	24.9	781.56	$\pm$ 35.06	$\pm$ 48.15	0.145	34.7	547.23	$\pm$ 28.51	$\pm$ 33.64			
0.16–0.20	0.179	25.0	781.65	$\pm$ 29.10	$\pm$ 41.66	0.179	34.6	599.62	$\pm$ 25.34	$\pm$ 32.05			
0.20–0.24	0.217	24.8	800.84	$\pm$ 28.87	$\pm$ 37.85	0.219	34.8	525.05	$\pm$ 23.38	$\pm$ 24.94			
0.24–0.30	0.266	24.7	710.72	$\pm$ 22.16	$\pm$ 29.93	0.266	34.8	535.99	$\pm$ 19.38	$\pm$ 22.65			
0.30–0.36	0.324	24.9	619.56	$\pm$ 20.88	$\pm$ 24.73	0.324	34.7	448.17	$\pm$ 17.52	$\pm$ 17.57			
0.36–0.42	0.382	24.6	480.40	$\pm$ 17.89	$\pm$ 19.00	0.383	34.6	335.53	$\pm$ 15.03	$\pm$ 13.26			
0.42–0.50	0.450	24.6	386.48	$\pm$ 14.03	$\pm$ 16.94	0.450	34.7	266.73	$\pm$ 11.62	$\pm$ 11.54			
0.50–0.60	0.534	24.8	268.87	$\pm$ 10.54	$\pm$ 14.44	0.534	34.6	188.79	$\pm$ 8.72	$\pm$ 9.94			
0.60–0.72	0.638	24.8	155.38	$\pm$ 7.35	$\pm$ 10.81	0.640	34.8	117.64	$\pm$ 6.15	$\pm$ 7.98			
0.72–0.90						0.769	34.3	57.26	$\pm$ 3.55	$\pm$ 5.23			
$p_T$	40 < $\theta$ < 50						50 < $\theta$ < 60						
	$\langle p_T \rangle$	$\langle \theta \rangle$	$d^2\sigma/dpd\Omega$				$\langle p_T \rangle$	$\langle \theta \rangle$	$d^2\sigma/dpd\Omega$				
			$\langle p_T \rangle$	$\langle \theta \rangle$	$d^2\sigma/dpd\Omega$	$d^2\sigma/dpd\Omega$			$\langle p_T \rangle$	$\langle \theta \rangle$	$d^2\sigma/dpd\Omega$	$d^2\sigma/dpd\Omega$	
0.10–0.13	0.115	45.0	445.22	$\pm$ 29.76	$\pm$ 35.55		0.145	55.0	405.84	$\pm$ 25.01	$\pm$ 26.17		
0.13–0.16	0.146	44.8	480.39	$\pm$ 26.93	$\pm$ 29.95		0.179	54.9	363.56	$\pm$ 19.37	$\pm$ 19.60		
0.16–0.20	0.180	44.8	413.93	$\pm$ 20.62	$\pm$ 22.29		0.219	54.7	350.54	$\pm$ 19.17	$\pm$ 16.72		
0.20–0.24	0.220	44.8	457.24	$\pm$ 22.01	$\pm$ 21.99		0.268	54.7	305.74	$\pm$ 14.86	$\pm$ 13.33		
0.24–0.30	0.269	44.9	410.04	$\pm$ 16.92	$\pm$ 17.39		0.329	54.8	237.38	$\pm$ 13.11	$\pm$ 9.85		
0.30–0.36	0.327	44.8	320.08	$\pm$ 14.93	$\pm$ 12.65		0.387	54.8	192.51	$\pm$ 11.70	$\pm$ 8.01		
0.36–0.42	0.387	44.8	290.06	$\pm$ 14.46	$\pm$ 12.04		0.456	54.4	158.93	$\pm$ 8.96	$\pm$ 7.34		
0.42–0.50	0.457	44.7	187.44	$\pm$ 9.76	$\pm$ 8.38		0.543	54.5	87.86	$\pm$ 5.89	$\pm$ 5.01		
0.50–0.60	0.543	45.0	122.14	$\pm$ 7.05	$\pm$ 6.72		0.652	55.1	59.02	$\pm$ 4.42	$\pm$ 4.34		
0.60–0.72	0.650	44.6	75.98	$\pm$ 4.92	$\pm$ 5.42		0.792	54.8	23.91	$\pm$ 2.21	$\pm$ 2.41		
0.72–0.90	0.791	45.0	38.19	$\pm$ 2.81	$\pm$ 3.71		1.007	55.0	4.59	$\pm$ 0.60	$\pm$ 0.74		
$p_T$	60 < $\theta$ < 75						75 < $\theta$ < 90						
	$\langle p_T \rangle$	$\langle \theta \rangle$	$d^2\sigma/dpd\Omega$				$\langle p_T \rangle$	$\langle \theta \rangle$	$d^2\sigma/dpd\Omega$				
			$\langle p_T \rangle$	$\langle \theta \rangle$	$d^2\sigma/dpd\Omega$	$d^2\sigma/dpd\Omega$			$\langle p_T \rangle$	$\langle \theta \rangle$	$d^2\sigma/dpd\Omega$	$d^2\sigma/dpd\Omega$	
0.13–0.16	0.146	67.2	316.38	$\pm$ 18.88	$\pm$ 19.80	0.145	82.3	262.44	$\pm$ 19.50	$\pm$ 17.40			
0.16–0.20	0.178	67.2	291.08	$\pm$ 14.19	$\pm$ 15.04	0.179	82.1	249.45	$\pm$ 13.36	$\pm$ 12.68			
0.20–0.24	0.218	67.3	283.27	$\pm$ 14.08	$\pm$ 12.93	0.219	82.0	217.97	$\pm$ 12.30	$\pm$ 9.68			
0.24–0.30	0.268	66.9	218.14	$\pm$ 10.23	$\pm$ 9.39	0.266	82.2	172.32	$\pm$ 9.24	$\pm$ 7.58			
0.30–0.36	0.327	66.5	170.16	$\pm$ 9.09	$\pm$ 7.26	0.327	82.5	112.02	$\pm$ 7.51	$\pm$ 5.36			
0.36–0.42	0.387	67.0	130.78	$\pm$ 7.97	$\pm$ 5.93	0.386	81.4	77.62	$\pm$ 6.21	$\pm$ 4.04			
0.42–0.50	0.456	66.3	100.28	$\pm$ 5.96	$\pm$ 5.05	0.456	82.1	63.59	$\pm$ 4.65	$\pm$ 3.83			
0.50–0.60	0.541	66.4	57.64	$\pm$ 3.89	$\pm$ 3.63	0.543	80.6	34.15	$\pm$ 3.03	$\pm$ 2.64			
0.60–0.72	0.651	66.6	31.39	$\pm$ 2.62	$\pm$ 2.57	0.645	82.6	16.27	$\pm$ 1.91	$\pm$ 1.64			
0.72–0.90	0.794	67.3	10.86	$\pm$ 1.18	$\pm$ 1.23	0.786	81.4	5.74	$\pm$ 0.83	$\pm$ 0.81			
0.90–1.25	1.012	65.3	2.76	$\pm$ 0.40	$\pm$ 0.47	1.001	80.2	1.09	$\pm$ 0.25	$\pm$ 0.22			
$p_T$	90 < $\theta$ < 105						105 < $\theta$ < 125						
	$\langle p_T \rangle$	$\langle \theta \rangle$	$d^2\sigma/dpd\Omega$				$\langle p_T \rangle$	$\langle \theta \rangle$	$d^2\sigma/dpd\Omega$				
			$\langle p_T \rangle$	$\langle \theta \rangle$	$d^2\sigma/dpd\Omega$	$d^2\sigma/dpd\Omega$			$\langle p_T \rangle$	$\langle \theta \rangle$	$d^2\sigma/dpd\Omega$	$d^2\sigma/dpd\Omega$	
0.13–0.16	0.147	97.3	232.74	$\pm$ 17.36	$\pm$ 14.90	0.143	114.1	208.25	$\pm$ 13.17	$\pm$ 11.62			
0.16–0.20	0.178	97.1	193.13	$\pm$ 11.77	$\pm$ 9.63	0.177	113.5	152.93	$\pm$ 9.20	$\pm$ 6.98			
0.20–0.24	0.219	97.4	153.56	$\pm$ 10.54	$\pm$ 6.74	0.217	113.1	91.48	$\pm$ 6.98	$\pm$ 4.17			
0.24–0.30	0.268	96.8	116.27	$\pm$ 7.62	$\pm$ 5.16	0.267	113.9	60.75	$\pm$ 4.71	$\pm$ 3.19			
0.30–0.36	0.325	97.2	72.90	$\pm$ 5.95	$\pm$ 3.74	0.327	114.0	35.80	$\pm$ 3.63	$\pm$ 2.45			
0.36–0.42	0.387	95.8	50.50	$\pm$ 4.89	$\pm$ 3.19	0.387	112.9	20.45	$\pm$ 2.67	$\pm$ 1.78			
0.42–0.50	0.453	96.6	36.53	$\pm$ 3.58	$\pm$ 2.95	0.456	112.3	12.85	$\pm$ 1.77	$\pm$ 1.43			
0.50–0.60	0.543	97.3	19.29	$\pm$ 2.29	$\pm$ 2.05	0.537	113.7	5.99	$\pm$ 1.08	$\pm$ 0.86			
0.60–0.72	0.648	97.2	7.54	$\pm$ 1.28	$\pm$ 1.06	0.643	112.4	2.75	$\pm$ 0.63	$\pm$ 0.52			
0.72–0.90	0.778	98.2	2.39	$\pm$ 0.53	$\pm$ 0.46	0.780	112.3	0.45	$\pm$ 0.17	$\pm$ 0.12			
0.90–1.25	1.007	94.8	0.55	$\pm$ 0.16	$\pm$ 0.15	0.946	110.2	0.08	$\pm$ 0.04	$\pm$ 0.03			